Analysis of estrogen profiles including methoxyestrogen glucuronides: method validation and applicability to human plasma and breast tissue

Analyse von Estrogenprofilen einschließlich Methoxyestrogenglucuroniden: Methodenvalidierung und Anwendbarkeit auf menschliches Plasma und Brustgewebe

Doctoral thesis for a doctoral degree at the Graduate School of Life Sciences

Julius-Maximilians-Universität Würzburg

Section Biomedicine

Jeniffer Calderón Giraldo

From Medellín, Colombia

Würzburg 2020

Affidavit

I hereby confirm that my thesis entitled “Analysis of estrogen profiles including methoxyestrogen glucuronides: method validation and applicability to human plasma and breast tissue” is the result of my own work. I did not receive any help or support from commercial consultants. All sources and/or materials applied are listed and specified in the thesis.

Furthermore, I confirm that this thesis has not yet been submitted as part of another examination process neither in identical nor in a similar form.

Würzburg 2020

Submitted on

_____

Chair Person: _____

Evaluators of the written thesis

Prof. Dr. Leane Lehmann
Supervisor - 1. Evaluator: _____

Prof. Dr. Helga Stopper
2. Evaluator: _____

Examiners of the public defense

Prof. Dr. Leane Lehmann
1. Examiner: _____

Prof. Dr. Helga Stopper
2. Examiner: _____

Prof. Dr. Günter Vollmer
3. Examiner: _____

Date of the public defense

_____

Doctoral certificate awarded on

_____

To Johannes

Acknowledgment

I want to express my gratitude to Professor Dr. Leane Lehmann for allowing me to work in her research group and for the suggestions and criticism that contributed to the successful conclusion of this work.

I would like to thank the German *Excellence Initiative* and the Graduate School of Life Sciences, University of Würzburg, for my doctoral fellowship. In the same way, I would like to thank the DAAD for the complementary fellowship.

I also would like to thank Dr. Carolin Kleider for her guidance and support during the development of my investigation and her feedback during the writing of this thesis.

I thank Dr. Harald Esch for his support in literature research, and his help and support during my first steps as a Doctoral researcher in a new place.

I thank Daniela Pemp for her help with some statistical analysis and with the GC-MS/MS analysis. I also would like to thank Tine Albrecht for her help with the GC-MS/MS analysis.

I would like to thank Rene Hauptstein for his comments, help with R, and just for being there when I need it.

I thank all my other dear colleagues Guy Eshun, Ghanya Al-Naqeb, Tobias Jaud, Miriam Macziol, Marina Kretzschmar and Benjamin Spielmann for the nice time, help and together work.

I also thank all the master students I had the opportunity to work with, especially to Daniel Walter, Miriam Raps and Lukas Häfner.

To my dear friends Carlos Mario and Juan Pablo, for always lifting me.

To my family for always believing in me.

And last but not least, I would like to say thank you to my lovely husband for his unconditional love and encouragement. I wouldn’t be writing this without your support.

Contents

Abbreviations

ACN	Acetonitrile
ADT	Adipose tissue
AFB	Ammonium formiate buffer
approx.	Approximately
BCRP	Breast cancer resistance protein
BMI	Body mass index
BRK	Bayerisches Rotes Kreuz
BSTFA	N,O – Bis (trimethylsilyl) trifluoroacetamide with1.0% Trimethylchlorosilane
CE	Collision energy
COMT	Catechol-*O*-methyltransferase
CYPs	Cytochrome P450 monooxygenases
CXP	Cell exit potential
DHEA	Dehydroepiandrosterone
DMSO	Dimethyl sulfoxide
DNA	Deoxyribonucleic acid
DP	Declustering potential
DTT	1,4-Dithiothreitol
ESI	Electrospray ionization
E1	Estrone
E1-G	Estrone-3-glucuronide
E1-S	Estrone-3-sulfate
E2	17β-Estradiol
E2-3-G	17β-Estradiol-3-glucuronide
E2-3-S	17β-Estradiol-3-sulfate
E2-17-S	17β-Estradiol-17-sulfate
e.g.	Exempli gratia
ePS	Enhanced product ion scan
FA	Formic acid
FDA	Food and Drug Administration
G	Glucuronides

GC	Gas chromatography
GS1	Nebulizer gas
GS2	Turbogas
GLT	Glandular tissue
HPLC	High performance liquid chromatography
2-HO-E2	2-hydroxyestradiol
4-HO-E2	4-hydroxyestradiol
16α-HO-E2	16α-hydroxyestradiol
2-HO-E1	2-hydroxyestrone
4-HO-E1	4-hydroxyestrone
16α-HO-E1	16α-hydroxyestrone
IS	Ion spray voltage
ISs	Internal standards
LC	Liquid chromatography
LOD	Limit of detection
LOQ	Limit of quantification
2-MeO-E2	2-methoxyestradiol
4-MeO-E2	4-methoxyestradiol
2-MeO-E2-3-G	2-methoxyestradiol-3-glucuronide
4-MeO-E2-3-G	4-methoxyestradiol-3-glucuronide
2-MeO-E2-17-G	2-methoxyestradiol-17-glucuronide
4-MeO-E2-17-G	4-methoxyestradiol-17-glucuronide
2-MeO-E1	2-methoxyestrone
4-MeO-E1	4-methoxyestrone
2-MeO-E1-G	2-methoxyestrone-3-glucuronide
4-MeO-E1-G	4-methoxyestrone-3-glucuronide
MeOH	Methanol
Min	Minute (s)
MRM	Multiple reaction monitoring
MS	Mass spectrometry
m/z	mass/charge ratio
NH_3	Ammonia
OATPs	Organic anion-transporting polypeptides
o.c	On column

Q	Quadrupole
Ql	Qualifier
Qn	Quantifier
RDS	Relative standard deviation
R^2	Coefficient of correlation
S	Sulfate
SAM	S-adenosylmethionine
SD	Standard deviation
Sec	Seconds
S/N	Signal to noise ratio
SPE	Solid phase extraction
STS	Steroid sulfatase
SULTs	Sulfotransferases
t_R	Retention time
UDPGA	Uridine 5’-diphospho-glucuronic acid
UGTs	Uridine 5’-diphospho-glucuronosyltransferases
UHPLC	Ultra high performance liquid chromatography
UV/Vis	Ultraviolet-visible

1. Introduction

Estrogens, namely 17β-estradiol (E2) and estrone (E1) are considered to play an important role in the initiation and promotion of breast cancer (summarized in Raftogianis et al., 2000), a malignancy responsible for around 500,000 deaths per year (summarized in Ghislain et al., 2016).

Two major mechanisms have been postulated to explain the carcinogenic effects of estrogens: (1) the estrogen receptor-mediated stimulation of breast cell proliferation with a concomitant enhanced rate of mutations and (2) the metabolism of hydroxylated estrogens to quinone derivatives which can react with the DNA (Russo and Russo, 2006, summarized in Yager and Davidson, 2006). Nevertheless, as a detoxifying mechanism, E1, E2, and their hydroxylated and methoxylated metabolites are reversibly conjugated into sulfates and glucuronides devoid of biological activity (summarized in Guillemette et al., 2004). Yet, despite the key detoxifying function of these conjugates, the study of their circulating levels face some significant problems: (1) analysis by techniques such as radioimmunoassay lack specificity and accuracy and requires enzymatic/chemical hydrolysis before analysis, being unable to differentiate between sulfates and glucuronides (summarized in Stanczyk et al., 2007, summarized in Wang et al., 2016), (2) very little knowledge in healthy women, which has been identified as a barrier to advance in breast cancer research (summarized in Liu, 2000), and (3) far fewer studies in pre- than in postmenopausal women (summarized in Samavat and Kurzer, 2015).

Therefore, to get more insights into the research of breast cancer etiology and prevention, the analysis of circulating levels of estrogens (including metabolites and conjugates) in women without breast cancer through reliable analytical techniques, is required.

1.1. Estrone and 17β-estradiol: formation and circulating levels

E2 and E1 are the most important estrogens in circulation and E2 is considered the most biologically active estrogen (summarized in Samavat and Kurzer, 2015).

The leading site of E2 and E1 biosynthesis in premenopausal women are the ovaries and peripheral tissue expressing aromatase (summarized in Africander and Storbeck, 2018, summarized in Rizner, 2013). In the ovaries, E2 and E1 are biosynthesized from cholesterol via pregnenolone, 17-hydroxypregnenolone, dehydroepiandrosterone (DHEA) and androstenedione (summarized in Miller and Auchus, 2011). In peripheral tissues, E2 and E1 are biosynthesized from DHEA and androstenedione derived from the adrenal cortex (summarized in Miller and Auchus, 2011). In postmenopausal women, the ovaries cease their activity causing a dramatic decrease in the production of E2 and E1. Therefore, adipose peripheral tissue including that of the breast becomes the major source of E2 and E1 (summarized in Africander and Storbeck, 2018).

After biosynthesis, E2 and E1 readily diffuse across membranes without the intervention of transporters (Oren et al., 2004). In blood, E2 can be found unbound or non-covalently bound to binding proteins such as the sex hormone-binding globulin and albumin (Dunn et al., 1981)(Figure 1).

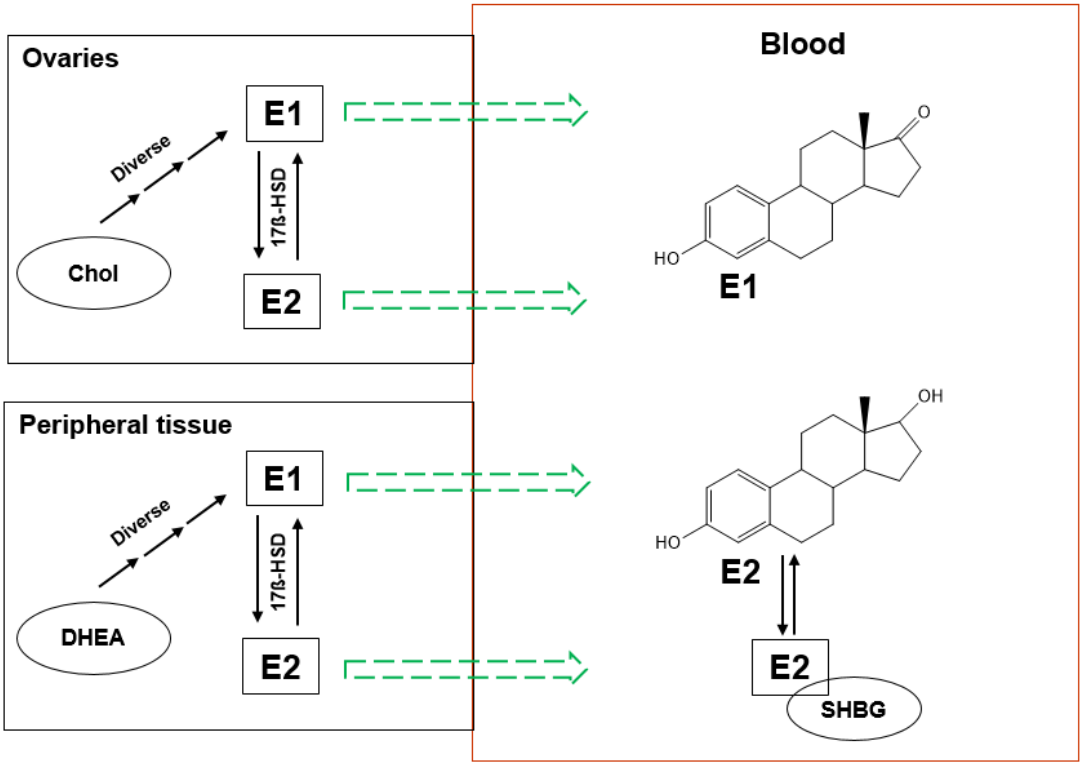

Figure 1: E1 and E2 released to circulation. Chol, cholesterol; 17β-HSD, 17β-hydroxysteroid dehydrogenase; SHBG, sex hormone-binding globulin or albumin. Green dashed arrows indicate freely diffusion across membranes.

Because of the role of estrogens in breast cancer etiology, information about their circulating levels has important relevance. Accordingly, quantification methods such as immunoassay have been applied. Nevertheless, this method suffers poor specificity and accuracy due to cross-reactivity and variation batch-to-batch of the antibodies, causing misinterpretations in epidemiologic studies (summarized in Wang et al., 2016). Therefore, analytical methods such as liquid and gas chromatography (LC and GC, respectively) coupled to mass spectrometry (MS), have become a golden tool (summarized in Denver et al., 2019a, Poschner et al., 2017).

Circulating levels reported for E1 and E2 range from tens to hundreds of fmol/mL. However, due to the declined activity of the ovaries during the menopause, these circulating levels differ between pre- and postmenopausal women (Table 1).

Table 1: Reported plasma/serum levels of E1 and E2 in pre- and postmenopausal women. The sources for this overview correspond to studies in plasma/serum samples from pre- and postmenopausal healthy women and using GC or LC as quantification techniques. Data from studies including both women with endometrial cancer (+) and healthy women as control matches, were summarized only for the healthy cohort. FP, follicular phase; LP, luteal phase; (P), plasma; *median; **mean; ***geometric mean; †range; ? healthy status not clearly specified.

Study population	fmol/mL		Analytical method	Reference
	E1	E2		
Premenopausal healthy women (*n*=20)	119	181	LC-MS	Coburn et al. (2019)***
Postmenopausal healthy women (*n*=26)	41	14		
Postmenopausal healthy women (*n*=110)	68	12	GC-MS	Audet-Delage et al. (2018)* +
Premenopausal women (*n*=27)	133-473	191-720	LC-MS	Faqehi et al. (2016)† (P) ?
Postmenopausal women (*n*=20)	22-78	29-51		

Premenopausal healthy women (n=10)	178	139	GC-MS	Caron et al. (2015)**
Postmenopausal healthy women (*n*=20)	125	31		
Postmenopausal healthy women (*n*=110)	68	12	LC-MS	Audet-Walsh et al. (2011)*+
Premenopausal healthy women (*n*=29)	372 in the early FP	203 in the early FP	LC-MS	Rothman et al. (2011)**
Postmenopausal healthy women (*n*=19)	138	11		
Postmenopausal healthy women (*n*=110)	78	22	GC-MS	Lepine et al. (2010)**+
Premenopausal healthy women (*n*=19)	142 (FP); 280 (LP)	141 (FP); 381 (LP)	GC-MS	Caron et al. (2009)**
Postmenopausal healthy women (*n*=10)	120	24		
Premenopausal healthy women (*n*=4)	186 (FP); 199 (LP)	235 (FP); 267 (LP)	LC-MS	Xu et al. (2007)**
Postmenopausal healthy women (*n*=2)	121	55		

1.2. Estrogen metabolic pathways and circulating levels

At the beginning of their metabolic pathway, E1 and E2 interconvert into each other through the action of the 17β-HSDs. Furthermore, E1 and E2 undergo oxidative metabolism (phase I) and conjugative metabolism (phase II) which includes (i) oxidation to hydroxylated derivates by cytochrome P450 monooxygenases (CYPs), (ii) methylation by catechol-*O*-methyltransferase (COMT), (iii) sulfonation by sulfotransferases (SULTs) and (iv) glucuronidation by uridine 5'-diphospho-glucuronosyltransferases (UGTs) (summarized in Blair, 2010, summarized in Guillemette et al., 2004) (Figure 2).

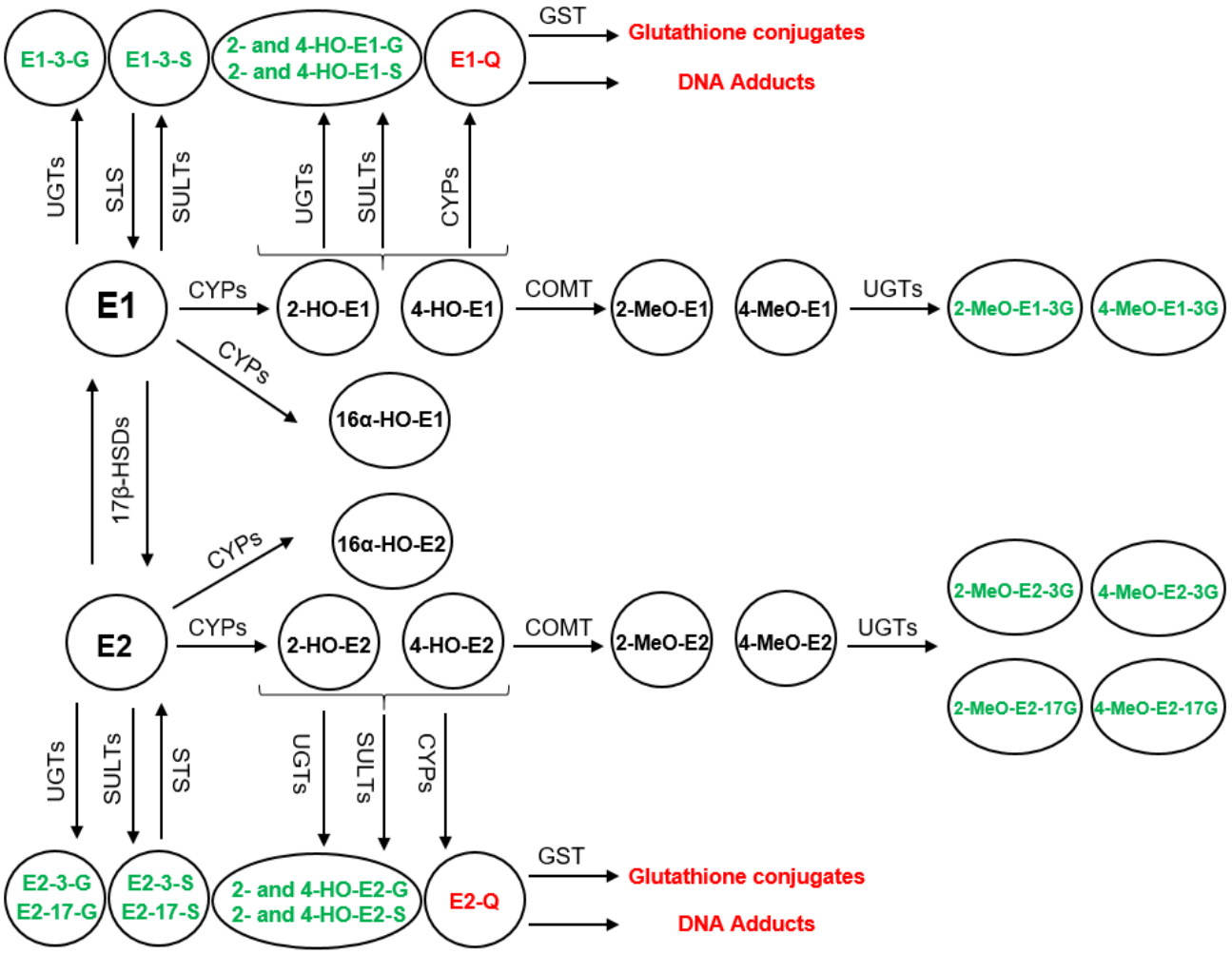

Figure 2: (Biotrans)formation pathways (partial) of estrogens (detoxifying metabolites in green and genotoxic metabolites in red). E1 and E2 interconvert into each other by 17β-HSDs and are conjugated to sulfates (-S) by SULTs, which can be hydrolyzed back to their corresponding parent estrogen by STS. Moreover, E1 and E2 are conjugated to glucuronides (-G) by UGTs or oxidized by a set of CYPs to 2- and 4-hydroxyestrogens. Hydroxyestrogens are sulfonated by SULTs, glucuronidated by UGTs, conjugated to glutathione by GST or methoxylated by the COMT to 2- and 4-methoxyestrogens. Furthermore, UGTs can glucuronidate the methoxyestrogens to methoxyestrogen glucuronides. The metabolites included in this figure are those subjected to analysis in the present investigation, excluding the genotoxic metabolites (red) and the hydroxyestrogen conjugates. 17β-HSDs, 17β-hydroxysteroid dehydrogenase; STS, steroid sulfatase; UGTs Uridine 5'-diphospho-glucuronosyltransferases; CYPs, cytochrome P450 monooxygenases; SULTs, sulfotransferases; GST, glutathione-s-transferase; COMT, catechol-*O*-methyltransferase.

1.2.1. Hydroxylation

E1 and E2 are hydroxylated at positions C2, C4 and C16 in a pathway catalyzed by CYP isoforms to produce 2- and 4-hydroxyestrone (2-OH-E1 and 4-OH-E1), 2- and 4-hydroxyestradiol (2-OH-E2 and 4-OH-E2), and 16α-hydroxyestrone/estradiol (16-α-OH-E1/E2) (Lepine et al., 2010, summarized in Samavat and Kurzer, 2015).

Several CYP isoforms responsible for catalyzing the formation of these oxidative metabolites are expressed in extrahepatic tissues such as the breast (summarized in Blair, 2010, Lee et al., 2003). The CYP isoforms 1A1, 1A2 and 3A4 catalyze the hydroxylation of both E2 and E1 to 2-OH-E1/E2 or 4-OH-E1/E2, whereas CYP1B1 can hydroxylate E2 and E1 at position 4 (summarized in Blair, 2010) and the CYP isoforms 3A5, 3A7, and 2C8 catalyze the hydroxylation of E1 and E2 at position 16 (Lee et al., 2003, summarized in Rizner, 2013). However, hydroxylation at position 2 has been related as quantitatively the predominant one, followed by position 4 (Lee et al., 2003), which is associated with greater carcinogenic potential (summarized in Cavalieri and Rogan, 2011).

Both E1 and E2 hydroxylated derivates are further involved in a metabolic redox cycle generating reactive quinones, semiquinones and free radicals, directly linked with DNA damage and subsequent carcinogenesis activity (summarized in Rizner, 2013, Zhang et al., 2007).

The analysis of circulating levels of hydroxyestrogens has been a challenge due to: (1) short half-lives (substrates for the COMT, Chapter 1.2.2), (2) temperature-liable nature and (3) low concentrations (Denver et al., 2019b). Yet, even the most recent studies using reliable analytical techniques such as GC-MS or LC-MS reported circulating levels of hydroxyestrogens only as of the sum of conjugated and unconjugated forms after enzymatic hydrolysis, and in the order from tens to hundreds of fmol/mL, with lower levels in post- than in premenopausal women (Table 2). In studies determining the combined concentrations of conjugated and unconjugated forms of hydroxyestrogens after enzymatic hydrolysis with β-glucuronidase, levels of unconjugated hydroxyestrogens were not detected without hydrolysis (Xu et al., 2007).

Table 2: Reported serum levels of hydroxyestrogens in pre- and postmenopausal women. The sources for this overview correspond to studies in serum samples from pre- and postmenopausal healthy women using LC as the quantification technique and reporting the ¥sum of conjugated and unconjugated forms after enzymatic hydrolysis (studies reporting levels of hydroxyestrogens without hydrolysis were not identified). Data from studies including women with breast (++) or endometrial cancer (+) and healthy women as control matches, were summarized only for the healthy cohort. FP, follicular phase; LP, luteal phase; NA, not available; ND, not detected; X, not analyzed; *median; **mean; ***geometric mean.

Study population	fmol/mL					Analytical method	Reference
	2-HO-E1	2-HO-E2	4-HO-E1	4-HO-E2	16α-HO-E1		
Premenopausal healthy women (*n*=20)	228	69	17	ND	112	LC-MS	Coburn et al. (2019) ¥***
Postmenopausal healthy women (*n*=26)	67	35	7	ND	39		
Postmenopausal healthy women (*n*=110)	NA	X	X	X	X	LC-MS	Audet-Delage et al. (2018) ¥*+
Postmenopausal healthy women (*n*=423)	69	36	22	ND	39	LC-MS	Fuhrman et al. (2012) ¥*++
Premenopausal healthy women (*n*=2)	1251 (LP); 1046 (FP)	140 (LP); 96 (FP)	168 (LP); 163 (FP)	X	52 (LP); 97 (FP)	LC-MS	Xu et al. (2007) ¥**
Postmenopausal healthy women (*n*=2)	253	38	40	X	31		

1.2.2. Methylation

Detoxification of hydroxyestrogens occurs by COMT-mediated metabolism which catalyzes their methylation to form 4 different methoxyestrogens, namely 2- and 4-methoxyestrone (2-MeO-E1 and 4-MeO-E1) and 2- and 4-methoxyestradiol (2-MeO-E2 and 4-MeO-E2) (summarized in Blair, 2010). COMT is mainly located at the cytosolic fraction of liver cells and other organs such as the breast (summarized in Yager, 2012) and catalyzes in higher proportion the formation of 2-methoxyestrogens than 4-methoxyestrogens (summarized in Guillemette et al., 2004).

The methylation pathway is considered the most important and quantitatively the most active for hydroxyestrogens since COMT prevents their biotransformation into reactive glutathione conjugates and DNA adducts (summarized in Rizner, 2013).

Same as for the hydroxylated metabolites, the analysis of methoxyestrogens has been a challenge due to the low amount of circulating levels and the lack of sensitive techniques (Rangiah et al., 2011). Serum levels of 2-MeO-E1 and 2-MeO-E2 are reported as their free forms, meanwhile, levels of 4-MeO-E1 and 4-MeO-E2 are reported as the sum of conjugated and unconjugated forms, both cases in the order of tens of fmol/mL, with lower levels in post- than in premenopausal women (Table 3). In studies determining the combined concentrations of conjugated and unconjugated forms of methoxyestrogens after enzymatic hydrolysis with β-glucuronidase, levels of unconjugated 4-MeO-E1 and 4-MeO-E2 were not detected without hydrolysis (Xu et al., 2007).

Table 3: Reported serum levels of methoxyestrogens in pre- and postmenopausal women. The sources for this overview correspond to studies in serum samples from pre- and postmenopausal healthy women using LC as the quantification technique (reported levels of 2- and 4-methoxyestrogens correspond to the ¥sum of conjugated and unconjugated forms after enzymatic hydrolysis). Data from studies including both women with breast cancer (++) and healthy women as control matches, were summarized only for the healthy cohort. FP, follicular phase; LP, luteal phase; (BLQ) below the limit of quantification; ND, not detected; *median; **mean; ***geometric mean.

Study population	fmol/mL				Analytical method	Reference
	2-MeO-E1	2-MeO-E2	4-MeO-E1	4-MeO-E2		
Premenopausal healthy women (*n*=20)	47	20	7¥	2¥	LC-MS	Coburn et al. (2019)***
Postmenopausal healthy women (*n*=26)	12	13	3¥	1¥		
Postmenopausal healthy women (*n*=215)	15	2	4¥	2¥	LC-MS	Falk et al. (2013)*++
Postmenopausal healthy women (*n*=423)	7	5	3¥	3¥	LC-MS	Fuhrman et al. (2012)*++
Premenopausal healthy women (*n*=4)	51 (LP); 58 (FP)	13 (LP) (BLQ); 16 (FP) (BLQ)	ND	ND	LC-MS	Xu et al. (2007)**
Postmenopausal healthy women (*n*=2)	13	4 (BLQ)	ND	ND		

1.2.3. Sulfonation

The conjugation of estrogens to sulfates is catalyzed by members of the superfamily of SULTs, which count for at least 11 isoforms (summarized in Coughtrie, 2016). Conjugation of E1 and E2 into sulfates has been recognized as one of the major routes of inactivation since sulfates are not ligands for estrogen receptor (ER) (summarized in Raftogianis et al., 2000).

E1 is metabolized to estrone-3-sulfate (E1-S) at high concentrations by SULT1A1 and at low concentrations by SULT1E1 (summarized in Blair, 2010). While E1 diffuses through plasma membranes, E1-S needs protein transporters for intracellular import and efflux such as the Organic anion-transporting polypeptides (OATPs) and the Breast cancer resistance protein (BCRP) (Jarvinen et al., 2018, Pizzagalli et al., 2003). E1-S is the most abundant estrogen conjugate in circulation in comparison with all other estrogen sulfates and glucuronides (summarized in Raftogianis et al., 2000), and present in 10 to 50-fold higher concentrations than E1 and E2, respectively (Audet-Delage et al., 2018, Pasqualini et al., 1989). However, E1-S is hydrolyzed back to its precursor E1 by the Steroid sulfatase (STS) (summarized in Coughtrie, 2016). Therefore, circulating E1-S is considered a reservoir of E1 and indirectly of E2 (summarized in Blair, 2010).

On the other hand, E2 is metabolized to 17β-estradiol-3-sulfate (E2-3-S) by SULT1A1, SULT1E1, and SULT2A1 (summarized in Blair, 2010) and in a minor proportion to 17β-estradiol-17-sulfate (E2-17-S) by SULT2A1 (Wang and James, 2005). E2-3-S is hydrolyzed back to its precursor E2 by STS, therefore, this conjugate is also considered a reservoir of E2 during the menopause (summarized in Blair, 2010).

The high circulating levels of E1-S allowed its study for many decades. However, traditional analytical approaches such as immunoassay carry serious limitations including enzymatic or chemical hydrolysis which are unable to differentiate between sulfates and glucuronides. Therefore, those techniques have been replaced with more accurate and sensitive methods such as LC-MS (Corona et al., 2010). Using the last-mentioned technique, circulating levels reported for E1-S ranged from hundreds to thousands of fmol/mL, with higher levels in pre- than in postmenopausal women (Table 4).

Table 4: Reported serum levels of estrogen sulfates in pre- and postmenopausal women. The sources for this overview correspond to studies in serum samples from pre- and postmenopausal healthy women using LC as the quantification technique (without enzymatic hydrolysis). Data from studies including both women with endometrial cancer (+) and healthy women as control matches, were summarized only for the healthy cohort. FP, follicular phase; LP, luteal phase; OVX, ovariectomized; X, not analyzed; *median; **mean.

Study population	fmol/mL			Analytical method	Reference
	E1-S	E2-3-S	E2-17-S		
Postmenopausal healthy women (*n*=110)	485	X	X	LC-MS	Audet-Delage et al. (2018)*+
Postmenopausal healthy women (*n*=110)	485	X	X	LC-MS	Audet-Walsh et al. (2011)*+
Premenopausal healthy women (*n*=47)	2483	X	X	LC-MS	Labrie et al. (2011)**
Postmenopausal healthy women not OVX (*n*=442)	428	X	X		
Premenopausal healthy women (*n*=47)	4891	X	X	LC-MS	Corona et al. (2010)**
Postmenopausal healthy women (*n*=442)	1164	X	X		
Postmenopausal healthy women (*n*=110)	713	X	X	LC-MS	Lepine et al. (2010)**+

Premenopausal healthy women (*n*=19)	1826 (FP); 5479 (LP)	X	X	LC-MS	Caron et al. (2009)**
Postmenopausal healthy women (*n*=10)	1256	X	X		

1.2.4. Glucuronidation

Together with sulfonation, glucuronidation has been recognized as a major conjugative pathway of estrogens (summarized in Raftogianis et al., 2000). This conjugation is catalyzed by UGTs by transferring the glucuronide moiety from the uridine 5'-diphospoglucuronic acid (UDPGA) to a nucleophilic group of the substrate (Kallionpaa et al., 2015, summarized in Raftogianis et al., 2000).

Glucuronidation plays a pivotal role as a detoxifying process through the biotransformation of the estrogens into conjugates devoid of biological activity, thus, controlling their tissular concentrations (summarized in Yang et al., 2017). Hence, a dysregulation pattern of the UGTs is considered a critical factor to induce the risk of breast cancer development (Zhou et al., 2017).

Four different UGT families, UGT1, UGT2, UGT3, and UGT8 have been observed in humans (summarized in Yang et al., 2017) in the endoplasmic reticulum, and mostly expressed in the liver. However, other estrogen-sensitive organs such as the endometrium and the breast express considerable amounts of these enzymes (summarized in Guillemette et al., 2004, Kallionpaa et al., 2015, Lepine et al., 2004).

Experiments *in vitro* conducted by Lepine et al. (2004) concluded that besides E1, E2, and their hydroxylated metabolites, methoxyestrogens are also subjected to glucuronidation by UGTs, highlighting the possibility and importance to determine their presence in circulation. Yet, conjugation by glucuronidation depends on the specificity and regioselectivity of UGTs. In the cited study, using microsomal fractions from UGT1A- and UGT2B-HK293 cells and commercial UGT1A10, preference of these enzymes to perform the glucuronidation of E2 at position -3 over the -17 was

evidenced, whereas no hydroxylated or methoxylated derivate of E2 was conjugated at position -17 (Table 5), indicating differences in the amounts of the reaction products.

However, it is important to note that glucuronide conjugates could be hydrolyzed back to their parent form when they reach contact with intestinal microflora, which produces a large variety and amounts of glucuronidases (summarized in Yang et al., 2017).

Additionally, whereas E1 and E2 diffuse freely through the membranes, their negatively charged glucuronides require import protein transporters such as OATPs (summarized in Obaidat et al., 2012), and efflux protein transporters such as the multidrug resistance-associated protein and BCRP (Jarvinen et al., 2018). For example, Obaidat et al. (2012) determined that at least 4 OATPs isoforms can transport E2-17-G. Furthermore, in experiments conducted by Jarvinen et al. (2018), BCRP exhibited the highest transport rates for E1-G and E2-3-G. Nevertheless, to date, no protein transporters have been studied for hydroxy- or methoxyestrogen glucuronides.

Table 5: Conjugation of E1, E2 and their metabolites by UGT isoenzymes. X, conjugated; -, not conjugated; ?, no data available.

UGT	Substrate																		References
	E1	E2		2-HO					4-HO					2-MeO			4-MeO		
	3G	3G	17G	E1		E2			E1		E2			E1	E2		E1	E2	
				2G	3G	2G	3G	17G	3G	4G	3G	4G	17G	3G	3G	17G	3G	3G	17G
1A1	X	X	-	-	X	-	X	?	X	X	X	X	?	X	X	?	X	X	?	summarized in Guillemette et al. (2004), Lepine et al. (2010)
1A3	X	X	X	X	X	-	X	?	X	X	X	-	?	X	X	?	X	X	?	
1A4	-	-	-	-	-	-	-	?	-	-	-	-	?	-	-	?	-	-	?	
1A5	-	-	-	-	-	-	-	?	-	-	-	-	?	-	-	?	-	-	?	
1A6	-	-	-	-	-	-	-	?	-	-	-	-	?	-	-	?	-	-	?	
1A7	-	-	-	-	-	-	-	?	-	-	-	-	?	-	-	?	-	-	?	
1A8	X	X	-	X	X	X	X	?	X	X	X	X	?	X	X	?	X	X	?	
1A9	X	-	-	X	X	X	X	?	X	X	-	X	?	X	X	?	X	X	?	
1A10	X	X	-	-	-	-	-	?	-	-	-	X	?	X	X	?	X	X	?	
2B4	-	-	-	-	X	-	-	?	-	-	-	X	?	X	X	?	-	-	?	
2B7	-	-	X	-	X	-	X	?	-	X	-	X	?	-	-	?	-	-	?	
2B10	-	-	-	-	-	-	-	?	-	-	-	-	?	-	-	?	-	-	?	
2B11	-	-	-	-	-	-	-	?	-	-	-	-	?	-	-	?	-	-	?	
2B15	-	-	-	-	-	-	-	?	-	-	-	-	?	-	-	?	-	-	?	
2B17	-	-	-	-	-	-	-	?	-	-	-	-	?	-	X	?	-	-	?	
2B28	-	-	-	-	-	-	-	?	-	-	-	-	?	-	-	?	-	-	?	

In the last decade, the direct determination of circulating estrogen glucuronides by LC-MS has been useful to avoid hydrolysis and derivatization steps (Zhao et al., 2014). Using the mentioned technique, reported levels of circulating estrogen glucuronides are in the order of tens to hundreds of fmol/mL (Table 6).

Table 6: Reported serum levels of estrogen glucuronides in pre- and postmenopausal women. The sources for this overview correspond to studies in serum samples from pre- and postmenopausal healthy women using LC as the quantification technique. Data from studies including both women with endometrial cancer (+) and healthy women as control matches, were summarized only for the healthy cohort. FP, follicular phase; LP, luteal phase; (BLQ) below the limit of quantification; X, not analyzed; ND, not detected; *median; **mean.

Study population	fmol/mL			Analytical method	Reference
	E1-G	E2-3-G	E2-17-G		
Postmenopausal healthy women (*n*=110)	51	BLOQ (11 fmoL/mL)	X	LC-MS	Audet-Walsh et al. (2011)*+
Premenopausal healthy women (n=19)	121 (FP); 316 (LP)	23 (FP); 74 (LP)	ND	LC-MS	Caron et al. (2009)**
Postmenopausal healthy women (*n*=10)	69	19	ND		

Analysis of methoxyestrogen glucuronides

Investigations conducted by Caron et al. (2009) determined levels of 2-methoxyestrone-3-glucuronide (2-MeO-E1-G) and 2-methoxyestradiol-3-glucuronide (2-MeO-E2-3-G) in serum from premenopausal (*n* = 19) and postmenopausal (*n* = 10)

healthy women using LC-MS. In this study, median levels of 2-MeO-E1-G were 16 fmol/mL and 45 fmol/mL in premenopausal women in their follicular and luteal phase, respectively (detected in 71% of the samples), and 13 fmol/mL in postmenopausal women (detected in 50% of the samples). Moreover, levels of 2-MeO-E2-3-G were 6 fmol/mL and 7 fmol/mL in premenopausal women in their follicular and luteal phases, respectively (detected in 13% of the samples), and 14 fmol/mL in postmenopausal women (detected in 70% of the samples). Nevertheless, those levels of 2-MeO-E2-3-G in serum from premenopausal women were below the limit of quantification of 10 fmol/mL. Additionally, the same research group of the mentioned study reported median levels of 5 fmol/mL of both 2-MeO-E1-G and 2-MeO-E2-3-G in serum from postmenopausal healthy women (*n* = 110), which are below the LOQ of 10 fmol/mL (Audet-Walsh et al., 2011).

Nevertheless, concerning the analysis of circulating levels of 4-methoxyestrone-3-glucuronide (4-MeO-E1-G), 2-methoxyestradiol-17-glucuronide (2-MeO-E2-17-G), 4-methoxyestradiol-3-glucuronide (4-MeO-E2-3-G) and 4-methoxyestradiol-17-glucuronide (4-MeO-E2-17-G), no previous studies have been reported.

1.3. Correlation between circulating levels of estrone, 17β-estradiol, and their metabolites

Investigations performed by Caron et al. (2009) determined positive correlations between levels of E1, E2 and their conjugates in serum samples from premenopausal healthy women (*n* = 19) in their follicular (F) and luteal (L) phase. In this study, E2 correlated positively with E1-G (*r* = 0.58 F, *r* = 0.50 L) and E1 correlated positively with E1-G (*r* = 0.58 F, *r* = 0.56 L) and with 2-MeO-E1-G (*r* = 0.26 F, *r* = 0.36 L). Furthermore, E1-S correlated positively with E1-G (*r* = 0.46 F, *r* = 0.71 L) and with 2-MeO-E1-G (*r* = 0.22 F, *r* = 0.59 L). These observations suggest a link between E1, E2 and their conjugates before the menopause.

In serum from postmenopausal healthy women, investigations performed by Audet-Walsh et al. (2011) (*n* = 110) suggested positive correlations between levels of E1 and E2 (*r* = 0.88), E1-S (*r* = 0.59) and E1-G (*r* = 0.54), also between E2 and E1-S (0.54) and E1-G (*r* = 0.47) as well as between E1-S and E1-G (0.48). Moreover, investigations

conducted by Labrie et al. (2011), found significant positive correlations between serum levels of E1 and E2 (r = 0.80), E1 and E1-S (r = 0.62), and E2 and E2-S (r = 0.59) in serum from postmenopausal non-ovariectomized women (n = 442). These correlations may also suggest a link between E1, E2 and their conjugates, extended until the menopause.

1.4. Methoxyestrogen glucuronides in human breast tissue

The expression of diverse UGT isoforms (Table 7), as well as detected levels of 2-MeO-E1 in normal human breast tissue, have been previously reported (Pemp et al., 2019). These findings support the presence of the necessary machinery for the biosynthesis of methoxyestrogen glucuronides in the mammary gland. Nevertheless, to date, no studies about levels of methoxyestrogen glucuronides in human breast tissue specimens have been reported.

Table 7: UGT isoenzymes detected in normal human breast tissue.

Isoenzyme	References
UGT1A1 UGT1A3 UGT1A8 UGT1A9 UGT1A10 UGT2B7	Chouinard et al. (2006), Gestl et al. (2002), summarized in Guillemette et al. (2004), Starlard-Davenport et al. (2008), summarized in Tukey and Strassburg (2000)

2. Objectives

Estrogens, namely 17β-estradiol and estrone, are considered to play an important role in breast cancer initiation and promotion through the metabolism to quinone derivatives able to react with the DNA and the estrogen receptor-mediated stimulation of breast cell proliferation. As a detoxifying mechanism, estrone, 17β-estradiol, and their metabolites are reversibly conjugated into sulfates and glucuronides devoid of biological activity. Thus, circulating estrogen profiles in women without breast cancer may provide insights into breast cancer etiology.

In previous investigations conducted in our research group using a validated method for human plasma, levels of estrone, 17β-estradiol, and 2-methoxyestrone were determined by means of GC-tandem mass spectrometry, and levels of estrone-3-sulfate, 17β-estradiol-3-sulfate and estrone-3-glucuronide were determined by means of UHPLC-tandem mass spectrometry. Moreover, since different methoxylated derivates from estrone and 17β-estradiol are subjected to glucuronidation *in vitro* by various human uridine 5'-diphospho-glucuronosyltransferase isoenzymes, methoxyestrogen glucuronides might also occur in human plasma and/or tissues.

Therefore, this work aims to evaluate the possibility to include methoxyestrogen glucuronides into the existing method for the analysis of estrogens, and therewith, complement the analysis of estrogens profile in human plasma and breast tissue.

Since methoxyestrogen glucuronides and their corresponding deuterium-labeled analogues are not commercially available, their biosynthesis, extraction, identification, and quantification will be first conducted.

After the biosynthesis of the references, the existing UHPLC-tandem mass spectrometry-based method for the analysis of estrogen conjugates will be extended by 2-methoxy-estrone-3-glucuronide, 4-methoxy-estrone-3-glucuronide, 2-methoxy-estradiol-3-glucuronide, 4-methoxy-estradiol-3-glucuronide, 2-methoxy-estradiol-17-glucuronide, and 4-methoxy-estradiol-17-glucuronide. First, the substance-dependent and source-dependent parameters for mass spectrometric detection will be determined and the chromatographic resolution of the analytes will be optimized. Afterward, the specificity and selectivity, the analytical response of references, the limit of detection and limit of quantification, accuracy, precision, recovery, and stability will be determined with respect to the newly included analytes.

The extended UHPLC-tandem mass spectrometry-based method will be applied to the analysis of estrone-3-sulfate, estradiol-3/17-sulfate, estrone-3-glucuronide, 17β-estradiol-3-glucuronide and six different methoxyestrogen glucuronides in human plasma. Levels of estrone, 17β-estradiol, and their hydroxylated and methoxylated metabolites will be analyzed by an existing GC-tandem mass spectrometry-based method for human plasma. With the levels obtained, the profiles of metabolites will be discussed for the study population of pre- and postmenopausal women and compared with the current literature.

Finally, the applicability of the extended method for the analysis of methoxyestrogen glucuronides in human breast glandular and adipose tissue specimens derived from women without breast cancer will be evaluated.

3. Materials and methods

3.1. Materials

3.1.1. Equipment

Equipment	Name (Provider)
Analytic balance	Mettler Toledo AT21 comparator (Mettler Waagen GmbH, Switzerland)
Balance	Mettler Toledo AE 240 (Mettler Waagen GmbH, Switzerland)
	VWR LA21 4i (VWR International GmbH, Darmstadt, Germany)
Bio freezer	Ultra-freezer UF 755G (B Medical Systems S.àr.l., Hosingen, Luxemburg)
Centrifuges	Hettich EBA 12 (Andreas Hettich GmbH & Co. KG, Tuttlingen, Germany)
	Hettich Mikro 12-24, Typ 2070 (Andreas Hettich GmbH & Co. KG, Tuttlingen, Germany)
	Thermo Scientific Heraus™ Fresco™ 21 microcentrifuge (Thermo Electron LED GmbH LR 56495 D-37520, Osterode, Germany)
Electrode	Blueline 14 pH (Xylem Analytics Germany Sales GmbH & Co. KG – SI Analytics, Mainz, Germany)

Evaporator	Christ Evaporator RVC 2-25 CD plus with Cold Trap CT 04-50 SR (Martin Christ Freeze-drying devices GmbH, Osterode am Harz, Germany) with Membrane Pump MZ 2C (Vacuubrand GmbH + Co. KG, Wertheim, Germany)
Freeze dryer	Christ Alpha 1-4 LSC, (Martin Christ Freeze-drying devices GmbH, Osterode am Harz, Germany) with hybrid vacuum pump RC 6 (Vacuubrand GmbH + Co. KG, Wertheim, Germany)
GC-MS/MS	Varian Gas Chromatograph System 450-GC with Varian CP-8400 Autosampler and Varian 300-MS Triple Quad Mass spectrometer (Bruker Daltonik GmbH, Bremen, Germany)
HPLC	Agilent Technologies Series 1200 HPLC-System (Agilent Technologies, Waldbronn, Germany) -G1311A Quaternary pump -G1314B variable wavelength detector (VWD) -G1316A Column oven TCC -G1322A Degasser -G1329A Autosampler ALS -ChemStation software
HPLC Column	Luna C18 (2) RP-HPLC 250 x 4,6 mm, 5 µm Particle seize (Phenomenex, Aschaffenburg, Germany)

Magnetic and heating stirrer	IKA® RCT basic (IKA®-Werke GmbH & Co. KG, Staufen, Germany)
Millipore system	Water purification system Mili-Q® synthesis A10 and Quantum EX polishing cartridge with Millipak® end filter (Merck KGaA, Darmstadt, Germany)
Mixer	Multi Bio RS-24 (PeqLab Biotechnologie GmbH, Erlangen, Germany)
pH meter	inoLabR pH 720 (WTW, Weilheim, Germany)
Pipettes	Piston pipettes: 2-20µL, RAININ LTS Pipet-Lite L-20, (Mettler-Toledo, Oakland, US) 20-200 µL, Abimed discovery comfort, single-channel pipette (Kinesis GmbH, Langenfeld, Germany) 5-50 µL, 50-200 µL, Rotilabo®-micropipette Proline®, variable, (Carl Roth, Karlsruhe, Germany) 100-1000 µL, Eppendorf Research®, single-channel pipette (Eppendorf AG, Hamburg, Germany) Positive displacement pipettes: MICROMAN® (Gilson Inc., Middelton, USA) 10-100 µL, M100 50-250 µL, M250 100-1000 µL, M1000

	Multi dispenser: Multipette® plus (Eppendorf AG, Hamburg, Germany)
QTrap 5500 Mass spectrometer (ESI system)	QTrap 5500 LC-MS/MS system with Turbo V™ Ion Source and TurboIonSpray® Probe (ABSciex GmbH, Darmstadt; Germany) with Nitrogen generator NGM11-S (CMC Instruments GmbH, Eschborn, Germany)
Rotation shaker	Multi Bio RS-24 (Part No.: 320901006, PEQLAB Biotechnologie GmbH)
Solid-phase extraction (SPE) device	Chromabond® Vacuum chamber for 16 columns (Macherey-Nagel GmbH & Co, KG, Düren) with Vacuum pump PC 2004 VARIO (Vacuubrand GmbH + Co KG, Wertheim)
UHPLC System	Shimadzu Nexera X2 UHPLC-System (Shimadzu GmbH, Duisburg, Germany) -CBM-20A Communication Bus Module -CTO-30A Column oven -DGU-20A 5R Degasser -LC-30AD liquid chromatograph -SIL-20AC Autosampler
UHPLC Column	Gemini C18 50 x 2.0 mm, 3 µM particle size (Phenomenex, Aschaffenburg, Germany)
Ultrasonic bath	SONOREX SUPER RK100 (BANDELIN electronic GmbH & Co, Berlin, Germany)
Vortex	Vortex GLW L46 (A. Hartenstein, Laborbedarf GmbH, Würzburg, Germany

Water bath	Julabo, Typ SW 22 (Julabo Labortechnik GmbH, Seelbach, Germany)

3.1.2. Laboratory consumables

Laboratory consumable	**Name (Provider)**
Beakers with drain	100-500-600 mL (VWR International, Darmstadt, Germany)
Centrifuge tubes	15 mL conical centrifuge tubes (Sarstedt AG & Co. KG, Nümbrecht, Germany) 50 mL conical centrifuge tubes (Sarstedt AG & Co. KG, Nümbrecht, Germany)
Chromatography consumables	Vials: Screw-top vial 1.5 mL, 12x32 mm, brown, 8-425 (451101211, Klaus Trott, Chromatography accessories, Kriftel, Germany) Inserts: µ-use, 5x30 mm, ca. 100 µL (conical), point 15 mm (501105021, Klaus Trott, Chromatography accessories, Kriftel, Germany) µ-use, 6x30 mm, ca. 300 µL (conical, hanging), point 12-13 mm (501106010, Klaus Trott, Chromatography accessories, Kriftel, Germany)

	Caps: Screwcap PP, 8-425, NK/TEF, red, 1.3 mm (3011S1015, Klaus Trott, Chromatography accessories, Kriftel, Germany) Snap-on Cap PE, transparent, NK/PTFE (2511C1020, Klaus Trott, Chromatography accessories, Kriftel, Germany) Bounce: Bounce 5x20 mm (501167012, Klaus Trott, Chromatography accessories, Kriftel, Germany)
Cryos	1.8 mL with screw cap (72.379, Sarstedt, Nümbrecht, Germany)
Disposable syringe	20 mL, TERUMO (Terumo Corporation, Tokyo, Japan)
Glass culture tubes	GL 18, 100x16 mm with screw cap (RG09, A. Hartestein, Laborbedarf GmbH, Würzburg, Germany)
Micro-reaction tubes	Micro-reaction tubes 1.5 and 2 mL (72.690.001 and 72.690.002, Sarstedt AG & Co, Nümbrecht, Germany) SafeSeal micro-reaction tubes 2mL, PP (Sarstedt AG & Co., Nümbrecht, Germany)
Parafilm	Parafilm M®, 4 IN. X 125 FT. Rolle (Pechiney plastic packaging, Menasha, USA)

Pasteur pipettes	Glass: 230 mm (VWR International GmbH, Darmstadt, Germany) Plastic: Pasteur pipette, 5 mL nonsterile, graduated up to 1 mL (612-1684, VWR International GmbH, Darmstadt, Germany)
Pipettes Tips	For piston pipettes: 0.1-20 µL, RAININ LTS Pipet-Lite, (VWR International, West Chester, US) 200 µL transparent (70.762.002, Sarstedt AG & Co, Nümbrecht, Germany) 1000 µL transparent (70.762, Sarstedt AG & Co, Nümbrecht, Germany) For positive displacement pipettes: Microman® Piston with capillaries (neoLab Migge Laboratory accessories GmbH, Heidelberg, Germany) 10-100 µL, CP 100 50-250 µL, CP 250 100-1000 µL, CP 1000 Multi dispenser: Eppendorf Biopur® 1 mL (Eppendorf AG, Hamburg, Germany)
Schott bottles	500-1000 mL Duran (Duran Group GmbH, Wertheim, Germany)

Spatula	18/8 Stainless steel, 2mm wide (Neolab Laboratory accessories GmbH, Heidelberg, Germany)
SPE cartridges	Supelclean™ LC-18 SPE Tubes, 3 mL (57012, SUPELCO, Bellefonte, USA)
Test tubes	250 mL, borosilicate glass, spout and hexagonal base (Brand GmbH & Co. KG, Wertheim, Germany)
	500 mL, borosilicate glass, spout and hexagonal base (LMS, Ilmenau, Germany)
Volumetric Flask	25 mL, transparent (Paul Marienfeld GmbH & Co. KG, Lauda-Königshofen, Germany)
	500 mL, transparent (Duran Group, Wertheim, Germany)

3.1.3. Chemicals

Chemical	**Name (Provider)**
Acetic acid	Concentrated, p.a., (1858, Facility of chemicals University of Würzburg, Germany)
Acetonitrile (ACN)	HPLC grade approx. 99.9% Gradient Grade, (20060.320, VWR Chemicals, Fontenay-sous-Bois, France)

	HiPerSolv® CHROMANORM® for LC-MS, ≥99.9% (83640.320,0 VWR Chemicals, Fontenay-sous-Bois, France)
Alamethicin	(UN3462, AppliChem GmbH, Darmstadt, Germany)
Ammonia (NH_3)	25%, (1146, Facility of chemicals University of Würzburg, Germany)
	LiChropur for LC-MS, 25%, (5.33003.0050, Merck, KGaA, Darmstadt, Germany)
Chloroform	For analysis, approx. 1% Ethanol (3221, Riedel-de Haën AG, Seelze, Germany)
Dichloromethane	(1593, Fisher Scientific UK Limited, Leicestershire, UK)
Dimethyl sulfoxide (DMSO)	≥99.9%, ACS, spectrophotometric grade, (154938, Sigma-Aldrich, St. Louis, USA)
1,4-Dithiothreitol (DTT)	≥ 99%, p.a., (6908.1, Carl Roth GmbH + Co. KG, Karlsruhe, Germany)
D-Saccharin acid 1,4-lactone monohydrate	Saccharolactone, (029K3776, Sigma-Aldrich, St. Louis, USA)
17β-Estradiol (E2)	Fountain Limited, Derbyshire, UK
E2-16,16,17-d3 (E2-d3)	98 Atom-% D (491187, Sigma-Aldrich Chemie GmbH, Steinheim, Germany)
E2-3-G	Acid-free (Steraloids Inc., Newport, RI, USA)

E2-17-G	Acid-free (Steraloids Inc., Newport, RI, USA)
E2-3-S	Sodium salt (Steraloids Inc., Newport, RI, US)
E2-3-S-2,4,16,16-d4 (E2-3-S-d4)	Sodium salt, 98 Atom-% D, stabilized with TRIS, 50% w/w (D-5287, C/D/N Isotopes Inc., Pointe-Claire, QC, Canada)
E2-17-S	Sodium salt, (Steraloids Inc., Newport, RI, US)
Estrone (E1)	Fountain Limited, Derbyshire, UK
E1-16,16-d2 (E1-d2)	(E889051, Toronto Research Chemicals, North York, ON, Canada)
E1-G	Acid-free (Steraloids Inc., Newport, RI, USA)
E1-G-2,4,16,16-d4 (E1-G-d4)	Biosynthesized in the research group
E1-S	Sodium salt, w/TRIS (Catalog ID: 1887-5, Research Plus Inc., New Jersey, USA)
E1-S-2,4,16,16-d4 (E1-3-S-d4)	Sodium salt, >98 Atom-% D, stabilized with TRIS, 50% w/w (D-5272, C/D/N Isotopes Inc., QC, Canada)
2-hydroxyestradiol-16,16,17-d3 (2-HO-E2-d3)	Biosynthesized in our research group
4-hydroxyestradiol-16,16,17-d3 (4-HO-E2-d3)	Biosynthesized in our research group

16α-hydroxyestradiol-2,4,17-d3 (16α -HO-E2-d3)	Biozol Diagnostica Vertrieb GmbH, Eching, Germany)
2-hydroxyestrone-1,4,16,16-d4 (2-HO-E1-d4)	> 98 Atom-% D (D-5806, C/D/N Isotopes Inc., Pointe-Claire, QC, Canada)
4-hydroxyestrone-1,2,16,16-d4 (4-HO-E1-d4)	> 99 Atom-% D (D-5807, C/D/N Isotopes Inc., Pointe-Claire, QC, Canada)
16α-hydroxyestrone-2,4,6,6,9-d5 (16α-HO-E1-d5)	(H941902, Toronto Research Chemicals, North York, ON, Canada)
Ethanol	96%, denatured, (Facility of chemicals University of Würzburg, Germany)
Ethyl acetate	CHROMASOLV® for HPLC, ≥99.7%, (34858-1L, Sigma-Aldrich, St. Louis, USA)
Formic acid (FA)	98-100% for Analysis, ACS, (05314.3010, Bernd Kraft, Duisburg, Germany) For mass spectrometry ~98% (94318-250ML-F, Sigma Aldrich Chemie GmbH, Steinheim, Germany)
Glucuronidase (bovine liver)	Type B-1 ≥100000 units/g solid (G0251-1MU, Sigma-Aldrich Chemie GmbH, Steinheim, Germany)
Glucuronidase (*Helix pomatia*)	Type HP-2 152900 units/mL (G7017-10ML, Sigma-Aldrich Chemie GmbH, Steinheim, Germany)
Glycine	Reagent Plus ≥99%, (G7126-100G, Sigma-Aldrich, St. Louis, USA)

Heptane	CHROMASOLV® LC-MS, ≥99% (34999-2.5L, Sigma-Aldrich Chemie GmbH, Steinheim, Germany)
Histopaque® 1077	100 mL (Merk KGAa, Darmstadt, Germany)
Hydrochloric acid (HCl)	37%, for analysis, ACS (05430.4100, Bernd Kraft, Duisburg, Germany)
L-Ascorbic acid	(07F040031, VWR International GmbH, Darmstadt, Germany)
Magnesium chloride - Hexahydrate ($MgCl_2$ *$6H_2O$)	(25108.295, VWR International GmbH, Darmstadt, Germany)
Methanol (MeOH)	HPLC approx. 99.9% Gradient Grade, (12490.4700, Bernd Kraft, Duisburg, Germany)
	HiPerSolv® CHROMANORM® for HPLC LC-MS, (83638.320, VWR Chemicals, Fontenay-sous-Bois, France)
2-methoxy-17ß-estradiol (2-MeO-E2)	Fountain Limited, Derbyshire, UK
4-methoxy-17ß-estradiol (4-MeO-E2)	Fountain Limited, Derbyshire, UK
2-methoxyestrone (2-MeO-E1)	Acid-free (Steraloids Inc., Newport, RI, USA)
4-methoxyestrone (4-MeO-E1)	Acid-free (Steraloids Inc., Newport, RI, USA)
N, O-Bis (trimethylsilyl) trifluoroacetamide with 1% Trimethylchlorosilane (BSTFA)	≥ 98.5%, without Trimethylchlorosilane (15238-25ML, Sigma Aldrich Chemie GmbH, Steinheim, Germany)

Potassium chloride (KCl)	> 99.5%, p.a. ACS. ISO (6781.1, Carl Roth GmbH, Germany)
Potassium hydrogen phosphate (K_2HPO_4)	≥ 99%, p.a., water-free, (P749.1, Carl Roth, Karlsruhe, Germany)
Potassium dihydrogen phosphate (KH_2PO_4)	≥ 99%, p.a., ASC, (3904.1, Carl Roth, Karlsruhe, Germany)
2-Propanol	HiPerSolv® CHROMANORM® for HPLC (20880.320, VWR International, Fontenay-sous-Bois, France)
S-Adenosylmethionine (SAM)	(A9384, Sigma-Aldrich, St. Louis, USA)
Sodium bicarbonate (NaHCO3)	(S57611KG, Sigma-Aldrich, St. Louis, USA)
Uridine 5'-diphospho-glucuronic acid tri-sodium salt	98-100%, (U675125MG, Sigma-Aldrich, St. Louis, USA)
Water	Millipore®-Water (internal device)
	HiPerSolv® CHROMANORM® for LC-MS, (83645.320, VWR Chemicals, Fontenay-sous-Bois, France)

3.1.4. Buffers and solutions

3.1.4.1. Buffers

Ammonium acetate buffer (25 mM, pH 9.2): 710 µL of acetic acid were dissolved in 500 mL of water LC-MS grade and 940 µL of NH_3 (25%, MS grade) were dissolved in another 500 mL of water LC-MS grade. The ammonia solution was placed in a Schott bottle and the pH adjusted until 9.2 with the acetic acid solution. The buffer was stored at 4 °C and used within a maximum period of 14 days.

Ammonium formiate buffer (AFB) (10 mM, pH 4.75): 385 µL of FA (~98%, MS grade) were dissolved in 1 L Millipore water and 622 µL of NH_3 (25%) were dissolved in another liter of Millipore water. The ammonia solution was placed in a Schott bottle and the pH adjusted until 4.75 with the FA solution. The buffer was stored at room temperature and the pH was checked regularly.

Enzyme-hydrolysis buffer: 2 mg L-ascorbic acid were placed in a 2 mL reaction tube and dissolved with 500 µL of sodium acetate buffer (see below). After, 50 µL of β-glucuronidase were added. This solution was prepared fresh for every use.

Glycine-HCl buffer (0.7 M, pH 1.2): 5.27 g of glycine were dissolved in 70 mL of Millipore water and the pH adjusted until 1.2 with concentrated HCl. After, the solution was completed until 100 mL in a volumetric flask and stored at 4 °C.

Krebs-Henseleit buffer: 2 g D-glucose, 0.141 g $MgSO_4$, 0.16 g KH_2PO_4, 0.35 g KCl, 6.9 g NaCl, 0.373 g $CaCl_2 * 2H_2O$ and 2.1 g $NaHCO_3$ were dissolved in 1 L of Millipore water and the pH is adjusted to 7.2 with HCl.

Potassium phosphate buffer (0.1 M, pH 7.4): 1.36 g of KH_2PO_4 were dissolved in 100 mL of Millipore water and 1.74 g of K_2HPO_4 were dissolved in another 100 mL of

Millipore water. The K_2HPO_4 solution was placed in a beaker and the pH adjusted until 7.4 with the KH_2PO_4 solution. The buffer was stored in a Schott bottle at 4 °C.

Sodium acetate buffer (0.15M, pH 4.1): 123.4 mg of sodium acetate were dissolved in 10 mL of Millipore water and 861 µL of acetic acid were dissolved with Millipore water until 100 mL in a volumetric flask. The ammonium solution was placed in a Schott bottle and the pH adjusted until 4.1 with the acetic solution. The buffer was stored Schott bottle at 4 °C.

3.1.4.2. Other solutions

Solutions for liquid-liquid extraction

DTT (20 mM): 77.125 mg of DTT were added to a 25 mL volumetric flask and dissolved in AFB. The solution was stored at room temperature.

AFB (10 mM, pH 4.75): See above (Chapter 3.1.4.1).

Solutions for solid-phase extraction

MeOH with 0.1% FA: 500 µL of FA were placed in a 500 mL volumetric flask with some mL of MeOH LC-MS grade. After, the solution was completed until volume with MeOH LC-MS grade. The solution was stored at room temperature.

MeOH (0.1% FA) / AFB 20:80 v/v: 100 mL of MeOH with 0.1% FA were mixed with 400 mL AFB. The solution was stored at room temperature.

MeOH (0.1% FA) / AFB 90:10 v/v: 450 mL of MeOH with 0.1% FA were mixed with 50 mL AFB. The solution was stored at room temperature.

Solutions for HPLC and UHPLC

Ammonium acetate buffer (25mM, pH 9.2): See above (Chapter 3.1.4.1).

MeOH/Water (pH 3.0 FA; 50:50 v/v): 500 mL of MeOH were mixed with 500 mL of water (pH 3.0 with FA). The same solution was also prepared with LC-MS grade water. The solutions were stored at room temperature.

MeOH/Water (pH 3.0 FA; 60:40 v/v): 600 mL of MeOH were mixed with 400 mL of water (pH 3.0 with FA). The solution was stored at room temperature.

Water (0.1% FA): 500 µL of FA were placed in a 500 mL volumetric flask with some mL of water LC-MS grade. After, the solution was completed until the volume with water LC-MS grade. The solution was stored at room temperature.

Water (pH 3.0 FA): Millipore water was acidified with FA until pH 3.0. The solution was stored at room temperature.

Further solutions

ACN (5%): 500 µL of ACN LC-MS grade were dissolved in 9.5 mL of water LC-MS grade. The solution was stored at room temperature.

Alamethicin (5% DMSO): In a micro-reaction tube, 190 µL of potassium phosphate buffer were placed and 10 µL of a solution 5 mg/mL of alamethicin in 100% DMSO were added. The solution was stored at -20 °C.

$MgCl_2$ (247 mM): 50.3 mg of $MgCl_2$ *6H2O were dissolved in 1 mL of Millipore water and stored at -20 °C.

$MgCl_2$ (40 mM): 81.3 mg of $MgCl_2$ *6H2O were dissolved in 10 mL of Millipore water and stored at -20 °C.

Saccharolactone (234 mM): 22.5 mg of Saccharolactone were dissolved in 500 µL of potassium phosphate buffer and stored at -20 °C.

SAM (2.5 mg/ mL): 3.0 mg of SAM were dissolved in 120.5 µL of DMSO and stored at -20 °C until a maximum period of 7 days.

UDPGA (10 mM): 25.8 mg of UDPGA were dissolved in 4 mL of potassium phosphate buffer and stored at -20 °C.

3.1.5. Biological material

Rat liver microsomes (RLM): Previously prepared and aliquoted in our research group, containing 23.2 mg/mL of protein.

Rat liver cytosol (RLC): Previously prepared and aliquoted in our research group, containing ~ 25 mg/mL of protein.

Human plasma: Plasma samples derived from the Isocross study were obtained from 21 women without breast cancer undergoing mammoplasty reduction for cosmetic reasons, which agreed to donate blood on the day of the surgery. After plasmas were processed, aliquots of approx. 1 mL were stored at -80 °C until use (Chapter 3.2.8.1).

Furthermore, 4 plasma samples from female donors were purchased from the Bayerisches Rotes Kreuz (BRK).

Human breast glandular and adipose tissue: Breast glandular (GLT) and adipose (ADT) tissues were obtained from women without breast cancer undergoing reduction mammoplasty for cosmetic reasons, which agreed to donate the tissue on the day of the surgery. The tissue was separated, classified and stored at -80 °C until use (Chapter 3.2.8.2).

3.1.6. Software

Software	**Version, Provider**
Agilent ChemStation	Rev B.03.02, Agilent Technologies, Waldbronn, Germany
Analyst®	Version 1.6.2; AB Sciex, Darmstadt, Germany.
ChemDraw Professional	Version 16.0, CambridgeSoft, Cambridge, USA
EndNote	Version X8.2 (Bld 11343), Clarivate Analytics, Philadelphia, USA
MS Data Review	6.9.2, Varian, California, USA
Origin Pro	Version 2018b, OriginLab Corporation, Northampton, MA 01060, USA
R Studio	Version 3.0.1, R Core Team (2013), R Foundation for Statistical Computing,

	Vienna, Austria. URL http://www.R-project.org/
Valoo	2.6, analytic-software, Leer, Germany, URL http:// www.analytiksoftware. de/
Varian MS workstation, MS Data Review	Version 6.9.2, Varian Inc., CA, USA

3.2. Methods

3.2.1. Analytical methods

3.2.1.1. HPLC-UV/Vis

Analytical system: Agilent Technologies Series 1200 HPLC with degasser, quaternary pump, autosampler and UV/Vis detector at 280 nm. Analysis performed with a Luna C18 (2) RP-HPLC column, 250 x 4.6 mm, 5 µm particle size. The data acquisition was performed using the ChemStation software (Chapter 3.1.6).

CONJUGATES40_60

Flow: 0.9 mL/min
Injection volume: 10 µL

Elution: Eluent A: Water (pH 3.0 FA)

Eluent B: MeOH

Isocratic, 40% A and 60% B

CONJUGATES50_50

Flow: 0.9 mL/min

Injection volume: 10 µL

Eluent A: Water (pH 3.0 FA)

Eluent B: MeOH

Elution: Isocratic, 50% A and 50% B

CONJUGATES_GRAD8

Flow: 0.5 mL/min

Injection volume: 20 µL

Elution: Eluent A: Water (pH 3.0 FA)

Eluent B: MeO

Gradient:

Time (min)	Eluent A (%)	Eluent B (%)
0	80	20
50	30	70
60	30	70
70	20	80
75	80	20
90	80	20

METHOXY_E1_E2

Flow: 0.9 mL/min

Injection volume: 10 µL

Elution: Eluent A: Water (pH 3.0 FA)

Eluent B: MeO

Gradient:

Time (min)	Eluent A (%)	Eluent B (%)
0	40	60
20	40	60
35	20	80
37	20	80
47	40	60

3.2.1.2. UHPLC-ESI-MS/MS

Analytical system: Shimadzu Nexera X2 UHPLC with DGU-20A 5R degasser, SIL-30AC autosampler, CTO-30A column oven, binary pump and LC-30AD liquid chromatograph with CBM-20A Communications Bus Module. The mass spectrometer consists of an ABSciex QTrap 5500 hybrid system of triple quadrupole with a Turbo V™ ion source with TurbolonSpray® probe for electrospray ionization (ESI) and nitrogen generator NGM11-S. Analyses were performed with a Gemini C18 column, 50 x 2.0 mm, 3 µm particle size with security guard cartridges Gemini C18 column, 4 x 2.0 mm. The data acquisition was performed using the Analyst software (Chapter 3.1.6).

Method 1

Mode: multiple reaction monitoring (MRM)

Flow: 0.3 mL/min

Injection volume: 5 µL

Column oven temperature: 40 °C

Elution: Eluent A: Ammonium acetate buffer

Eluent B: ACN

Gradient:

Time (min)	Eluent A (%)	Eluent B (%)
0.00	95	5
0.50	95	5
3.00	79	21
10.00	50	50
15.50	0	100
18.50	0	100
20.00	95	5
30.00	95	5

From a time of 8 min. the eluent flow is switched to the solvent waste

Mass spectrometer conditions (Method 1)

The source-dependent and substance-dependent parameter settings fo method 1 are summarized in Tables 8-9.

Table 8: Source-dependent parameters for the UHPLC-MS/MS method 1. CUR, curtain gas; IS, ion spray voltage; GS1, nebulizer gas; TEM, temperature (source); GS2, turbogas.

Parameter	Setting
CUR	35 psi
IS	-3500 V
GS1	40 psi
TEM	550 °C
GS2	80 psi
Polarity	Negative

Table 9: Substance-dependent parameters for the UHPLC-MS/MS method 1. [a] In Q3, the first fragment corresponds to the quantifier and the second to the qualifier. t_R, retention time; DP, declustering potential; Q, quadrupole; m/z, mass charge ratio; CE, collision energy; CXP, cell exit potential.

Analyte	t_R	DP (V)	Q1 (m/z)	Q3 (m/z) [a]	CE (V)	CXP (V)
E2-3-G	4.8	-35	447.1	112.9	-28	-9
				174.8	-24	-17
E1-G	5.1	-30	445.1	113.0	-26	-9
				268.9	-46	-19
E1-G-d4	5.1	-140	449.1	112.9	-26	-11
				273.1	-50	-19
E2-17-S	5.8	-30	351.0	96.9	-44	-13
				79.9	-122	-11
E2-3-S	5.9	-30	351.0	271.1	-46	-21
				144.9	-70	-17
E2-3-S-d4	5.9	-30	355.0	275.1	-46	-21
				146.9	-70	-17
E1-S	6.3	-45	349.0	269.1	-42	-21
				145.0	-66	-11
E1-S-d4	6.3	-30	353.0	273.1	-44	-13
				146.9	-66	-13

Method 2

Mode: MRM

Flow: 0.4 mL/min

Injection volume: 5 µL

Column oven temperature: 50 °C

Elution: Eluent A: Ammonium acetate buffer

Eluent B: ACN

Gradient:

Time (min)	Eluent A (%)	Eluent B (%)
0.00	83	17
6.00	83	17
10.00	0	100
13.00	0	100
15.00	83	17
25.00	83	17

From a time of 8 min. the eluent flow is switched to the solvent waste

Method 3

Mode: enhanced product ion scan (ePS)

Flow: 0.3 mL/min

Injection volume: 5 µL

Column oven temperature: 50 °C

Elution: Eluent A: Ammonium acetate buffer

Eluent B: ACN

Gradient:

Time (min)	Eluent A (%)	Eluent B (%)
0.01	95	5
0.50	95	5
3.00	79	21
10.00	50	50
15.50	50	50
18.5*	0	100
20.00	0	100
30.00	95	5

*From a time of 18.50 min. the eluent flow is switched to the solvent waste

Method 4

Mode: ePS

Flow: 0.3 mL/min

Injection volume: 5 µL

Column oven temperature: 50 °C

Elution: Eluent A: Ammonium acetate buffer

Eluent B: ACN

Gradient:

Time (min)	Eluent A (%)	Eluent B (%)
0.00	95	5
0.50	95	5
15.50	0	100
18.50*	0	100
20.00	95	5
30.00	95	5

*From a time of 18.50 min. the eluent flow is switched to the solvent waste

3.2.1.3. GC-MS/MS

Analytical system: Varian 450 gas chromatograph with a Varian CP 8400 autosampler and coupled to a Varian 300 Triple Quad Mass Spectrometer. Analysis performed with a Supelco SLBTM-5ms capillary column, 30 m x 0.25 mm, 0.25 µm particle size. The data acquisition was performed using the Mass Data Review software (Chapter 3.1.6).

Mode: MRM

Flow: 1 mL/min

Injection volume: 2 µL (splitless)

Injector temperature: 250 °C

Column temperature: 60 °C →30 °C/min→250 °C→1.8 °C/min→275 °C

Carrier gas: Helium

Mass spectrometer conditions

The mass spectrometer and substance-dependent parameter settings for the GC-MS/MS method are summarized in Tables 10-11.

Table 10: Mass spectrometer parameters for the GC-MS/MS method. IS, ion spray voltage.

Parameter	Setting
Collision gas	Argon
IS	70 eV
Ion source	250 °C
Pressure impact chamber	1.6 mTorr
Transfer line	280 °C
Voltage detector	1265 V

Table 11: Substance-dependent parameters for the GC-MS/MS method. t_R, retention time; Q, quadrupole; m/z, mass charge ratio; CE, collision energy.

Analyte	t_R	Q1 (m/z)	Q3(m/z)	CE (V)	Dwell Time (s)
12.42-14.12 min					
E1	13.4	342.0	257.0	10.0	0.10
E1-d2	13.4	344.0	259.0	10.0	0.10
E1-d4	13.4	346.0	261.0	10.0	0.10
E2	13.8	416.0	285.0	13.0	0.10
E2-d3	13.8	419.0	285.0	13.0	0.10
E2-d4	13.8	420.0	287.0	13.0	0.10
14.12-20.34 min					
4-MeO-E1	14.8	372.0	342.0	12.0	0.08
4-MeO-E1-d4	14.8	376.0	342.0	12.0	0.08
4-MeO-E2	15.3	446.0	315.0	14.0	0.08
4-MeO-E2-d3	15.3	449.0	315.0	14.0	0.08
2-MeO-E1	15.4	372.0	342.0	12.0	0.08
2-MeO-E1-d4	15.4	376.0	342.0	12.0	0.08
2-HO-E1	15.5	430.0	345.0	16.0	0.08
2-HO-E1-d4	15.5	434.0	345.0	16.0	0.08
16α-HO-E1	15.9	430.0	286.0	8.0	0.08
16α-HO-E1-d5	15.9	435.0	291.0	8.0	0.08
2-MeO-E2	16.0	446.0	315.0	14.0	0.08
2-MeO-E2-d3	16.0	449.0	315.0	14.0	0.08
2-HO-E2	16.0	504.0	373.0	18.0	0.08
2-HO-E2-d3	16.0	507.0	373.0	18.0	0.08
4-HO-E1	16.3	430.0	345.0	16.0	0.08
4-HO-E1-d4	16.3	434.0	345.0	16.0	0.08
4-HO-E2	16.7	504.0	373.0	18.0	0.08
4-HO-E2-d3	16.7	507.0	373.0	18.0	0.08
16α-HO-E2	17.1	504.0	324.0	9.0	0.08
16α-HO-E2-d3	17.1	507.0	327.0	9.0	0.08

3.2.2. Biosynthesis of methoxyestrogen glucuronide references and their corresponding deuterated analogues

The glucuronidation of 2-MeO-E1, 4-MeO-E1, 2-MeO-E2 and 4-MeO-E2 was performed based on an existing method in our research group. The method for the glucuronidation of E1 was adopted and then adapted concerning the solubility of the references, thus, replacing the DMSO for MeOH as the solvent for the methoxyestrogens.

3.2.2.1. Glucuronidation of 2- and 4-methoxyestrone

The glucuronidation of 2-MeO-E1 was performed using a 2 mM stock solution 10% MeOH, and the protein fraction of RLM. The components used are listed in Table 12.

Table 12: Components for the glucuronidation of 2-MeO-E1.

Component	Concentration	Volume used (µL)	Concentration in the incubation probe (250 µL)
Protein (RML)	23.2 mg/mL	21.5	2 mg/mL
Alamethicin	250 µg/mL (5% DMSO)	50	50 µg/mL (1% DMSO)
$MgCl_2$	247	10	9.9 mM
2-MeO-E1	2 mM (10% MeOH)	25	200 µM (1% MeOH)
Saccharolactone	234 mM	10	9.4 mM
Potassium-phosphate buffer	0.1 M	33.5	-
UDPGA	10 mM	100	4 mM

Procedure: All the components were mixed over ice. The protein and the alamethicin were placed in a 2 mL micro-reaction tube and incubated for 15 min. After that time, all other components were added to the tube with the UDPGA as the last one. The enzymatic reaction started placing the tube in a water bath at 37 °C overnight and was stopped the next day by adding 500 µL Glycine-HCl buffer. Afterward, liquid-liquid

extraction with ethyl acetate was performed 3 times removing each time the organic phase to a glass tube. The combined organic phase containing the reaction product was evaporated at 90 mbar.

Isolation of the reaction product: The evaporated product was dissolved in 250 µL MeOH and 10-15 µL were injected in the HPLC-UV/Vis (method CONJUGATES40_60, Chapter 3.2.1.1) to verify the formation of the conjugate. After no interference peaks were detected, all performed biosynthesis were mixed in one glass tube, evaporated at 60 mbar and dissolved in 100 µL MeOH. Aliquots of this 100 µL containing the reaction product were injected (method CONJUGATES40_60, Chapter 3.2.1.1), and after separation of the product peak, the collection was carried out in a glass tube after passing the detector. For the collected product, the MeOH was removed by evaporation at 60 mbar and the aqueous phase was frozen and freeze-dried overnight. The reaction product was stored at -20 °C until identification (Chapter 3.2.3), quantification (Chapter 3.2.5) and preparation of the stocks solutions (Chapter 3.2.6).

The glucuronidation of 4-MeO-E1 was performed with the same methodology as for 2-MeO-E1, but using 5 µL of a 4-MeO-E1 stock solution 10 mM 100% in MeOH. After biosynthesis, isolation of the reaction product was also performed in the same way as for 2-MeO-E1.

3.2.2.2. Glucuronidation of 2- and 4-methoxyestradiol

The glucuronidation of 2-MeO-E2 and 4-MeO-E2 was performed using the same methodology as for the methoxylated derivates of E1, but using 5 µL of a 10 mM stock solution 100% in MeOH. These glucuronidations were performed by a master student within our research group.

Since both 2- and 4-MeO-E2 are glucuronidated at 2 different positions (-3 and -17), the synthesis of a blank with the same concentration in the incubation probe of the corresponding methoxyestradiol was conducted in performed to support the identification of the peaks. For this, the UDPGA was replaced with 100 µL of potassium phosphate buffer.

Isolation of the reaction products: The isolation of the reaction products was also performed as for the methoxylated metabolites of E1 using the method CONJUGATES40_60 (Chapter 3.2.1.1) for the glucuronidation products of 2-MeOE2 (2-MeO-E2-3-G and 2-MeO-E2-17-G) and the method CONJUGATES50_50 (Chapter 3.2.1.1) for the glucuronidation products of 4-MeOE2 (4-MeO-E2-3-G and 4-MeO-E2-17-G). Two peaks were collected in each case. The collected reaction products were stored at -20 °C until identification (Chapter 3.2.3), quantification (Chapter 3.2.5) and preparation of the stocks solutions (Chapter 3.2.6).

3.2.3. Identification of the methoxyestrogen glucuronides and the glucuronidation position

2- and 4-MeO-E1 can be glucuronidated only at position 3 of the molecule. However, even when only one peak was observed in each case after the biosynthesis, their identities were confirmed. Furthermore, 2- and 4-MeO-E2 can be glucuronidated at 2 different positions, -3 and -17. Thus, the identification of the 2 collected peaks in each case was conducted. This assignment was performed via UHPLC-MS/MS in ePS mode and with support of the literature. In every case, a precursor ion was selected at the first quadrupole (Q1) with a certain mass/charge ratio (m/z) to be later fragmented at the collision cell (Q2) with a settled collision energy value (CE). Finally, fragments were scanned at (Q3) which consists of a linear ion trap configured with fixed trap time.

3.2.3.1. Identification of 2- and 4-methoxyestrone-3-glucuronide

After the isolation of the reaction products (Chapter 3.2.2.1) the dried residues were dissolved in ACN 5% to solutions of approx. 0.29 ng/µL and 0.19 ng/µL of 2-MeO-E1-G and 4-MeO-E1-G, respectively, and injected to perform an ePS with fixed trap time. The evaluation of the chromatograms was carried out with the Analyst software ((Chapter 3.1.6).

2-MeO-E1-G was identified using the method 3 (Chapter 3.2.1.2) and 2 different CE of -20 V and -40 V were tested. For the 4-MeO-E1-G, the identification was carried out using the method 4 (Chapter 3.2.1.2) and 2 different CE of -20 V and -40 V were tested.

3.2.3.2. Identification and assignation of the glucuronidation position of 2- and 4-methoxyestradiol-3/17-glucuronide

After the isolation of the reaction products (Chapter 3.2.2.2), the dried residues were dissolved in ACN 5% to solutions of approx. 0.20 ng/µL and injected to perform an ePS with fixed trap time. The evaluation of the chromatograms was carried out with the Analyst software (Chapter 3.1.6), and the assignation of the glucuronidation position was supported by the obtained fragments and the literature (Gentili et al., 2002).

2-MeO-E2-3-G and 2-MeO-E2-17-G were identified using the method 4 (Chapter 3.2.1.2) and CE of -20 V, -30, -40, -50 and -60 V were tested. After the evaluation of the individual chromatograms, the most suitable CE was determined. At this CE, the most intense fragments were chosen, drawn and exanimated with the literature (Gentili et al., 2002). The same procedure was carried out with 4-MeO-E2-3-G and 4-MeO-E2-17-G by a master student within our research group.

3.2.4. Biosynthesis of deuterated methoxyestrogen glucuronides

For the identification and quantification of methoxyestrogen glucuronides in human plasma and breast tissue, deuterated internal standards (ISs) to spike the samples were needed. Since deuterated methoxyestrogens to further glucuronidation were not commercially available, their biosynthesis through methylation of deuterated hydroxyestrogens was first performed using an existing method in our research group.

3.2.4.1. Methylation of deuterated 2- and 4-hydroxyestrone

The methylation of 2- and 4-HO-E1-d4 using rat liver cytosol (RLC), was performed with the incubation mixture described in Table 13.

Table 13: Components for the methylation of 2- and 4-HO-E1-d4.

Component	Concentration	Volume used (µL)	Concentration in the incubation probe (1000 µL)
Potassium phosphate buffer	0.1 M	750	-
$MgCl_2$	40 mM	100	4 mM
2- or 4-HO-E1-d4	10 mM (100% DMSO)	10	100 µM (1% DMSO)
Protein (RLC)	~ 25 mg/mL	40	~ 1 mg/mL
SAM	2.5 mg/mL	100	25 µg/mL

Procedure: All components were placed together in a glass tube, with the SAM at the end. The incubation was performed for 90 min in a water bath at 37 °C and after that time, was stopped by adding 3 mL of ethyl acetate. Afterward, liquid-liquid extraction with ethyl acetate was performed 3 times removing each time the organic phase into a new glass tube. The combined organic phase containing the reaction product was evaporated at 90 mbar. To better identification of the products, a blank with the same concentration of the corresponding hydroxyestrogen in the incubation probe was conducted, replacing the SAM with potassium phosphate buffer.

Isolation of the reaction product: The evaporated product was dissolved in MeOH to approx. 40 µM (supposing that 100% of the 10 mM was methylated) and 10 µL were injected in the HPLC-UV/Vis (method METHOXY_E1_E2, Chapter 3.2.1.1) to verify the formation of the product and its concentration via 1 point calibration curve with references 80 µM of 2- or 4-MeO-E1. After the peak was identified, the remaining product with a known concentration was evaporated at 60 mbar and dissolved in 100 µL MeOH to inject aliquots of 10 µL x 8 times (collecting them in a glass tube after passing the detector). The MeOH was removed by evaporation at 60 mbar and the aqueous phase was frozen and freeze-dried overnight. Afterward, the collected reaction product with a known amount of fmol was dissolved in MeOH to approx. 50 µM and 10 µL were injected in the HPLC-UV/Vis (method METHOXY_E1_E2, Chapter 3.2.1.1) to verify its concentration via 1 point calibration curve with references 80 µM of 2- or 4-MeO-E1 (Appendix A1.15) to further glucuronidation.

3.2.4.2. Methylation of deuterated 2- and 4-hydroxyestradiol

The methylation of 2- and 4-HO-E2-d3 using RLC, was performed in the same way as 2- and 4-HO-E1-d4 (Chapter 3.2.4.1), verifying the concentration of the reaction products via 1 point calibration curve (Appendix A1.15), to further glucuronidation. Blanks were performed with the corresponding deuterated hydroxyestrogen.

3.2.4.3. Glucuronidation of deuterated methoxyestrogens

The glucuronidation of the deuterated methoxyestrogens was performed in the same way as for their corresponding undeuterated analogs (Chapter 3.2.2). The identification was performed using the retention time (t_R) of methoxyestrogen references, blanks, and the t_R of the peak of undeuterated methoxyestrogen glucuronides. The collected and identified reaction products were stored at -20 °C until quantification (Chapter 3.2.5) and preparation of the stock solutions (Chapter 3.2.6).

3.2.5. Methods for the quantification of biosynthesized references

Since methoxyestrogen glucuronides are not commercially available, their quantification with standardized references is not possible. Therefore, 2 different quantification methodologies were evaluated (Chapters 3.2.5.1-3.2.5.2.)

3.2.5.1. Absorbance difference: ratio factors

This quantification method using the absorbance difference consisted of the building of the ratio of peak areas of unconjugated E1 or E2 to those of their corresponding glucuronides at position -3 or -17 (ratio factors) (E1/E1-G; E2/E2-3-G and E2/G). After, the peak areas of the biosynthesized methoxyestrogen glucuronides were multiplied by these ratio factors and the obtained values were used to quantify the metabolite within a calibration curve of their corresponding methoxyestrogen. Thus, calibration curves of E1 with E1-G and E2 and with E2-3-G and E2-17-G were constructed.

3.2.5.1.1. Ratio factor of estrone and estrone-3-glucuronide

A calibration curve of both E1 and E1-G was constructed and the ratio factor was calculated as $\frac{peak\ area\ E1}{peak\ area\ E1-G}$ for each point of the calibration curve. The linear range of both calibration curves was 40-200 µM, which is the same calibration range of 2-MeO-E1 and 4-MeO-E1 (Table 15). The calibration curve was built from a stock solution 400 µM in MeOH of E1 + E1-G as follows:

71.4 µL of E1 (2240 µM) + 40 µL of E1-G (400 µM) + 288.6 µL MeOH

From this stock solution, 3 independent calibration curves were constructed (Table 14), and 10 µL of each calibration point were injected (method CONJUGATES40_60, Chapter 3.2.1.1) and evaluated using Origin Pro (Chapter 3.1.6). With the ratios of each point from all 3 calibration curves, the mean value (ratio factor) and its standard deviation (SD) and relative standard deviation (RSD) were calculated (Appendices A1.20-A1.21).

Table 14: Pipetting scheme to construct the calibration curves for the determination of the ratio factor E1/E1-G, within a concentration range from 40 µM to 200 µM. o.c., on column.

Calibration point	Concentration (µM)	pmol o.c.	Concentration of the stock solution (µM)	Volume from the stock solution (µL)	Volume. of MeOH (µL)
1	40	400	400	20	180
2	80	800		40	160
3	120	1200		60	140
4	160	1600		80	120
5	200	2000		100	100

Quantification of (deuterated) 2-MeO-E1-G and 4-MeO-E1-G

For the quantification of these metabolites, 5 point calibration curves of 2-MeO-E1 and 4-MeO-E1 were constructed from 1000 µM stock solutions in MeOH (Table 15). Both calibration curves were constructed 3 times independently, and 10 µL of each calibration point were injected (method CONJUGATES40_60, Chapter 3.2.1.1). The curves were evaluated using Origin Pro (Chapter 3.1.6). With the areas of 3 calibration curves, the SD and the RSD were calculated (Appendices A1.26-A1.29).

Table 15: Pipetting scheme to construct the calibration curve of 2-MeO-E1 or 4-MeO-E1, within a concentration range from 40 µM to 200 µM. o.c., on column.

Calibration point	Concentration (µM)	pmol o.c	Volume (µL) from the stock solution 2- or 4-MeO-E1 (100 µM)	Volume of MeOH (µL)
1	40	400	20	480
2	80	800	40	460
3	120	1200	60	440
4	160	1600	80	420
5	200	2000	100	400

The isolated peaks of the biosynthesized references (Chapter 3.2.2.1; Chapter 3.2.4.3) were dissolved in a volume of MeOH, and 10 µL of each reference were injected 3 times (Method CONJUGATES40_60, Chapter 3.2.1.1). The obtained areas were multiplied by the ratio factor $\frac{peak\ area\ E1}{peak\ area\ E1-G}$ and the corresponding values were inserted into the linear equation of the calibration curve (Appendix A1.34).

3.2.5.1.2. Ratio factors of estradiol and estradiol-3/17-glucuronide

Calibration curves of both E2 and E2-3-G and E2 and E2-17-G were constructed and the ratio factors were calculated as $\frac{peak\ area\ E2}{peak\ area\ E2-3-G}$ and $\frac{peak\ area\ E2}{peak\ area\ E2-17-G}$, respectively, for each point of these calibration curves. The linear range was 40-200 µM, which is

the same calibration range of 2-MeO-E2 and 4-MeO-E2. The calibration curves were constructed from stock solutions 400 µM in MeOH of E2 + E2-3-G and E2 + E2-17-G as follows:

50 µL of E2 (4000 µM) + 50 µL of E2-3-G (4000 µM) + 400 µL MeOH

50 µL of E2 (4000 µM) + 50 µL of E2-17-G (4000 µM) + 400 µL MeOH

The procedure to construct the calibration curves was the same as in Table 14 (Chapter 3.2.5.1.1), and the data was evaluated using Origin Pro (Chapter 3.1.6). With the ratios of each point from all 3 calibration curves, the mean values (ratio factors) and their SD and RSD were calculated (Appendices A1.22-A1.25).

Quantification of (deuterated) 2-MeO-E2-3-G and 2-MeO-E2-17-G

For the quantification of these metabolites, a 5 point calibration curve of 2-MeO-E2 was constructed from a 1000 µM stock solution in MeOH. The pipetting scheme is the same as in Table 15 (Chapter 3.2.5.1.1). The calibration curves were constructed 3 times independently, and 10 µL of each calibration point were injected (method CONJUGATES40_60, Chapter 3.2.1.1). The curves were evaluated using Origin Pro (Chapter 3.1.6). With the areas of 3 calibration curves, the SD and the RSD were calculated (Appendices A1.30-A1.31). Then, the isolated peaks of the biosynthesized references (Chapter 3.2.2.2; Chapter 3.2.4.3) were dissolved in a volume of MeOH, and 10 µL of each reference were injected 3 times (Method CONJUGATES40_60, Chapter 3.2.1.1). The obtained areas were multiplied by the corresponding ratio factor $\frac{peak\ area\ E2}{peak\ area\ E2{-}3{-}G}$ or $\frac{peak\ area\ E2}{peak\ area\ E2{-}17{-}G}$ and the resulting values were inserted into the linear equation of the calibration curve (Appendix A1.34).

Quantification of (deuterated) 4-MeO-E2-3-G and 4-MeO-E2-17-G

For the quantification of these metabolites, a 5 point calibration curve of 4-MeO-E2 was built from a 1000 µM stock solution in MeOH. The pipetting scheme is the same as in Table 15. The calibration curves were constructed 3 times independently, and 10

µL of each calibration point were injected (method CONJUGATES50_50, Chapter 3.2.1.1). The curves were evaluated using Origin Pro (Chapter 3.1.6). With the areas of 3 calibration curves, the SD and the RSD were calculated (Appendices A1.32-A1.33). Then, the isolated peaks of the biosynthesized references (Chapter 3.2.2.2; Chapter 3.2.4.3) were dissolved in a volume of MeOH, and 10 µL of each reference were injected 3 times (Method CONJUGATES50_50, Chapter 3.2.1.1). The obtained areas were multiplied by the corresponding ratio factor $\frac{peak\ area\ E2}{peak\ area\ E2-3-G}$ or $\frac{peak\ area\ E2}{peak\ area\ E2-17-G}$ and the resulting values were inserted into the linear equation of the calibration curve (Appendix A1.34).

3.2.5.2. Hydrolysis

This method consists of hydrolyzing back a glucuronide to its unconjugated form by enzymatic reaction with β-glucuronidase (e.g. 2-MeO-E2-3-G → 2-MeO-E2). If the amount of initial glucuronide is known and correct, the amount of unconjugated product after hydrolysis will be also known and can be quantified in a normal calibration curve of its corresponding methoxyestrogen. The procedure according to Xu et al. (2005), was first carried out with E2-3-G to test the suitability of the method, and after with biosynthesized 2-MeO-E2-3-G. β-glucuronidase from *Helix pomatia* was first used, but as the reaction product had several matrix interferences, it was replaced with β-glucuronidase from bovine liver which has no peroxidase activity.

Procedure:

Incubation and extraction: 40 µL of the substrate were placed in a glass tube with 500 µL of enzyme-hydrolysis buffer and the incubation was carried out overnight in a water bath at 37 °C. The next day, E1 as internal standard was added to the incubation probe and right after the reaction was stopped by adding 7 mL of dichloromethane. After, the reaction product was shaken for 30 min at 8 rpm in the rotation shaker. Finally, the organic phase was transferred to another glass tube and completely evaporated at 300 mbar.

Purification through solid phase-extraction: The evaporated product was dissolved in 2 mL of MeOH (0.1% FA) / AFB 20:80 v/v and the SPE was performed as follows:

A.	Conditioning of the cartridges:	2 x 2 mL MeOH with 0.1% FA 2 x 2 mL MeOH (0.1% FA) / AFB 20:80 v/v
B.	Sample load:	Probe (2mL)
C.	Washing:	2 x 2 mL MeOH (0.1% FA) / AFB 20:80 v/v
D.	Elution:	2 x 2 mL MeOH (0.1% FA) / AFB 90:10 v/v

After elution, the probe was evaporated at 60 mbar and dissolved in 100 µL MeOH.

3.2.5.2.1. Hydrolysis of 17β-estradiol-3-glucuronide

The hydrolysis of 17β-estradiol-3-glucuronide (E2-3-G) to E2 was performed as described in the procedure (Chapter 3.2.5.2) using 40 µL of an E2 solution 75 µM. Since E2 was not possible to be calculated, the percentage of hydrolysis was calculated by difference with the remaining E2-3-G which was not hydrolyzed, via 1 calibration point of E2-3-G (Appendix A1.35).

3.2.5.2.2. Hydrolysis of 2-methoxyestradiol-3-glucuronide

The hydrolysis of 2-MeO-E2-3-G to 2-MeO-E2 was performed as described in the procedure (Chapter 3.2.5.2) using 40 µL of a 2-MeO-E2-3-G solution approx. 75 µM (calculated with the ratio factor, Chapter 3.2.5.1.2). For quantification of the hydrolysis product, a 7 point calibration curve of 2-MeO-E2 with E1 as internal standard was built (Table 16) using stock solutions 100 µM of 2-MeO-E2 in MeOH and 150 µM of E1 in MeOH. The linear range of 2-MeO-E2 was 10-40 µM.

The calibration curve was constructed 3 times independently, and 20 µL of each calibration point were injected (method CONJUGATES_GRAD8, Chapter 3.2.1.1). The curves were evaluated using Origin Pro (Chapter 3.1.6). With the areas of all 3 calibration curves, the SD and the RSD were calculated (Appendices A1.36-A1.37). With the calibration curve, the hydrolysis product, 2-MeO-E2 was quantified (Appendix A1.38).

Table 16: Pipetting scheme to construct the calibration curve of 2-MeO-E2 using E1 as internal standard, within a concentration range from 10 µM to 40 µM. o.c., on column.

Calibration point	Concentration (µM)	pmol o.c. of E2	Volume (µL) from the E2 stock solution (100 µM)	Volume (µL) from the E1 stock solution (150 µM)	Volume of MeOH (µL)
1	10	200	10		70
2	15	300	15		65
3	20	400	20		60
4	25	500	25	20	55
5	30	600	30		50
6	35	700	35		45
7	40	800	40		40

3.2.6. Stock solutions of biosynthesized methoxyestrogen glucuronides

Stock solutions with a known concentration of biosynthesized methoxyestrogen glucuronides were prepared to further work in plasma and tissue samples. For this, the remaining volumes after the quantification process (Chapter 3.2.5.1) were evaporated at 60 mbar and dissolved in MeOH to a concentration of 10 ng/µL. From this stock solutions, work solutions of 100 pg/µL in MeOH were prepared with a dilution of 1:100.

3.2.7. Optimization of the substance-dependent and source-dependent parameters for the *Multiple Reaction Monitoring* method

To apply the existing UHPLC-MS/MS method in the MRM negative mode for the analysis of estrogen conjugates to the analysis of methoxyestrogen glucuronides, the instrument settings substance-dependent parameters (Chapter 3.2.7.1) and source-dependent parameters (Chapter 3.2.7.2) needed to be first optimized. The negative mode was selected since the ionization of the conjugates, which are polar molecules, will be enhanced. With the 2 most intense mass transitions (product ions), the analyte can be quantified (mass transition of the quantifier, Qn) and identified (mass transition of the qualifier, Ql), since the ratio of the intensity of the Qn to the Ql is equally and unique for a specific analyte.

3.2.7.1. Substance-dependent parameters

The optimization of the substance-dependent parameters was performed using the fragment ions selected from the literature which were also used for the identification of the glucuronidation position (Chapter 3.2.3), and the stock solutions 100 pg/µL (Chapter 3.2.6). Individual solutions of 10-20 pg/µL were prepared from the corresponding stock solution 100 pg/µL (Table 17) and injected individually via syringe pump at a flow rate of 7 µL/min with an intensity of at least 5 x 10^5 counts per second (cps) in the range of the expected m/z (± 50 Da), to check the presence of the precursor ion. Subsequently, the software-based *Automatic Compound Optimization* was performed by injecting the biosynthesized references with the syringe pump and the declustering potential (DP), which brings the precursor ion into the vacuum chamber with maximum intensity, was optimized at Q1. With the optimal DP obtained from a range of 1-300 V in increments of 5 V, a product ion scan for the precursor ion was performed. The CE was determined in a range of 5-13 V in increments of 2 V for the 8 most intense fragment ions, and the cell exit potential (CXP) (Q2 and Q3) was determined in a range of 0-55 V in increments of 2 V.

Table 17: Concentration of the biosynthesized methoxyestrogen glucuronides for the substance-dependent parameters optimization.

Reference	Concentration in pg/µL
2-MeO-E1-G	20
4-MeO-E1-G	20
2-MeO-E2-3-G	10
2-MeO-E2-17-G	20
4-MeO-E2-3-G	10
4-MeO-E2-17-G	20

3.2.7.2. Source-dependent parameters

The optimization of the source-dependent parameters for the biosynthesized references was performed using a mix prepared from the stock solutions 10-100 pg/µL (Table 18). Each biosynthesized reference was pipetted together in a vial, then the mix was evaporated at 30 mbar and dissolved in 100 µL MeOH. The mix was injected and analyzed in MRM negative mode using the method 2 with the previously optimized substance-specific parameters (Chapter 3.2.1.2). Each source-dependent parameter was tested at 3 different levels (Table 19), with the curtain gas (CUR) fixed at 35 psi.

Table 18: Pipetting scheme and concentration in the mix of biosynthesized references used for the source-dependent parameters optimization.

Reference	Concentration of the stock solution (pg/µL)	Volume from the stock solution (µL)	Concentration in pg/µL in 100µL mix (fmol/µL)
2-MeO-E1-G 2-MeO-E1-G-d4	100	10	10
4-MeO-E1-G 4-MeO-E1-G-d4	10	30	3
2-MeO-E2-3-G 2-MeO-E2-3-G-d3	100	10	10
2-MeO-E2-17-G 2-MeO-E2-17-G-d3	100	15	15
4-MeO-E2-3-G 4-MeO-E2-3-G-d3	10	50	15
4-MeO-E2-17-G 4-MeO-E2-17-G-d3	100	15	5

Table 19: Source-dependent parameters optimized at 3 different levels. TEM, temperature (source); IS, ion spray voltage; GS1, nebulizer gas; GS2, turbogas.

Source parameter	Experiment	Level	Fixed parameters
TEM (°C)	1 2 3	450 500 550	IS = -3500 V; GS1 = 40 psi; GS2 = 80 psi
IS (V)	1 2 3	-3000 -3500 -4000	Temp = 550 °C; GS1 = 40 psi; GS2 = 80 psi
GS1 (psi)	1 2 3	40 50 60	Temp = 550 °C; IS = -3500 V; GS2 = 70 psi
GS2 (psi)	1 2 3	40 50 60	Temp = 550 °C; IS = -3500 V; GS1 = 40 psi

3.2.8. Preparation of human plasma and breast tissue specimens

The blood and breast tissue specimens were collected from women without breast cancer undergoing mammoplasty reduction for cosmetic reasons on the day of the surgery. The personal information such as age, parity and menopausal status, etc., was collected in a questionnaire before the surgery day (Appendix A3.1).

3.2.8.1. Human plasma

In a 15 mL centrifuge tube containing the whole blood, an equal amount Histopaque® 1077 was added slowly with a Pasteur pipette and then centrifuged at 440 gravities for 40 min. After centrifugation, the plasma (upper part) was taken and divided into aliquots of approx. 1 mL in micro-reaction tubes of 1.5 mL, and stored at -80 °C until use. The fraction containing the mononuclear cells were further processed to be used by someone else in other investigations.

3.2.8.2. Human breast tissue

As fast as possible, samples were placed in ice-cold Krebs buffer and the adipose and glandular fractions were separated. Every separated piece was weighed and stored in cryos and then frozen in liquid nitrogen. Afterward, samples were stored at -80 °C until grinding. The grinding process was performed by hammering portions of approx. 200 mg in liquid nitrogen between 4 to 6 times in a custom-made stainless steel mortar. The resulting powder was placed in a pre-tared cryo and after register the exact weight, samples were stored at -80 °C until use.

3.2.9. Extraction of metabolites from human plasma and breast tissue

3.2.9.1. Human plasma

The plasma samples stored at -80 °C were thawed on ice. For each extraction series, a blank was also extracted in the same way as the plasma, to verify no contamination of the samples with E1 or E2. In this blank, the plasma is replaced with AFB buffer. For the quantification, mixtures of references that do not undergo extraction were used.

The workup consisted of a liquid-liquid extraction followed by an SPE, and then, either derivatization for the GC-MS/MS analysis, or dilution for the LC-MS/MS analysis. Before the workup, the blank, the plasma samples, and the reference were spiked with the mixture of ISs (deuterated analogs) containing the metabolites to be analyzed in the GC-MS/MS or the UHPLC-MS/MS (Table 20). For the references, GC-mix 1 and GC-mix 2 were pipetted together in one vial to GC-MS/MS analysis, and the remaining standards were pipetted in another vial for UHPLC-MS/MS analysis. No deuterated analogs of E2-3-S and E2-17-S were available, thus, samples were not spiked but another vial containing 695 fmol and 3121 fmol, respectively, was used to determine qualitatively these metabolites using their t_R.

Table 20: Internal standards list, fmol added in the spiking volume to the plasma samples.

	Internal standard	Volume (to spike) (µL)	fmol added
GC-Mix 1 (in ACN)	E1-d2	50	110
	E2-d3		109
	2-MeO-E1-d4		115
	4-MeO-E1-d4		115
	2-MeO-E2-d3		115
	4-MeO-E2-d3		115
	16α-HO-E1-d5		96
	16α-HO-E1-d3		1030
GC-Mix 2 (in ACN with 0.1% FA)	2-HO-E1-d4	50	3444
	4-HO-E1-d4		3444
	2-HO-E2-d3		3432
	4-HO-E2-d3		3432
To LC (in ACN)	E1-S-d4	10	133
To LC (in MeOH)	E1-G-d4	10	3964
To LC (in ACN)	E2-3-S-d4	10	396
Mixture of deuterated methoxyestrogen glucuronides to LC (in MeOH) (See validation Chapter 3.2.10.1)	2-MeO-E1-G-d4	10	1157
	4-MeO-E1-G-d4		144
	2-MeO-E2-3G-d3		602
	2-MeO-E2-17-G-d3		1938
	4-MeO-E2-3G-d3		449
	4-MeO-E2-17-G-d3		4776

Liquid-liquid extraction: 3 mL of chloroform were placed in a silanized glass tube and the standard references listed in Table 19 were added. After, 200 µL of DTT and between 1-1.2 mL of AFB were added to the tube (the mL of AFB depends on the mL available of plasma since the aqueous phase has to complete 2 mL between the 200 µL of DTT, the AFB, and the plasma). Then, a defined volume of plasma (between 0.8-1 mL) was added and the mixture was centrifuged for 5 min at 5000 rpm.

Thereafter, the organic phase was placed in another silanized tube and the extraction was repeated twice with 1 mL chloroform each. The combined organic phases were placed together an evaporated at 60 mbar to further SPE. The tube with the remaining aqueous phase was centrifuged 10 min at 5000 rpm and the supernatant was removed to another glass tube. Then, 5 mL of ACN were added to precipitate the proteins with vigorous vortex and centrifugation for 10 min. After precipitation, the remaining aqueous phase was frozen at -20 °C and freeze-dried overnight to further SPE.

Solid-phase extraction: The SPE of both organic and aqueous phases was performed independently, but the procedure was the same. The corresponding dried phase was dissolved in 2 mL of MeOH (0.1% FA) / AFB 20:80 v/v and loaded into the SPE cartridges previously conditioned with 2 times 2 mL of MeOH with 0.1% FA and 2 times 2 mL of MeOH (0.1% FA) / AFB 20:80 v/v. In the case of the aqueous phase, the samples were dissolved in a 2 mL micro-reaction tube and centrifuged at 14,800 rpm for 10 min before loading the cartridge. After the load of the samples, the cartridges were washed with 2 times 2 mL of MeOH (0.1% FA) / AFB 20:80 v/v and the samples were eluted with 2 times 2 mL of MeOH (0.1% FA) / AFB 90:10 v/v. Finally, the eluates were evaporated at 20 mbar overnight.

Derivatization and dissolution of the organic and aqueous phases, respectively: The dried remainder from the organic phase was derivatized with 30 µL of BSTFA and injected on the GC-MS/MS (Chapter 3.2.1.3) for the analysis of E1, E2 and their hydroxyl and methoxyl derivates. The dried residue from the aqueous phase was dissolved in 50 µL of ACN 5% and injected on the UHPLC-MS/MS for the analysis of the estrogen conjugates and methoxyestrogen glucuronides (Chapter 3.2.1.2).

3.2.9.2. Human breast tissue

The breast tissue samples stored at -80 °C were thawed on ice. Same as for plasma, a blank was performed in each extraction series and samples were also spiked with the same references (Table 20).

Liquid-liquid extraction, solid-phase extraction, and derivatization or dissolution: A rack was soaked in liquid nitrogen and the cryos containing the powdered tissue were placed on it. Afterward, 500 µL of chloroform, the references (Table 20), and 500 mg of silibeads were added. The cryos were manually shaken and placed into the cell disruptor for 2 sec. at 6.5 m/sec, 3 times at 4 °C. The content of the cryos was transferred to silanized glass tubes and the cryos were washed 3 times with 1, 1 and 0.5 mL of chloroform, collecting all these washing steps together. Once the organic phase was completely transferred to the glass tube, the liquid-liquid extraction (without the ACN precipitation for the aqueous phase) was performed as for the plasma. The glass tubes collecting the organic phase were pre-weighted to determine the oil content by gravimetry. Once the liquid-liquid extractions were carried out, the SPE and derivatization/dissolution of the samples were performed to GC-MS/MS or UHPLC-MS/MS analysis, in the same way as for plasma.

3.2.10. Validation of the extended method for the detection and quantification of methoxyestrogen glucuronides

The existing method for the quantification of estrogen conjugates by means of UHPLC-MS/MS in the MRM negative mode was extended to the specific detection and quantification of methoxyestrogen glucuronides.

3.2.10.1. Mixture of Internal standards

The fmol of deuterated methoxyestrogen glucuronides present in 10 µL of the mixture of ISs used to spike the samples (described in Table 20, Chapter 3.2.9), were calculated to ensure areas about 3 times their LOD levels (Appendix A2.10). The

pipetting scheme to prepare the mixture of ISs is described in Table 21, where references were pipetted together in a vial, evaporated at 30 mbar and then dissolved in 1 mL of MeOH.

Table 21: Pipetting scheme of the mixture of ISs.

Reference	Concentration of stock solution (pg/µL)	Volume of stock solution (µL)
2-MeO-E1-G-d4	1000	55.6
4-MeO-E1-G-d4	100	69
2-MeO-E2-3G-d3	1000	29
2-MeO-E2-17-G-d3	600	155.5
4-MeO-E2-3G-d3	500	43.2
4-MeO-E2-17-G-d3	10000	23

3.2.10.1.1. Peak shape evaluation

The evaluation of the peak shape of the deuterated methoxyestrogen glucuronides in the mixture of ISs was visually assessed as recommended (https://www.shimadzu.com/an/support/lib/lctalk/92/abnormalpeakshapes.htm, last access: December 2019) (Figure 3).

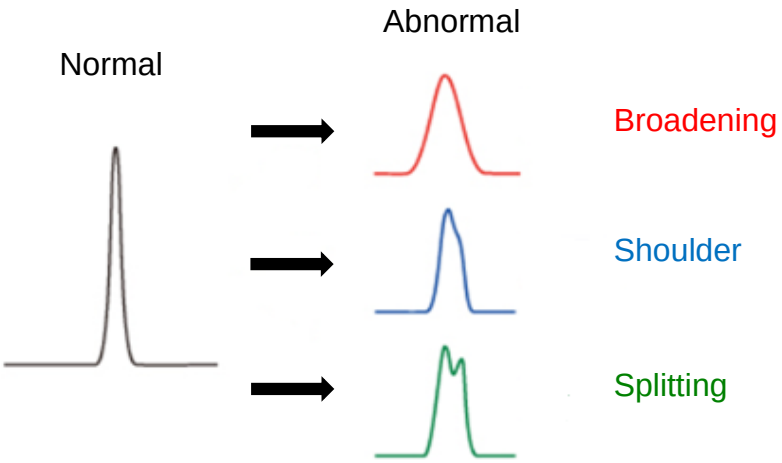

Figure 3: Example of normal and abnormal peak shapes.

3.2.10.1.2. Chromatographic resolution of the peaks

The chromatographic resolution (Rs) of the deuterated methoxyestrogen glucuronides in the mixture of ISs was assessed as recommended, using the following formula:

$$Rs = 1.18 * (\frac{tR2-tR1}{W0.5h1+w0.5h2})$$

With t_R as the retention time for each peak ($t_R1 < t_R2$) and W0.5h as the full with at half maximum of each peak (https://www.shimadzu.com/an/hplc/support/lib/lctalk/resol-1.html, last access: December 2019).

3.2.10.1.3. Quantifier/Qualifier ratio

The Qn/Ql ratios were constructed with the raw peak areas of each methoxyestrogen glucuronide as:

$$\frac{Qn}{Ql} = \frac{Peak\ area\ at\ Qn\ transition}{Peak\ area\ at\ Ql\ transition}$$

With Qn as the product ion which gives the most intense peak area, and the Ql the product ion which gives the second most intense peak area.

3.2.10.1.4. Isotopes of methoxyestrogen glucuronides

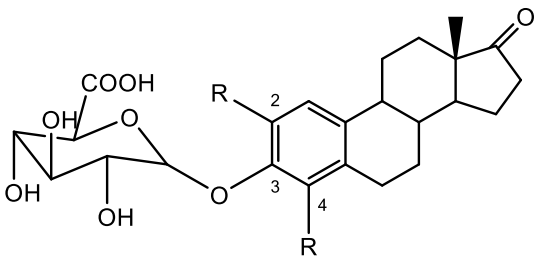

R = Methoxy
R2 = 2-MeO-E1-G
R4 = 4-MeO-E1-G

Isotopes m/z: 477.21 (27.0%), 478.21 (3.5%), 478.21 (1.8%)

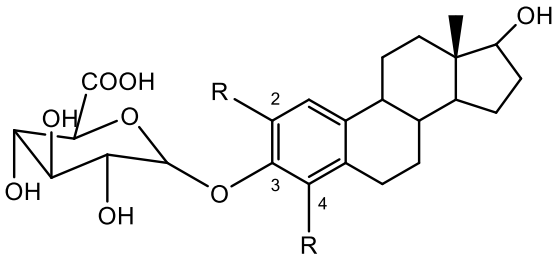

R = Methoxy
R2 = 2-MeO-E2-3-G
R4 = 4-MeO-E2-3-G

Isotopes m/z: 479.22 (27.0%), 480.23 (2.7%), 480.22 (1.8%)

Figure 4: Isotopes of methoxyestrogen glucuronides. Isotopes of 2- and 4-MeO-E2-17-G are the same as for 2- and 4-MeO-E2-3-G

3.2.10.2. Recovery

The recovery of the analytes was calculated with the formula:

Recovery (%) = (peak area of the analyte in plasma/ peak area of the reference) *100

3.2.10.3. Analytical response of deuterated and non-deuterated methoxyestrogen glucuronides

Quantification of methoxyestrogen glucuronides was performed using the ratios of their peak areas to those of their corresponding deuterated analogs by applying the rule of proportion (Chapter 3.2.11.2). Therefore, it was important to verify that the analytical response between non-deuterated and deuterated methoxyestrogen glucuronides was the same when linear increases in the concentration were made. Thus, a mixture of methoxyestrogen glucuronides was prepared (Table 22) in a way that ratios of fmol of non-deuterated methoxyestrogen glucuronides to the fmol of deuterated methoxyestrogen glucuronides (in 10 µL of the ISs mixture, Chapter 3.2.9.1, Table 20) were between 0.5 and 2.0. If the analytical response (peak areas) of the analytes increments in the same way as the fmol were increased, ratios of peak areas of non-deuterated/deuterated methoxyestrogen glucuronides after UHPLC-MS/MS analysis should be between 0.50 and 2.0, too.

For this, methoxyestrogen glucuronides were pipetted together in a vial, then the mixture was evaporated at 30 mbar and dissolved in 100 µL MeOH. Thereafter, 3 independent plasma samples were spiked with 10 µL, 20 µL and 40 µL of this mixture, respectively, and 10 µL of the mixture of ISs to reach the desired fmol ratios (Figure 5). The procedure was carried out on 3 different days.

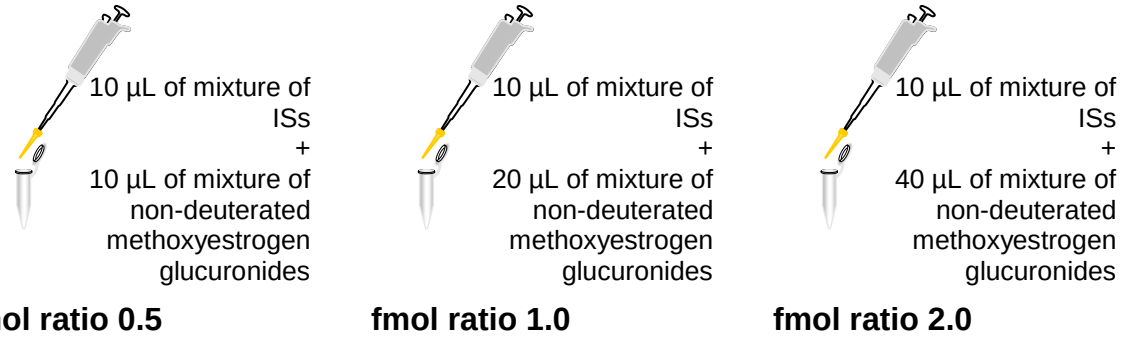

Figure 5: Schematic procedure for the spiking of plasma samples to reach ratios of fmol of no-deuterated methoxyestrogen glucuronides to fmol of deuterated methoxyestrogen glucuronides (in the mixture of ISs) of 0.5, 1.0 and 2.0.

Table 22: Pipetting scheme to prepare the mixture of methoxyestrogen glucuronides to reach ratios of fmol of no-deuterated to deuterated methoxyestrogen glucuronides (in the mixture ISs) of 0.5, 1.0 and 2.0.

Reference	Concentration of stock solution (pg/µL)	Volume of stock solution to the mix (µL)	Volume of mix added to the plasma (µL)	fmol added to the plasma	Ratios of fmol of the reference to that of its corresponding deuterated analog
2-MeO-E1-G	100	27.5	10	557	0.50
			20	1154	1.00
			40	2308	2.00
4-MeO-E1-G	10	34	10	71	0.49
			20	142	0.99
			40	284	1.98
2-MeO-E2-3G	100	14.5	10	303	0.50
			20	606	1.01
			40	1212	2.01
2-MeO-E2-17-G	100	46.5	10	972	0.50
			20	1943	1.00
			40	3887	2.01
4-MeO-E2-3G	100	11	10	230	0.51
			20	460	1.02
			40	919	2.05
4-MeO-E2-17-G	100	114	10	2382	0.50
			20	4765	1.00
			40	9529	2.00

3.2.10.4. Limit of detection and limit of quantification

Both limits of detection (LOD) and quantification (LOQ) levels were calculated in spiked plasma samples. The LOD was calculated as a concentration (fmol/mL) with a response of a signal to noise ratio (S/N) $\geq$ 3. For this, a mixture of deuterated methoxyestrogen glucuronides with the same concentration as in Table 18 (Chapter 3.2.7.2) was prepared and injected using the method 2 (Chapter 3.2.1.2). The calculations were performed using the following formula (where the noise was calculated using the script "S-to-N" from the Analyst software, Chapter 3.1.6):

$$\text{LOD (fmol/mL)} = \frac{\left(\frac{noise*3}{heigh\ of\ deuterated\ standard\ peak} * fmol\ of\ deuterated\ standard\right)}{V\ (mL)}$$

After the determination of the LOD levels for each methoxyestrogen glucuronide, the LOQ was established statistically as the maximum LOD, ensuring an S/N> 10 (Appendix A2.10).

3.2.10.5. Accuracy and precision

Both accuracy and precision were calculated in spiked plasma samples. The accuracy and precision of the method were calculated near the suggested LOQ level of each methoxyestrogen glucuronide (Complete data file available in the accompanying disc). For this purpose, a mixture containing fmol of each methoxyestrogen glucuronide near to their respective LOQ was prepared (Table 23). The methoxyestrogen glucuronides were pipetted together in a vial, then the mixture was evaporated at 30 mbar and dissolved in 200 µL MeOH. Samples were spiked with 20 µL of this mixture and 10 µL of the mixture of ISs. After the extraction procedure, plasma samples were injected using the method 2 (Chapter 3.2.1.2). The procedure was performed with 3 independent replicates, in 3 different days.

Table 23: Pipetting scheme to prepare the mix containing the fmol of each methoxyestrogen glucuronide near to the suggested LOQ level.

Reference	Concentration of stock solution (pg/µL)	Volume of stock solution (µL)	Concentration added to the plasma (fmol/mL)
2-MeO-E1-G	100	17	357
4-MeO-E1-G	50	15	157
2-MeO-E2-3G	100	15	313
2-MeO-E2-17-G	100	146	3051
4-MeO-E2-3G	100	22	430
4-MeO-E2-17-G	100	174	3636

The accuracy was calculated with the following formula:

Accuracy (%) = (calculated concentration / nominal concentration) * 100

The precision was calculated as the RSD with the following formula:

Precision (% RSD) = (SD/mean) * 100

3.2.10.6. Stability

3.2.10.6.1. Stability of stock solutions

A mixture with methoxyestrogen glucuronides was prepared with the same concentration described in Table 18 (Chapter 3.2.7.2). All references were pipetted together in a vial, evaporated and dissolved in 400 µL MeOH. Thereafter, 6 individual vials were prepared by pipetting 50 µL out of this mixture in each of them and evaporating them again. The first vial was dissolved in 50 µL ACN 5% and stored immediately at -20 °C as the reference or time 0 (t0). The other vials were also stored at -20 °C and were dissolved one per month until completing 5 months. When the last

vial was dissolved, all vials were injected and the stability (%) was calculated using as 100% the reference or t0 with the formula:

Stability (%) = (peak area at t_x *100) / raw peak area at t0

With t_x as the corresponding month.

3.2.10.6.2. Stability of samples in the autosampler

The stability of samples in the autosampler (4 °C) was tested in spiked plasmas (3 independent replicates) with a mixture containing certain fmol of each methoxyestrogen glucuronide (Table 24). The methoxyestrogen glucuronides were pipetted together in a vial, then the mixture was evaporated at 30 mbar and dissolved in 200 µL MeOH. Samples were spiked with 20 µL of this mixture and 10 µL of the mixture of ISs. After the extraction procedure, plasma samples were injected using the method 2 (Chapter 3.2.1.2), then left in the autosampler for 24 h and injected again. The stability (%) was calculated by comparing the fmol of non-deuterated methoxyestrogen glucuronides obtained at t0 with the fmol obtained after 24 h in the autosampler using the formula:

Stability (%) = (fmol found after 24 h * 100) / fmol found at t0.

Table 24: Pipetting scheme to prepare the mix of methoxyestrogen glucuronides to test the stability in plasma samples after 24 h stored in the autosampler.

Reference	Concentration of stock solution (pg/µL)	Volume of stock solution (µL)	Concentration added to the plasma (fmol/mL)
2-MeO-E1-G	100	22	462
4-MeO-E1-G	50	24	252
2-MeO-E2-3G	100	20	418
2-MeO-E2-17-G	100	168	3510
4-MeO-E2-3G	100	27	564
4-MeO-E2-17-G	100	197	4012

3.2.10.6.3. Stability of samples after freeze/thaw cycles

The stability after freeze/thaw cycles was tested in spiked plasma samples (3 independent replicates) with the same mixture described in Table 24. Samples were spiked with 20 µL of this mixture and 10 µL of the mixture of ISs. After the extraction procedure, plasma samples were injected using the method 2 (Chapter 3.2.1.2) and stored at -20° C. During 4 days, samples were thawed and frozen, one time per day. After the fourth day, samples were injected again and the stability (%) was calculated using as 100% the reference or t0 with the formula:

Stability (%) = (fmol found after the fourth day of freeze/thaw * 100) / fmol found at t0

3.2.11. Analysis of circulating estrogen profiles in women without breast cancer

3.2.11.1. Quantification of estrone, 17β-estradiol, hydroxyestrogens, and methoxyestrogens by means of GC-MS/MS

After extraction and derivatization, samples were analyzed by means of GS-MS/MS with a method previously established in our research group (Chapter 3.2.1.3). The quantification of the analytes was performed by someone else. The LOD and LOQ levels were also provided from other studies (Table 25).

Table 25: LOD and LOQ levels of E1, E2, hydroxyestrogens, and methoxyestrogens.

Metabolite	LOD (fmol/mL)	LOQ (fmol/mL)	Obtained from
E1	4	8	Samples derived from the Isocross study (*n* = 15)
E2	6	12	
2-MeO-E1	7	30	
2-MeO-E2	12	25	Samples derived from another study (*n* = 111)
4-MeO-E1	15	29	
4-MeO-E2	10	30	

3.2.11.2. Quantification of estrogen conjugates and methoxyestrogen glucuronides by means of UHPLC-MS/MS

After extraction and dissolution, samples were analyzed by means of UHPLC-MS/MS (Chapter 3.2.1.2). Each metabolite was identified by its t_R and the Qn/Ql ratio (Chapter 3.2.10.1.3). E1-S, E1-G, E2-3-S, E2-17-S, and E2-3-G were analyzed with a method previously established in our research group and the LOD and LOQ levels were provided from other studies (Table 26).

Table 26: LOD and LOQ levels of estrogen conjugates.

Metabolite	LOD (fmol/mL)	LOQ (fmol/mL)	Obtained from
E1-S	22	40	Samples derived from another study (*n* = 111)
E1-G	163	249	
E2-3-S	54	109	
E2-17-S	253	401	
E2-3-G	720	937	

E1-G

Quantification of E1-G was performed through the linear curve y = 0.00463x + 0.02589 and using the ratios of the peak areas of E1-G to that of E1-G-d4 (from 0.14 to 1.44). Nevertheless, if a ratio was < 0.137, quantification was performed by one-point calibration (the lowest one) as:

$$\text{E1-G (fmol/mL)} = \frac{\left(\frac{area\ E1-G}{\frac{area\ E1-G-d4}{0.137}} * 291.115\right)}{V\ (mL)}$$

And LOD levels were calculated with the response-factor of 1.64 as:

$$\text{E1-G LOD (fmol/mL)} = \frac{\frac{noise*3}{heigh\ of\ E1-G-d4\ peak} * \frac{1}{1.64} * fmol\ E1-G-d4}{V\ (mL)}$$

E1-S

Quantification of E1-S was performed using ratios of the peak areas of E1-S to that of E1-S-d4 and the fmol of E1-S-d4 (Table 20, Chapter 3.2.9.1).

E2-3-G

As no deuterated standard for this metabolite is available, quantification was performed by the rule of proportion using the peak areas of E1-G-d4 as:

$$\text{E2-3-G (fmol/mL)} = \frac{\left(\frac{E2-3-G}{\frac{area\ E1-G-d4}{0.758}} * 1561\ fmol\right)}{V\ (mL)}$$

E2-3-S

Quantification of E2-3-S was performed through the linear curve y = 0.01465x + 0.00348 and using the ratios of the peak areas of E2-3-S to that of E2-3-S-d4 (from 0.095 to 0.709). Nevertheless, if a ratio was < 0.095, quantification was performed by one-point calibration (the lowest one) as:

$$\text{E2-3-S (fmol/mL)} = \frac{\left(\frac{area\ E2-3-S}{\frac{area\ E2-3-s-d4}{0.095}} * 59.82\right)}{V\ (mL)}$$

And LOD levels were calculated with the response-factor of 0.6 as:

$$\text{E2-3-S LOD (fmol/mL)} = \frac{\frac{noise*3}{heigh\ of\ E2-3-S-d4\ peak} * \frac{1}{0.6} * fmol\ E2-3-S-d4}{V\ (mL)}$$

E2-17-S

As no deuterated standard for this metabolite is available, quantification was performed by the rule of proportion using the area of E2-3-S-d4 as:

$$\text{E2-17-S (fmol/mL)} = \frac{\left(\frac{area\ E2-17-S}{\frac{area\ E2-3-s-d4}{0.902}} * 694.5\right)}{V\ (mL)}$$

Methoxyestrogen glucuronides

Quantification of methoxyestrogen glucuronides (when present) was performed using ratios of the peak areas of the non-deuterated to that of the deuterated analogs and the fmol of the deuterated analogs (Table 20, Chapter 3.2.9.1). If no level was detected, a LOD was calculated as described in Chapter 3.2.10.4.

3.2.12. Statistics

Statistics were performed using the software Origin Pro, R studio and Valoo (Chapter 3.1.6). Data were graphically checked for normal distribution and variance homogeneity or using the Shapiro-Wilk test. For calibration curves, linearity and homoscedasticity were verified with Valoo. For comparison of 2 groups, t-Test (normally distributed) or paired Wilcoxon test (small sample size or non-normal distributed) were performed, and *p*-values were adjusted using the method of Holm in R. For comparison of a population with a reference value, single sample t-Test was performed. For the correlation analyses, rank-based Spearman correlation coefficient were performed using the R-scripts previously provided by the Chair of Mathematical Statistics with application in Biometrics of the University of Dortmund.

The R scripts used are the following:

- ***Correlation analysis***

```
corX <- rcorr(as.matrix(X[,c(1:5)]), type=c("spearman"))
X.r <- data.frame(cor Xt$r)
X.P <- data.frame(cor X$P)
write.table(X.r,' X _R.csv', sep=",")
write.table(X.P,' X _p.csv', sep=",")
```

With X as the group (pre- or postmenopausal women) to be correlated.

- ***p-values adjustment***

```
p.adjustment(method = “holm”,c(p-value 1, p-value n)
```

3.2.13. Literature research

For the search of scientific literature in our research group, it is recommended to use EndNote to build our library.

All the members of our group may have access to every library in the case that specific information is needed, or when a person is leaving the group, the reason why is also very important to document how the Library was built, by writing the next information:

- Research date
- Exact terms: “Key Words”
- The number of hits by using those “Key Words”
- The platform used: PubMed (NLM), LISTA (EBSCO), etc.

For the use, the “Key Words”, is necessary to consider how are they use in the literature. For example, when one term is made from two (e.g. diconjugates), it is necessary to perform the search with and without space (“di conjugates” and “diconjugates”).

The Library should be refresh at least once per year and with the tool “Find duplicates” keep only the new papers.

The documentation of the literature research can be consulted in the accompanying CD.

4. Results and discussion

In order to investigate the possibility to include methoxyestrogen glucuronides into an existing method for the analysis of estrogens in human plasma and breast tissue (including conjugates and metabolites) by means of GC- and UHPLC-MS/MS, compound references of methoxyestrogen glucuronides which are not commercially available were biosynthesized, identified and quantified (Chapter 4.1). Followed by the biosynthesis of the references, the selectivity and specificity, recovery, analytical response of references, limits of detection and quantification, accuracy, precision, and stability were determined with respect to the newly included analytes in human plasma. (Chapter 4.2). To determine the profiles of estrogens in human plasma from women without breast cancer, the extended UHPLC-MS/MS method was applied to the analysis of E1-S, E2-3/17-S, E1-G, E2-3-G, and methoxyestrogen glucuronides and the existing GC-MS/MS method was applied to the analysis of E1, E2 and their hydroxylated and methoxylated metabolites (Chapters 4.3-4.4).
Finally, the applicability of the extended method to the analysis of methoxyestrogen glucuronides in human breast GLT and ADT specimens derived from women without breast cancer was evaluated (Chapter 4.5).

4.1. Biosynthesis of methoxyestrogen glucuronide references and their corresponding deuterated analogues

Methoxyestrogen glucuronides are polar metabolites expected to be found in circulation (Chapter 1.2.4). Because of the important detoxifying role, the study of methoxyestrogen glucuronides through reliable analytical techniques is essential. Since compound references of methoxyestrogen glucuronides for method development and optimization and for quantification are not commercially available, the biosynthesis of these metabolites was required.

Thus, methoxyestrogen glucuronides and their corresponding deuterated analogues were biosynthesized and identified (Chapters 4.1.1-4.1.3). Then, biosynthesized references were quantified (Chapter 4.1.4) and the substance- and source-dependent

parameters were optimized for the use of the UHPLC-MS/MS method in the MRM negative mode (Chapter 4.1.5).

The method already established in our working group for the biosynthesis of E1-G was used as a reference. This method includes the use of microsomal fractions from rat liver which expresses considerable amounts of hepatic UGTs such as UGTA1 and UGTA3 (Daidoji et al., 2005) involved in the glucuronidation of methoxyestrogens (Chapter 1.2.4). However, regarding their specificity, UGTs can conjugate both E1, E2, and their oxidized derivates at different positions (Chapter 1.2.4, Table 5). Therefore, differences between the obtained amounts of biosynthesized methoxyestrogen glucuronides were expected.

4.1.1. Glucuronidation of 2- and 4-methoxyestrone and identification of the methoxyestrogen glucuronides

The method for the biosynthesis of 2-MeO-E1-G and 4-MeO-E1-G using 2-MeO-E1 and 4-MeO-E1 as substrate, respectively, was previously described (Chapter 3.2.2.1). Because of their molecular structure, glucuronidation of both molecules is only possible at position -3 where the hydroxy group is available (Figure 6). It has been reported that at least 6 different isoforms of the UGTs can catalyze the glucuronidation of 2-MeO-E1-G, and 5 different the glucuronidation of 4-MeO-E1-G (Chapter 1.2.4, Table 5), from which 2 of them, UGT1A1 and UGT1A3, are present in the microsomal fraction from both human and rat liver (Chen et al., 2018).

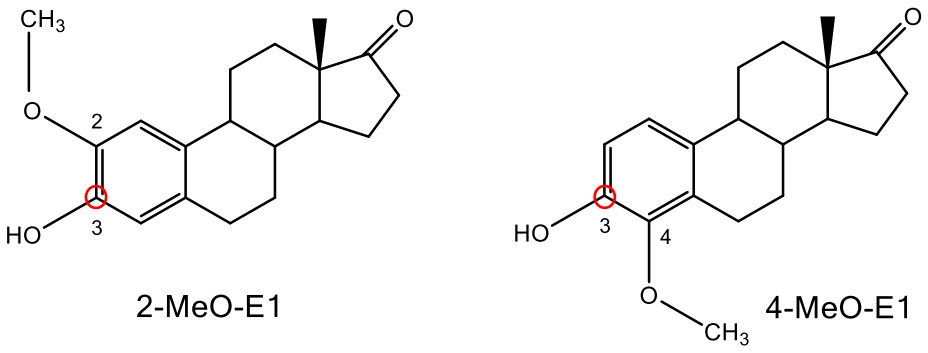

Figure 6: Chemical structure from 2-MeO-E1 and 4-MeO-E1, showing the hydroxy group available for glucuronidation at the position -3.

After biosynthesis, extraction, and injection of 2-MeO-E1-G (Method CONJUGATES40_60, Chapter 3.2.1.1), two peaks at 19 and 41 min were observed (Appendix A1.1). As the t_R of the peak of 2-MeO-E1 reference was 40 min, it can be concluded that the peak at 19 min corresponds to the 2-MeO-E1-G. In the case of 4-MeO-E1-G, two peaks at 24 and 40 min were observed (Appendix A1.2). Because the t_R of the peak of 4-MeO-E1 reference was 42 min (Appendix A1.2), it can be concluded that the peak at 24 min corresponds to the 4-MeO-E1-G. In both cases, this was further confirmed with the isolated reaction products (Chapter 3.2.2.1) through the ion fragments obtained by ePS (Chapter 3.2.1.2).

As an example, Figure 7 illustrates the collision-induced fragmentation of 2-MeO-E1-G, with some of the most abundant expected fragment ions.

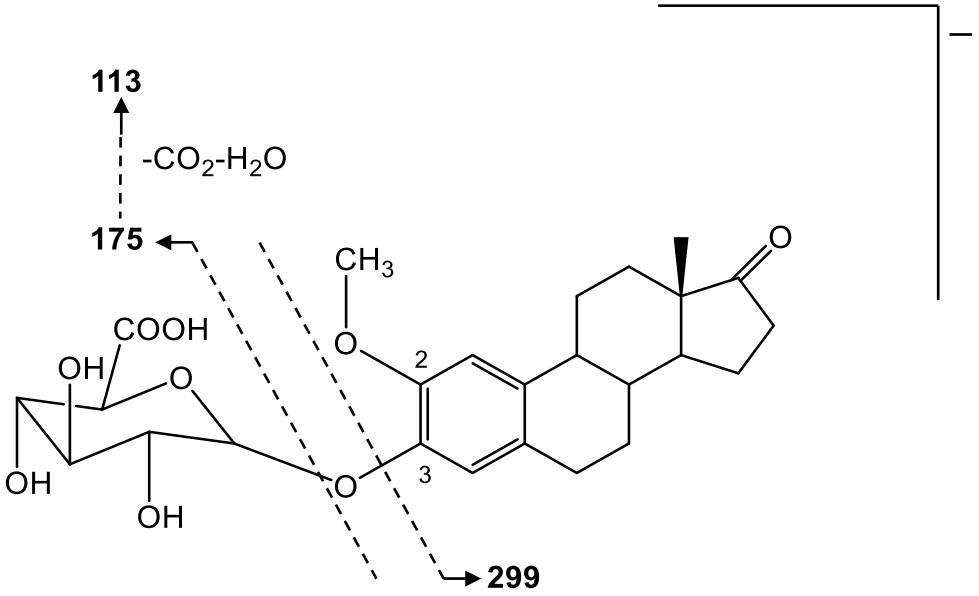

Figure 7: Collision-induced fragmentation of biosynthesized 2-MeO-E1-G (ESI in the MRM negative ion mode, CE = -20 V). Precursor ion $[M-H]^{--}$ = 475.

In the ePS of 2- and 4-MeO-E1-G, the 3 most abundant fragment ions for both molecules were (in order) m/z= 475, 175 and 113 (Appendices A1.3-A1.4). m/z = 475 corresponds to the parent ion $[M-H]^-$, but m/z = 175 was the key ion indicating the fragmentation of the molecule which gives the loss of the glucuronic acid attached at

the position -3. Finally, m/z = 113 indicates the subsequent loss of the carboxyl group from the glucuronic acid.

After identification of the chromatographic peaks, all biosynthesized products were collected together (Chapter 3.2.2.1) and stored at -20 °C until quantification (Chapter 3.2.5.1.1).

4.1.2. Glucuronidation of 2- and 4-methoxyestradiol and identification of the methoxyestrogen glucuronides and the position of the glucuronidation

The method for the biosynthesis of 2-MeO-E2-3-G, 2-MeO-E2-17-G, 4-MeO-E2-3-G and 4-MeO-E2-17-G using 2-MeO-E2 and 4-MeO-E2 as substrate, was previously described (Chapter 3.2.2.2). Glucuronidations of 2- and 4-MeO-E2 are possible either at position -3 or position -17 where the hydroxy groups are available (Figure 8). Furthermore, experiments conducted by Lepine et al. (2004) with HK293 cells and similar conditions to the biosynthesis here performed, concluded that the glucuronidation of estrogens at position -3 was predominant over the position -17 (Chapter 1.2.4, Table 5). Thus, as a first insight, it was hypothesized that biosynthesis of products glucuronidated at position -3 will be predominant over those glucuronidated at position -17.

The biosynthesis of both 2-MeO-E2-3-G and -17-G was performed by a master student within our research group and in both cases, a blank was performed in parallel.

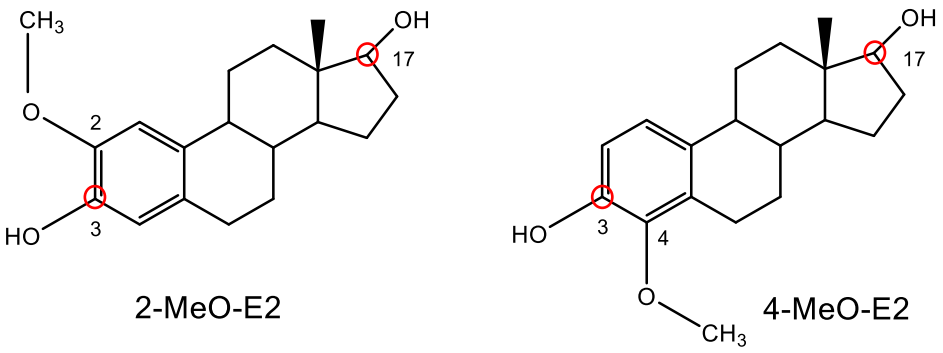

Figure 8: Chemical structure from 2-MeO-E2 and 4-MeO-E2, showing the hydroxy groups available for glucuronidation at the position -3 and -17.

After biosynthesis, extraction, and injection of the reaction products of 2-MeO-E2 (Method CONJUGATES40_60, Chapter 3.2.1.1), 3 main peaks at 13, 20 and 35 min were observed (Appendix A1.5). As the t_R of the peak of 2-MeO-E2 in the blank of the biosynthesis was 34 min (Appendix A1.5) it can be concluded that the peaks at 13 and 20 min are the biosynthesized conjugates. Then, the assignment of the glucuronidation position of both peaks was performed with the isolated reaction products (Chapter 3.2.2.2) through the ion fragments from their structures obtained by ePS (Chapter 3.2.1.2). As a first insight, due to findings in the literature, it was expected that the chromatographic peak with the highest area (13 min) corresponds to 2-MeO-E2-3-G.

To identify the position of glucuronidation, both mass spectra (Appendices A1.6-A1.7) were compared between them and the literature from Gentili et al. (2002) which conducts also an ePS scan in the negative mode for the investigation of different estrogen metabolites. Gentili et al. (2002) investigated the estrogen glucuronides but not the methoxyestrogen glucuronides. Then for a proper comparison, m/z = 30 which corresponds to the mass of the methoxyl group was added to the precursor and other fragment ions.

As in the case of 2- and 4-MeO-E1-G, the ions m/z = 175 and 113, indicate the fragmentation of the molecule which gives the loss of the glucuronic acid and the subsequent loss of the carboxyl group. Furthermore, a comparison of the mass spectra of the isolated peak at 13 min (Appendix A1.6) with the spectra of E2-3-G and E2-17-G from Gentili et al. (2002), shows in parallel the fragments m/z = 477.0, 301.0 and 113.0. Comparing the mass spectra of the isolated peak at 20 min (Appendix A1.7) with the spectra of E2-3-G and E2-17-G from Gentili et al. (2002), the fragments m/z= 477.0 and 301.0 were also comparable.

At this point, comparing both isolated peaks with the literature gave only the confirmation about the structure, but still, the identification of the glucuronidation position was missing. Nevertheless, a comparison between mass spectra from both isolated peaks at 13 and 20 min have shown that the fragments m/z = 340.3 and 355.0 showed up only in for the peak at 20 min. Through analysis of the structure after collision-induced fragmentation, these fragments are seen only when the molecule has been conjugated at the position -17 (Figures 9A-B), confirming the theory that the isolated peak at 20 min corresponds to the 2-MeO-E2-17-G.

In the case of the reaction products of 4-MeO-E2, after biosynthesis, extraction and injection (Method CONUUGATES50_50, Chapter 3.2.1.1), 3 main peaks at 16, 17 and 33 min were observed (Appendix A1.8). As the t_R of the peak of 4-MeO-E2 in the blank of the biosynthesis was 32 min (Appendix A1.8), it can be concluded that the peaks at 16 and 17 min were the biosynthesized conjugates.

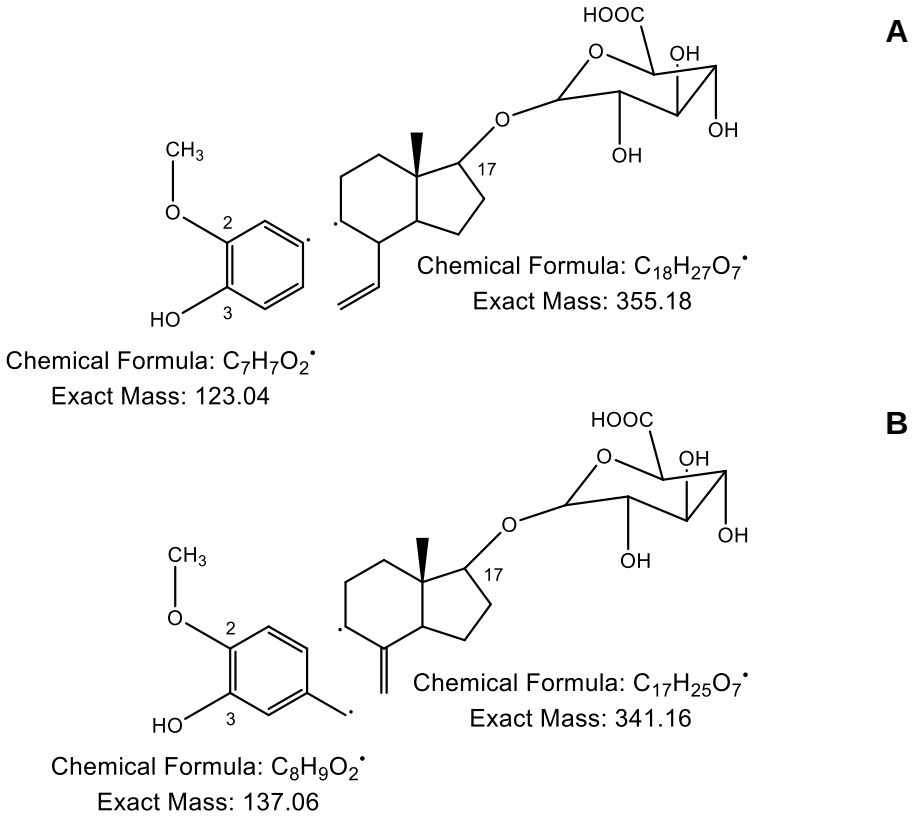

Figure 9: Collision-induced fragmentation of biosynthesized 2-MeO-E2-17-G (ESI in the negative ion mode, CE = -40 V), showing the fragment ions m/z = 341 Da (A) and m/z = 355 Da (B).

The confirmation of the structure and identification of the glucuronidation position for the 4-MeO-E2-conjugates were conducted in the same way as for the 2-MeO-E2-conjugates conjugates and performed by a master student within our research group. In a coordinated work, it was concluded that the isolated peak at 17 min corresponds to the 4-MeO-E2-3-G (Appendix A1.9), and the isolated peak at 16 min corresponds to the 4-MeO-E2-17-G (Appendix A1.10).

After identification of the chromatographic peaks, all biosynthesized products were collected together (Chapter 3.2.2.2) and stored at -20 °C until quantification (Chapter 3.2.5.1.1).

4.1.3. Biosynthesis of deuterated methoxyestrogens glucuronides

The existing method for the analysis of estrogen conjugates involves the use of ISs (deuterated analogues) to spike the plasma samples (Chapter 3.2.9, Table 20). Therefore, for the extended method, the biosynthesis of deuterated methoxyestrogen glucuronides was required. Deuterated methoxyestrogens to perform the glucuronidation are not commercially available, consequently, the methylation of deuterated hydroxyestrogens to deuterated methoxyestrogens was first performed. For this, a method already established in our working group for the methylation of deuterated hydroxyestrogens and using the cytosolic fraction from rat liver was applied as a reference (Chapter 3.2.4). The methylation occurs through the addition of a methyl group derived from the SAM and catalyzed by the COMT, which is mainly located in the liver cytosols (Chapter 1.2.2).

4.1.3.1. Methylation of deuterated hydroxyestrogens

The method for the methylation of 2-HO-E1-d4, 4-HO-E1-d4, 2-HO-E2-d3, and 4-HO-E2-d3 using the cytosolic fraction from rat liver was previously described (Chapters 3.2.4.1-3.2.4.2). In all cases, blanks were performed in parallel.

After biosynthesis, extraction and injection of the reaction products (method METHOXYE1_E2, Chapter 3.2.1.1), 2-methoxyestrone-1, 4, 16, 16-d4 (2-MeO-E1-d4); 4-methoxyestrone-1, 2, 16, 16-d4 (4-MeO-E1-d4); 2-methoxyestradiol-16, 16, 17-d3 (2-MeO-E2-d3) and 4-metoxyestradiol-16, 16, 17-d3 (4-MeO-E2-d3) were identified in the chromatogram using the t_R of the peaks of the non-deuterated analogues (2- and 4-MeO-E1 and 2- and 4-MeO-E2, 80 µM in MeOH), and by the t_R of the peaks observed in the blanks of the biosynthesis containing 2- or 4-HO-E1, or 2- or 4-HO-E2, regarding the substrate in question, at a concentration of 100 µM in the incubation probe. The

identity of the products based on the t_R of the chromatographic peaks (Appendices A1.11-A1.14) is summarized in Table 27.

Table 27: Identification of deuterated methoxyestrogens by the t_R of the peaks of the corresponding methoxyestrogen reference (80 µM) and by the t_R of the peak of the corresponding hydroxyestrogen (100 µM) observed in the blank of the biosynthesis. t_R, retention time.

Expected molecule	t_R (min) of peaks in the chromatogram of the biosynthesis	t_R (min) of 2- or 4-MeO-E1 / 2- or 4-MeO-E2	t_R (min) of 2- or 4-HO-E1 / 2- or 4-HO-E2 in the blank	Conclusion
2-MeO-E1-d4	1-> 28 2-> 30	28	15	The peak at 28 min correspond to the 2-MeO-E1-d4
4-MeO-E1-d4	1-> 17 2-> 28	28	17	The peak at 28 min correspond to the 4-MeO-E1-d4
2-MeO-E2-d3	1-> 33 2-> 36	34	22	The peak at 33 min correspond to the 2-MeO-E2-d3
4-MeO-E2-d3	1-> 31 2-> 36	32	18	The peak at 31 min correspond to the 4-MeO-E2-d3

Once the reaction products were identified, they were manually collected (Chapters 3.2.4.1-3.2.4.2) and quantified stock solutions of 2-MeO-E1-d4 (40.80-51.37 µM), 4-MeO-E1-d4 (31.61-53.93 µM), 2-MeO-E2-d3 (37.65-41.00 µM), and 4-MeO-E2-d3 (40.45-42.87 µM) were prepared (calculations available in Appendix A1.15) to further glucuronidation (Chapter 4.1.3.2).

4.1.3.2. Glucuronidation of the biosynthesized deuterated methoxyestrogens

After the biosynthesis of deuterated methoxyestrogens, the glucuronidation was performed in the same way as for their non-deuterated analogues with the method previously described (Chapter 3.2.4.3). As the obtained stock solutions of deuterated methoxyestrogens varied in amount and concentration (Appendix A1.15), for each glucuronidation was taken a volume that ensured 50 mmol in the reaction probe, which were the same mmol present in the 250 µL of the reaction probe for the glucuronidation of the non-deuterated analogues (Chapters 3.2.2.1-3.2.2.2). In all cases, blanks were performed in parallel.

After the biosynthesis, extraction, and injection of the reaction products (method CONJUGATES40_60 for 2-methoxy products and method CONJUGATES50_50 for 4-methoxy products, Chapter 3.2.1.1), deuterated methoxyestrogen glucuronides were identified in the chromatogram using the t_R of the peaks of the methoxy references 80 µM in MeOH (2- and 4-MeO-E1 and 2- and 4-MeO-E2), and by the t_R of the peaks observed in the blanks of the biosynthesis containing 2- or 4-MeO-E1, or 2- or 4-MeO-E2, regarding the substrate in question, at a concentration of 200 µM in the incubation probe. As deuterated- and non-deuterated methoxyestrogens are analogue molecules, the identification of the reaction products was also supported by the t_R of the peaks of the non-deuterated methoxyestrogen glucuronides (Chapters 4.1.1-4.1.2). The identity of the products based on the t_R of the chromatographic peaks (Appendices A1.16-A1.19) is summarized in Table 28.

After identification of the chromatographic peaks, all biosynthesized products were collected together (Chapter 3.2.4.3) and stored at -20 °C until quantification (Chapter 4.1.4).

Table 28: Identification of deuterated methoxyestrogen glucuronides by the t_R of the peaks of the corresponding methoxyestrogen reference (80 µM) and by the t_R of the peak of the corresponding methoxyestrogen (200 µM) observed in the blank of the biosynthesis. t_R, retention time.

Expected molecule	t_R (min) of the peaks in the chromatogram of the biosynthesis	t_R (min) of 2- or 4-MeO-E1 / 2- or 4-MeO-E2	t_R (min) of 2- or 4-MeO-E1 / 2- or 4-MeO-E2 in the blank	Conclusion
2-MeO-E1-G-d4	1-> 15 2-> 21	34	1-> 22 2-> 33	The peak at 15 min correspond to the 2-MeO-E1-G-d4
4-MeO-E1-G-d4	1-> 20 2-> 38	37	38	The peak at 20 min correspond to the 4-MeO-E1-G-d4
2-MeO-E2-3-G-d3 and 2-MeO-E2-17-G-d3	1-> 16 2-> 24 3-> 40	42	40	The peak at 16 min correspond to the 2-MeO-E2-3-G-d3 and at 24 to 2-MeO-E2-17-G-d3
4-MeO-E2-3-G-d3 and 4-MeO-E2-17-G-d3	1-> 20 2-> 24 3-> 27 4-> 29 5-> 45	46	45	The peak at 29 min correspond to the 4-MeO-E2-3-G-d3 and at 27 to 4-MeO-E2-17-G-d3

4.1.4. Quantification of biosynthesized references

Since methoxyestrogen glucuronides are not commercially available, a quantification method for the amount of the biosynthesized references to prepare the stock/work solutions was required. Hence, two different methods were assessed:

(A) Using the difference in the absorbance of the chromatographic peaks between the unconjugated and conjugated estrogens (commercially available) (Chapter 4.1.4.1). This quantification method consisted of determining the peak area ratio (ratio factor) of free E1 or E2 to their corresponding glucuronides at position 3- or 17- (E1/E1-G; E2/E2-3-G and E2/E2-17-G) at each point of the calibration curve. The peak areas of the biosynthesized methoxyestrogen glucuronides were multiplied by this ratio factors and the obtained values were introduced into the calibration curve of their corresponding methoxyestrogen to have the concentration in the solution of biosynthesized product.

(B) Through enzymatic hydrolysis of the conjugates to their unconjugated form. This method consists of hydrolyzing back a glucuronide to its unconjugated form by enzymatic reaction with β-glucuronidase (e.g. E2-3-G → E2) (Chapter 4.1.4.2). If the amount of initial glucuronide is known, the amount of unconjugated product after hydrolysis should be also known (expected) and can be quantified using a calibration curve with E1 as the internal standard, due to the structural similarity with E2.

4.1.4.1. Quantification through the ratio factor

The ratio factors were built through five-point calibration curves (each of them 3 times independently) of the mentioned E1/E1-G (Chapter 3.2.5.1.1; Appendices A1.20-A1.21), E2/E2-3-G (Chapter 3.2.5.1.2; Appendices A1.22-A1.23) and E2/E2-17-G (Chapter 3.2.5.1.2; Appendices A1.24-A1.25). After, the mean ratio factors were calculated for each analyte (summarized in Table 29).

Table 29: Ratio factors E1/E1-G, E2/E2-3-G, and E2/E2-17-G obtained through five-point calibration curves, each of them 3 times (*n* = 15).

	E1/E1-G	E2/E2-3-G	E2/E2-17-G
Ratio factor (mean)	1.70	1.80	1.07
SD	0.01	0.03	0.01
RSD (%)	0.74	1.68	0.51

The similarity in the ratios between conjugates on which glucuronidation occurs at the position 3- (1.70 and 1.80) may be possible due to the conjugation direct on the chromophore of the molecule, different in the case of glucuronidation at position 17- which has no influence on the chromophore, giving a smaller ratio value (1.10).

With these ratios, the next step was to construct the calibration curves of the respective non-deuterated methoxyestrogens. Thus, five-point calibration curves of 2-MeO-E1 (Chapter 3.2.5.1.1; Appendices A1.26-A1.27), 4-MeO-E1 (Chapter 3.2.5.1.1; Appendices A1.28-A1.29), 2-MeO-E2 (Chapter 3.2.5.1.2; Appendices A1.30-A1.31) and 4-MeO-E2 (Chapter 3.2.5.1.2; Appendices A1.32-A1.33), were constructed, each of them as a mean of the 3 independent calibration curves.

With the ratio factor and the methoxyestrogen calibration curves, the identified, isolated and stored references were quantified as described in Chapters 3.2.5.1.1-3.2.5.1.2. The quantifications are summarized in Table 30 and the detailed calculation procedure can be found in Appendix A1.34.

Table 30: Quantified solutions of biosynthesized references using the ratio factor.

Biosynthesized reference	Volume available (µL)	Corresponding ratio factor	Corresponding calibration curve	Concentration of biosynthesized reference (µM)
2-MeO-E1-G	904.2	1.70	2-MeO-E1,	114.54
2-MeO-E1-G-d4	580.2		y=0.21787x-4.73051	76.17
4-MeO-E1-G	539.0		4-MeO-E1,	87.30
4-MeO-E1-G-d4	362.3		y=0.09705x+2.93642	73.77
2-MeO-E2-3-G	2270.0	1.80	2-MeO-E2,	92.39
2-MeO-E2-3-G-d3	1797.3		y=0.23647x-3.14305	75.12
4-MeO-E2-3-G	450.0		4-MeO-E2,	95.34
4-MeO-E2-3-G-d3	180.1		y=0.10387x-7.44091	59.77
2-MeO-E2-17-G	660.0	1.07	2-MeO-E2,	88.31
2-MeO-E2-17-G-d3	340.3		y=0.23647x-3.14305	42.89
4-MeO-E2-17-G	450.0		4-MeO-E2,	48.03
4-MeO-E2-17-G-d3	219.1		y=0.10387x-7.44091	47.98

With the available volume of the solutions after quantification and their respective concentrations (Table 30), the amount (µg) of each reference was calculated (Appendix A1.34) and illustrated in Figure 10.

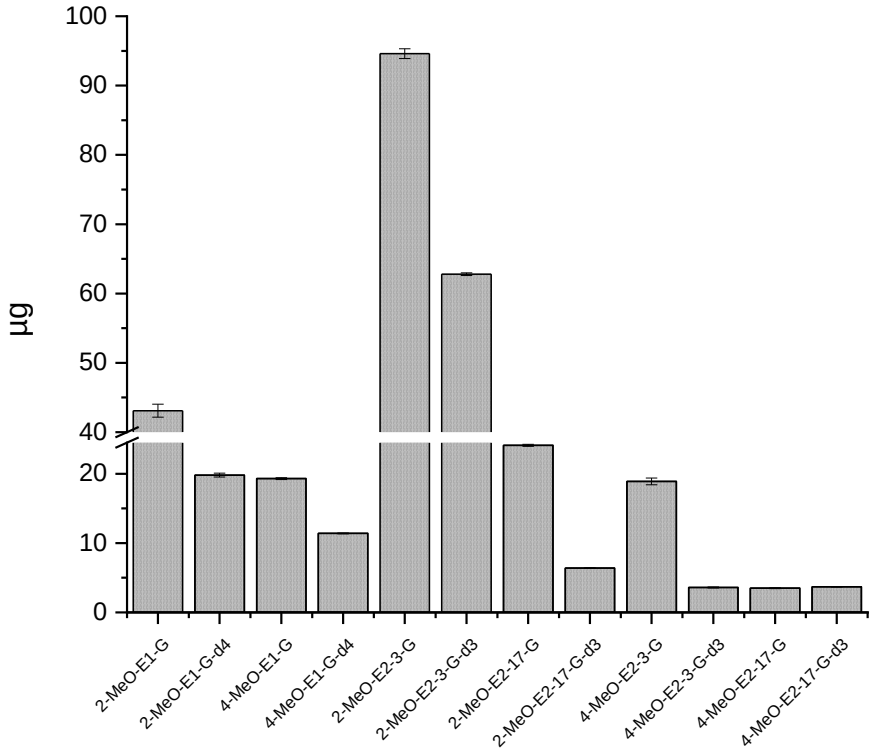

Figure 10: Amount (µg ± SD) of biosynthesized references.

The biosynthesized amounts of (deuterated)-methoxyestrogen glucuronides between 3.45 µg (4-MeO-E2-17-G-d3) and 94.61 µg (2-MeO-E2-3-G) (Appendix A1.34), were sufficient for further analyses.

4.1.4.2. Quantification through enzymatic hydrolysis

If the quantification using the ratio factor is correct (Chapter 4.1.4.1), the calculated nmol of methoxyestrogen glucuronides should remain constant after hydrolysis to their original form. Yet, even when quantification through enzymatic hydrolysis is a time-consuming method, it was necessary to prove that the quantification of biosynthesized references using the ratio factor was correct. Since the amount of biosynthesized references is very limited, the hydrolysis method was optimized with E2-3-G which is commercially available (Chapter 4.1.4.2.1) and then performed only with biosynthesized 2-MeO-E2-3-G (Chapter 4.1.4.2.2).

4.1.4.2.1. Optimization of the hydrolysis method using 17β-estradiol-3-glucuronide

The hydrolysis method of E2-3-G to E2 using β-glucuronidase from the bovine liver according to Xu et al. (2005), was previously described (Chapter 3.2.5.2.1). After hydrolysis, extraction, and purification through SPE, the reaction product was analyzed by means of HPLC-UV/Vis (method CONJUGATES50_50, Chapter 3.2.1.1). Nevertheless, the quantification of E2 was not possible due to a big matrix peak at the same t_R (Figure 11). Because E2-3-G was not 100% hydrolyzed, an alternative way was to quantify it (small peak Figure 11A) and then calculate the fmol of E2 by difference (fmol added of E2-3-G – fmol remaining after hydrolysis of E2-3-G = fmol of E2).

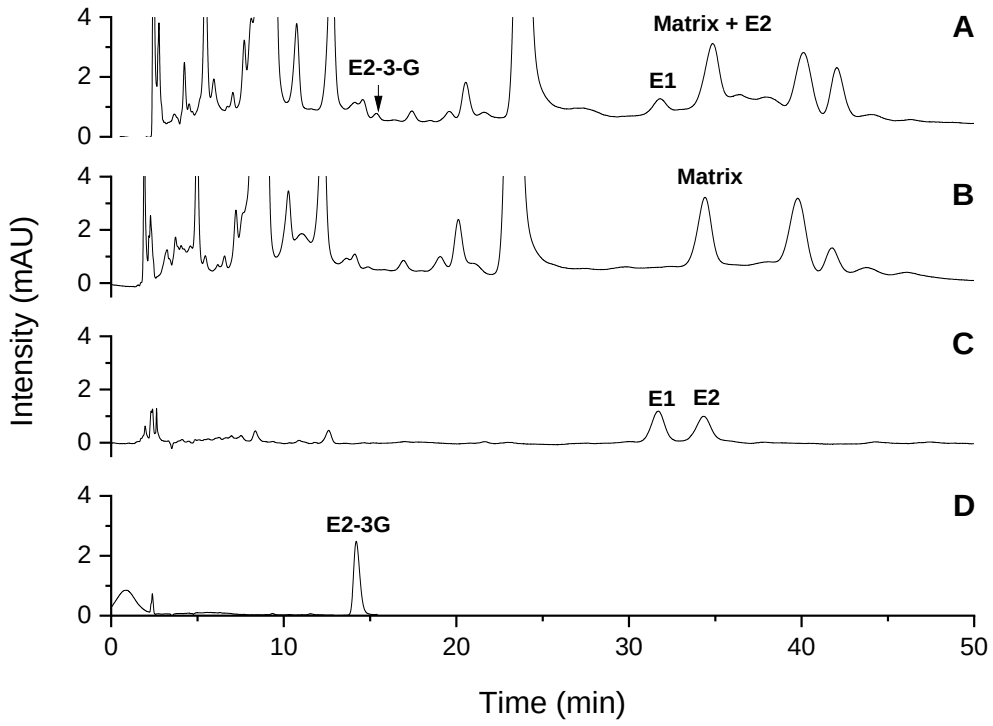

Figure 11: HPLC-UV/Vis chromatogram after hydrolysis of E2-3-G (A); a blank of the hydrolysis showing the matrix peak at the same t_R of E2 (B); a mix reference of E1+E2 30 µM (C) and a reference of E2-3-G 150 µM (D). The measurement was performed using the method CONJUGATES50_50 (Chapter 3.2.1.1).

The remaining E2-3-G, identified by the t_R of the peak of a reference of E2-3-G 150 µM (Figure 11A), was manually isolated and collected through HPLC separation (method CONJUGATES50_50, Chapter 3.2.1.1) to be evaporated and freeze-dried overnight. After isolation, the E2-3-G was identified and quantified by means of UHPLC-MS/MS via a one-point calibration. For this purpose, an E2-3-G reference was dissolved until a concentration which gives an area approx. near to the area of the isolated E2-3-G from the hydrolysis (3.1 x 10^4 counts). Then, the E2-3-G reference dissolved until 64 nM, gave an area of 3.4 x 10^5 counts. Through this single point, the remaining E2-3-G has a concentration of 20.9 nM (contains 3.48 pmol, Appendix A1.35). This means that from the initial 3000 pmol used for the hydrolysis (40 µL of solution 75 µM, Chapter 3.2.5.2.1), 0.1% was not hydrolyzed, giving a hydrolysis value of 99.9% (Appendix A1.35).

4.1.4.2.2. Hydrolysis of 2-methoxyestradiol-3-glucuronide

Once the hydrolysis method with E2-3-G was optimized (Chapter 4.1.4.2.1), biosynthesized 2-MeO-E2-3-G was hydrolyzed using β-glucuronidase from the bovine liver with the method previously described (Chapter 3.2.5.2.2). After extraction and SPE purification, the reaction product was analyzed via HPLC-UV/Vis. Nevertheless, the hydrolysis product (2-MeO-E2) identified by the t_R of the peak of a reference 2-MeO-E2, was too small to be quantified in a calibration curve (Figure 12A).

To overcome this, 20 µL of the hydrolysis product were spiked with 20 µL of a mix reference of 2-MeO-E2 30 µM + E1 50 µM to enhance the concentration of 2-MeO-E2. As a result, the peak of 2-MeO-E2 had an area that can be used for quantification through a calibration curve (Figure 13A).

Thereby, quantification of 2-MeO-E2 after hydrolysis was performed by using a seven-point extern calibration curve of 2-MeO-E2 with E1 50 µM as internal standard (Chapter 3.2.5.2.2, Appendices A1.36-A1.37). In this way, the calculated concentration of 26.9 µM gave a recovery of 128.2%, which means 28% was over-quantified using this method (Appendix A1.38).

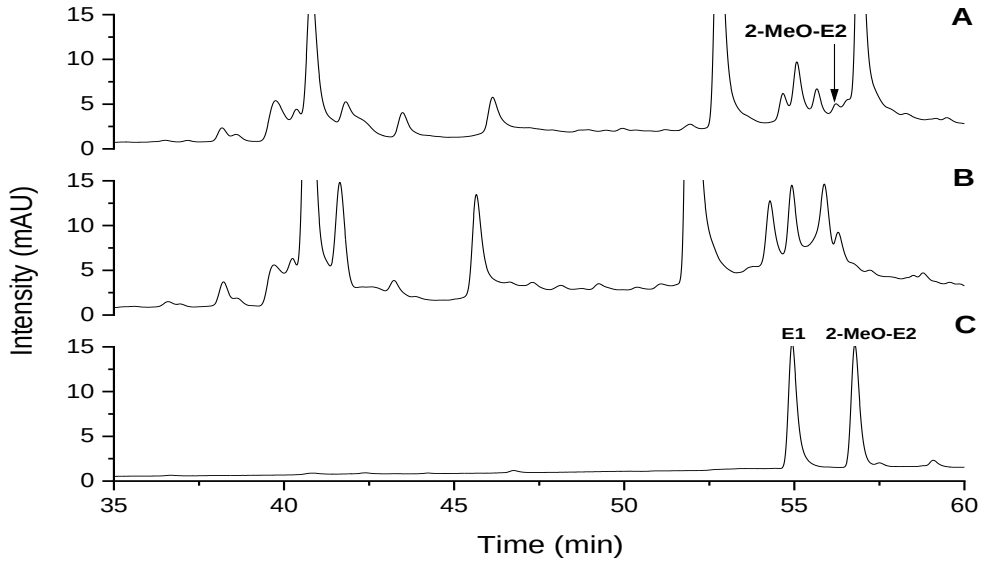

Figure 12: HPLC-UV/Vis chromatogram after hydrolysis of 2-MeO-E2-3-G (A); a blank of the hydrolysis (B) and a mix reference of 2-MeO-E2 30 µM + E1 50 µM. The measurement was performed using the method CONJUGATES_GRAD8 (Chapter 3.2.1.1).

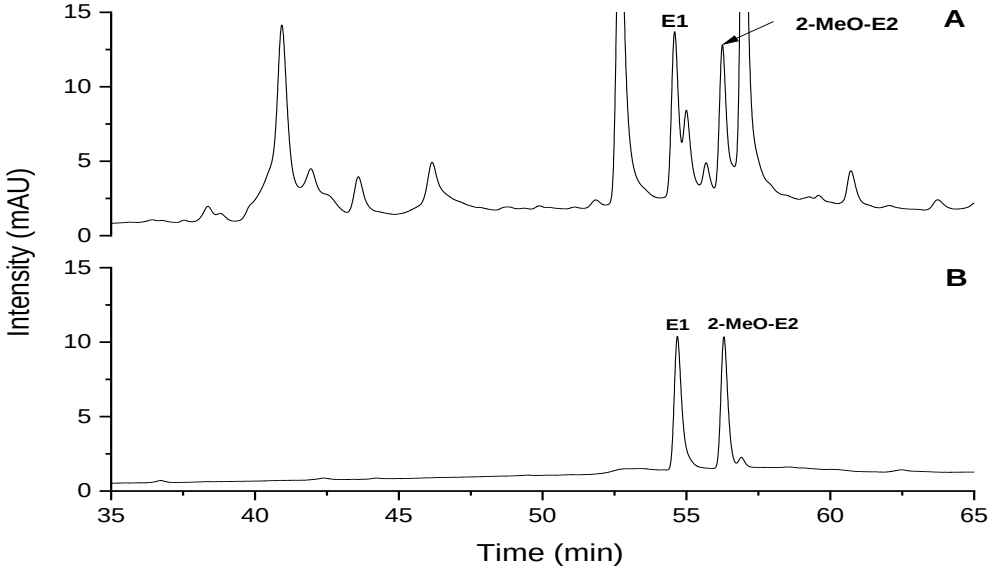

Figure 13: HPLC-UV/Vis chromatogram of the hydrolysis of 2-MeO-E2-3-G after spiking (A) and a mix reference of 2-MeO-E2 30 µM + E1 50 µM (B). The measurement was performed using the method CONJUGATES_GRAD8 (Chapter 3.2.1.1).

4.1.5. Optimization of the substance-dependent and source-dependent parameters for the *Multiple Reaction Monitoring* method

An existing UHPLC-MS/MS method in MRM negative mode for the sensitive and specific detection and quantification of estrogen conjugates was extended by the analysis of methoxyestrogen glucuronides. Therefore, the substance-dependent (dependent on the analyte) and source-dependent parameters (influenced by the LC conditions) were optimized with respect to the newly included analytes. In this measurement mode, a deprotonated ion with a specific m/z ratio is selected in Q1 and then fragmented in Q2 (the collision cell). Subsequently, only one fragment ion (product ion) with a specific m/z ratio passes through Q3, which is detected in the detector (Figure 14).

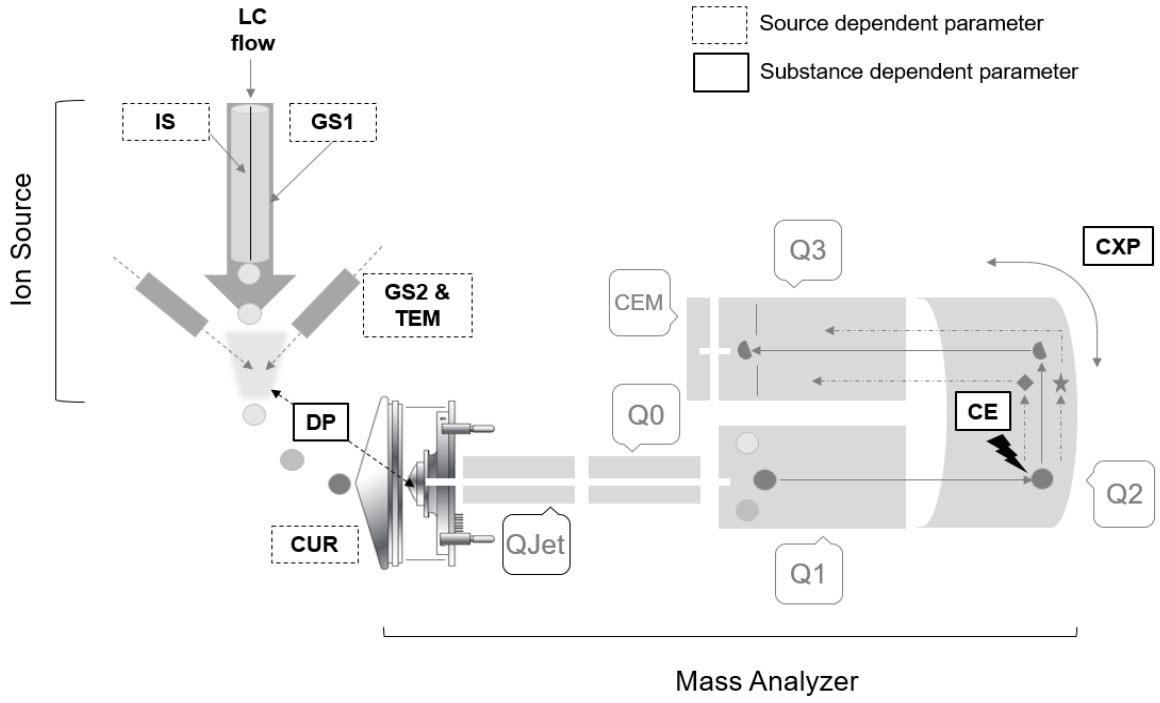

Figure 14: Illustration of the setup of the ESI ion source and the mass analyzer of the ESI-MS/MS system (Chapter 3.1.1). For the use of the MRM method, the substance-dependent parameters (continues black squares, declustering potential (DP), collision energy (CE), cell exit potential (CXP)), and the source- dependent parameters (dashed black squares, curtain gas (CUR), Ion spray voltage (IS), nebulizer gas (GS1), temperature (TEM) and turbogas (GS2)) were optimized. Q, quadrupole; CEM, Continuous Electron Multiplier.

4.1.5.1. Substance-dependent parameters

The substance-dependent parameters were optimized individually through *Automatic Compound Optimization* as described in Chapter 3.2.7.1. For all conjugates, 4 fragments were selected. The optimized substance-dependent parameters of CE and CXP with a pre-optimized DP are summarized in Table 31.

Table 31: Substance-dependent parameters for the most intensive fragment ions of biosynthesized methoxyestrogen glucuronides. m/z, mass charge ratio; DP, declustering potential; CE, collision energy; CXP, cell exit potential.

Conjugate	Precursor m/z (Da)	DP (V)	Fragments m/z (Da)	CE (V)	CXP (V)
2-MeO-E1-G	475	-25	117.0	-12	-5
			113.0	-26	-17
			284.1	-56	-13
			89.0	-44	-43
4-MeO-E1-G	475	-20	117.0	-12	-9
			89.0	-18	-11
			137.0	-10	-11
			284.1	-50	-19
2-MeO-E2-3-G	477	-30	113.0	-28	-9
			286.1	-56	-25
			135.0	-32	-13
			221.0	-24	-19
2-MeO-E2-17-G	477	-45	113.0	-32	-9
			301.2	-36	-21
			135.0	-20	-11
			74.9	-70	-11
4-MeO-E2-3-G	477	-65	113.0	-28	-7
			286.1	-54	-15
			174.9	-24	-23
			285.2	-76	-29
4-MeO-E2-17-G	477	-5	113.0	-32	-17
			301.1	-36	-21
			74.9	-70	-13
			286.0	-48	-31

The two fragments with the highest intensity were selected, with the first most intensive as the Qn (for quantification) and the second as the Ql (for identification through the unique ratio Qn/Ql). Subsequently, the substance-specific parameters were enhanced and established for both Qn and Ql (Table 32).

Table 32: Substance-dependent parameters for the Qn and Ql of biosynthesized references in MRM negative mode. t_R, retention time, DP, declustering potential; Q, quadrupole; CE, collision energy; CXP, cell exit potential, Qn. quantifier; Ql, qualifier.

Conjugate	t_R (min)	DP (V)	Q1 (m/z)	Q3 (m/z)	CE (V)	CXP (V)	$\frac{Qn}{Ql}$
2-MeO-E1-3G	2.64±0.20	-25	475.1	112.9	-26	-17	1.7
				283.9	-56	-13	
2-MeO-E1-3G-d_4	2.18±0.30		479.1	112.9	-26	-17	1.5
				288.0	-56	-13	
4-MeO-E1-3G	4.00±0.31	-25	475.1	112.9	-26	-17	2.2
				283.9	-56	-13	
4-MeO-E1-3G-d_4	3.22±0.46		479.1	112.9	-26	-17	1.9
				288.0	-56	-13	
2-MeO-E2-3G	1.57±0.12	-30	477.1	113.0	-28	-9	1.5
				286.1	-56	-25	
2-MeO-E2-3G-d_3	1.36±0.16		480.1	113.0	-28	-9	1.5
				289.1	-56	-25	
2-MeO-E2-17G	3.02±0.23	-30	477.1	113.0	-28	-9	1.4
				301.2	-36	-21	
2-MeO-E2-17G-d_3	2.47±0.35		480.1	113.0	-28	-9	1.2
				304.1	-36	-21	
4-MeO-E2-3G	3.39±0.26	-30	477.1	113.0	-28	-9	1.9
				286.1	-56	-25	
4-MeO-E2-3G-d_3	2.83±0.41		480.1	113.0	-28	-9	1.8
				289.1	-56	-25	
4-MeO-E2-17G	2.21±0.17	-30	477.1	113.0	-28	-9	1.3
				301.2	-36	-21	
4-MeO-E2-17G-d_3	1.84±0.24		480.1	113.0	-28	-9	1.1
				304.1	-36	-21	

4.1.5.2. Source-dependent parameters

After the optimization of the substance-dependent parameters, the source-dependent parameters were also optimized using a mixture of all biosynthesized references (Chapter 3.2.7.2) and the method 2 in MRM negative mode (Chapter 3.2.1.2). Thus, the Gas 1 (GS1, nebulizer gas), Gas 2 (GS2, turbogas), temperature (TEM) and IS were optimized at 3 different levels (each), using the curtain gas flow (CUR) at 35 psi (Table 19, Chapter 3.2.7.2). The mixture was injected 12 times (3 levels for all 4 optimized parameters, Appendix A1.39), and the combination with the most intensive peak areas (Figure 15) was selected: source temperature 550 °C, GS1 = 60 psi, GS2 = 70 psi and IS = -3500 V.

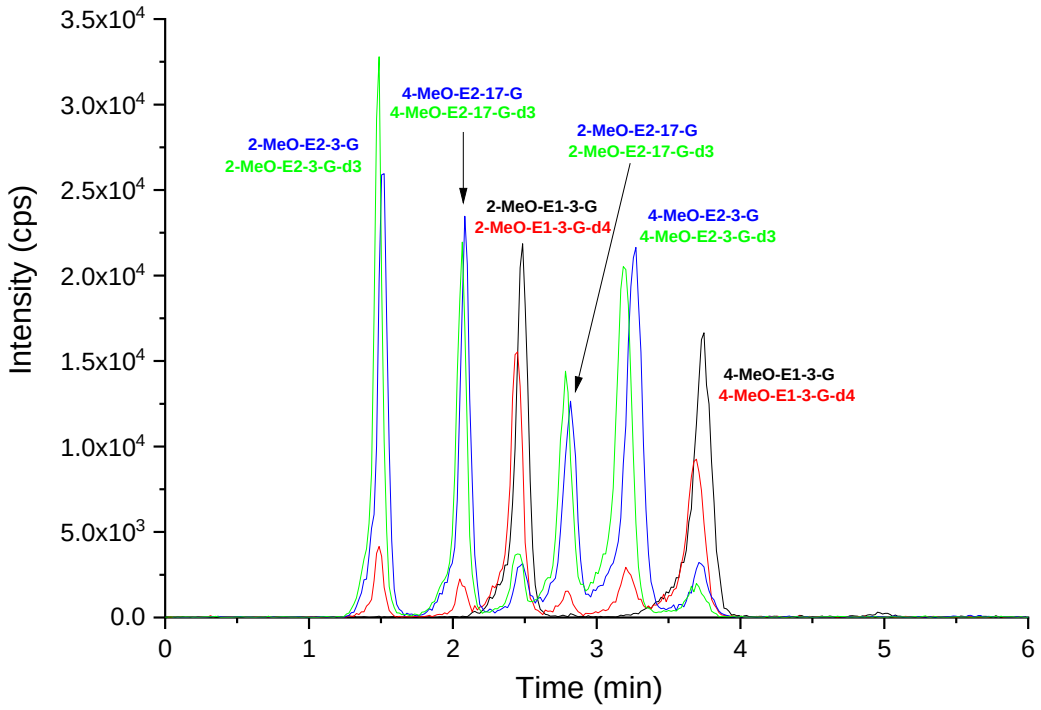

Figure 15: Chromatogram of overlying MRM-transitions of biosynthesized references by UHPLC-MS/MS. Resolution between analytes was achieved using the method 2 (Chapter 3.2.1.2) with TEM = 550 °C, GS1 = 60 psi, GS2 = 70 psi and IS = -3500 V.

4.2. Validation of the extended method for the detection and quantification of methoxyestrogen glucuronides

Validation is defined by the International Organization of Standardization as the ability of an analytical method to provide reliable and reproducible results based on examination and provision of strong evidence (summarized in Araujo, 2009).

The validation of the extended method for the specific detection and quantification by means of UHPLC-MS/MS of methoxyestrogen glucuronides was developed with regard to the Food and Drug Administration guideline (FDA, 2018) because of its appropriateness in the validation of bioanalytical methods such as chromatographic assays that quantitatively determine metabolites in biological matrices such as plasma. The method using deuterated methoxyestrogen glucuronides as ISs (Chapter 4.2.1) was validated concerning the parameters recommended by the cited guideline of specificity and selectivity (Chapter 4.2.2), recovery (Chapter 4.2.3), the analytical response of the references (Chapter 4.2.4), the LOD, LOQ, accuracy and precision (Chapter 4.2.5), and stability (Chapter 4.2.6). The dilution effects, a parameter also recommended in this guideline, was not validated.

4.2.1. Internal Standards

The internal standards are structurally similar analogs, mostly stable isotope-labeled compounds, added to calibration curves and samples to facilitate the quantification (FDA, 2018) and identification of a target molecule through the unique Qn/Ql ratio and t_R. The ISs are added before the extraction process to ensure the same conditions as for the interested analytes (Zenkevich and Makarov, 2007).

In the present validation, samples were spiked with a mixture of the ISs containing an appropriate amount of each biosynthesized –d3 and -d4 methoxyestrogen glucuronide to ensure S/N values more than 3 times the LOD of each conjugate (Chapter 3.2.10.1). The suitability of this mixture for quantification/identification purposes was assessed by proving that the components do not interfere with each other or with their non-deuterated analogues by (i) the chromatographic resolution of the peaks (Chapter 4.2.1.1) and (ii) the study of interferences with isotopes (Chapter 4.2.1.2).

4.2.1.1. Chromatographic resolution of the peaks

The chromatographic resolution of the peaks was achieved using a Gemini C18 column using as mobile phase ammonium acetate buffer 25 mM, pH 9.2 (A) and ACN (B) with isocratic elution at 17% (B) (Chapter 3.2.1.2).

The peak shapes were assessed visually as recommended (https://www.shimadzu.com/an/support/lib/lctalk/92/abnormalpeakshapes.htm, last access: December 2019, Chapter 3.2.10.1.1). In the present validation, good peak shape and no co-elution or overlapping between peaks were observed for 2- and 4-MeO-E1-G-d_4, 2- and 4-MeO-E2-3G-d_3 and 2- and 4-MeO-E2-17G-d_3. Additionally, no peaks were detected at the same t_R of deuterated methoxyestrogen glucuronides in both Qn and Ql transitions of their corresponding non-deuterated analogs (Appendices A2.1-A2.3). Nevertheless, the chromatographic peaks of 2-MeO-E2-17-G-d3 and 4-MeO-E2-3-G-d3, and 4-MeO-E2-17-G-d3 and 2-MeO-E1-G (as an isotope) eluted adjoining with a narrow time-window (Figure 16).

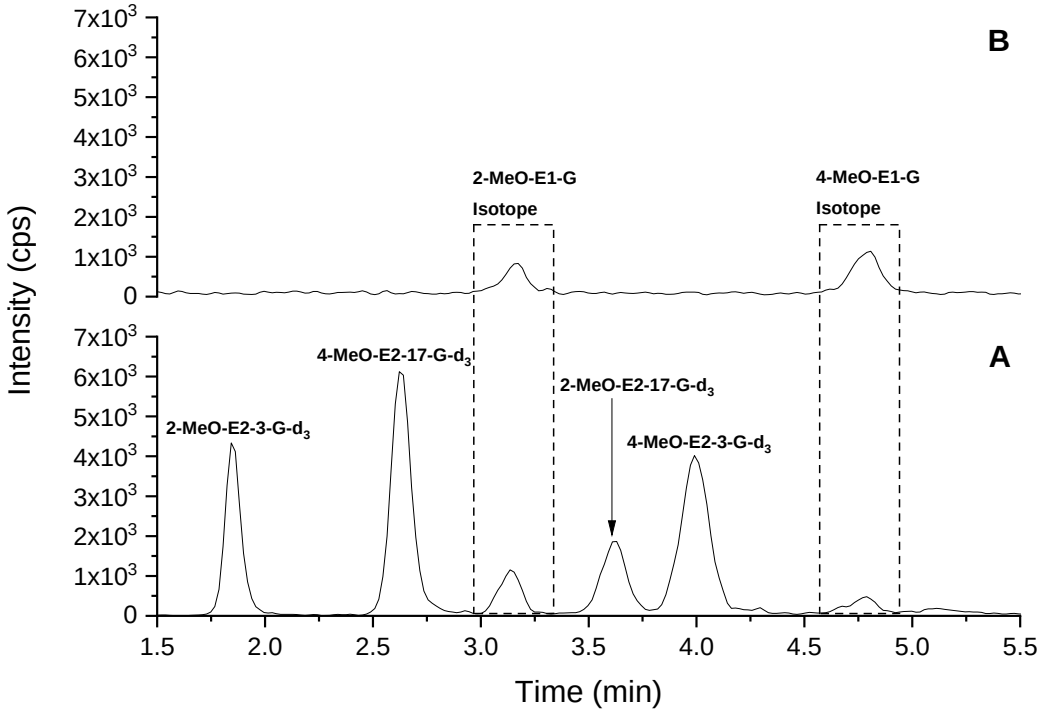

Figure 16: Chromatogram of MRM-transitions of (A) deuterated 2- and 4-methoxyestradiol glucuronides (Qn transition m/z=480.100/113.000) and (B) 2- and 4-methoxyestradiol glucuronides (Qn transition m/z=477.100/113.000). m/z, mass charge ratio.

Accordingly, the resolution between the chromatographic peaks of 2-MeO-E2-17-G-d3 and 4-MeO-E2-3-G-d3 and between 4-MeO-E2-17-G and 2-MeO-E1-G (as an isotope) was calculated using the formula previously described (Chapter 3.2.10.1.2, https://www.shimadzu.com/an/hplc/support/lib/lctalk/resol-1.html, last access: December 2019). As recommended, a resolution value $\geq$ 1.5 assures that the peaks are enough separated. Therefore, the calculated values above 1.5 ensured an appropriated separation between the mentioned analytes (Table 33).

Table 33: Peak resolution values between conjugates which eluted adjoining. *Individual data values available in Appendix A2.4.

Conjugates which eluted adjoining	Peak resolution*	Range	Conclusion
2-MeO-E2-17-G-d3 and 4-MeO-E2-3-G-d3	2.74	1.69-3.33	The chromatographic resolution between the adjoining peaks is optimum
4-MeO-E2-17-G and 2-MeO-E1-G (as an isotope)	2.06	1.93-2.18	

4.2.1.2. Possible interferences of isotopes

To prove that (possible) isotopes are not interfering with the identification of methoxyestrogens glucuronides, each conjugate was analyzed with respect to the mixture of ISs. Thus, isotopes of deuterated and undeuterated methoxyestrogen glucuronides were obtained by sketching their molecules in ChemDraw (Chapter 3.2.10.1.4) and their m/z= $[M-H]^-$ were compared between them. When a peak of these isotopes would appear at the same t_R of another methoxyestrogen glucuronide, the identity was confirmed by the Qn/Ql ratios. For this, the Qn/Ql ratios of the isotopes were calculated from 3 independent injections (Appendix A2.5) and compared with the Qn/Ql ratio of the conjugate with the same m/z= $[M-H]^-$ (Table 34).

Table 34: Analysis of (possible) isotopes which may interfere with the identification and quantification of methoxyestrogens glucuronides. [a] Isotope may interfere with m/z = $[M-H]^-$ of 2- and 4-MeO-E2-3G and 2- and 4-MeO-E2-17G; [b] Isotope may interfere with m/z = $[M-H]^-$ of 2- and 4-MeO-E1-G-d_4; [c] Mean value from 3 independent measurements (individual data values available in Appendix A2.5);. -, not calculated since no isotope will interfere; m/z, mass/charge ratio; Qn, quantifier; Ql, qualifier.

Reference	m/z = $[M-H]^-$	Qn/Ql ratio	Isotopes (m/z) (Abundance in %)	Qn/Ql ratio of common Isotopes with other m/z = $[M-H]^-$ [c]
2-MeO-E1-G-d4	479.1	1.56	481.23 (27%); 482.24	-
4-MeO-E1-G-d4		1.90	(2.7%); 482.23 (1.8%)	
2-MeO-E1-G	475.1	1.54	477.21[a] (27%); 478.21	10.18±0.19
4-MeO-E1-G		2.03	(3.5%); 482.21 (1.8%)	11.21±6.92
2-MeO-E2-3-G-d3	480.1	1.64	484.24 (27%); 483.25	-
2-MeO-E2-17-G-d3		1.19	(2.7%); 483.24 (1.8%)	
2-MeO-E2-3-G	477.1	1.69	479.22[b] (27%); 480.23	6.76±1.19
2-MeO-E2-17-G		1.36	(2.7%); 480.22 (1.8%)	7.68±2.25
4-MeO-E2-3-G-d3	480.1	1.81	484.24 (27%); 483.25	-
4-MeO-E2-17-G-d3		1.14	(2.7%); 483.24 (1.8%)	
4-MeO-E2-3-G	477.1	1.87	479.22[b] (27%); 480.23	7.23±0.42
4-MeO-E2-17-G		1.29	(2.7%); 480.22 (1.8%)	9.15±2.52

As observed in Table 34, the (possible) isotope of 2- and 4-MeO-E1-G (477.21, 27%) could interfere with the m/z = $[M-H]^-$ of 2-and 4-MeO-E2-3-G and 2-and 4-MeO-E2-17-G. Also, the isotope of 2- and 4-MeO-E2-3-G (479.22, 27%) could interfere with the $[M-H]^-$ of 2-and 4-MeO-E1-G-d4. Nevertheless, all ratios of the isotopes are higher than the Qn/Ql ratios of the conjugates with the same m/z = $[M-H]^-$ (Table 35), thus, they will not be wrongly identified. Therefore, the use of the mixture of ISs is suitable for the quantification/identification of methoxyestrogen glucuronides.

.2.2. Specificity and Selectivity

The specificity, wrongly understood as an equivalent of the selectivity, is defined as the ability of the analytical method to eliminate interferences by producing a response only for the target compound. Since this is almost impossible to reach in chromatographic assays for biological matrices, a more appropriate term is the selectivity which is defined as the ability of an analytical method to produce a response for the target compound which is distinguishable from all other responses (summarized in Araujo, 2009).

Therefore, the specificity of the method was ensured by the specific substance-dependent and source-dependent parameters (Chapter 4.1.5), and the selectivity was assured by determining unique Qn/Ql ratio values, including the evaluation of possible interferences with isotopes (Chapter 4.2.1.2).

Quantifier / Qualifier ratio

The ratio value between the peak areas of the Qn to that of the Ql of the methoxyestrogen glucuronides supports their specific identification in the case a matrix peak is eluting at the same t_R of the mentioned compounds. During the optimization of the substance-dependent parameters (Chapter 4.1.5.1, Table 32) the t_R and Qn/Ql ratios were acquired. Nevertheless, to set ratio values with acceptable SD, numerous extractions were performed and more accurate Qn/Ql ratios were established (Table 35).

Table 35: Median and range of Qn/Ql ratios (*n* = 30) for biosynthesized deuterated and non-deuterated methoxyestrogen glucuronides obtained from references (*n* = 10), spiked blanks (*n* = 10), and spiked plasma samples (*n* = 10). Qn, quantifier; Ql, qualifier. Individual data values available in Appendices A2.6-A2.7.

Conjugate	Qn/Ql	Range
2-MeO-E1-3G	1.54	1.05-2.12
2-MeO-E1-3G-d_4	1.56	1.19-1.87
4-MeO-E1-3G	2.03	1.20-2.58
4-MeO-E1-3G-d_4	1.90	1.24-2.73
2-MeO-E2-3G	1.69	1.25-2.21
2-MeO-E2-3G-d_3	1.64	1.15-1.93
2-MeO-E2-17G	1.36	1.08-1.69
2-MeO-E2-17G-d_3	1.19	0.91-1.76
4-MeO-E2-3G	1.87	1.53-2.69
4-MeO-E2-3G-d_3	1.81	1.40-2.10
4-MeO-E2-17G	1.29	1.07-1.53
4-MeO-E2-17G-d_3	1.14	1.01-1.23

Because plasma is a very complex biological matrix, the ranges of Qn/Ql ratios observed in Table 35 can be expected.

4.2.3. Recovery

The recovery is defined as the efficiency in the extraction process of the analytical method. The recovery does not need to be 100% but should be consistent and reproducible for the analytes and the ISs (FDA, 2018). Moreover, when the analyte of interest has concentration levels in the order of fmol and there is a bias due to matrix effects, recoveries up to 40% could be accepted (Gustavo González and Ángeles Herrador, 2007).

For the present method, validation of the recovery was determined by spiking plasma samples with the mixture of ISs and after the extraction procedure (Chapter 3.2.9.1), recoveries were calculated (Chapter 3.2.10.2) and ranged from 50.91% (4-MeO-E1-G) to 62.17% (2-MeO-E2-3-G) (Figure 17).

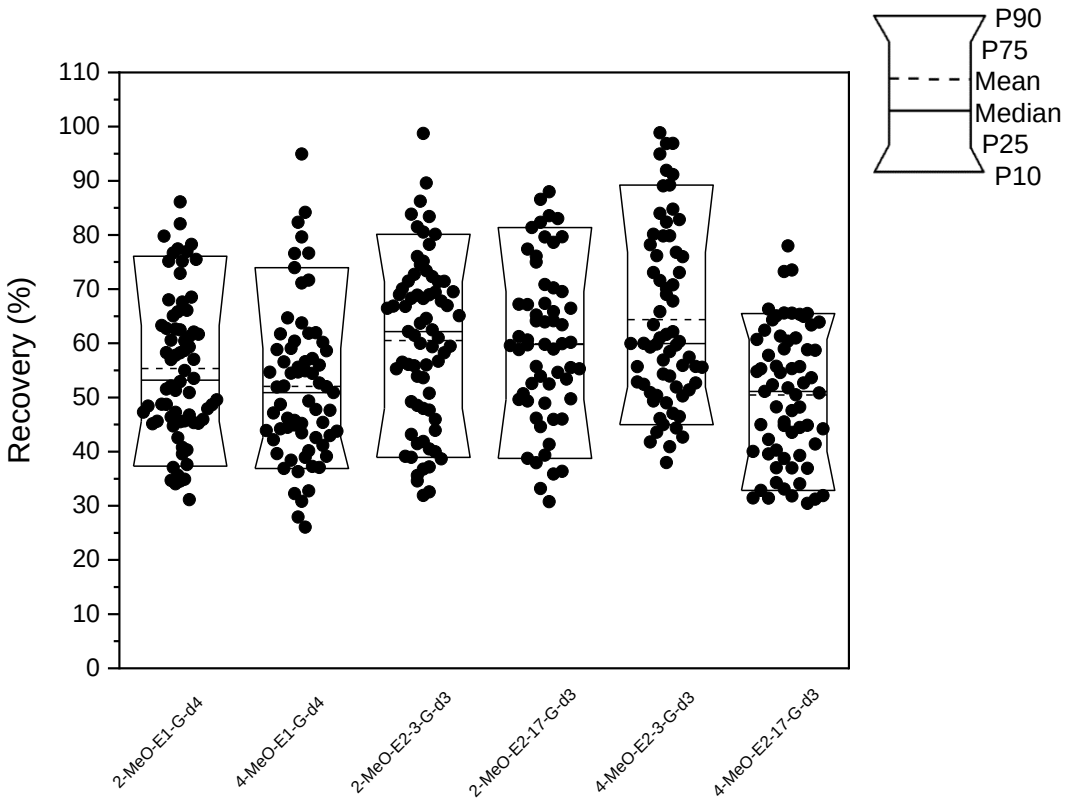

Figure 17: Recoveries (%) of 2-MeO-E1-G-d4 (*n* = 70), 4-MeO-E1-G-d4 (*n* = 67), 2-MeO-E2-3G-d3 (*n* = 71), 2-MeO-E2-17G-d3 (*n* =59), 4-MeO-E2-3G-d3 (*n* = 66) and 2-MeO-E2-17G-d3 (*n* = 65) in human plasma. P, percentile. Complete box-plot chart statistics available in Appendix A2.8.

Unintentional hydrolysis of analytes during the workup was previously discarded within a master thesis developed within our working group. Yet, recoveries of 4-MeO-E1-G-d4 and 4-MeO-E2-17G-d3 were around 50% (Figure 17). However, because of the use of the mixture of ISs, equal losses for the analytes can be assured, making the results less dependent on high recoveries, since it corrects/compensate the variability due to theses losses during the sample extraction.

4.2.4. Analytical response of deuterated and non-deuterated methoxyestrogen glucuronides

There is no knowledge about the range of circulating levels of methoxyestrogen glucuronides. Therefore, the establishment of calibration curves without knowing a range of concentration would be not meaningful. Instead, the analytical response of the methoxyestrogen glucuronides was assessed for the setting of the LOQ levels (quantification of accuracy and precision, Chapter 4.2.5.3) and for the quantification of the analytes (if present) by using the ratios of the peak areas of non-deuterated/ deuterated conjugates.

The analytical response of the methoxyestrogen glucuronides was determined by adding the mixture of ISs and known amounts of their corresponding non-deuterated methoxyestrogen glucuronides in a way that ratios of fmol of non-deuterated/ deuterated conjugates were between 0.5 and 2.0 (Chapter 3.2.10.3). If the analytical response (peak areas) of the conjugates increments in the same way as the fmol were increased, it would be expected that after UHPLC-MS/MS analysis, the ratios of peak areas of non-deuterated/deuterated conjugates would be between 0.50 and 2.0, too. The range of fmol of methoxyestrogen glucuronides used to build those ratios was between 71 fmol/mL (4-MeO-E1-G) and 9529 fmol/mL (4-MeO-E2-17-G) (Chapter 3.2.10.3, Table 22), which covers the LOQ range of the analytes (Chapter 4.2.5).

To observe if there is a significant difference between the expected (reference ratios) and obtained ratios, single sample t-Tests were performed (Chapter 3.2.12). The single sample t-Test determines if the median value of a population is significantly different from a hypothesized/reference value, therefore, it was appropriate for this purpose. As a result, with exception of 2-MeO-E2-17-G, no significant differences (with $p < 0.05$ as the standard significance level) were found between the expected and found ratios of peak areas of non-deuterated/deuterated conjugates in spiked plasmas (Table 36). Moreover, an increment in the ratios of fmol from 0.5 to 1.0 and from 1.0 to 2.0 provide a similar response in the ratios of peak areas given by those fmol (Table 36). Therefore, levels of conjugates in plasma (if present) could be quantified using the peak area ratios of deuterated/non-deuterated methoxyestrogen glucuronides. This was further verified by calculating the accuracy and precision at the suggested LOQ level using this method (Chapter 4.2.5.3).

Table 36: Comparison between the expected and obtained ratios of peak areas of non-deuterated/deuterated methoxyestrogen glucuronides in spiked plasma samples through single sample t-Test ($p < 0.05$) with subsequent *p*-value adjustment using the method of Holm. Except for 2-MeO-E2-17-G, no significant differences were found between the expected and obtained ratios. *Individual data values and exact *p*-values available in Appendix A2.9.

Conjugate ratio	fmol ratio	Expected area ratio	Obtained area ratio* (mean, $n = 3$)	*p*-value*
2-MeO-E1-G / 2-MeO-E1-G-d_4	0.50	0.50	0.62±0.03	0.22035
	1.00	1.00	1.20±0.15	0.19838
	2.00	2.00	2.44±0.27	0.10048
4-MeO-E1-G to 4-MeO-E1-G-d_4	0.49	0.49	0.64±0.05	0.26929
	0.99	0.99	1.20±0.28	0.28638
	1.98	1.98	2.22 [a]	0.28638
2-MeO-E2-3G to 2-MeO-E2-3G-d_3	0.50	0.50	0.60±0.15	0.45960
	1.01	1.01	1.15±0.11	0.12855
	2.01	2.01	2.28±0.43	0.22035
2-MeO-E2-17G to 2-MeO-E2-17G-d_3	0.50	0.50	-	-
	1.00	1.00	0.58 [a]	-
	2.01	2.01	1.42±0.59	0.44336
4-MeO-E2-3G to 4-MeO-E2-3G-d_3	0.51	0.51	0.56 [a]	0.45960
	1.02	1.02	1.13±0.19	0.25299
	2.05	2.05	2.12 [a]	0.45960
4-MeO-E2-17G to 4-MeO-E2-17G-d_3	0.50	0.50	0.71±0.05	0.22035
	1.00	1.00	1.42±0.30	0.26488
	2.00	2.00	2.90±0.55	0.22035

4.2.5. Limit of detection, limit of quantification, accuracy, and precision

The LOD is the lowest amount that can be reliably detected and identified (summarized in Kruve et al., 2015). In chromatographic methods is usually estimated based on the S/N and corresponds to a concentration with a response of S/N > 3 (Kruve et al., 2015). The LOQ is defined as the lowest concentration of an analyte which can be accurately and precisely quantified, with a response of around S/N > 10 (Chandran and Singh, 2007).

The accuracy is defined as the closeness of the result obtained to the nominal value and the precision is defined as the closeness of agreement between values obtained by replicate measurements under specific conditions (summarized in Araujo, 2009). In the present validation, the accuracy and precision were determined at the suggested LOQ levels.

4.2.5.1. Limit of detection

Individual LOD levels were determined by spiking at least 20 plasma samples with deuterated methoxyestrogen glucuronides and using the calculation previously described (Chapter 3.2.10.4). For the present method, median LOD levels in human plasma of 183 fmol/mL (2-MeO-E1-G), 66 fmol/mL (4-MeO-E1-G), 165 fmol/mL (2-MeO-E2-3-G), 1022 fmol/mL (2-MeO-E2-17-G), 76 fmol/mL (4-MeO-E2-3-G) and 569 fmol/mL (4-MeO-E2-17-G) were determined (Figures 18A-18B).

Median LOD levels of 183 fmol/mL (2-MeO-E1-G) and 165 fmol/mL (2-MeO-E2-3-G) determined with the present method are higher than LOQ levels of 10 fmol/mL reported by Caron et al. (2009) for both same metabolites (LOD levels, as well as the method to calculate LOQ levels, are not shown). Thus, levels of 2-MeO-E1-G and 2-MeO-E2-3-G detected in the cited study would not be detected with the present method (Chapter 1.2.4). However, the method applied by Caron et al. (2009) is only specific for estrogen glucuronides and methoxyestrogen glucuronides and differs in sample preparation and analysis (Chapter 4.2.7). Additionally, (possible) levels of 2- and 4-MeO-E2-17-G, 4-MeO-E1-G, and 4-MeO-E2-3-G were not investigated by Caron et al. (2009).

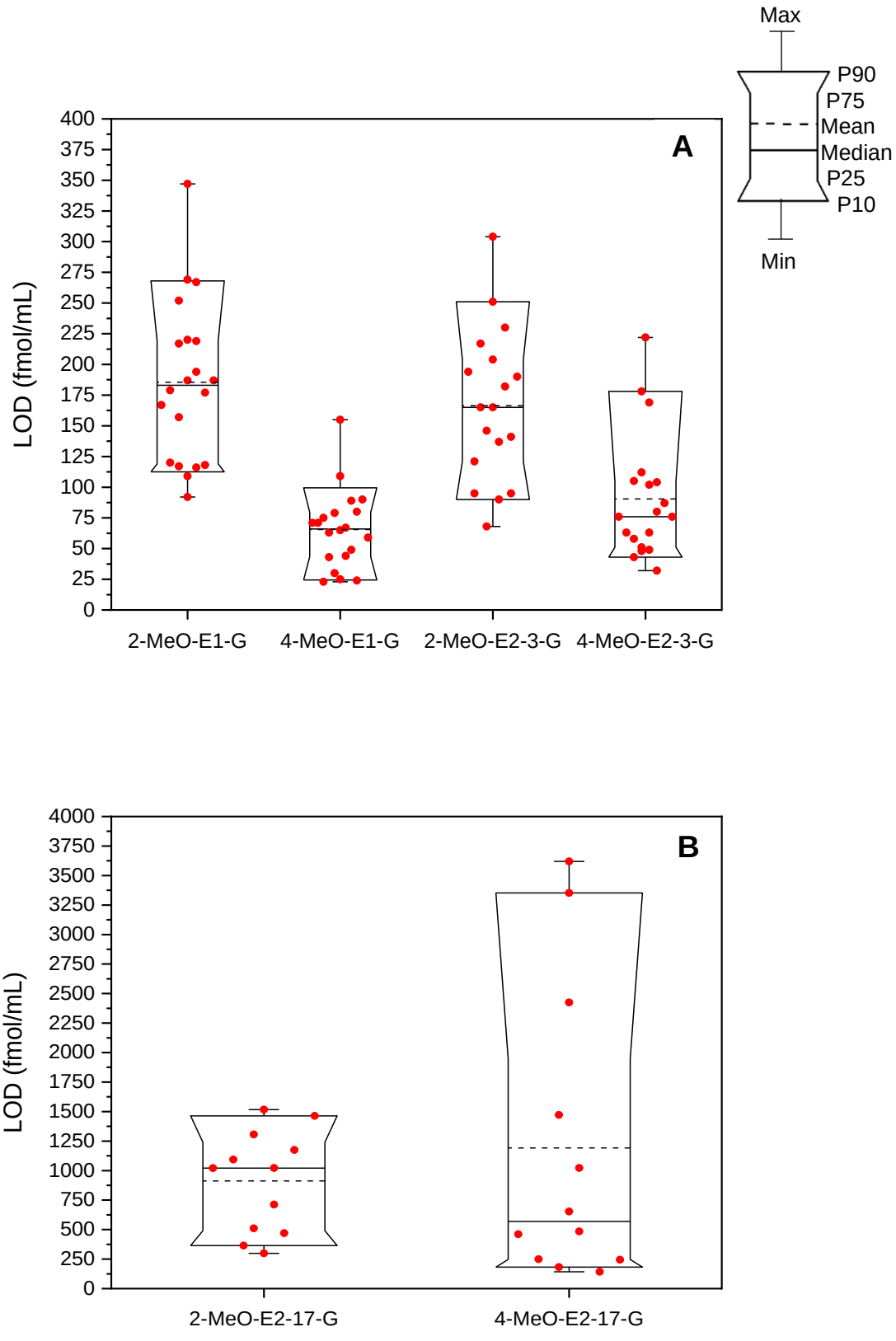

Figure 18: LOD levels in human plasma (fmol/mL) of **(A)** 2-MeO-E1-G (*n* = 20), 4-MeO-E1-G (*n* = 20), 2-MeO-E2-3-G (*n* = 18), 4-MeO-E2-3-G (*n* = 19) and **(B)** 2-MeO-E2-17-G (*n* = 12), 4-MeO-E2-17-G (*n* = 12). Complete box-plot charts statistics available in Appendix A2.10.

4.2.5.2. Limit of quantification

The maximum LOD levels for each conjugate were determined as the LOQ, which ensures S/N values > 10 (Chapter 3.2.10.4). Thus LOQ levels of 347 fmol/mL (2-MeO-E1-G), 155 fmol/mL (4-MeO-E1-G), 304 fmol/mL (2-MeO-E2-3-G), 3636 fmol/mL (2-MeO-E2-17-G), 460 fmol/mL (4-MeO-E2-3-G) and 3636 fmol/mL (4-MeO-E2-17-G) were determined. Moreover, accuracy and precision at the LOQ level were evaluated in order to determine if, from those fmol/mL, quantification of the analytes will be accurate and precise.

4.2.5.3. Accuracy and precision at the suggested limit of quantification

During the validation of an analytical method, it is recommended to assess both accuracy and precision at 3 different concentration levels based on sample concentrations (FDA, 2018). Nevertheless, in the plasma samples screened to this point, levels of endogenous methoxyestrogen glucuronides had not been detected, therefore, the accuracy and precision were determined at the suggested LOQ levels.

Thus, plasma samples were independently processed 3 times at 3 different days for intra- and inter-day accuracy and intra- and inter-day precision (repeatability and intermediate precision) by spiking them with the concentrations (fmol/mL) near to the suggested LOQ levels (Chapter 3.2.10.5). After extraction and injection, calculations were performed as previously described (Chapter 3.2.10.5) and as acceptance criteria, FDA (2018) recommends accuracies within $\pm$20% the nominal concentration and precision of $\pm$ 20% of RDS, at the LOQ level.

At the fmol/mL near to the suggested LOQ levels, intra-day accuracies between 92.80% (2-MeO-E2-3-G) – 188.02% (4-MeO-E2-17-G) and precisions between 1.85% (2-MeO-E2-3-G) - 18.74% (2-MeO-E2-17-G) were found (Table 37). Additionally, inter-day accuracies between 86.40% (2-MeO-E2-17-G) – 142.17% (4-MeO-E2-17-G) and precisions between 7.72% (4-MeO-E2-3-G) – 33.36% (2-MeO-E2-17-G) were found (Table 37). Accuracies and precisions of 2- and 4-MeO-E2-17-G were out of specification, therefore, analysis of these conjugates could be qualitative but not quantitative. For the other 4 methoxyestrogen glucuronides, accuracies and precisions in between the specifications enable their quantitative analysis.

Table 37: Mean values of intra- and inter-day accuracy and precision of methoxyestrogen glucuronides in human plasma at the suggested LOQ levels. [a] Data reported as percentages (%);[b] out of specification.

Conjugate	fmol/mL at the LOQ level	Real fmol/mL added	Accuracy [a] (*n*=3)	Precision [a] (*n*=3)
Intra-day assays				
2-MeO-E1-G	347	357	106.66±3.57	3.35
4-MeO-E1-G	155	157	97.87±16.77	17.14
2-MeO-E2-3-G	304	313	92.80±1.72	1.85
2-MeO-E2-17-G	3636	3051	108.14±20.27[b]	18.74
4-MeO-E2-3-G	460	460	106.89±3.00	2.81
4-MeO-E2-17-G	3636	3636	188.02±23.02[b]	12.24
Inter-day assays				
2-MeO-E1-G	347	357	98.69±12.17	12.33
4-MeO-E1-G	155	157	109.60±16.88	15.40
2-MeO-E2-3-G	304	313	106.67±10.18	10.11
2-MeO-E2-17-G	3636	3051	86.40±28.82[b]	33.36 [c]
4-MeO-E2-3-G	460	460	98.43±7.60	7.72
4-MeO-E2-17-G	3636	3636	142.17±25.87[b]	18.19

4.2.6. Stability

Stability has been defined by the FDA (2018) as the lack of degradation of an analyte in a given matrix under specific storage and use conditions. For the present validation, the stability of the stock solutions of biosynthesized deuterated methoxyestrogen glucuronides (Chapter 4.2.6.1), stability of spiked plasma samples stored in the autosampler (Chapter 4.2.6.2) and stability of spiked plasma samples after freeze/thaw cycles (Chapter 4.2.6.3) were assessed.

4.2.6.1. Stability of stock solutions

The stability of stock solutions of biosynthesized references was measured during 5 months at a storage temperature of -20 °C and was calculated as a percentage % by comparing the raw areas obtained every month with the time zero (t0) (Chapter 3.2.10.6.1).

During 5 months, the stabilities of the biosynthesized references ranged from 97.18% (4-MeO-E1-G) to 134.31% (4-MeO-E2-3-G) (Figure 19).

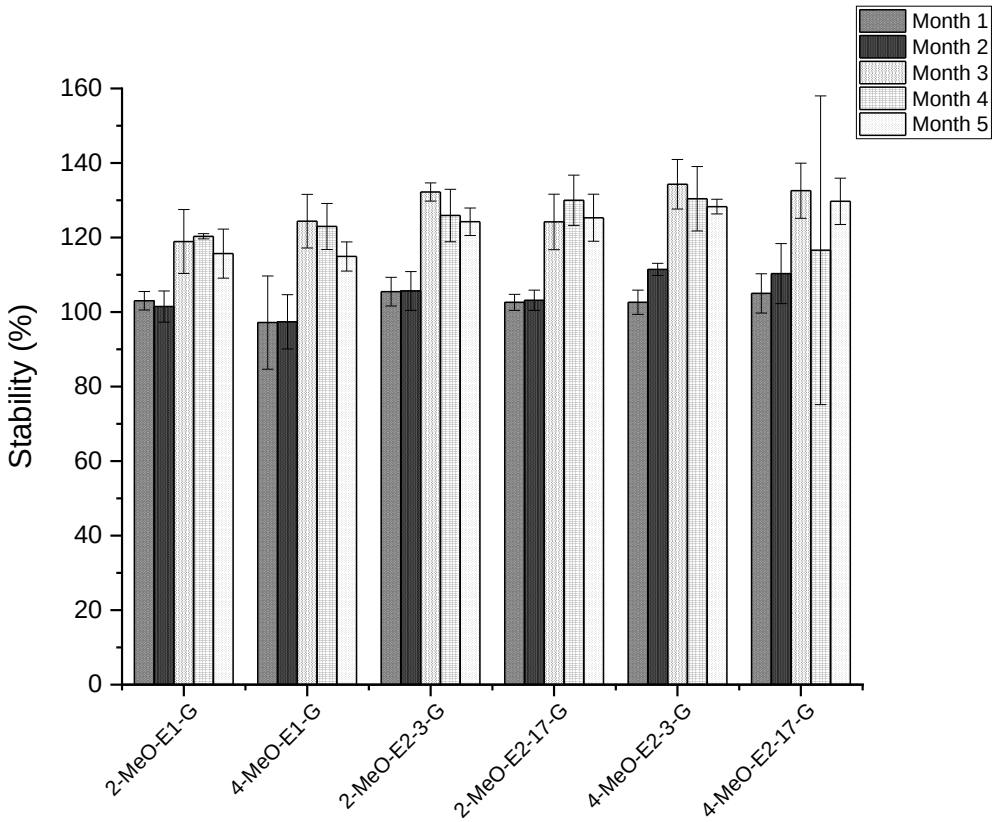

Figure 19: Mean values of stability (%) with their respective SD (whiskers) of methoxyestrogen glucuronides for 5 months at -20 °C. Individual data values available in Appendix A2.11.

Biosynthesized references were stable during 5 months at the storage conditions. High stability values above 100% could be due to fluctuations in the mass spectrometer source after maintenance.

4.2.6.2. Stability of samples in the autosampler

The FDA (2018) guideline recommends assessing the stability of the biological matrix in the autosampler to discard possible damage of the sample and subsequently of the analyte of interest when long-batches, which require a long time of injection, may bias the results after the sample preparation. Thus, the stability of plasma samples stored in the autosampler was assessed by spiking them with 10 µL of the mixture of ISs and with 20 µL of a mixture of methoxyestrogen glucuronides containing 252-4117 fmol/mL (Chapter 3.2.10.6.2). Then, plasma samples were extracted, injected (t0) and stored in the autosampler which holds a temperature of approx. 4 °C. After 24 h, plasma samples were injected again and the stability was calculated as previously described in Chapter 3.2.10.6.2. The stability values expressed as percentages are summarized in Table 38.

To assess whether there was a significant difference in the fmol added to the plasma samples after the 24 h, a t-Test with subsequent *p*-values adjustment using the method of Holm was performed. No significant differences were found (Appendix A2.12).

Table 38: Mean values of stability (%) of spiked plasma samples after 24 h stored in the autosampler. SD, standard deviation; RSD, relative standard deviation; * individual data values and *p*-values available in Appendix A2.12.

Conjugate	Stability (%)* (*n* = 3)	SD	RSD (%)
2-MeO-E1-G	105.27	2.53	2.40
4-MeO-E1-G	91.37	6.70	7.34
2-MeO-E2-3-G	102.84	7.00	6.81
2-MeO-E2-17-G	100.77	10.72	10.64
4-MeO-E2-3-G	96.59	3.62	3.74
4-MeO-E2-17-G	102.38	7.36	7.19

As observed in Table 38, methoxyestrogen glucuronides in extracted plasma samples remain stable after 24 h stored in the autosampler, between 91.37% (4-MeO-E1-G) and 105.27% (2-MeO-E1-G).

4.2.6.3. Stability of samples after freeze/thaw cycles

To evaluate if handling, storage conditions or the need for a second injection affects the stability of the samples and subsequently the analytes of interest, the stability after freeze/thaw cycles was assessed. This was performed by spiking plasma samples with 10 µL of the mixture of ISs and with 20 µL of a mixture of methoxyestrogen glucuronides containing 252-4117 fmol/mL (Chapter 3.2.10.6.3). After plasma extraction, samples were injected (t0) and stored at -20 °C. During four days, plasma samples were thawed and frozen and re-injected on the fourth day. Thereafter, the stability was calculated as previously described (Chapter 3.2.10.6.3). The stability values expressed as percentages are summarized in Table 39.

To assess whether there was a significant difference in the fmol added to the plasma samples after the fourth day of freeze/thaw cycles, a t-Test with subsequent *p*-values adjustment using the method of Holm was performed. No significant differences were found (Appendix A2.13).

Table 39: Mean values of stability (%) of spiked plasma samples after freeze/thaw cycles for 4 days. SD, standard deviation; RSD, relative standard deviation; * individual data values and *p*-values available in Appendix A2.13.

Conjugate	Stability (%)* (*n* = 3)	SD	RSD
2-MeO-E1-3G	102.39	6.90	6.74
4-MeO-E1-3G	103.81	4.19	4.04
2-MeO-E2-3G	99.39	8.42	8.47
2-MeO-E2-17G	100.08	3.46	3.46
4-MeO-E2-3G	95.71	4.07	4.25
4-MeO-E2-17G	96.10	6.21	6.47

As observed in Table 39, methoxyestrogen glucuronides in extracted plasma samples remain stable after 4 cycles/days of freezing/thawing, between 95.71% (4-MeO-E2-3-G) and 103.81% (4-MeO-E1-G).

4.2.7. Applicability of the extended method to the analysis of methoxyestrogen glucuronides in human plasma

As previously discussed (Chapter 1.2.4), studies *in vitro* concluded that methoxyestrogens are subjected to glucuronidation by UGTs, giving the possibility to find methoxyestrogen glucuronides in circulation (Lepine et al., 2004). Moreover, in a study conducted by Caron et al. (2009), serum levels of 2-MeO-E1-G and 2-MeO-E2-3-G were detected in pre- and postmenopausal healthy women. However, no data about circulating levels (if present) of 2-MeO-E2-17-G, 4-MeO-E1-G or 4-MeO-E2-3/17-G, have been previously reported. Therefore, an existing method for the analysis of estrogen conjugates in plasma by means of UHLPC-MS/MS was extended by the analysis of 6 different methoxyestrogen glucuronides and was validated with respect to these newly included metabolites.

With the present method, losses up to 50% in the recovery of the analytes during the work-up, reduced its sensitivity which resulted in higher LODs of 2-MeO-E1-G and 2-MeO-E2-3-G (in the order of hundreds of fmol/mL) when they were compared with the limits of quantification (in the order of tens of fmol/mL) reported by Caron et al. (2009). Those contrast can be attributed to differences between the analytical methods such as:

- The use of different amounts of serum and sample preparation, including different types of SPE cartridges, eluents, and order in the extraction procedure. In the cited study, estrogen sulfates were extracted and processed separately from the estrogen glucuronides, meanwhile with the method used in the present study, both types of conjugates were extracted and processed together.
- The use of different chromatographic columns and eluents.
- Different source- and substance-dependent parameters, including the IS, TEM, DP, and CE.

Additionally, no limits of detection of 4-MeO-E1-G or 4-MeO-E2-3-G, which were in the order of tens of fmol/mL with the present method, have been previously reported. However, the extended method could be applied to the analysis in human plasma of 2- and 4-MeO-E1-G and 2- and 4-MeO-E2-3-G due to the following reasons: (1) Good sensitivity with LOD levels as low as tens to hundreds of fmol/mL. (2) Proportional analytical response. (3) The method has shown to be accurate and precise. (4) With

the existing method, the LOD, as well as circulating levels of the glucuronide E1-G, are in the order of hundreds of fmol/mL. Thus, levels in the order of hundreds of fmol/mL (if present) of the mentioned methoxyestrogen glucuronides could be detected with the extended method. (5) Stability of the compound references in spiked plasma samples.

Concerning 2- and 4-MeO-E2-17-G, the extended method could be applied for their qualitative but not quantitative analysis due to the following reasons: (1) Poor (non-proportional) analytical response which could be attributed to a less ionization of these molecules compared to those conjugated at position 3. As a consequence, high LODs (in the order of hundreds to thousands of fmol/mL) indicated that the method would be not sensitive enough for the quantitative analysis of these two conjugates. (2) Accuracies and precisions out of specifications.

4.3. Sample collection and characterization of the study population

The plasma samples selected for the present investigation (*n* = 25) derived from the Isocross study (*n* = 21) and the BKR (*n* = 4).

Plasma samples derived from the Isocross study (1-21) were obtained from women without breast cancer undergoing mammoplasty reduction for cosmetic reasons. On the day of the surgery, plasma samples were prepared from the blood (Chapter 3.2.8.1) and stored at -80 °C until analysis. Furthermore, these 21 female donors filled out a questionnaire with information about factors affecting estrogens metabolism such as the menopausal status and age, height and weight, among others (Chapters 4.3.1-4.3.2).

Plasmas 22-25 were purchased from the BKR and belong to healthy female donors. No specific information about plasmas 22-25 was known, thus, they were included in the profile analysis of free estrogens and their metabolites, but not in the discussion between pre-, and postmenopausal women.

4.3.1. Questionnaire

Multiple factors such as age, menopausal status, and body mass index (BMI), among others, modify circulating levels of estrogens (Key, 2011), and therefore, the levels of their metabolites. Thus, the information concerning those factors was compiled in a questionnaire (Appendix A3.1). The BMI was calculated using the information about the height and weight of the female donors. The menopausal status was determined by the age with regard to the findings of Tsilidis et al. (2011) on which in a study population of German women (n > 27,000), no woman younger than 45 years old was postmenopausal and no woman older than 53 years old was premenopausal.

4.3.2. Characterization of the study population

With the information collected in the questionnaire (Chapter 4.3.1, Appendix A3.1), the 21 female donors were classified with regard to their age (Chapter 4.3.2.1),

menopausal status (Chapter 4.3.2.2), BMI (Chapter 4.3.2.3), parity (Chapter 4.3.2.4), smoking habits, alcohol consumption and the intake of hormone active drugs (HAD) (Chapter 4.3.2.5).

4.3.2.1. Classification by age

Female donors were normally distributed by age (Shapiro-Wilk test, $p = 0.22394$ at the 0.05 level), and ranged between 19 and 64 years old with a mean value of 46 and a median of 49 (Figure 20). This is near to the general German women population which has a mean age of 47.5 years old (https://www.laenderdaten.de/bevoelkerung/medianalter.aspx, last access: December 2019).

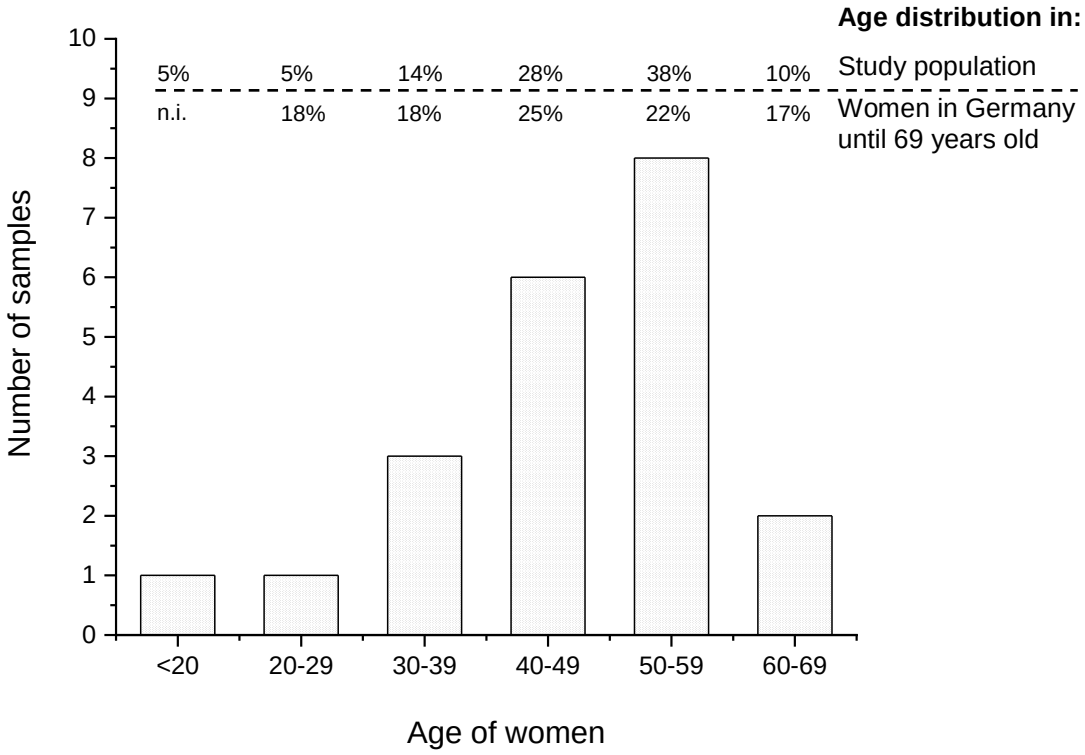

Figure 20: Classification by age of the female donors in the present investigation derived from Isocross study ($n = 21$), compared with the female population in Germany (until 69 years old). n.i., no information.

4.3.2.2. Classification by menopausal status

Tsilidis et al. (2011) found that in a population study of German women (*n* > 27,000), no woman younger than 45 years old was postmenopausal and no woman older than 53 years old was premenopausal. Therefore, (with a high probability) the classification by the menopausal status of the 21 female donors was: premenopausal women (*n* =9, 43%), perimenopausal women (*n* = 5; 24%) and postmenopausal women (*n* = 7; 33%) (Figure 21).

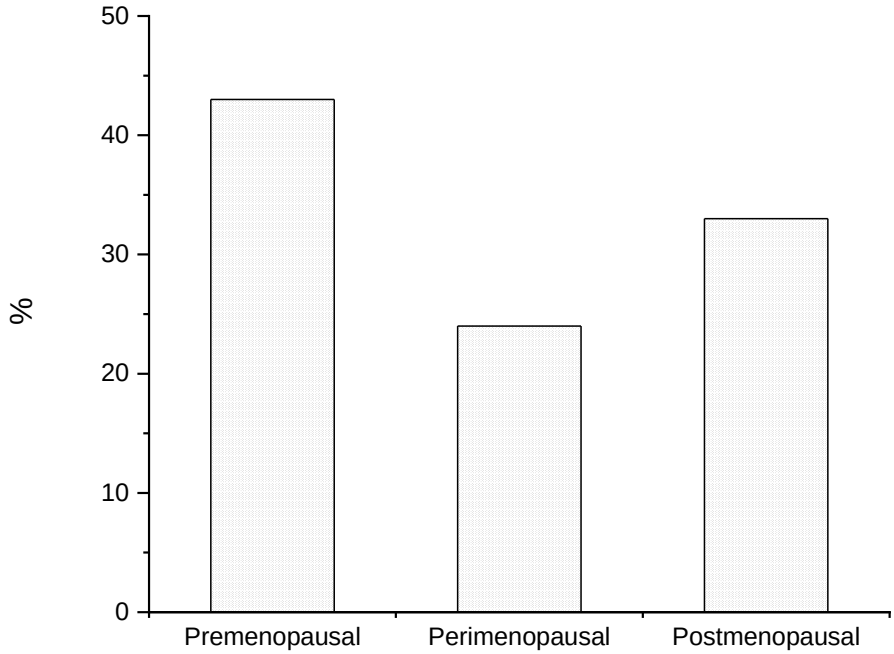

Figure 21: Classification by menopausal status of the female donors in the present investigation derived from Isocross study (*n* = 21). Premenopausal (<46 years old), perimenopausal (46-52 years old), postmenopausal (≥ 53 years old).

4.3.2.3. Classification by body mass index

According to the World Health Organization, BMI classification, from the female donors derived from the Isocross study (*n* = 21), 2 women (9.5%) were classified with a normal

(BMI 18.50-24.99), 11 women (52.4%) as pre-obese (BMI 25.00-29.99) and 8 women (38.1%) as obese (BMI≥30) (Figure 22).

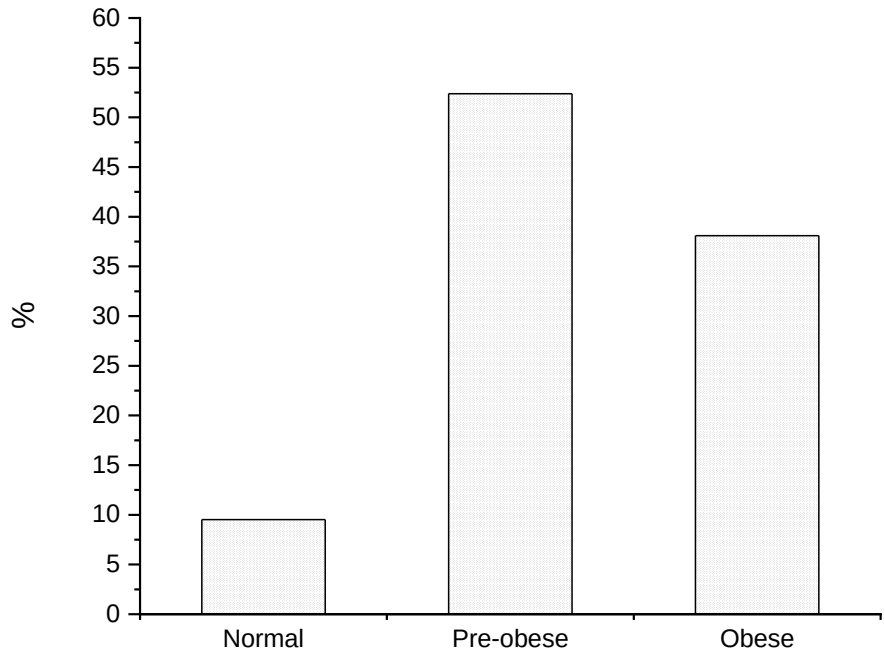

Figure 22: Classification by BMI of the female donors in the present investigation derived from Isocross study (*n* = 21).

4.3.2.4. Classification by parity

Within the 21 women derived from the Isocross study, 16 (76%) were parous and 5 (24%) were nulliparous. Furthermore, 13 women (81%), had between 2-3 children meanwhile 2 women (13%) had one child and one woman (6%) had 4 children.

4.3.2.5. Classification by smoking habits, alcohol consumption, and hormone active drugs

From the 21 female donors, only 2 women (10%) had smoking habits meanwhile the other 19 women (90%) were ex-smokers or did not have smoking habits. Regarding the intake of hormone active drugs, 18 (86%) women reported no intake and the other 3 women (14%) reported the intake of hormonal preparations.

Moreover, 12 women (57%) were non-alcohol consumers, 5 women (24%) used to ingest < 20 g / week of alcohol and 3 women (14%) used to ingest > 20 g / week of alcohol. The information about alcohol consumption in one woman (5%) was unknown.

4.4. Analysis of circulating estrogen profiles in women without breast cancer

Following the metabolic pathways of estrogens (including metabolites and conjugates), their circulating profiles in 25 women of different menopausal statuses and without breast cancer were analyzed as E1 and E2 (Chapter 4.4.1), estrogen conjugates (Chapter 4.4.2), hydroxylated and methoxylated metabolites of estrogens (Chapter 4.4.3), and methoxyestrogen glucuronides (Chapter 4.4.4). Thereafter, correlation analysis between E1, E2 and their conjugates (present in more than 30% of the samples) were performed (Chapter 4.4.5).

From the 21 plasma samples derived from the Isocross study selected for the present investigation, 10 samples were previously analyzed in 2014 with respect to E1, E2, their conjugates and their hydroxylated and methoxylated metabolites. In those analyses, levels of E1, E2, E1-S, and 2-MeO-E1 were detected. Therefore, results from 2014 were compared with the results obtained in the present investigation for the mentioned analytes in those 10 common samples (Chapter 4.4.1-4.4.3).

The LOD and LOQ levels of E1, E2, and 2-MeO-E1 were previously established with plasma samples derived from the Isocross study in 2014 (Chapter 3.2.11.1). The LOD and LOQ levels for E1-S, E1-G, E2-3-S, E2-3-G, E2-17-S, and other methoxyestrogens were taken from another study (n = 111) conducted in our research group in parallel with the present investigation since no LOD or LOQ levels were previously established for these analytes (Chapter 3.2.11.2).

4.4.1. Determination of estrone and 17β-estradiol

Because of the key role of estrogens in breast cancer etiology (Russo and Russo, 2006), the measurement of serum/plasma levels of E1 and E2 is essential (summarized in Stanczyk et al., 2007). Using specific MS-based methodologies, circulating levels of E1 and E2 have been reported in the order of tens to hundreds of fmol/mL (Chapter 1.1). In the present study, both E1 and E2 were analyzed by means of GC-MS/MS in plasma samples from women without breast cancer.

E1 was detected in 100% of the samples (n = 25) above the LOQ of 8 fmol/mL, with levels between 24-824 fmol/mL (median 94 fmol/mL, Figure 23). Furthermore, in the

10 samples derived from the Isocross study analyzed in 2014 and analyzed again in the present study, median levels of E1 of 105 fmol/mL and 119 fmol/mL, respectively, were comparable (paired Wilcoxon test, p = 0.92188). Complete levels of comparison and statistical tests available in Appendix A4.2.

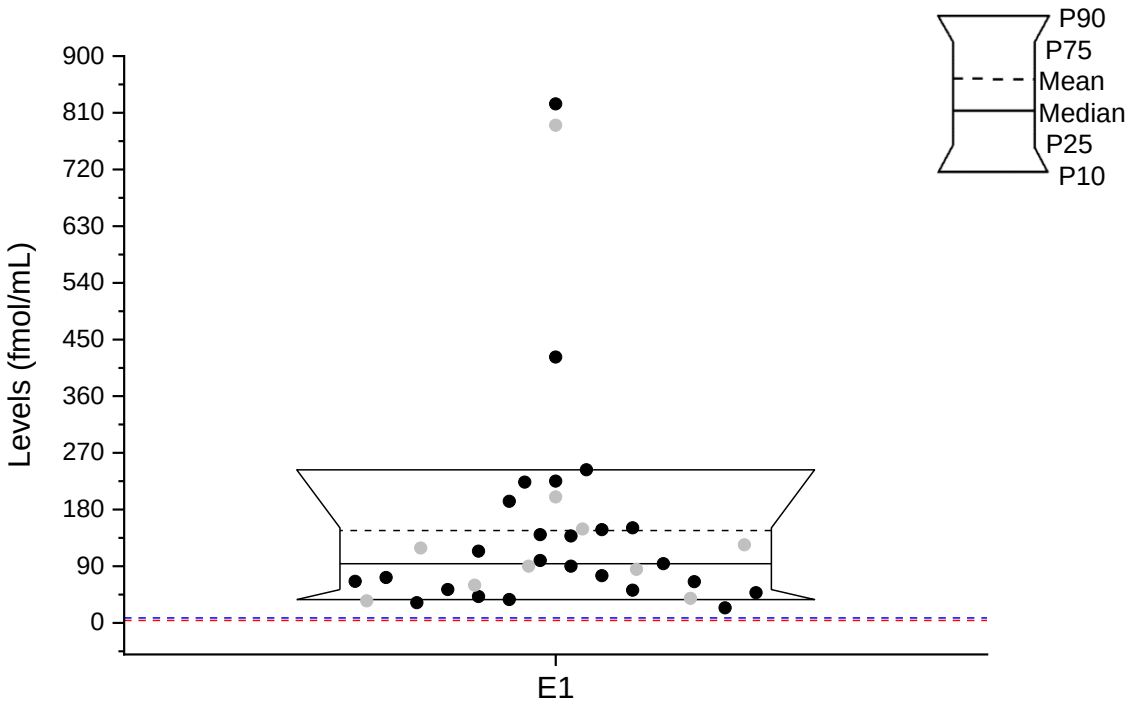

Figure 23: Levels of E1 (black dots, n = 25) in plasma samples from women without breast cancer determined by means of GC-MS/MS (Chapter 3.2.1.3). --- LOD; --- LOQ; P, percentile. Complete box-plot chart statistics available in Appendix A4.1. Light grey dots indicate those samples which were analyzed in 2014 (n = 10).

E2 was detected in 88% of the samples (n = 22) above the LOQ of 12 fmol/mL, with levels of 14-900 fmol/mL (median 37 fmol/mL, Figure 24). Additionally, in 8% of the samples (n = 2), E2 levels were below the LOQ and in 4% (n = 1) below the LOD of 6 fmol/mL (Appendix A4.3). In the 10 samples derived from the Isocross study analyzed in 2014 and analyzed again in the present study, median levels of E2 of 130 fmol/mL and 162 fmol/mL, respectively, were comparable (paired Wilcoxon test, p = 0.86523 at

the 0.05 level). Complete levels of comparison and statistical tests available in Appendix A4.4.

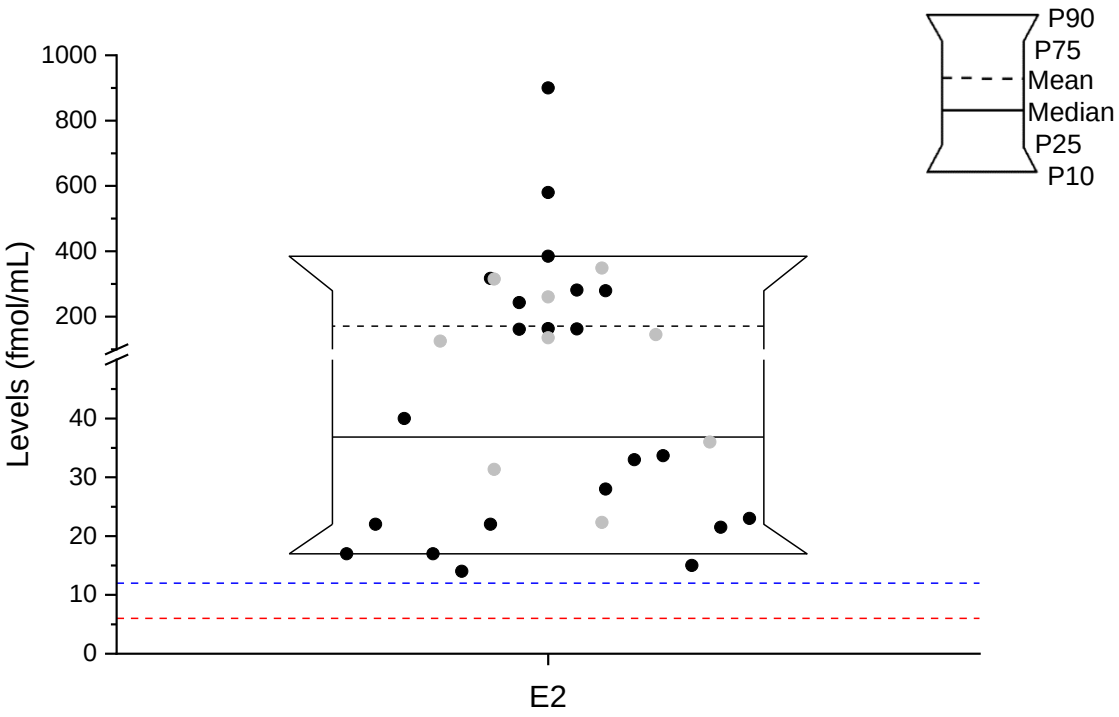

Figure 24: Levels of E2 (black dots, *n* = 22) in plasma samples from women without breast cancer determined by means of GC-MS/MS (Chapter 3.2.1.3). --- LOD; --- LOQ; P, percentile. Complete box-plot chart statistics available in Appendix A4.3. Light grey dots indicate those samples which were analyzed in 2014 (*n* = 10).

To compare the levels of E1 and E2 detected in the present study with the current literature, plasma samples were divided with regard to the menopausal status of the female donors. This excludes plasma samples obtained from the BRK (*n* = 4), and plasma samples from perimenopausal women (*n* = 5) since this categorization does not meet the literature.

In premenopausal women (*n* = 9), E1 levels were 37-422 fmol/mL (median 138 fmol/ml) and in postmenopausal women (*n* = 7) were 24-94 fmol/mL (median 48 fmol/mL) (Figure 25). These levels are strongly supported by several previous studies determining levels of E1 by means of GC-MS or LC-MS (Chapter 1.1, Table 1).

Furthermore, lower median levels of E1 in postmenopausal women than in premenopausal women, agree with the findings in the literature, too (Chapter 1.1).

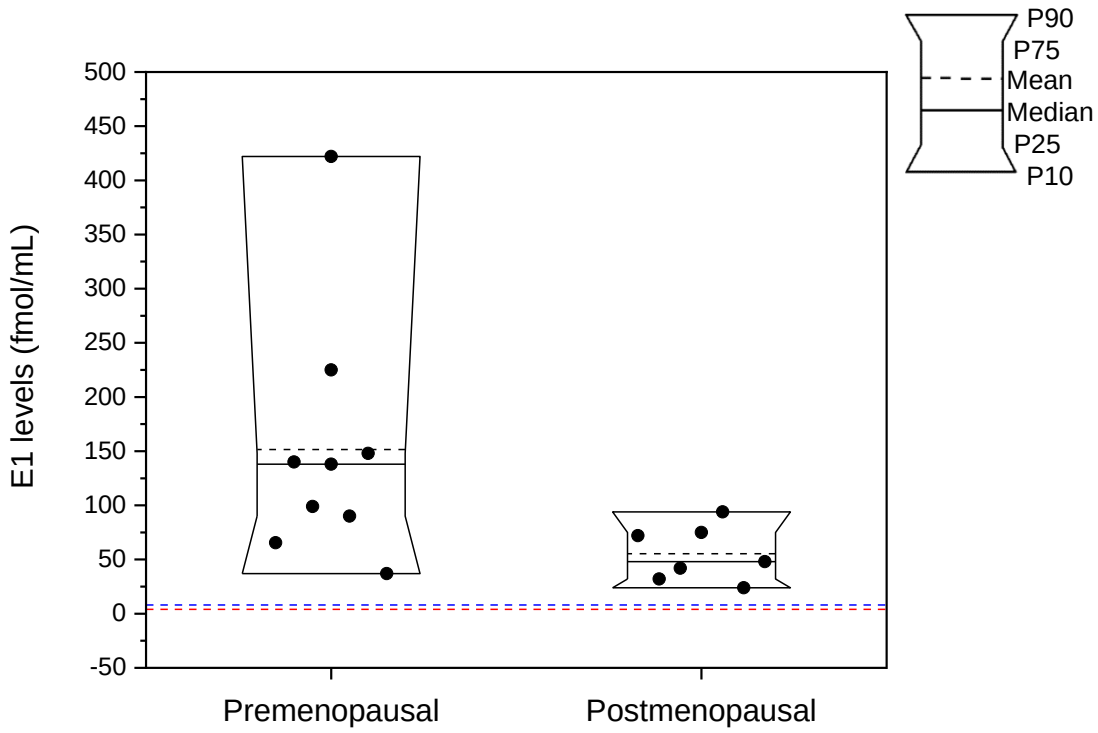

Figure 25: Levels of E1 in premenopausal (*n* = 9) and postmenopausal (*n* = 7) women without breast cancer determined by means of GC-MS/MS (Chapter 3.2.1.3). P, percentile. Complete box-plot chart statistics available in Appendix A4.5.

Moreover, in premenopausal women (*n* = 9), E2 levels were 13-900 fmol/mL (median 162 fmol/mL) and in postmenopausal women (*n* = 6) were 17-34 fmol/mL (median 22 fmol/mL) (Figure 26). These levels are also strongly supported by several previous studies determining levels of E2 by means of GC-MS or LC-MS (Chapter 1.1, Table 1). Additionally, lower median levels of E2 in postmenopausal women compared with premenopausal women, agree with findings from the literature (Chapter 1.1, Table 1).

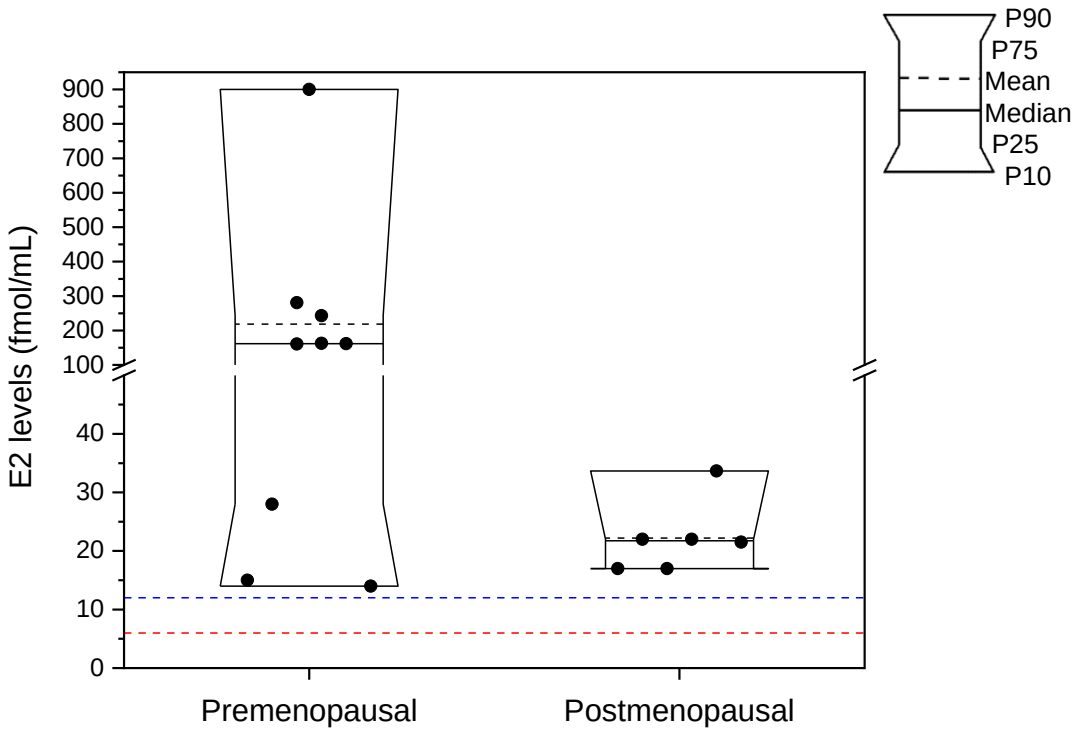

Figure 26: Levels of E2 in premenopausal (*n* = 9) and postmenopausal (*n* = 6) women without breast cancer determined by means of GC-MS/MS (Chapter 3.2.1.3). P, percentile. Complete box-plot chart statistics available in Appendix A4.6.

Median levels of E2 were higher than those of E1 in plasma samples from premenopausal women and lower than those of E1 in plasma samples from postmenopausal women. Both findings agree with the literature which indicates that the production and release of E2 decrease dramatically after menopause (Africander and Storbeck, 2018, Chapter 1.1).

Ratios of levels of 17β-estradiol to that of estrone

To determine the fold difference between levels of E1 and E2 with regard to the menopausal status and to compare with the literature, individual ratios of E2 levels to E1 levels (ratios E2/E1) were determined in plasma samples with calculated levels of

E2 above the LOQ of 12 fmol/mL from premenopausal (*n* = 9) and postmenopausal (*n* = 6) women without breast cancer.

As previously described, the ovaries cease the activity during the menopause decreasing the production of E2. Thus, E1 becomes the major estrogen at this stage (Chapter 1.1). For this reason, it would be expected that ratios E2/E1 in postmenopausal women would be lower than in premenopausal women.

In the present study, ratios E2/E1 in premenopausal women were 0.1-2.1 (median 1.2) and in postmenopausal women were 0.3-0.7 (median 0.4) (Figure 27).

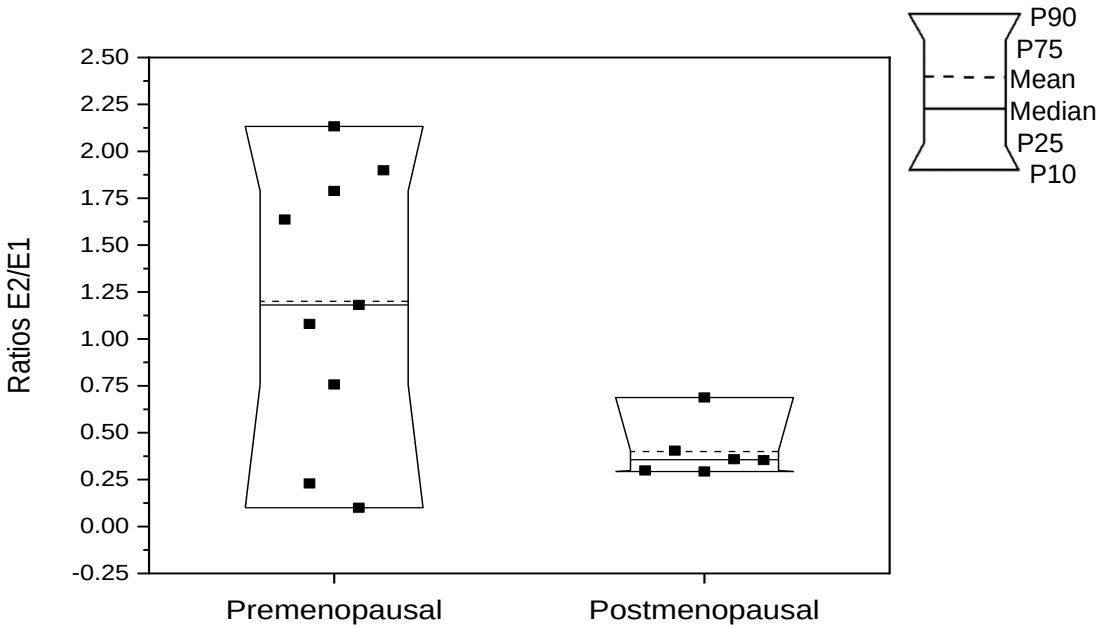

Figure 27: Ratios of E2 levels to E1 levels (ratios E2/E1) in plasma samples from premenopausal (*n* = 9) and postmenopausal (*n* = 6) women without breast cancer. P, percentile. Complete box-plot chart statistics in Appendix A4.7.

As expected, median ratios E2/E1 in postmenopausal women were lower than in premenopausal women, supporting the predominance of E1 over E2 during the menopause (Chapter 1.1, Table 1). Conversely, median ratios E2/E1 were > 1 in premenopausal women support higher levels of E2. These findings are strongly supported by the literature on which median ratios E2/E1 (calculated with reported

mean/median levels of E1 and E2, Appendix A4.30) are about 3-fold higher in serum from premenopausal women than in serum from postmenopausal women.

4.4.2. Determination of estrone and 17β-estradiol conjugates

Conjugation to sulfates and glucuronides is recognized as one of the major routes of estrogens biotransformation which leads to their inactivation (summarized in Raftogianis et al., 2000). Because of their important function as detoxifying metabolites, the analysis of circulating levels of estrogen sulfates and glucuronides has been improving during the last years, replacing immunoassays for more accurate techniques such as LC coupled to MS (Chapters 1.2.3-1.2.4).

In the present study, E1-S (Chapter 4.4.2.1), E1-G (Chapter 4.4.2.2), E2-3-S (Chapter 4.4.2.3), E2-3-G and E2-17-S (Chapter 4.4.2.4) were analyzed by means of UHPLC-MS/MS in plasma samples from women without breast cancer.

4.4.2.1. Determination of estrone-3-sulfate

E1-S is reported as the most abundant circulating estrogen with levels in the order of hundreds to thousands of fmol/mL (Chapter 1.2.3). Since E1 was detected in all plasma samples (Chapter 4.4.1), it would be expected to detect E1-S in all of them, too.

In the present study, E1-S was detected in 100% of the samples (n = 25) above the LOQ of 40 fmol/mL with levels of 134-11082 fmol/mL (median 761 fmol/mL, Figure 28). Furthermore, in the 10 samples derived from the Isocross study analyzed in 2014 and analyzed again in the present study, median levels of E1-S of 1532 fmol/mL and 1239 fmol/mL, respectively, were comparable (paired Wilcoxon test, p = 0.43164 at the 0.05 level). Complete levels of comparison and statistical tests available in Appendix A4.9.

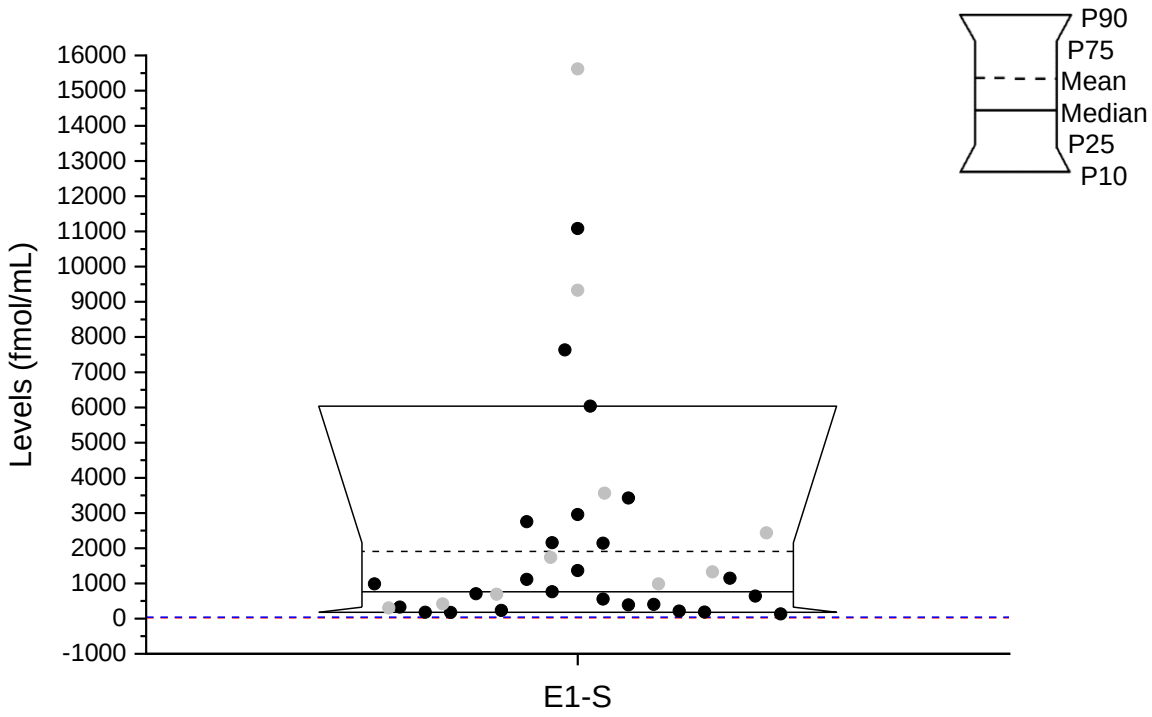

Figure 28: Levels of E1-S (black dots, *n* = 25) in plasma samples from women without breast cancer determined by means of UHPLC-MS/MS (Chapter 3.2.1.2). ---LOD; --- LOQ; P, percentile. Complete box-plot chart statistics available in Appendix A4.8. Light grey dots indicate those samples which were analyzed in 2014 (*n* = 10).

To compare levels of E1-S determined in the present study with those from the current literature, plasma samples were divided with regard to the menopausal status of the female donors. This excludes plasma samples obtained from the BRK (*n* = 4), and from perimenopausal women (*n* = 5) since this categorization does not meet the literature.

In premenopausal women (*n* = 9), E1-S levels were 176-7634 fmol/mL (median 1363 fmol/ml) and in postmenopausal women (*n* = 7) were 179-1144 fmol/mL (median 704 fmol/mL) (Figure 29). These levels are supported by previous studies determining E1-S in serum from pre and postmenopausal women by means of LC-MS (Chapter 1.2.3, Table 4).

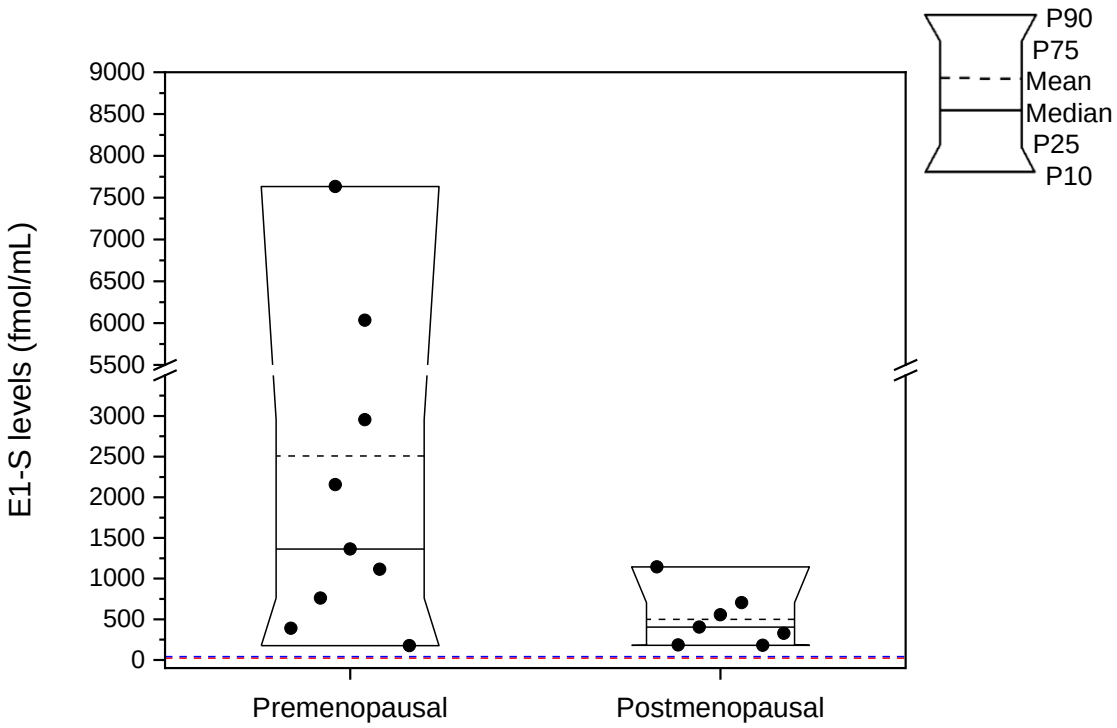

Figure 29: Levels of E1-S in premenopausal (*n* = 9) and postmenopausal (*n* = 6) women without breast cancer determined by means of UHPLC-MS/MS (Chapter 3.2.1.2). P, percentile. Complete box-plot chart statistics available in Appendix A4.10.

Ratios of levels of estrone-3-sulfate to that of estrone

To determine the fold difference between levels of E1-S and its precursor E1 in the plasma samples from the present study, individual ratios of E1-S levels to E1 levels (ratios E1-S/E1) were determined in pre- (*n* = 9) and postmenopausal (*n* = 7) women without breast cancer. Serum levels of E1-S have been reported to be up to 50-fold higher than its unconjugated precursor E1 (Chapter 1.2.3). Thus, it would be expected that individual ratios of E1-S levels to E1 levels (ratios E1-S/E1) would be > 1.

In premenopausal women from the present study, ratios E1-S/E1 were 2.7-30.1 (median 15.1) and in postmenopausal women were 5.8-15.9 (median 7.5) (Figure 30).

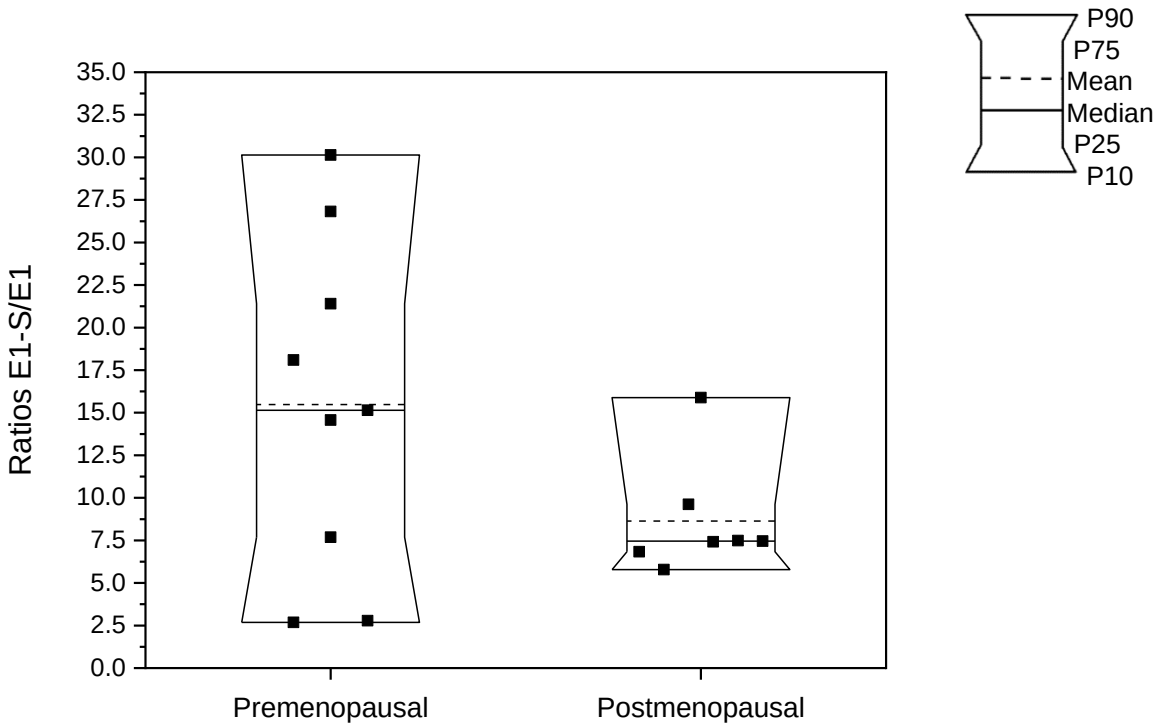

Figure 30: Ratios of E1-S levels to E1 levels (ratios E1-S/E1) in plasma samples from premenopausal (*n* = 9) and postmenopausal (*n* = 7) women without breast cancer. P, percentile. Complete box-plot chart statistics in Appendix A4.11.

The median E1-S/E1 ratios in both pre- and postmenopausal women are in line with those calculated with mean/median E1-S and E1 levels reported in the literature (Appendix A4.30). As previously described, both E1-S and E1 levels were lower during the menopause (Chapters 4.4.1, 4.4.2.1). Thus, as expected, median ratios E1-S/E1 were lower (half) in postmenopausal than in premenopausal women.

4.4.2.2. Determination of estrone-3-glucuronide

Previous studies determining circulating levels of estrogen conjugates by means of LC-MS evidenced that E1-G is the second most abundant conjugate after E1-S, with serum levels in the order of tens to hundreds of fmol/mL in pre- and postmenopausal women (Chapters 1.2.3-1.2.4).

In the present study, E1-G was detected in 28% of the samples (*n* = 7) above the LOQ of 249 fmol/mL with levels of 258-544 fmol/mL (median 416 fmol/mL, Figure 31). Additionally, in 24% of the samples (*n* = 6) E1-G levels were below the LOQ, in 36% (*n* = 9) below the LOD, and in 12% (*n* = 3) were n.d. due to interferences with matrix peaks (Appendix A4.12). All detected levels were in plasma samples from premenopausal women except for one with 305 fmol/mL which corresponds to a perimenopausal woman and one with 414 fmol/mL which corresponds to one plasma from the BRK. In postmenopausal women, no levels above the LOD of 163 fmol/mL were detected.

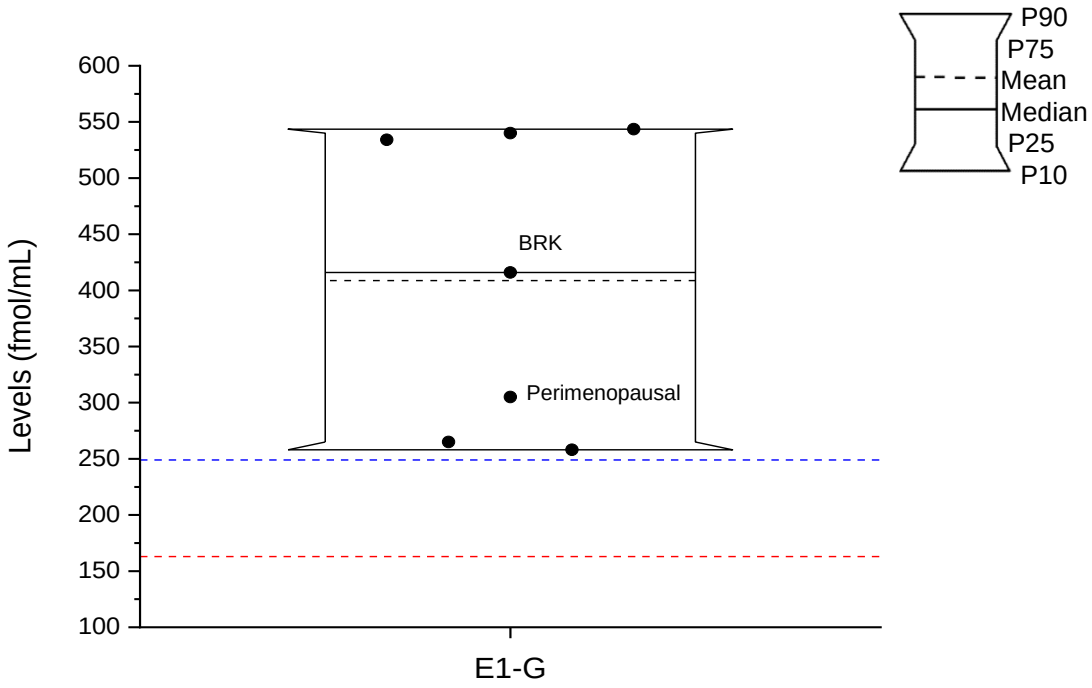

Figure 31: Levels of E1-G (*n* = 7) in plasma samples from women without breast cancer determined by means of UHPLC-MS/MS (Chapter 3.2.1.2). ---LOD; --- LOQ; P, percentile. Complete box-plot chart statistics available in Appendix A4.12.

In contrast with the literature, E1-G levels were not detected in plasma samples from postmenopausal women (Chapter 1.2.4, Table 6). Yet, with the method here applied, the LOD of E1-G (163 fmol/mL) is about 15-fold higher than the LOQ of 11 fmol/mL established by Audet-Walsh et al. (2011) and Caron et al. (2009). Thus, levels of E1-

G of tens of fmol/mL in postmenopausal women detected in the cited studies could not have been detected with the present method. Conversely, in premenopausal women, median levels of E1-G detected in the present study were slightly above median levels of 316 fmol/mL previously reported by Caron et al. (2009).

Ratios of levels of estrone-3-glucuronide to that of estrone and estrone-3-sulfate

In previous investigations, Caron et al. (2009) determined that in serum from premenopausal healthy women, E1-G levels were above E1 levels, whereas in postmenopausal healthy women, E1 levels were about the double of E1-G. In contrast, Audet-Walsh et al. (2011) determined that in serum from postmenopausal healthy women, E1-G levels were above E1 levels. Therefore, to determine the fold difference in plasma samples from the present study and to compare with the literature, individual ratios of E1-G levels to E1 levels (ratios E1-G/E1) were calculated. Ratios were established by using calculated levels of E1 and E1-G (*n* = 5) in premenopausal women since no levels above the LOQ were detected in postmenopausal women.

Thus, in premenopausal women, ratios E1-G/E1 were 1.3-5.5 (median 1.9, Figure 32).

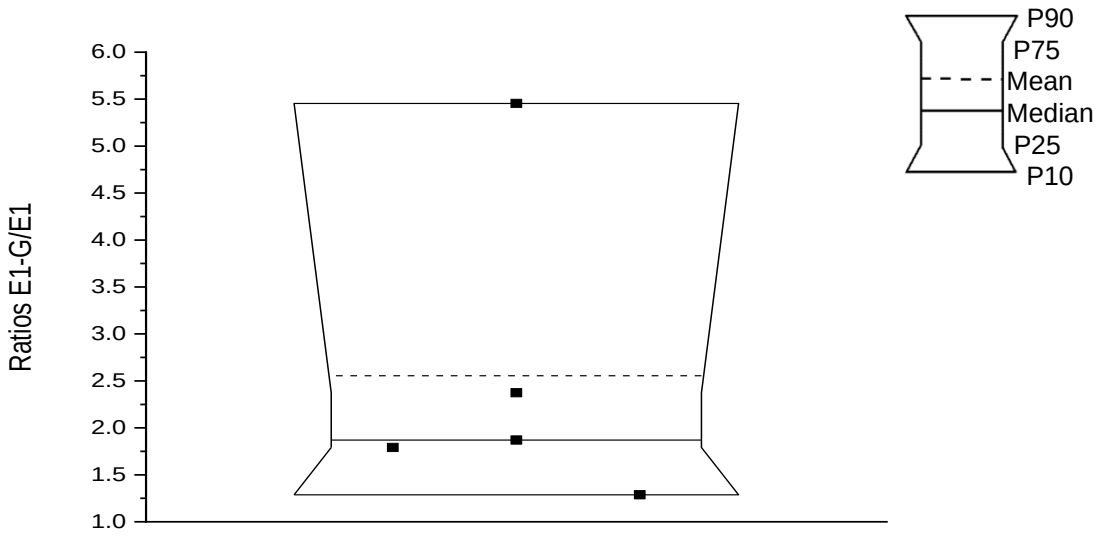

Figure 32: Ratios of E1-G levels to E1 levels (ratios E1-G/E1) in plasma samples from premenopausal women without breast cancer (*n* = 5). P, percentile. Complete box-plot chart statistics in Appendix A4.13.

As expected, ratios E1-G/E1 in premenopausal women were > 1, supporting higher amounts of E1-G over its precursor E1 in plasmas with both metabolites detected. This is in line with findings from Caron et al. (2009) on witch serum levels of E1-G were higher than E1 in premenopausal women. Moreover, ratios E1-G/E1 (calculated with median levels reported in the cited study, Appendix A4.30) were also comparable.

Furthermore, to determine the fold difference between both conjugates of E1, individual ratios of E1-G levels to E1-S levels (ratios E1-G/E1-S) were established by using calculated levels of E1-S and E1-G (*n* = 5) in premenopausal women. Since E1-S has been reported in higher concentrations than E1 and E1-G (Chapter 1.2.3), it would be expected to have ratios E1-G/E1-S < 1.

Thus, ratios E1-G/E1-S in premenopausal women were 0.07-0.71 (median 0.09) (Figure 33).

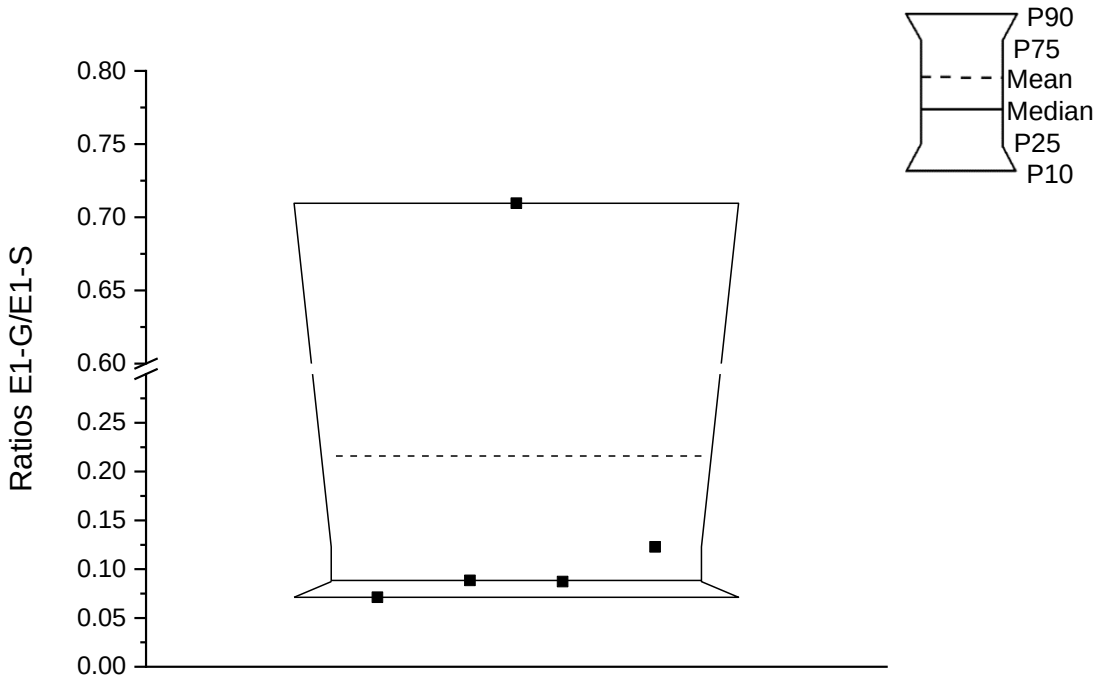

Figure 33: Ratios of E1-G levels to E1-S levels (ratios E1-G/E1-S) in plasma samples from premenopausal women without breast cancer (*n* = 5). P, percentile. Complete box-plot chart statistics in Appendix A4.14.

As expected, median ratios E1-G/E1-S were all < 1, supporting predominance of E1-S as the E1-conjugate present in the highest amounts in circulation. This is in line with findings from Caron et al. (2009) in premenopausal healthy women, on which E1-S serum levels were higher than E1-G as well as ratios E1-G/E1-S (calculated with median levels reported in the cited study, Appendix A4.30).

4.4.2.3. Determination of 17β-estradiol-3-sulfate

At least 3 different SULT isoforms are known for catalyzing the conjugation of E2 into E2-3-S (Chapter 1.2.3). Yet, in previous investigations determining the serum profile of estrogens and their conjugates by means of LC-MS/MS in pre- and postmenopausal healthy women, no levels of E2-3-S have been reported (Chapter 1.2.3, Table 4). However, in another study conducted in our research group (*n* = 111) and using the same UHPLC-MS/MS method, E2-3-S was detected in 68% of the plasma samples from premenopausal women above the LOQ of 109 fmol/mL, but no levels were detected in plasma samples from postmenopausal women.

In the present study, E2-3-S was detected in 24% of the samples (*n* = 6) above the LOQ of 109 fmol/mL with levels of 111-329 fmol/mL (median 171 fmol/mL, Figure 34). Additionally, in 4% of the samples (*n* = 1), E2-3-S levels were below the LOQ, in 60% (*n* = 15) below the LOD of 54 fmol/mL, and in 2% (*n* = 3) were established as n.d. due to interferences with matrix peaks (Appendix A4.15). All detected levels were in plasma samples from premenopausal women except for one with 168 fmol/mL which corresponds to a perimenopausal woman. In postmenopausal women, no levels above the LOD of 54 fmol/mL were detected.

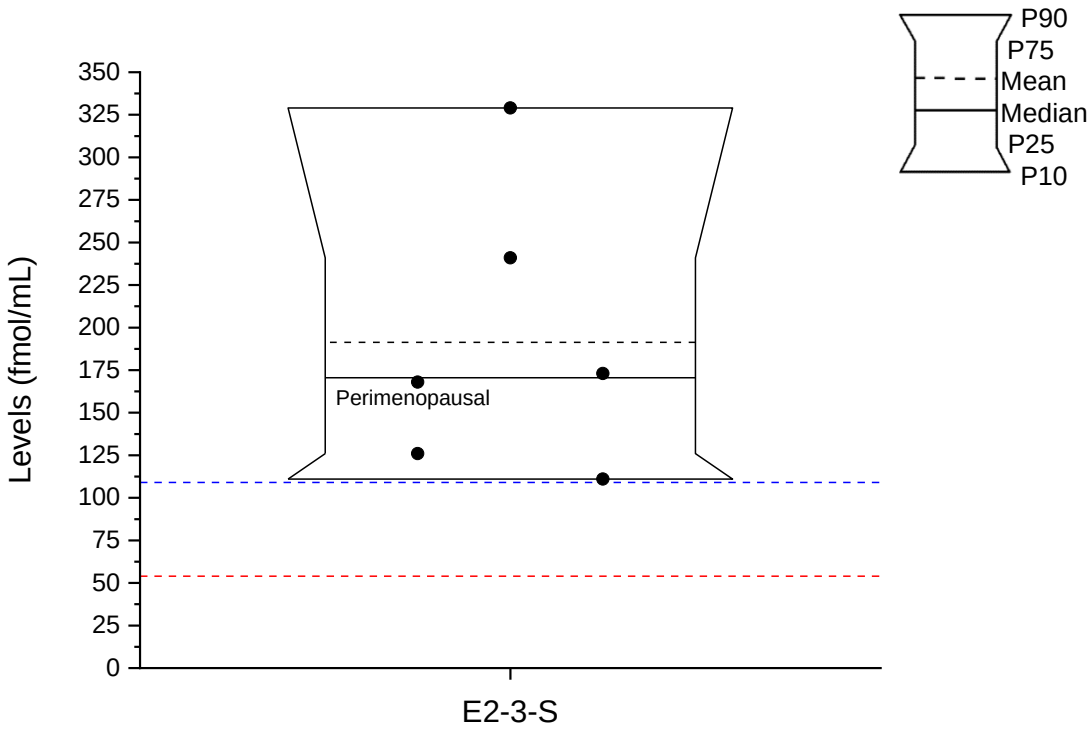

Figure 34: Levels of E2-3-S (*n* = 6) in plasma samples from women without breast cancer determined by means of UHPLC-MS/MS (Chapter 3.2.1.2). ---LOD; --- LOQ; P, percentile. Complete box-plot chart statistics available in Appendix A4.15.

In comparison with another study conducted in our research group, E2-3-S was detected in premenopausal women, and no levels were detected in postmenopausal women. Furthermore, E2-3-S was detected in those plasmas with E2 levels above the median (37 fmol/mL, Chapter 4.4.1). Thus, it can be hypothesized that during the menopause, E2-3-S could not serve as a depot of E2, and its biosynthesis to further release into circulation is also affected by the lower levels of E2.

Ratios levels of 17β-estradiol-3-sulfate to that of 17β-estradiol

To determine the fold difference of E2-3-S with respect to its parent E2 in the plasma samples from the present study, individual ratios of E2-3-S levels to E2 levels (ratios E2-3-S/E2) were calculated. Ratios were established by using calculated levels of E2

and E2-3-S (*n* = 5) in plasma samples from premenopausal women above the LOQ of 109 fmol/mL. Since E2-3-S was detected in those plasma samples with levels of E2 above the median (Chapter 4.4.1), it would be expected to have ratios E2-3-S/E2 < 1.

Thus, ratios E2-3-S/E2 in premenopausal women were 0.37-6.18 (median 0.69) (Figure 35).

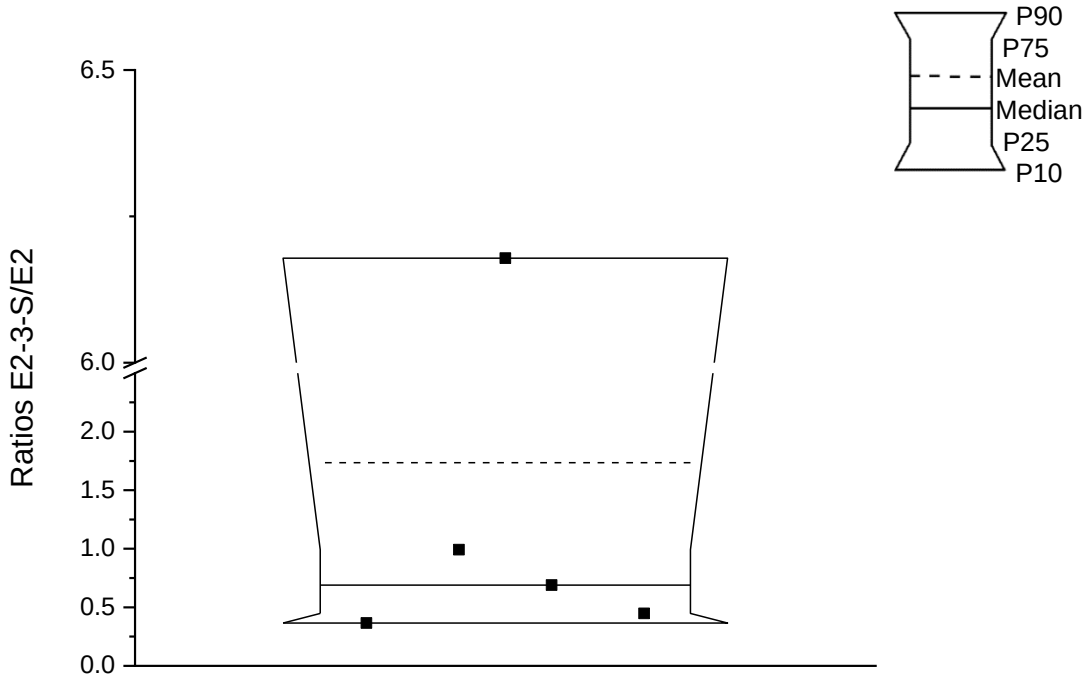

Figure 35: Ratios of E2-3-S levels to E2 levels (ratios E2-3-S/E2) in plasma samples from premenopausal women without breast cancer (*n* = 5). P, percentile. Complete box-plot chart statistics in Appendix A4.16.

Median E2-3-S/E2 ratios support the presence of major levels of E2 in plasma samples from premenopausal women, but no data for comparison was identified in the literature.

4.4.2.4. Determination of other conjugates of 17β-estradiol: 17β-estradiol-3-glucuronide and 17β-estradiol-17-sulfate

As previously described, E2 is further conjugated to E2-3-G and E2-17-S by UGT and SULT isoforms, respectively (Chapters 1.2.3-1.2.4). In studies determining serum levels of estrogen conjugates by means of LC-MS, no levels of E2-17-S have been reported. In the case of E2-3-G, Caron et al. (2009) detected levels in 70% and 40% of the serum samples from pre- and postmenopausal healthy women, respectively, above the LOQ of 11 fmol/mL (Chapter 1.2.4, Table 6).

In the present study, levels of E2-3-G and E2-17-S were less than 720 and 253 fmol/mL, respectively. This is in accordance with previous results in plasma samples derived from the Isocross study analyzed in 2014 (n = 10) and plasma samples from another study conducted in our research group (n = 111) using the same analytical method.

Since the LOD of E2-3-G of 720 fmol/mL is very above the LOQ level of 11 fmol/mL determined by Caron et al. (2009), detected levels in pre and postmenopausal healthy women of 19-74 fmol/mL could not have been detected with the method applied in this study.

4.4.3. Determination of oxidative metabolites of estrogens

Additionally to direct conjugation, estrogens undergo extensive oxidative phase I metabolism. This metabolic pathway produces hydroxyestrogens, hydroxyl derivates catalyzed by different hepatic and extrahepatic CYPs (Chapter 1.2.1). After hydroxylation, hydroxyestrogens undergo phase II metabolism catalyzed by the COMT, producing methoxyestrogens (Chapter 1.2.2).

In this chapter, the analysis by means of GC-MS/MS of hydroxyestrogens (Chapter 4.4.3.1), 2-MeO-E1 (Chapter 4.4.3.2.1) and other methoxyestrogens under their LOD levels (Chapter 4.4.3.2.2) is described.

4.4.3.1. Determination of hydroxyestrogens

A predominant metabolic pathway of estrogens is an A and D ring hydroxylation to form hydroxyestrogens, which are further oxidized to reactive quinones and semiquinones linked with breast cancer initiation (Chapter 1.2.1). Circulating mean/median levels reported for hydroxyestrogens by chromatographic techniques correspond mainly to the sum of the conjugated (as sulfates and glucuronides) and unconjugated forms after enzymatic hydrolysis (Chapter 1.2.1, Table 2). Yet, levels corresponding to their free forms are usually undetected in serum from healthy women (Xu et al., 2007).

In the present study, both 16α-HO-E1 and 16α-HO-E2 were analyzed in 88% of the samples (*n* = 22), and levels were less than 41 and 370 fmol/mL, respectively. 2-HO-E1 was analyzed in 60% of the samples (*n* = 15) and 2-HO-E2 in 80% of the samples (*n* = 20) and levels were less than 748 and 952 fmol/mL, respectively. Finally, both 4-HO-E1/E2 were analyzed in 52% of the samples (*n* = 13) and levels were less than 1177 and 2223 fmol/mL, respectively (Boxplot charts and statistic of all hydroxyestrogens analyzed in the present study available in Appendices A4.17-A4.19). These results are in accordance with previous results in plasma samples derived from the Isocross study analyzed in 2014 (*n* = 10) and plasma samples from another study conducted in our research group (*n* = 111) using the same analytical method, on which no levels of hydroxyestrogens were detected.

Moreover, previously reported mean/median serum levels of hydroxyestrogens corresponding to the sum of the free and conjugated forms (Chapter 1.2.1, Table 2) would not have been detected with the method here applied, which only determines the free forms and does not involve enzymatic hydrolysis.

In the present study, high LODs, as well as low recoveries and evaluability of hydroxyestrogens were found. Except for 16α-HO-E1, all hydroxyestrogens have median recoveries under 32% (Appendix A4.20). Yet, their presence in the plasma samples from the present study cannot be discarded accurately. Possible reasons could be the low detectability of the references and the probable instability of the hydroxyestrogens during sample preparation (Denver et al., 2019b).

4.4.3.2. Determination of methoxyestrogens

Methylation of hydroxyestrogens catalyzed by the COMT occurs for both E1 and E2 at positions 2 and 4 of the molecule producing 2- and 4-MeO-E1 and 2- and 4-MeO-E2 (Chapter 1.2.2). Using chromatographic techniques, circulating levels of 2-MeO-E1/E2 have been often reported as their free forms, meanwhile, 4-MeO-E1/E2 have been reported as the sum of the conjugated (as sulfates and glucuronides) and unconjugated forms after enzymatic hydrolysis, since free forms are usually undetected (Chapter 1.2.2, Table 3).

4.4.3.2.1. Determination of 2-methoxyestrone

Within the metabolic pathway of methoxyestrogens, 2-MeO-E1 has been reported as the predominant one in circulation (Chapter 1.2.2). Previous studies determining mean/median serum levels of this metabolite in pre- and postmenopausal healthy women reported amounts up to tens of fmol/mL (Chapter 1.2.2, Table 3).

In the present study, 2-MeO-E1 was detected in 20% of the samples (*n* = 5) above the LOQ of 30 fmol/mL with levels of 51-164 fmol/mL (median 90 fmol/mL). Form these 5 samples, 2 were from premenopausal women (90 and 108 fmol/mL, respectively), two from perimenopausal women (51 and 164 fmol/mL, respectively) and one corresponds to one plasma from the BRK (71 fmol/mL) (Figure 36). From these 5 samples, 3 were analyzed also in 2014, but just one plasma from a perimenopausal woman exhibited levels of 2-MeO-E1 of 202 fmol/mL. Moreover, in 24% of the samples (*n* = 6) levels of 2-MeO-E1 were below the LOQ of 30 fmol/mL and in 56% (*n* = 14) were below the LOD of 7 fmol/mL (Appendix A4.21). In postmenopausal women, no levels above the LOQ of 30 fmol/mL were detected.

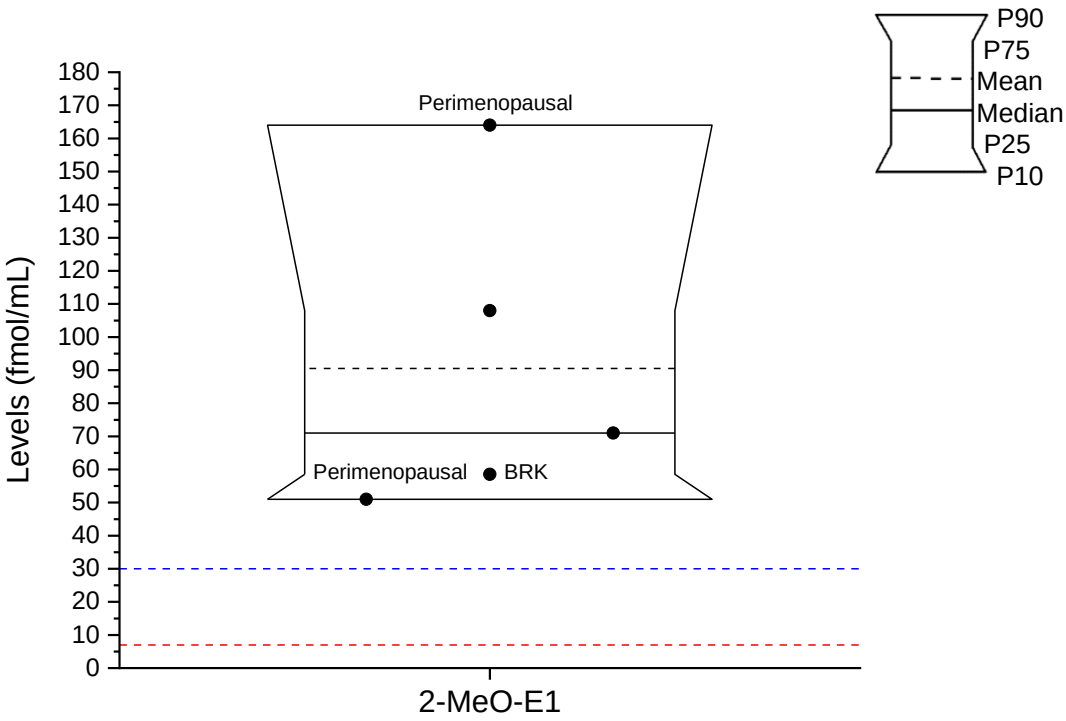

Figure 36: Levels of 2-MeO-E1 (*n* = 5) in plasma samples from women without breast cancer determined by means of GC-MS/MS (Chapter 3.2.1.3). ---LOD; --- LOQ; P, percentile. Complete box-plot chart statistics available in Appendix A4.21.

Levels of 2-MeO-E1 detected in plasma samples from premenopausal women in the present study (90-108 fmol/mL) are comparable with those reported by Coburn et al. (2019) and Xu et al. (2007) (Chapter 1.2.2, Table 3). No levels of 2-MeO-E1 above the LOQ of 30 fmol/mL were detected in postmenopausal women, however, levels reported in other studies (Chapter 1.2.2, Table 3) would have been detected with the method applied in this study.

Ratios of levels of 2-MeO-E1 to that of E1

Median plasma levels of E1 (94 fmol/mL, Chapter 4.4.1) are comparable with those of 2-MeO-E1 (90 fmol/mL), from which ratios of 2-MeO-E1 levels to E1 levels (ratios 2-MeO-E1/E1) < 1 would be expected. However, whereas E1 was detected in 100% (*n*

= 25) of the study population, 2-MeO-E1 was detected only in 20% (*n* = 5), and from there, only 8% (*n* = 2) belong to premenopausal women. For these 2 samples, to determine the fold difference and to compare with the current literature, ratios 2-MeO-E1/E1 were established by using calculated levels of E1 and 2-MeO-E1 (*n* = 2). Thus, ratios 2-MeO-E1/E1 in premenopausal women were 0.26 and 0.64. These ratios are comparable with those from the literature (calculated with reported mean/median levels of 2-MeO-E1 and E1, Appendix A4.30).

In the 2 plasma samples from premenopausal women with detected 2-MeO-E1 levels, levels of E1, E1-S and E-G were above the median (Appendix A4.29). Therefore, it could be hypothesized that in plasmas with lower levels of E1, the conjugation pathway to sulfates and glucuronides would be predominant over the methylation pathway.

4.4.3.2.2. Evaluation of methoxyestrogens under their limits of detection

Besides 2-MeO-E1, 2-MeO-E2 and 4-MeO-E1/E2 were also analyzed by GC-MS/MS. Previous studies determining serum-free levels of 2-MeO-E2 in pre- and postmenopausal healthy women, have reported that this metabolite is often not detected, or is near or below the LOQ level (Chapter 1.2.2, Table 3). Moreover, serum levels of 4-MeO-E1 and 4-MeO-E2 in pre- and postmenopausal healthy women have been usually undetected as their free forms but detected as the sum of their free and conjugated forms (as sulfates and glucuronides) after enzymatic hydrolysis, with levels below tens to tens of fmol/mL (Chapter 1.2.2, Table 3).

In the present study, 2-MeO-E2 and 4-MeO-E1 were analyzed in 100% of the samples (*n* = 25) and levels were less than 15 and 10 fmol/m, respectively (Boxplot charts and statistics available in Appendix A4.22). Furthermore, 4-MeO-E2 was analyzed in 96% of the samples (*n* = 24) with levels less than 15 fmol/mL, and in one sample (4%) was n.d. due to interferences with matrix peaks (Boxplot charts and statistics are available in Appendix A4.22). These results are comparable with those obtained in the common 10 samples derived from the Isocross study analyzed in 2014 (complete levels of comparison and statistical tests available in Appendices A4.23-A4.25).

Serum levels of free 2-MeO-E2 reported by Coburn et al. (2019) would not have been detected with the method here applied since the LOD of the cited study is 0.33 fmol/mL. Furthermore, serum levels of 4-MeO-E1/E2 reported as the sum of the conjugated and unconjugated forms (Chapter 1.2.2, Table 3) would not have been detected with the method here applied which was designed to detect only the free forms and does not involve enzymatic hydrolysis.

Although LODs of 4-MeO-E1 (10 fmol/ml) and 4-MeO-E2 (15 fmol/mL) were comparable with 2-MeO-E1 (7 fmol/mL), the first 2 metabolites were not detected in any plasma sample. This could be explained by the fact that in normal estrogen-sensitive tissues, the hydroxylation at position 2 occurs in preference over the position 4 (Stack et al., 2014), reducing the chances for 4-MeO-E1/E2 to be biosynthesized.

4.4.4. Determination of methoxyestrogen glucuronides

Previous studies reported that methoxyestrogens are subjected to glucuronidation *in vitro* by different human UGT isoenzymes, leading to the possibility to find methoxyestrogen glucuronides in circulation (Lepine et al., 2004). Because of the key role of estrogen conjugates as detoxifying metabolites, the study of circulating levels of methoxyestrogen glucuronides is essential. Nevertheless, due to the lack of sensitive and accurate analytical techniques and compound references, this study remains incomplete. To the date, serum levels of only 2-MeO-E1-G and 2-MeO-E2-3-G in pre- and postmenopausal healthy women have been reported by one research group (Chapter 1.2.4), and no previous reports of the analysis of 4-MeO-E1-G, 4-MeO-E2-3-G or 2- and 4-MeO-E2-17-G have been published.

In the present study, after the biosynthesis of reference compounds (Chapter 4.1) and the validation of the extended method by means of UHPLC-MS/MS for the analysis of methoxyestrogen glucuronides (Chapter 4.2), 2- and 4-MeO-E1-G, 2-and 4-MeO-E2-3-G and 2- and 4-MeO-17-G were analyzed in 25 plasma samples from women without breast cancer.

4.4.4.1. Determination of 2-methoxyestrone-3-glucuronide

As previously mentioned, levels of 2-MeO-E1-G were detected in serum from pre- and postmenopausal healthy women in the order of tens of fmol/mL (Chapter 1.2.4).

In the present study, 2-MeO-E1-G was detected in 8% of the plasma samples (*n* = 2) with levels of 93 and 51 fmol/mL in one premenopausal and one perimenopausal woman, respectively. In 84% of the samples (*n* = 21), levels of 2-MeO-E1-G were less than 183 fmol/mL plasma and in 8% (*n* = 2) were established as n.d. due to interferences with the matrix (Appendix A4.26).

In the two samples with detected levels of 2-MeO-E1-G, besides E1 and E1-S, levels of E1-G and 2-MeO-E1 were also detected (Appendix A4.29). Specifically, E1 levels were above the P75, E1-S levels were above the P90 and E1-G had a LOQ level for the perimenopausal woman and a level above the P90 for the premenopausal woman. Furthermore, in both women with detected levels of 2-MeO-E1-G, levels of 2-MeO-E1 were above the median. Surprisingly, despite the differences between the LOD levels of 2-MeO-E1-G and its precursor 2-MeO-E1 (183 fmol/mL and 7 fmol/mL, respectively), detected levels of 2-MeO-E1 of 51 fmol/mL and 108 fmol/mL and of 2-MeO-E1-G of 51 fmol/mL and 93 fmol/mL in the same peri and postmenopausal women, respectively, were comparable (Appendix A4.29). Thus, it could be hypothesized that a pattern of conjugation to 2-MeO-E1-G should be expected in those plasmas with high levels of its precursor 2-MeO-E1, which was also detected in plasmas with levels of E1 and its conjugates above the P75.

Ratios of levels of 2-methoxyestrone-3-glucuronide to that of estrone and methoxyestrone

An association between ratios of free estrogens/hydroxyestrogens and breast cancer has been postulated in breast cancer patients and matching controls (Sampson et al., 2017). Given these associations, ratios of individual detoxifying estrogen metabolites such as methoxyestrogen glucuronides may provide important information by establishing fold difference patterns.

Therefore, ratios of levels of 2-MeO-E1-G to levels of E1 (2-MeO-E1-G/E1) and ratios of levels of 2-MeO-E1-G to levels of 2-MeO-E1 (2-MeO-E1-G/2-MeO-E1) were

determined for the samples with individual LOQ levels of 2-MeO-E1-G (*n* = 2). Thus, ratios 2-MeO-E1-G/E1 were 0.23 and 0.22 and ratios 2-MeO-E1-G/2-MeO-E1 were 0.004 and 0.002.

Ratios 2-MeO-E1-G/E1 were comparable with those calculated with median levels of 2-MeO-E1-G and E1 in serum from premenopausal women reported by Caron et al. (2009) (Appendix A4.30). Yet, no literature to compare ratios 2-MeO-E1-G/2-MeO-E1 was identified.

Because of the small number of plasma samples with detected levels of 2-MeO-E1-G, to conclude about these ratios would not be meaningful. However, this information could be the starting point for further investigations in studies with larger cohorts. Proper validation of these findings could serve as opportunities for breast cancer prevention when individual ratios are modified e.g. by modifying the lifestyles.

4.4.4.2. Evaluation of other methoxyestrogen glucuronides

As previously described, levels of 2-MeO-E2-3-G in serum from pre- and postmenopausal healthy women were reported in the order of tens of fmol/mL, and no levels of other methoxyestrogens have been reported (Chapter 1.2.4).

With the method applied in the present study, 2-MeO-E2-3-G has a LOD (165 fmol/mL) higher than the LOQ reported by Caron et al. (2009) (11 fmol/mL, LOD not reported). Therefore, reported levels of 2-MeO-E2-3-G in the cited study would not be detected.

Although LODs of 2-MeO-E2-3-G (165 fmol/mL), 4-MeO-E1-G (66 fmol/mL) and 4-MeO-E2-3-G (76 fmol/mL) were lower than the LOD of 2-MeO-E1-G (183 fmol/mL), levels of the first 3 metabolites were not detected in any plasma sample (Appendices A4.27-A4.28). Furthermore, due to poor analytical response and high LODs, levels higher than 1022 of 2-MeO-E2-17-G and 569 of 4-MeO-E2-17-G of fmol/mL plasma can be excluded.

Because of the results obtained in Chapter 4.4.4.1, it was hypothesized that a pattern of conjugation to 2-MeO-E1-G should be expected in those plasmas with detected levels of its precursor 2-MeO-E1 above the median. Thus, when no levels of 4-MeO-E1 or 2- and 4-MeO-E2 were detected in any plasma (Chapter 4.4.3.2.2), a conjugation

pattern to 4-MeO-E1-G, 2-MeO-E2-3-G, 4-MeO-E2-3-G and 4-MeO-E2-17-G would be unlikely.

However, to interpret LOD levels in the context of this part of the metabolic pathway, a comparison between LOD levels of methoxyestrogen glucuronides and their precursors (Table 40) should be addressed.

Table 40: Comparison of LOD levels (fmol/mL) between methoxyestrogens (previously obtained in other studies, Chapter 3.2.11.1) and methoxyestrogen glucuronides.

Parent methoxyestrogen	LOD (fmol/mL)	Methoxyestrogen glucuronide	LOD (fmol/mL)
2-MeO-E1	7	2-MeO-E1-G	183
4-MeO-E1	15	4-MeO-E1-G	66
2-MeO-E2	12	2-MeO-E2-3G	165
		2-MeO-E2-17G	1022
4-MeO-E2	10	4-MeO-E2-3G	76
		4-MeO-E2-17G	569

LODs of methoxyestrogen glucuronides are higher than the LODs of their respective methoxyestrogen. Therefore, it could be expected that levels of methoxyestrogen glucuronides would not be detected below the LODs of the respective methoxyestrogen, or in between the gap of LODs of both conjugated and unconjugated analytes. This means that as in the present study the presence of more than 10 fmol 4-MeO-E1, 15 fmol 2-MeO-E2 and 15 fmol/mL 4-MeO-E2 per mL plasma can be excluded, same levels of 4-MeO-E1-G, 2-MeO-E2-3-G, 2-MeO-E2-17-G, 7 4-MeO-E2-3-G and 4-MeO-E2-17-G could be also excluded.

However, detected levels of 2-MeO-E1-G of 51 fmol/mL and 93 fmol/mL are in between the gap of the LODs of both conjugated and unconjugated forms. Therefore, the possible reasons why methoxyestrogen glucuronides were not detected in circulation could be also:

- **Enzymatic specificities**

The methylation of hydroxyestrogens catalyzed by the COMT is carried out in lesser amounts for 4-HO-E1/E2 compared with 2-HO-E1/E2 (summarized in Guillemette et al., 2004). For instance, methylation products of 4-HO-E1/E2, as precursors of 4-MeO-E2-3/17-G, would have fewer levels available for the biosynthesis of the later mentioned conjugates. Additionally, no specific activity of UGTs for the conjugation of methoxyestrogens at position -17 has been reported (Chapter 1.2.4, Table 5). Therefore, the biosynthesis of 2- and 4-MeO-E2-17-G could not be completely assumed.

- **Transport proteins**

Whereas estrogens are able to freely diffuse through biological membranes, their conjugates need active transport to cross them. Investigations conducted by Jarvinen et al. (2018) determined the specificity and role of efflux transporters in the disposition of estrogen glucuronides in humans (Chapter 1.2.4). Nevertheless, no studies of this type have been conducted in methoxyestrogen glucuronides. For these molecules, the methyl group either at position 2- or 4- of the corresponding estrogen may represent a steric impediment for the binding to those transporters or the molecule may stay attached to the membrane, modifying the permeability, and perhaps, decreasing circulating levels.

Therefore, in the samples from the present study population analyzed with the extended UHPLC-MS/MS method, the presence of more than 68 (4-MeO-E1-G), 121 (2-MeO-E2-3-G), 2098 (2-MeO-E2-17-G), 2098 (4-MeO-E2-3-G) and 2219 (4-MeO-E2-17-G) fmol/mL plasma can be excluded (Appendices A4.27-A4.28).

4.4.5. Correlation between levels of estrone, 17β-estradiol, and estrone-3-sulfate with regard to the menopausal status

Significant strong correlations between circulating levels of free estrogens and estrogen conjugates in pre- and postmenopausal healthy women have been previously reported (Chapter 1.3). Yet, the data available in premenopausal women are more limited than in postmenopausal women (Chapter 1.3).

Therefore, to contribute with more data in premenopausal women and to compare with the current literature, correlation analyses were performed and compared between premenopausal (up to 45 years old) and postmenopausal women without breast cancer (up 53 years old). Since there were extreme levels of estrogens and their metabolites which may bias the correlation coefficient, the rank-based Spearman correlation coefficient was used. Statistical correlation analyses were performed using the R-scripts previously provided by the Chair of Mathematical Statistics with application in Biometrics of the University of Dortmund (Chapter 3.2.12). Furthermore, estrogen metabolites that were not detected in more than 30% of the samples were excluded from the correlation analyses (E1-G, E2-3-S, and 2-MeO-E1).

Spearman's correlation coefficients among plasma levels of E1, E2, and E1-S in pre (n = 9) and postmenopausal women (n = 7) from the present study were calculated, showing positive associations in all cases (Table 41).

Table 41: Spearman's correlation coefficients among levels of E1, E2 and E1-S in plasma from pre- (n = 9) and postmenopausal (n = 7) women without breast cancer. Correlations in the light grey background shown to be statistically significant (p < 0.05, Appendix A4.31).

Menopausal status		E1	E2	E1-S
Premenopausal	E1	1.00	0.78	0.70
Postmenopausal		1.00	0.77	0.86
Premenopausal	E2		1.00	0.90
Postmenopausal			1.00	0.69
Premenopausal	E1-S			1.00
Postmenopausal				1.00

In plasmas from premenopausal women, significant positive correlations were observed among levels of E1, E2, and E1-S, which may suggest a link between circulating amounts of estrogens and their conjugates. These findings are in line with those from Caron et al. (2009), which determined that a significant correlation exists between serum levels of unconjugated estrogens and their corresponding conjugated metabolites in premenopausal healthy women (n = 19) during their follicular and luteal phase (Chapter 1.3).

Moreover, in plasma from postmenopausal women, significant positive correlations were observed between levels of E1 and E2 and between E1 and E1-S. These observations may also suggest a link between circulating amounts of E1 and E1-S during the menopause. Furthermore, moderate (far from R = 1 but above 0.5) no significant correlation (p > 0.05, Appendix A4.31) was observed between levels of E2 and E1-S, which may be attributed to the declining of E2 levels during the menopause (summarized in Africander and Storbeck, 2018). These observations are in line with findings by Audet-Walsh et al. (2011) (n = 110) and Labrie et al. (2011) (n = 438) in serum from postmenopausal healthy women, on which significant associations between E1 and E2, and moderate associations between E2 and E1-S were reported (Chapter 1.3).

As observed, an association between plasma levels of E1 and E2, and between E1 and its conjugate E1-S was present regardless of the menopausal status. Nevertheless, it is very important to note that correlation analyses in small sample sizes (n < 25) have shown to give normal to poor approximations (de Winter et al., 2016), which may bias the results. Accordingly, further validation of the approaches here related (even when consistent with previous reports, Chapter 1.3), is required in a larger sample population.

4.5. Analysis of methoxyestrogen glucuronides in normal glandular and adipose tissue specimens from women without breast cancer

In previous results in normal GLT and ADT specimens derived from the Isocross study, besides 2-MeO-E1, no other methoxyestrogen was detected. One reason for this could be that they are present in their glucuronide form. This hypothesis is supported by the presence of several UGT isoforms in normal breast tissue (Chapter 1.4). Since biosynthesized references and the validated analytical method are now available for the specific detection and quantification of these metabolites in human plasma, the possibility to apply the same method in normal human GLT and ADT specimens was evaluated.

Recovery (%) and LOD levels (fmol/g) in normal human glandular and adipose breast tissue specimens

The recovery (%) and LOD levels (fmol/g) of methoxyestrogen glucuronides were determined in both GLT and ADT specimens derived from the Isocross study (Chapter 3.2.8.2). Samples were spiked with deuterated biosynthesized references, extracted (Chapter 3.2.9.2) and analyzed by means of UHPLC-MS/MS using the method previously described (Chapter 3.2.1.2).

Thus, recoveries in GLT (n = 18) and ADT (n = 12) were determined. Median recoveries in GLT were 4-24% (4-MeO-E2-17-G - 4-MeO-E1-G) and in ADT were 13-37% (2-MeO-E2-17-G - 4-MeO-E2-3-G) (Figure 37). The median recovery value of 2-MeO-E1-G in plasma, which was the only methoxyestrogen glucuronide detected in the present study, was 53% (Chapter 4.2.3). Therefore, when the highest recoveries in GLT and ADT were 24% and 37%, respectively, the chance to find any methoxyestrogen glucuronide would be very rare, if levels are expected in the range of tens to hundreds of fmol/g as other estrogen glucuronides.

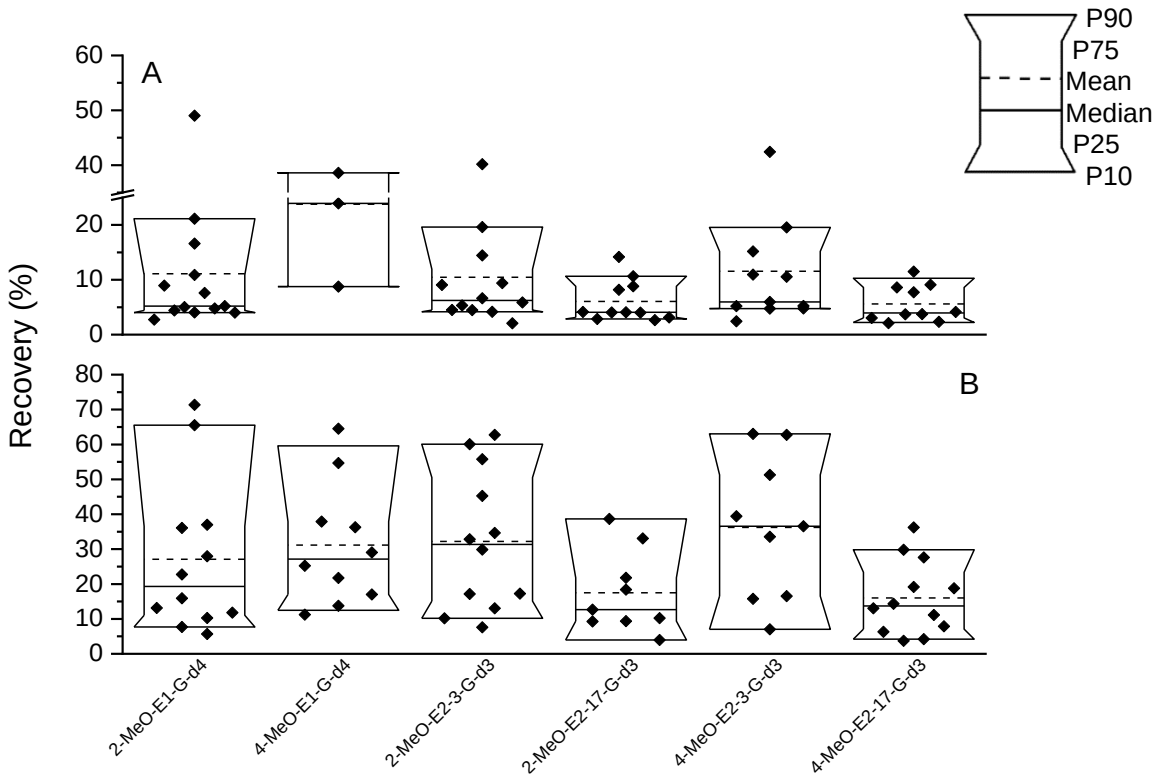

Figure 37: Recoveries (%) of methoxyestrogen glucuronides in (A) GLT and (B) ADT from women without breast cancer determined by means of UHPLC-MS/MS (Chapter 3.2.1.2). P, percentile. Complete box-plot chart statistics available in Appendices A4.32-A43.33.

Moreover, LOD levels in GLT (*n* = 18) and ADT (*n* = 12) were also determined. Median LOD levels in GLT were 399-10523 fmol/g (4-MeO-E2-3-G - 4-MeO-E2-17-G) and in ADT were 111-3751 fmol/g (2-MeO-E2-3-G - 4-MeO-E2-17-G) (Figures 38-39). In plasma, median LOD levels were in the range of 66-1022 fmol/mL (4-MeO-E1-G - 2-MeO-E2-17-G). Therefore, when LOD levels in GLT and ADT are too high compared with plasma (Chapter 4.2.5.1), the chance to find any of these metabolites in tissue specimens would be very rare, if levels are expected in the range of tens to hundreds of fmol/g as other estrogen glucuronides.

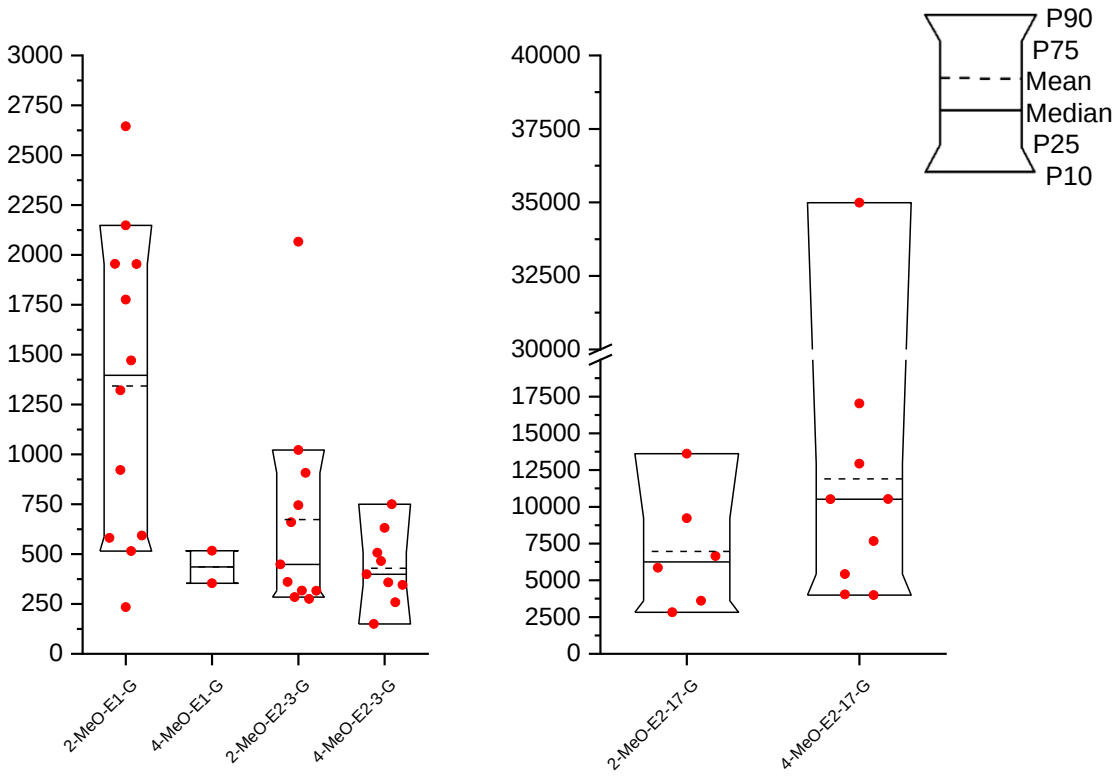

Figure 38: LOD levels (fmol/g) of methoxyestrogen glucuronides in GLT from women without breast cancer determined by means of UHPLC-MS/MS (Chapter 3.2.1.2). P, percentile. Complete box-plot chart statistics in Appendix A4.34.

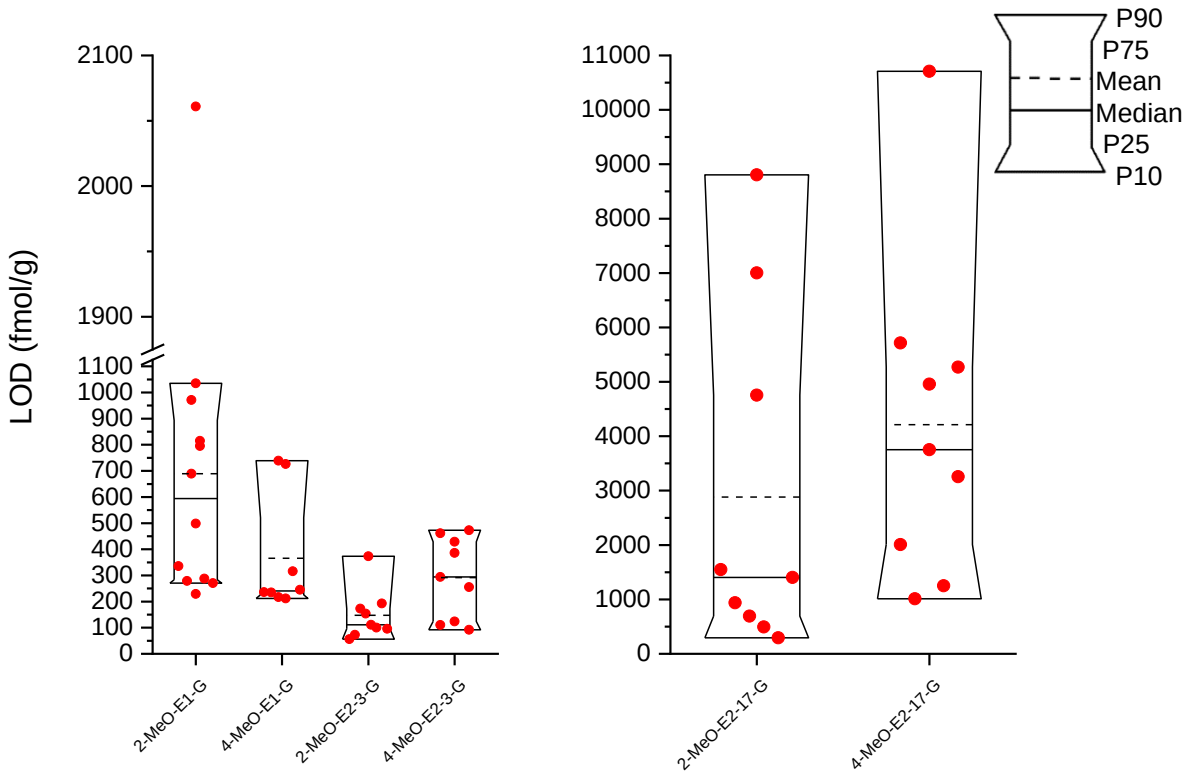

Figure 39: LOD levels (fmol/g) of methoxyestrogen glucuronides in ADT from women without breast cancer determined by means of UHPLC-MS/MS (Chapter 3.2.1.2). P, percentile. Complete box-plot chart statistics in Appendix A4.35.

Evaluating the applicability of the analytical method for the quantification of methoxyestrogen glucuronides in tissue specimens, low recoveries, and high LOD levels compared with plasma were found (Table 42).

Table 42: Comparison between median recoveries (%) and median LOD levels in plasma (Appendix A2.8, Appendix A2.10) with GLT and ADT.

Conjugate	Recovery (%)			LOD (fmol/mL or g)		
	Plasma	GLT	ADT	Plasma	GLT	ADT
2-MeO-E1-G	53	5	19	183	1396	594
4-MeO-E1-G	51	24	27	66	436	241
2-MeO-E2-3-G	62	6	31	165	448	111
2-MeO-E2-17-G	59	4	12	1022	6249	1404
4-MeO-E2-3-G	60	6	37	76	399	294
4-MeO-E2-17-G	51	4	14	569	10523	3751

Moreover, in many analyses of tissue specimens, no signals were observed in the extracted ion chromatograms of the specific transitions of methoxyestrogen glucuronides. Therefore, validation of the method and further analysis were not pursued.

In consequence, it was not possible to apply the UHPLC-MS/MS method to the analysis of methoxyestrogen glucuronides in human plasma to human breast ADT and GLT specimens.

5. Summary

Estrogens play a key role in breast cancer development. However, not all estrogen metabolites have the same effect. Therefore, the knowledge on the profile of circulating estrogens in healthy women is of importance. However, most methods used for the analysis of estrogens do either not target conjugated estrogens or detect only the sum of the respective free and conjugated form. Accordingly, this work aimed to evaluate the possibility to include methoxyestrogen glucuronides into an existing method for the analysis of estrogens, and therewith, complement the analysis of estrogen profiles in human plasma and breast tissue from women without breast cancer.

First, microsomal protein fractions from rat liver were used to biosynthesize six different methoxyestrogen glucuronides and their corresponding deuterium analogues to serve as reference compounds. Deuterated analogues were synthesized *in vitro* by methylation and glucuronidation of deuterated hydroxyestrogens. Identities of the products were verified by UHPLC-tandem mass spectrometry in enhanced product ion scan mode. Quantification using the peak area ratio of estrone and 17β-estradiol to their corresponding glucuronides and calibration curves of their methoxylated derivates confirmed amounts of reference compound synthesized in the microgram range which were sufficient for further analysis. For these references, the most intense precursor and fragment ions were determined and their respective peak intensities and chromatographic separation were optimized.

For the validation of the method, the mixture of deuterated analogues (internal standards) was separated exhibiting a good chromatographic resolution of the peaks as well as no interference with possible isotopes. The specificity of the analytical method was ensured by the specific substance- and source-dependent parameters and the selectivity by quantifier/qualifier ratios. The recoveries were between 51% (4-methoxyestrone-3-glucuronide) and 62% (2-methoxyestradiol-3-glucuronide). All conjugates exhibit a proportional analytical response except for 2-methoxyestradiol-17-glucuronide. The limits of detection and quantification in plasma were between 66 fmol/mL (4-methoxyestrone-3-glucuronide) and 1022 fmol/mL (2-methoxyestradiol-17-glucuronide) and between 155 fmol/mL (4-methoxyestrone-3-glucuronide) and 3636 fmol/mL (2- and 4- methoxyestradiol-17-glucuronide), respectively. At the suggested limits of quantification, intra- and inter-day accuracies of 93% (2-methoxyestradiol-3-glucuronide) to 110% (4-methoxyestrone-3-glucuronide) and intra- and inter-day

precisions of 2% (2-methoxyestradiol-3-glucuronide) to 15% (4-methoxyestrone-3-glucuronide) were achieved. For 2- and 4-methoxyestradiol-17-glucuronide, accuracies and precisions up to 188% and 33%, respectively, were out of specification. Biosynthesized references were stable at the storage conditions for at least five months, as well as in spiked plasma samples stored in the autosampler for one day, and after freeze/thaw cycles during four days. Since accuracies and precisions are in line with the FDA (2018) recommendations, and because of the recoveries above 50%, the limits of detection in the range of tens to hundred fmol/mL, and the proportional analytical response of the references, the extended method could be applied for the quantitative analysis of 2- and 4-methoxyestrone-3-glucuronide and 2- and 4-methoxyestradiol-3-glucuronide in human plasma. Because of accuracies and precisions out of specification, poor analytical response and higher limits of detection, the extended method was not optimum for the quantitative analysis in plasma of 2- and 4-methoxyestradiol-17-glucuronide, but the qualitative analysis could be performed.

After validation, the extended UHPLC-tandem mass spectrometry-based method and the existing GC-tandem mass spectrometry-based method were used to analyze estrone and 17β-estradiol, their hydroxylated and methoxylated metabolites, estrone-3-sulfate, estradiol-3 and -17-sulfate, estrone-3-glucuronide, 17β-estradiol-3-glucuronide and six different methoxyestrogen glucuronides in plasmas derived from nine premenopausal, five perimenopausal and seven postmenopausal women as well as from four women of unknown menopausal statuses.

As expected, estrone and 17β-estradiol were detected at levels from tens to hundreds of fmol/mL and estrone-3-sulfate at levels from hundreds to thousands of fmol/mL. Estrone-3-glucuronide was detected above its limit of quantification in 28% of the samples at levels of hundreds of fmol/mL, but no levels were detected in postmenopausal women, contrasting with Caron et al. (2009). 17β-estradiol-3-sulfate was detected above its limit of quantification in 24% of the samples at levels from tens to hundreds of fmol/mL. No data was identified for comparison. Levels of 17β-estradiol-3-glucuronide and 17β-estradiol-17-sulfate were less than 720 and 253 fmol/mL, respectively, therefore, levels reported by Caron et al. (2009) of 17β-estradiol-3-glucuronide of tens of fmol/mL would not be detected with the present method. Levels of hydroxyestrogens were less than 41 (16α-hydroxyestrone) to 2223 (4-hydroxyestradiol) fmol/mL. 2-methoxyestrone was detected above its limit of quantification in 20% of the samples at levels of tens to hundreds of fmol/mL. Levels

of 2-methoxyestradiol were less than 15 fmol/mL, contrasting with the literature reporting levels in the order of tens of fmol/mL. Levels of 4-methoxyestrone/estradiol were less than 10 and 15 fmol/mL, respectively. Contrasts with reported levels may be due to differences in the analytical methods.

With the extended method, 2-methoxyestrone-3-glucuronide was detected in plasmas from one premenopausal and one perimenopausal woman which exhibited levels of 2-methoxyestrone above the median. However, levels reported by Caron et al. (2009) for 2-methoxyestrone/estradiol-3-glucuronide would not be detected due to differences in the method and limits of detection. Furthermore, the presence of more than 66 (4-methoxyestrone-3-glucuronide), 165 (2-methoxyestradiol-3-glucuronide) and 76 (4-methoxyestradiol-3-glucuronide) fmol/mL could be excluded. Because the analytical method could be applied for the qualitative analysis of 2- and 4-methoxyestradiol-17-glucuronide levels less than 3636 fmol/mL of both analytes could be excluded.

Since only free estrogens and estrone-3-sulfate were detected in more than 30% of the samples, Spearman´s rank correlation analyses were performed only between them. As expected, positive correlations were observed among estrone, 17β-estradiol, and estrone-3-sulfate in premenopausal and postmenopausal women, respectively.

Finally, the extended method cannot be applied for the analysis of methoxyestrogen glucuronides in human adipose and glandular breast tissue specimens due to very low recoveries and higher limits of detection compared to those in plasma.

In summary, the quantitative analysis of 2- and 4-methoxyestrone-3-glucuronide and 2- and 4-methoxyestradiol-3-glucuronide and the qualitative analysis of 2- and 4-methoxyestradiol-17-glucuronide could be included in an existing method to complement the analysis of estrogen profiles and yielded the expected results in a defined test population of twenty-five plasma samples derived from women with various menopausal statuses. This is the first time that such a broad spectrum of estrogens (including metabolites and conjugates) has been analyzed together in human plasma from women without breast cancer. Therefore, the present method constitutes a tool for further investigations in hormone-dependent diseases.

6. Zusammenfassung

Estrogene spielen eine zentralle Rolle bei der Entstehung von Brustkrebs. Jedoch haben nicht alle Estrogenmetabolite die gleiche Wirkung. Deshalb ist das Wissen über das Profil der zikulierenden Estrogene bei gesunden Frauen von entscheidender Bedeutung. Die meisten Methoden zur Analyse von Estrogenen zielen jedoch entweder nicht auf konjugierte Estrogene ab oder erfassen nur die Summe der jeweiligen freien und konjugierten Form. Gegenstand der vorliegenden Arbeit war demzufolge, die Möglichkeit der Einbeziehung von Methoxyestrogenglucuroniden in eine bestehende Methode zur Analyse von Estrogenen zu evaluieren und somit die Analyse von Estrogenprofilen im menschlichen Plasma und im Brustgewebe von Frauen ohne Brustkrebs zu ergänzen.

Zunächst wurden mikrosomale Proteinfraktionen aus Rattenleber zur Biosynthese von sechs verschiedenen Methoxyestrogenglucuroniden, die als Referenzverbindungen dienen sollten. Deuterierte Analoga wurden *in vitro* durch Methylierung und Glucuronidierung kommerziell erhältlicher deuterierter Hydroxyestrogene synthetisiert. Die Identität der Produkte wurde durch UHPLC-Tandem-Massenspektrometrie im Produktionenscan-Modus verifiziert. Die Quantifizierung der Methoxyglucuronide erfolgte unter Verwendung der Peakflächenverhältnisse von Estron und 17β-Estradiol zu ihren entsprechenden Glucuroniden und Kalibrierungskurven ihrer methoxylierten Derivate und bestätigte die Synthese von mikrogramm Mengen der Referenzen. Dies war für die weitere Analyse ausreichend. Für diese Referenzen wurden die intensivsten Vorläufer- und Fragmentionen bestimmt, und ferner ihre jeweiligen Peakintensitäten sowie die chromatographische Trennung optimiert.

Für die Validierung der Methode wurde das Gemisch der deuterierten Analoga (interne Standards) getrennt, wobei eine gute chromatographische Auflösung der Peaks sowie keine Interferenz mit möglichen Isotopen auftrat. Die Spezifität der analytischen Methode wurde durch die bestimmten stoff- und quellenabhängigen Parameter und die Selektivität durch „quantifier/qualifier“-Verhältnisse sichergestellt. Die Wiederfindungen lagen zwischen 51% (4-Methoxyestron-3-Glucuronid) und 62% (2-Methoxyestradiol-3-Glucuronid). Alle Konjugate ergaben ein der Menge proportionales analytisches Signal, mit Ausnahme des 2-Methoxyestradiol-17-Glucuronid. Die Nachweis- und Quantifizierungsgrenzen im Plasma lagen zwischen 66 fmol/mL (4-

Methoxyestron-3-Glucuronid) und 1022 fmol/mL (2-Methoxyestradiol-17-Glucuronid) bzw. zwischen 155 fmol/mL (4-Methoxyestron-3-Glucuronid) und 3636 fmol/mL (2- und Methoxyestradiol-17-Glucuronid). Bei den vorgeschlagenen Quantifizierungsgrenzen wurden intra- und inter-Tages-Richtigkeiten von 93% (2-Methoxyestradiol-3-Glucuronid) bis 110% (4-Methoxyestron-3-Glucuronid) und intra- und inter-Tages-Präzisionen von 2% (2-Methoxyestradiol-3-Glucuronid) bis 15% (4-Methoxyestron-3-Glucuronid) erreicht. Bei 2- und 4-Methoxyestradiol-17-Glucuronid lagen die Richtigkeiten und Präzisionen bis zu 188% bzw. 33% außerhalb der Spezifikation. Die biosynthetischen Referenzen waren bei den Lagerungsbedingungen mindestens fünf Monate lang stabil, auch in aufgestockten Plasmaproben, die im Autosampler während eines Tages bzw. nach Gefrier-/Auftauzyklen über vier Tage gelagert wurden. Da die Grenzwerte den Empfehlungen der FDA (2018) entsprechen Wiederfindungsrate über 50% betragen, die Nachweisgrenzen im Bereich von zehn bis hundert fmol/mL liegen, sowie der proportionalen analytischen Reaktion der Referenzen, könnte die erweiterte Methode für die quantitative Analyse von 2- und 4-Methoxyestron-3-glucuronid und 2- und 4-Methoxyestradiol-3-glucuronid im Humanplasma angewendet werden. Aufgrund der außerhalb der Spezifikation liegenden Genauigkeit und Präzision, der schlechten analytischen Reaktion und der höheren Nachweisgrenzen war die erweiterte Methode nicht optimal für die quantitative Analyse von 2- und 4-Methoxyestradiol-17-Glucuronid in Plasma, aber die qualitative Analyse konnte durchgeführt werden.

Nach der Validierung wurden die erweiterte, auf der UHPL-Tandem-Massenspektrometrie basierende Methode zur Analyse von Estron-3-Sulfat, 17β-Estradiol-3- und -17-Sulfat, Estron-3-Glucuronid, 17β-Estradiol-3-Glucuronid und sechs verschiedene Methoxyestrogenglucuronide und die bestehende, auf der GC-Tandem-Massenspektrometrie basierende Methode zur Analyse von Estron und 17β-Estradiol, ihrer hydroxylierten und methoxylierten Metaboliten in Plasmen angewendet, die von neun prämenopausalen, fünf perimenopausalen und sieben postmenopausalen Frauen sowie von vier Frauen mit unbekanntem Menopausenstatus stammen.

Wie erwartet wurden Estron und 17β-Estradiol in Konzentrationen von zehn bis Hunderten von fmol/mL und Estron-3-Sulfat in Konzentrationen von Hunderten bis Tausenden von fmol/mL nachgewiesen. Estron-3-Glucuronid wurde in 28% der Proben bei Konzentrationen von Hunderten von fmol/mL oberhalb seiner Bestimmungsgrenze nachgewiesen, aber bei postmenopausalen Frauen wurden im

Gegensatz zu Caron et al. (2009) keine Gehalte festgestellt. 17β-Estradiol-3-Sulfat wurde in 24% der Proben in Konzentrationen von zehn bis Hunderten von fmol/mL oberhalb seiner Bestimmungsgrenze nachgewiesen. Es wurden keine Daten zum Vergleich identifiziert. Die Werte von 17β-Estradiol-3-Glucuronid und17β-Estradiol-17-Sulfat lagen unter 720 bzw. 253 fmol/mL, aber die von Caron et al. (2009) berichteten Werte von 17β-Estradiol-3-Glucuronid von zehn fmol/mL würden mit unserer Methode nicht erfasst. Die Gehalte an Hydroxyestrogenen betrugen weniger als 41 (16α-Hydroxyestron) bis 2223 (4-Hydroxyestradiol) fmol/mL. 2-Methoxyestron wurde in 20% der Proben bei Gehalten von zehn bis hundert fmol/mL oberhalb seiner Bestimmungsgrenze nachgewiesen. Die 2-Methoxyestradiol-Konzentration lag unter 15 fmol/mL, während die Literatur über Konzentrationen in der Größenordnung von zehn fmol/mL berichtete. Die Werte von 4-Methoxyestron/Estradiol betrugen weniger als 10 bzw. 15 fmol/mL. Unterschiede mit den berichteten Werten können auf Unterschiede in den Analysemethoden zurückzuführen sein.

Mit der erweiterten Methode, 2-Methoxyestron-3-Glucuronid wurde bei einer prämenopausalen und einer perimenopausalen Frau, die 2-Methoxyestron-Spiegel über dem Median aufwiesen. Die von Caron et al. (2009) berichteten Werte für 2-Methoxyestron/Estradiol-3-Glucuronid konnten jedoch aufgrund von Unterschieden in der Methode und den Nachweisgrenzen nicht nachgewiesen werden. Außerdem, konnte das Vorhandensein von mehr als 66 (4-Methoxyestron-3-glucuronid), 165 (2-Methoxyestradiol-3-glucuronid) und 76 (4-Methoxyestradiol-3-glucuronid) fmol/mL ausgeschlossen werden. Da die analytische Methode für die quantitative Analyse von 2- und 4-Methoxyestradiol-17-Glucuronid angewendet werden konnte, konnten Konzentrationen von weniger als 3636 fmol/mL beider Analyten ausgeschlossen werden.

Da nur freie Estrogene und Estron-3-Sulfat in mehr als 30% der Proben nachgewiesen wurden, wurde die Spearman'sche Rangkorrelationsanalyse nur zwischen ihnen durchgeführt. Erwartungsgemäß wurden signifikante positive Korrelationen zwischen Estron, 17β-Estradiol und Estron-3-Sulfat bei prämenopausalen und postmenopausalen Frauen beobachtet.

Schließlich kann die erweiterte Methode nicht für die Analyse von Methoxyestrogenglucuroniden in menschlichen Fett- und Drüsengewebeproben

angewendet werden, da die Wiederfindung sehr gering ist und die Nachweisgrenzen im Vergleich zu denen im Plasma höher sind.

Zusammenfassend lässt sich sagen, dass die quantitative Analyse von 2- und 4-Methoxyestrone-3-glucuronid und 2- und 4-Methoxyestradiol-3-glucuronid sowie die qualitative Analyse von 2- und 4-Methoxyestradiol-17-glucuronid in eine bestehende Methode zur Ergänzung der Analyse von Estrogenprofilen aufgenommen werden konnte und die erwarteten Ergebnisse in einer definierten Testpopulation von fünfundzwanzing Plasmaproben von Frauen mit unterschiedlichem Menopausestatus lieferte. Dies ist das erste Mal, dass ein so breites Spektrum von Estrogenen (einschliesslich Metaboliten und Konjugaten) zusammen in menschlichem Plasma von Frauen analysiert wurde. Daher stellt die vorliegende Methode ein Instrument für weitere Untersuchungen bei hormonabhängigen Erkrankungen dar.

7. References

AFRICANDER, D. & STORBECK, K. H. 2018. Steroid metabolism in breast cancer: Where are we and what are we missing? *Mol Cell Endocrinol,* 466**,** 86-97.

ARAUJO, P. 2009. Key aspects of analytical method validation and linearity evaluation. *J Chromatogr B Analyt Technol Biomed Life Sci,* 877**,** 2224-34.

AUDET-DELAGE, Y., GREGOIRE, J., CARON, P., TURCOTTE, V., PLANTE, M., AYOTTE, P., SIMONYAN, D., VILLENEUVE, L. & GUILLEMETTE, C. 2018. Estradiol metabolites as biomarkers of endometrial cancer prognosis after surgery. *J Steroid Biochem Mol Biol,* 178**,** 45-54.

AUDET-WALSH, E., LEPINE, J., GREGOIRE, J., PLANTE, M., CARON, P., TETU, B., AYOTTE, P., BRISSON, J., VILLENEUVE, L., BELANGER, A. & GUILLEMETTE, C. 2011. Profiling of endogenous estrogens, their precursors, and metabolites in endometrial cancer patients: association with risk and relationship to clinical characteristics. *J Clin Endocrinol Metab,* 96**,** E330-9.

BLAIR, I. A. 2010. Analysis of estrogens in serum and plasma from postmenopausal women: past present, and future. *Steroids,* 75**,** 297-306.

CARON, P., AUDET-WALSH, E., LEPINE, J., BELANGER, A. & GUILLEMETTE, C. 2009. Profiling endogenous serum estrogen and estrogen-glucuronides by liquid chromatography-tandem mass spectrometry. *Anal Chem,* 81**,** 10143-8.

CARON, P., TURCOTTE, V. & GUILLEMETTE, C. 2015. A chromatography/tandem mass spectrometry method for the simultaneous profiling of ten endogenous steroids, including progesterone, adrenal precursors, androgens and estrogens, using low serum volume. *Steroids,* 104**,** 16-24.

CAVALIERI, E. L. & ROGAN, E. G. 2011. Unbalanced metabolism of endogenous estrogens in the etiology and prevention of human cancer. *J Steroid Biochem Mol Biol,* 125**,** 169-80.

CHANDRAN, S. & SINGH, R. S. P. 2007. Comparison of various international guidelines for analytical method validation. *Phramazie,* 62.

CHEN, A., ZHOU, X., CHENG, Y., TANG, S., LIU, M. & WANG, X. 2018. Design and optimization of the cocktail assay for rapid assessment of the activity of UGT enzymes in human and rat liver microsomes. *Toxicol Lett,* 295**,** 379-389.

CHOUINARD, S., TESSIER, M., VERNOUILLET, G., GAUTHIER, S., LABRIE, F., BARBIER, O. & BELANGER, A. 2006. Inactivation of the pure antiestrogen fulvestrant and other synthetic estrogen molecules by UDP-glucuronosyltransferase 1A enzymes expressed in breast tissue. *Mol Pharmacol,* 69**,** 908-20.

COBURN, S. B., STANCZYK, F. Z., FALK, R. T., MCGLYNN, K. A., BRINTON, L. A., SAMPSON, J., BRADWIN, G., XU, X. & TRABERT, B. 2019. Comparability of serum, plasma, and urinary estrogen and estrogen metabolite measurements by sex and menopausal status. *Cancer Causes Control,* 30**,** 75-86.

CORONA, G., ELIA, C., CASETTA, B., DA PONTE, A., DEL PUP, L., OTTAVIAN, E. & TOFFOLI, G. 2010. Liquid chromatography tandem mass spectrometry assay for fast and sensitive quantification of estrone-sulfate. *Clin Chim Acta,* 411**,** 574-80.

COUGHTRIE, M. W. H. 2016. Function and organization of the human cytosolic sulfotransferase (SULT) family. *Chem Biol Interact,* 259**,** 2-7.

DAIDOJI, T., GOZU, K., IWANO, H., INOUE, H. & YOKOTA, H. 2005. UDP-glucuronosyltransferase isoforms catalyzing glucuronidation of hydroxy-polychlorinated biphenyls in rat. *Drug Metab Dispos,* 33**,** 1466-76.

DE WINTER, J. C., GOSLING, S. D. & POTTER, J. 2016. Comparing the Pearson and Spearman correlation coefficients across distributions and sample sizes: A tutorial using simulations and empirical data. *Psychol Methods,* 21**,** 273-90.

DENVER, N., KHAN, S., HOMER, N. Z. M., MACLEAN, M. R. & ANDREW, R. 2019a. Current strategies for quantification of estrogens in clinical research. *J Steroid Biochem Mol Biol,* 192**,** 105373.

DENVER, N., KHAN, S., STASINOPOULOS, I., CHURCH, C., HOMER, N. Z. M., MACLEAN, M. R. & ANDREW, R. 2019b. Data for analysis of catechol estrogen metabolites in human plasma by liquid chromatography tandem mass spectrometry. *Data Brief,* 23**,** 103740.

DUNN, J. F., NISULA, B. C. & RODBARD, D. 1981. Transport of steroid hormones: binding of 21 endogenous steroids to both testosterone-binding globulin and corticosteroid-binding globulin in human plasma. *J Clin Endocrinol Metab,* 53**,** 58-68.

FALK, R. T., BRINTON, L. A., DORGAN, J. F., FUHRMAN, B. J., VEENSTRA, T. D., XU, X. & GIERACH, G. L. 2013. Relationship of serum estrogens and estrogen metabolites to postmenopausal breast cancer risk: a nested case-control study. *Breast Cancer Res,* 15**,** R34.

FAQEHI, A. M. M., COBICE, D. F., NAREDO, G., MAK, T. C. S., UPRETI, R., GIBB, F. W., BECKETT, G. J., WALKER, B. R., HOMER, N. Z. M. & ANDREW, R. 2016. Derivatization of estrogens enhances specificity and sensitivity of analysis of human plasma and serum by liquid chromatography tandem mass spectrometry. *Talanta,* 151**,** 148-156.

FDA 2018. Guidance for Industry-Bioanalytical Method Validation *FDA, U.S*.

FUHRMAN, B. J., SCHAIRER, C., GAIL, M. H., BOYD-MORIN, J., XU, X., SUE, L. Y., BUYS, S. S., ISAACS, C., KEEFER, L. K., VEENSTRA, T. D., BERG, C. D., HOOVER, R. N. & ZIEGLER, R. G. 2012. Estrogen metabolism and risk of breast cancer in postmenopausal women. *J Natl Cancer Inst,* 104**,** 326-39.

GENTILI, A., PERRET, D., MARCHESE, S., MASTROPASQUA, R., CURINI, R. & DI CORCIA, A. 2002. Analysis of Free Estrogens and their Conjugates in Sewage and River Waters by Solid-Phase Extraction then Liquid Chromatography-electrospary-Tandem Mass Spectrometry. *Chromatographia,* 56**,** 25-32.

GESTL, S. A., GREEN, M. D., SHEARER, D. A., FRAUENHOFFER, E., TEPHLY, T. R. & WEISZ, J. 2002. Expression of UGT2B7, a UDP-glucuronosyltransferase implicated in the metabolism of 4-hydroxyestrone and all-trans retinoic acid, in normal human breast parenchyma and in invasive and in situ breast cancers. *Am J Pathol,* 160**,** 1467-79.

GHISLAIN, I., ZIKOS, E., COENS, C., QUINTEN, C., BALTA, V., TRYFONIDIS, K., PICCART, M., ZARDAVAS, D., NAGELE, E., BJELIC-RADISIC, V., CARDOSO, F., SPRANGERS, M. A. G., VELIKOVA, G., BOTTOMLEY, A., EUROPEAN ORGANISATION FOR, R., TREATMENT OF CANCER QUALITY OF LIFE, G., BREAST CANCER, G. & HEADQUARTERS, E. 2016. Health-related quality of life in locally advanced and metastatic breast cancer: methodological and clinical issues in randomised controlled trials. *Lancet Oncol,* 17**,** e294-e304.

GUILLEMETTE, C., BELANGER, A. & LEPINE, J. 2004. Metabolic inactivation of estrogens in breast tissue by UDP-glucuronosyltransferase enzymes: an overview. *Breast Cancer Res,* 6**,** 246-54.

GUSTAVO GONZÁLEZ, A. & ÁNGELES HERRADOR, M. 2007. A practical guide to analytical method validation, including measurement uncertainty and accuracy profiles. *TrAC Trends in Analytical Chemistry,* 26**,** 227-238.

JARVINEN, E., DENG, F., KIDRON, H. & FINEL, M. 2018. Efflux transport of estrogen glucuronides by human MRP2, MRP3, MRP4 and BCRP. *J Steroid Biochem Mol Biol,* 178**,** 99-107.

KALLIONPAA, R. A., JARVINEN, E. & FINEL, M. 2015. Glucuronidation of estrone and 16alpha-hydroxyestrone by human UGT enzymes: The key roles of UGT1A10 and UGT2B7. *J Steroid Biochem Mol Biol,* 154**,** 104-11.

KEY, T. J. 2011. Endogenous oestrogens and breast cancer risk in premenopausal and postmenopausal women. *Steroids,* 76**,** 812-5.

KRUVE, A., REBANE, R., KIPPER, K., OLDEKOP, M. L., EVARD, H., HERODES, K., RAVIO, P. & LEITO, I. 2015. Tutorial review on validation of liquid chromatography-mass spectrometry methods: part II. *Anal Chim Acta,* 870**,** 8-28.

LABRIE, F., MARTEL, C. & BALSER, J. 2011. Wide distribution of the serum dehydroepiandrosterone and sex steroid levels in postmenopausal women: role of the ovary? *Menopause,* 18**,** 30-43.

LEE, J. M., ANDERSON, P. C., PADGITT, J. K., HANSON, J. M., WATERS, C. M. & JOHNSON, J. A. 2003. Nrf2, not the estrogen receptor, mediates catechol estrogen-induced activation of the antioxidant responsive element. *Biochim Biophys Acta,* 1629**,** 92-101.

LEPINE, J., AUDET-WALSH, E., GREGOIRE, J., TETU, B., PLANTE, M., MENARD, V., AYOTTE, P., BRISSON, J., CARON, P., VILLENEUVE, L., BELANGER, A. & GUILLEMETTE, C. 2010. Circulating estrogens in endometrial cancer cases and their relationship with tissular expression of key estrogen biosynthesis and metabolic pathways. *J Clin Endocrinol Metab,* 95**,** 2689-98.

LEPINE, J., BERNARD, O., PLANTE, M., TETU, B., PELLETIER, G., LABRIE, F., BELANGER, A. & GUILLEMETTE, C. 2004. Specificity and regioselectivity of the conjugation of estradiol, estrone, and their catecholestrogen and methoxyestrogen metabolites by human uridine diphospho-glucuronosyltransferases expressed in endometrium. *J Clin Endocrinol Metab,* 89**,** 5222-32.

LIU, E. T. 2000. Breast cancer research: where we are and where we should go. *Breast Cancer Res,* 2**,** 73-6.

MILLER, W. L. & AUCHUS, R. J. 2011. The molecular biology, biochemistry, and physiology of human steroidogenesis and its disorders. *Endocr Rev,* 32**,** 81-151.

OBAIDAT, A., ROTH, M. & HAGENBUCH, B. 2012. The expression and function of organic anion transporting polypeptides in normal tissues and in cancer. *Annu Rev Pharmacol Toxicol,* 52**,** 135-51.

OREN, I., FLEISHMAN, S. J., KESSEL, A. & BEN-TAL, N. 2004. Free diffusion of steroid hormones across biomembranes: a simplex search with implicit solvent model calculations. *Biophys J,* 87**,** 768-79.

PASQUALINI, J. R., GELLY, C., NGUYEN, B. L. & VELLA, C. 1989. Importance of estrogen sulfates in breast cancer. *J Steroid Biochem,* 34**,** 155-63.

PEMP, D., KLEIDER, C., SCHMALBACH, K., HAUPTSTEIN, R., GEPPERT, L. N., KOLLMANN, C., ICKSTADT, K., ECKERT, P., NESHKOVA, I., JAKUBIETZ, R., ESCH, H. L. & LEHMANN, L. 2019. Qualitative and quantitative differences in estrogen biotransformation in human breast glandular and adipose tissues: implications for studies using mammary biospecimens. *Arch Toxicol,* 93**,** 2823-2833.

PIZZAGALLI, F., VARGA, Z., HUBER, R. D., FOLKERS, G., MEIER, P. J. & ST-PIERRE, M. V. 2003. Identification of steroid sulfate transport processes in the human mammary gland. *J Clin Endocrinol Metab,* 88**,** 3902-12.

POSCHNER, S., ZEHL, M., MAIER-SALAMON, A. & JAGER, W. 2017. Simultaneous quantification of estrogens, their precursors and conjugated metabolites in human breast cancer cells by LC-HRMS without derivatization. *J Pharm Biomed Anal,* 138**,** 344-350.

RAFTOGIANIS, R., CREVELING, C., WEINSHILBOUM, R. & WEISZ, J. 2000. Estrogen metabolism by conjugation. *J Natl Cancer Inst Monogr***,** 113-24.

RANGIAH, K., SHAH, S. J., VACHANI, A., CICCIMARO, E. & BLAIR, I. A. 2011. Liquid chromatography/mass spectrometry of pre-ionized Girard P derivatives for quantifying estrone and its metabolites in serum from postmenopausal women. *Rapid Commun Mass Spectrom,* 25**,** 1297-307.

RIZNER, T. L. 2013. Estrogen biosynthesis, phase I and phase II metabolism, and action in endometrial cancer. *Mol Cell Endocrinol,* 381**,** 124-39.

ROTHMAN, M. S., CARLSON, N. E., XU, M., WANG, C., SWERDLOFF, R., LEE, P., GOH, V. H., RIDGWAY, E. C. & WIERMAN, M. E. 2011. Reexamination of testosterone, dihydrotestosterone, estradiol and estrone levels across the menstrual cycle and in postmenopausal women measured by liquid chromatography-tandem mass spectrometry. *Steroids,* 76**,** 177-82.

RUSSO, J. & RUSSO, I. H. 2006. The role of estrogen in the initiation of breast cancer. *J Steroid Biochem Mol Biol,* 102**,** 89-96.

SAMAVAT, H. & KURZER, M. S. 2015. Estrogen metabolism and breast cancer. *Cancer Lett,* 356**,** 231-43.

SAMPSON, J. N., FALK, R. T., SCHAIRER, C., MOORE, S. C., FUHRMAN, B. J., DALLAL, C. M., BAUER, D. C., DORGAN, J. F., SHU, X. O., ZHENG, W., BRINTON, L. A., GAIL, M. H., ZIEGLER, R. G., XU, X., HOOVER, R. N. & GIERACH, G. L. 2017. Association of Estrogen Metabolism with Breast Cancer Risk in Different Cohorts of Postmenopausal Women. *Cancer Res,* 77**,** 918-925.

STACK, D. E., RITONYA, J., JAKOPOVIC, S. & MALOLEY-LEWIS, B. 2014. Regioselective deuterium labeling of estrone and catechol estrogen metabolites. *Steroids,* 92**,** 32-8.

STANCZYK, F. Z., LEE, J. S. & SANTEN, R. J. 2007. Standardization of steroid hormone assays: why, how, and when? *Cancer Epidemiol Biomarkers Prev,* 16**,** 1713-9.

STARLARD-DAVENPORT, A., LYN-COOK, B. & RADOMINSKA-PANDYA, A. 2008. Identification of UDP-glucuronosyltransferase 1A10 in non-malignant and malignant human breast tissues. *Steroids,* 73**,** 611-20.

TSILIDIS, K. K., ALLEN, N. E., KEY, T. J., DOSSUS, L., LUKANOVA, A., BAKKEN, K., LUND, E., FOURNIER, A., OVERVAD, K., HANSEN, L., TJONNELAND, A., FEDIRKO, V., RINALDI, S., ROMIEU, I., CLAVEL-CHAPELON, F., ENGEL, P., KAAKS, R., SCHUTZE, M., STEFFEN, A., BAMIA, C., TRICHOPOULOU, A., ZYLIS, D., MASALA, G., PALA, V., GALASSO, R., TUMINO, R., SACERDOTE, C., BUENO-DE-MESQUITA, H. B., VAN DUIJNHOVEN, F. J., BRAEM, M. G., ONLAND-MORET, N. C., GRAM, I. T., RODRIGUEZ, L., TRAVIER, N., SANCHEZ, M. J., HUERTA, J. M., ARDANAZ, E., LARRANAGA, N., JIRSTROM, K., MANJER, J., IDAHL, A., OHLSON, N., KHAW, K. T., WAREHAM, N., MOUW, T., NORAT, T. & RIBOLI, E. 2011. Oral contraceptive use and reproductive factors and risk of ovarian cancer in the European Prospective Investigation into Cancer and Nutrition. *Br J Cancer,* 105**,** 1436-42.

TUKEY, R. H. & STRASSBURG, C. P. 2000. Human UDP-glucuronosyltransferases: metabolism, expression, and disease. *Annu Rev Pharmacol Toxicol,* 40**,** 581-616.

WANG, L. Q. & JAMES, M. O. 2005. Sulfotransferase 2A1 forms estradiol-17-sulfate and celecoxib switches the dominant product from estradiol-3-sulfate to estradiol-17-sulfate. *J Steroid Biochem Mol Biol,* 96**,** 367-74.

WANG, Q., MESAROS, C. & BLAIR, I. A. 2016. Ultra-high sensitivity analysis of estrogens for special populations in serum and plasma by liquid chromatography-mass spectrometry: Assay considerations and suggested practices. *J Steroid Biochem Mol Biol,* 162**,** 70-9.

XU, X., ROMAN, J. M., ISSAQ, H. J., KEEFER, L. K., VEENSTRA, T. D. & ZIEGLER, R. G. 2007. Quantitative measurement of endogenous estrogens and estrogen metabolites in human serum by liquid chromatography-tandem mass spectrometry. *Anal Chem,* 79**,** 7813-21.

XU, X., VEENSTRA, T. D., FOX, S. D., ROMAN, J. M., ISSAQ, H. J., FALK, R., SAAVEDRA, J. E., KEEFER, L. K. & ZIEGLER, R. G. 2005. Measuring fifteen endogenous estrogens simultaneously in human urine by high-performance liquid chromatography-mass spectrometry. *Anal Chem,* 77**,** 6646-54.

YAGER, J. D. 2012. Catechol-O-methyltransferase: characteristics, polymorphisms and role in breast cancer. *Drug Discov Today Dis Mech,* 9**,** e41-e46.

YAGER, J. D. & DAVIDSON, N. E. 2006. Estrogen carcinogenesis in breast cancer. *N Engl J Med,* 354**,** 270-82.

YANG, G., GE, S., SINGH, R., BASU, S., SHATZER, K., ZEN, M., LIU, J., TU, Y., ZHANG, C., WEI, J., SHI, J., ZHU, L., LIU, Z., WANG, Y., GAO, S. & HU, M. 2017. Glucuronidation: driving factors and their impact on glucuronide disposition. *Drug Metab Rev,* 49**,** 105-138.

ZENKEVICH, I. G. & MAKAROV, E. D. 2007. Chromatographic quantitation at losses of analyte during sample preparation. Application of the modified method of double internal standard. *J Chromatogr A,* 1150**,** 117-23.

ZHANG, Y., GAIKWAD, N. W., OLSON, K., ZAHID, M., CAVALIERI, E. L. & ROGAN, E. G. 2007. Cytochrome P450 isoforms catalyze formation of catechol estrogen quinones that react with DNA. *Metabolism,* 56**,** 887-94.

ZHAO, Y., BOYD, J. M., SAWYER, M. B. & LI, X. F. 2014. Liquid chromatography tandem mass spectrometry determination of free and conjugated estrogens in breast cancer patients before and after exemestane treatment. *Anal Chim Acta,* 806**,** 172-9.

ZHOU, X., ZHENG, Z., XU, C., WANG, J., MIN, M., ZHAO, Y., WANG, X., GONG, Y., YIN, J., GUO, M., GUO, D., ZHENG, J., ZHANG, B. & YIN, X. 2017. Disturbance of Mammary UDP-Glucuronosyltransferase Represses Estrogen Metabolism and Exacerbates Experimental Breast Cancer. *J Pharm Sci,* 106**,** 2152-2162.

8. Appendix

A1 Biosynthesis of methoxyestrogen glucuronide references and their corresponding deuterated analogues

A1.1 HPLC-UV/Vis chromatograms of biosynthesized 2-MeO-E1-G (A) and a reference of 2-MeO-E1 80 µM (B). The measurement was performed using the method CONJUGATES 40_60 (Chapter 3.2.1.1).

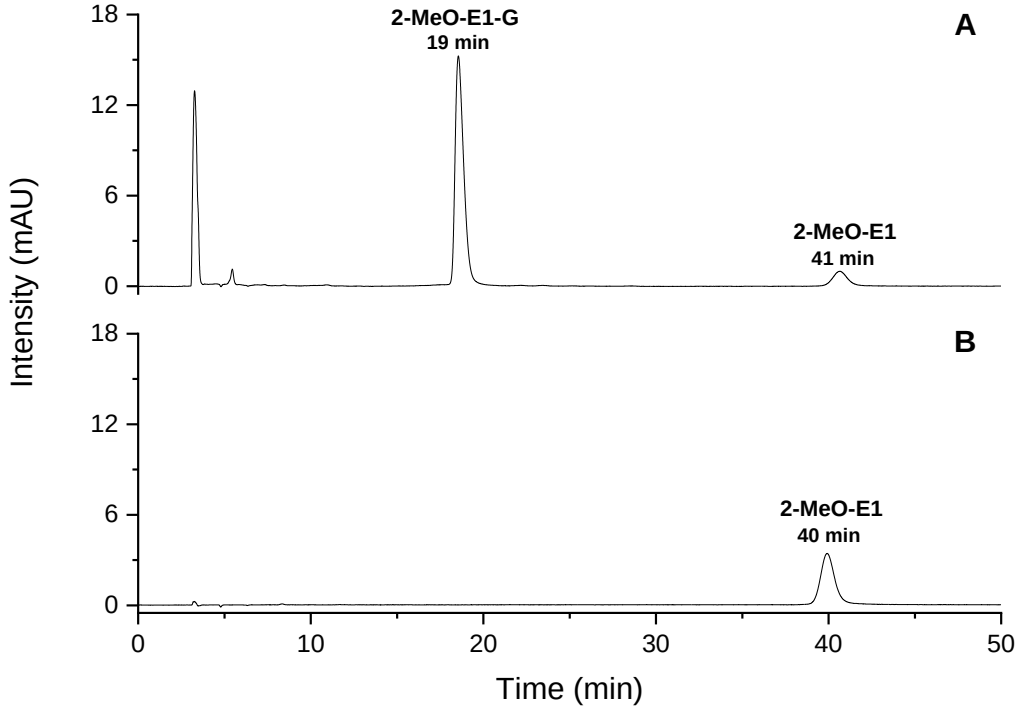

A1.2 HPLC-UV/Vis chromatograms of biosynthesized 4-MeO-E1-G (A) and a reference of 4-MeO-E1 80 µM (B). The measurement was performed using the method CONJUGATES 40_60 (Chapter 3.2.1.1).

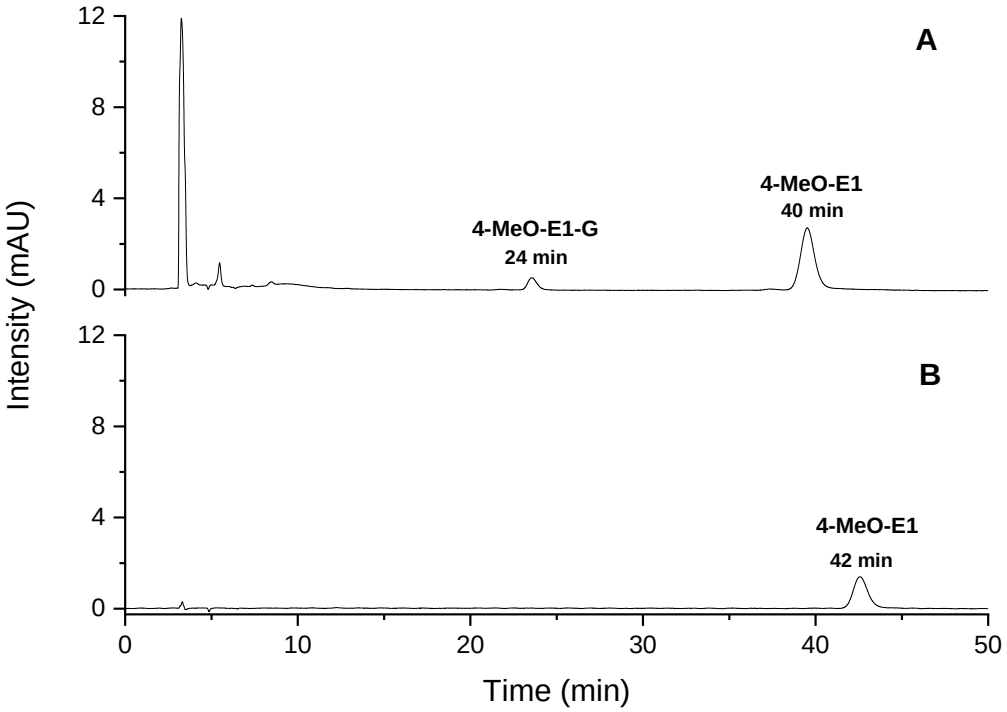

A1.3 Enhanced product ion scan spectrum of the isolated peak of 2-MeO-E1-G with a CE of -20 V using the method 3 (Chapter 3.2.1.2)

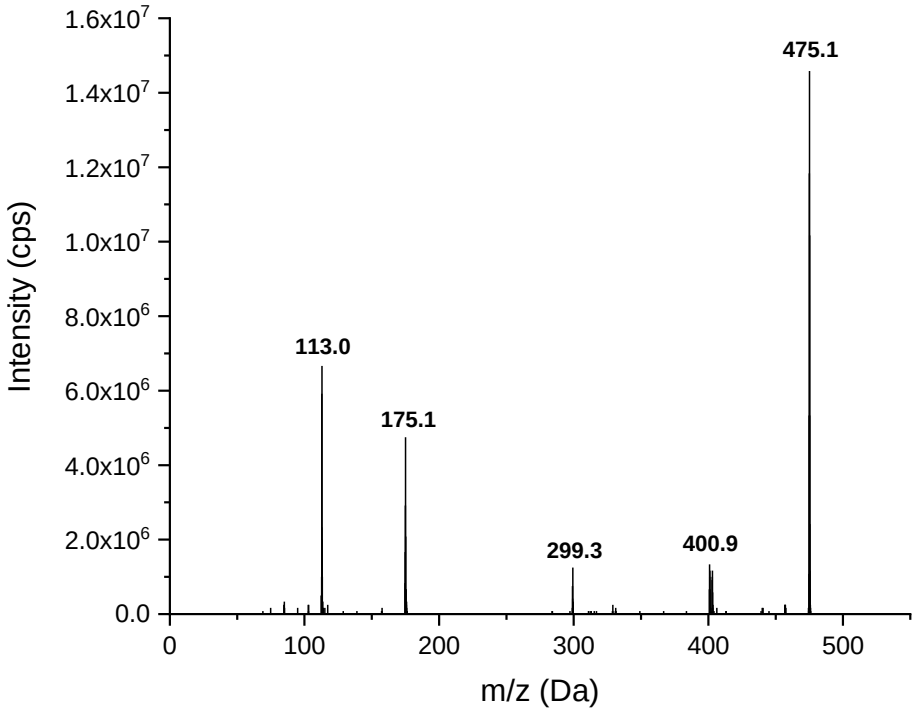

A1.4 Enhanced product ion scan spectrum of the isolated peak of 4-MeO-E1-G with a CE of -20 V using the method 3 (Chapter 3.2.1.2)

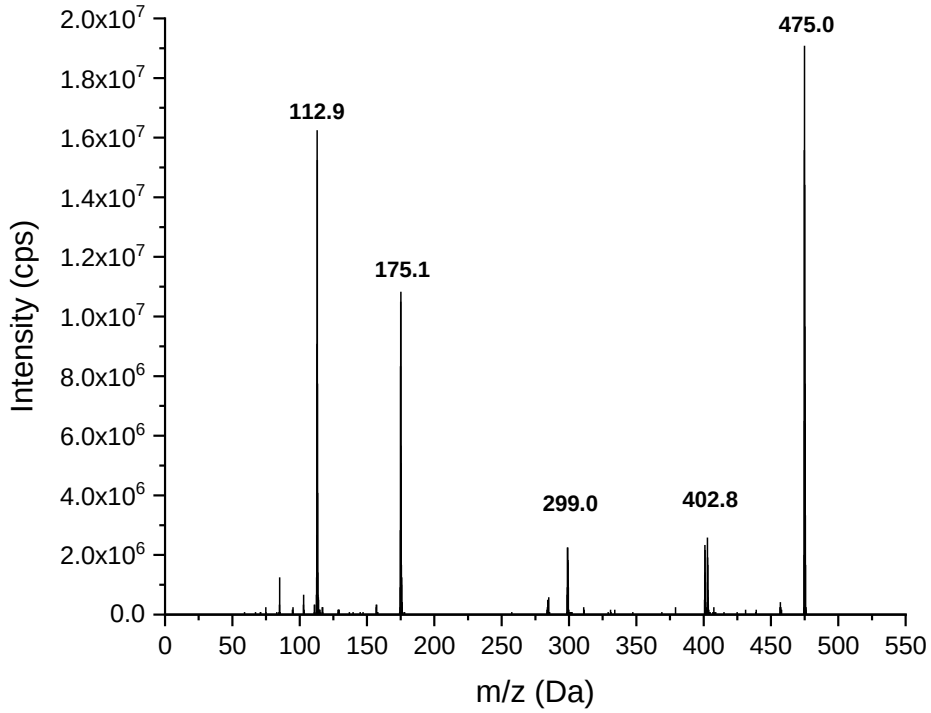

A1.5 HPLC-UV/Vis chromatograms of biosynthesized 2-MeO-E2-3-G and 2-MeO-E2-17-G (A) and a blank of the biosynthesis with 2-MeO-E2 200 µM (B). The measurement was performed using the method CONJUGATES 40_60 (Chapter 3.2.1.1).

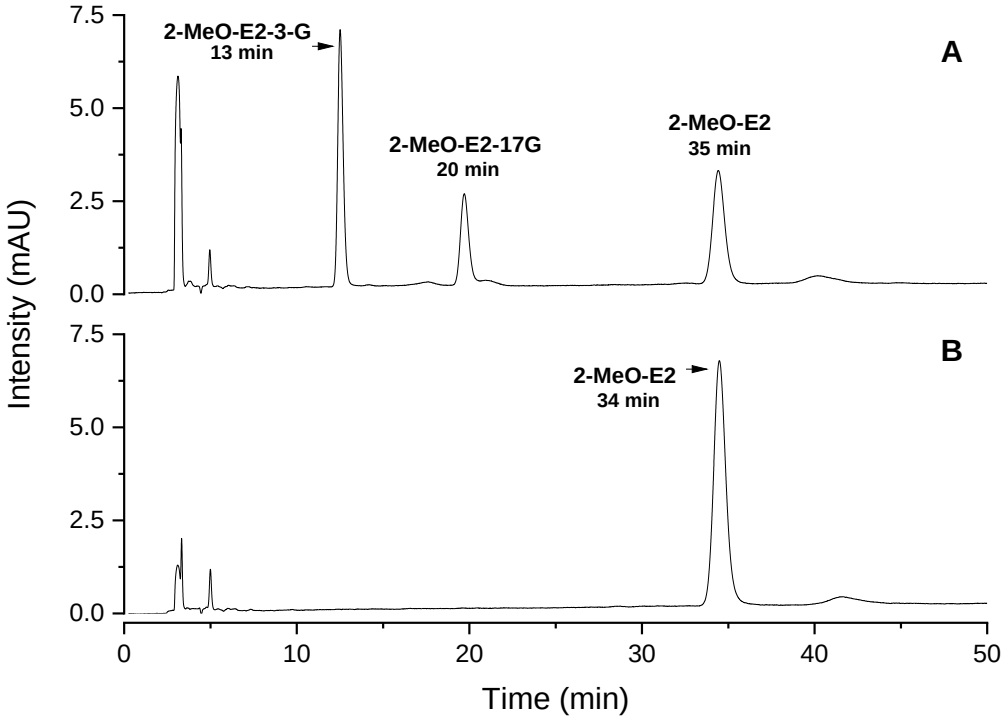

A1.6 Enhanced product ion scan spectrum of the isolated peak at 13 min (suspected 2-MeO-E2-3-G) with a CE of -40 V using the method 4 (Chapter 3.2.1.2).

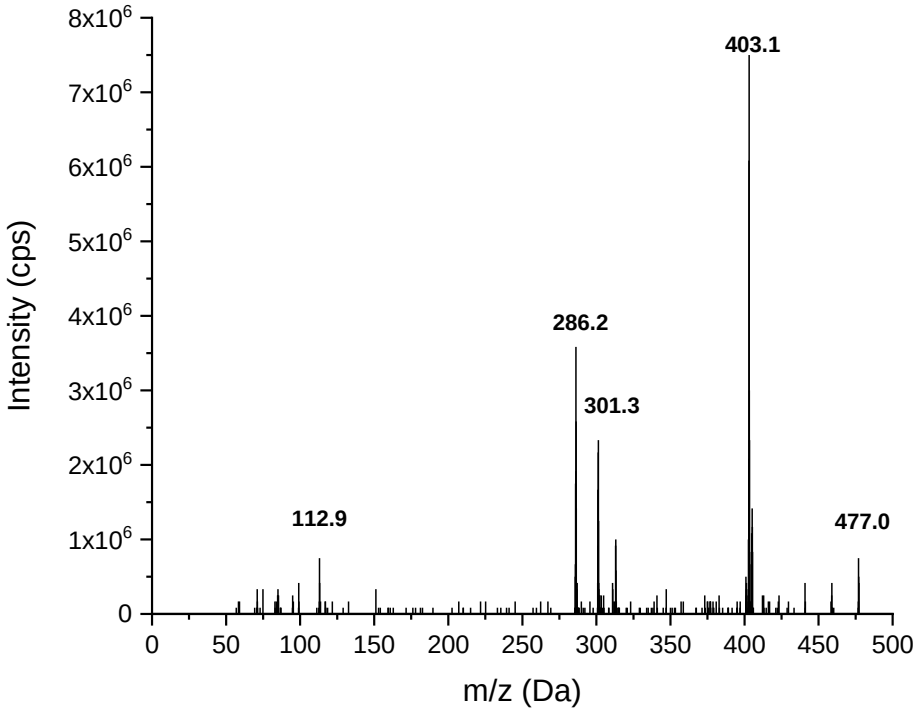

A1.7 Enhanced product ion scan spectrum of the isolated peak at 20 min (suspected 2-MeO-E2-17-G) with a CE of -40 V using the method 4 (Chapter 3.2.1.2).

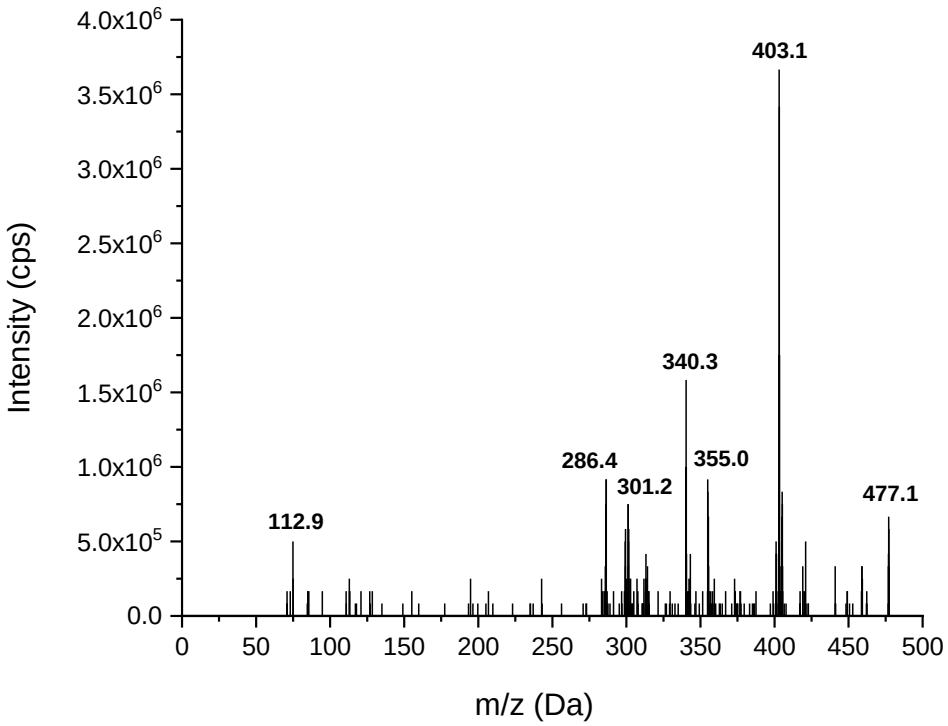

A1.8 HPLC-UV/Vis chromatograms of biosynthesized 4-MeO-E2-3-G and 4-MeO-E2-17-G (A), and a blank of the biosynthesis with 4-MeO-E2 200 µM (B). The measurement was performed using the method CONJUGATES 50_50 (Chapter 3.2.1.1).

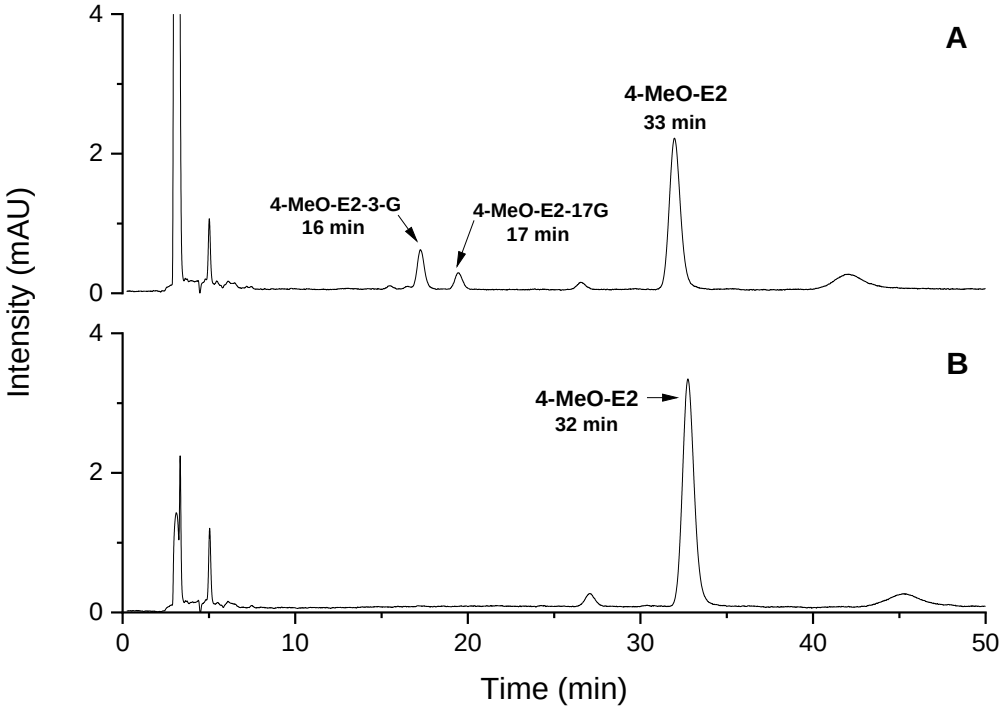

A1.9 Enhanced product ion scan spectrum of the isolated peak at 17 min (suspected 4-MeO-E2-3-G) with a CE of -40 V using the method 4 (Chapter 3.2.1.2).

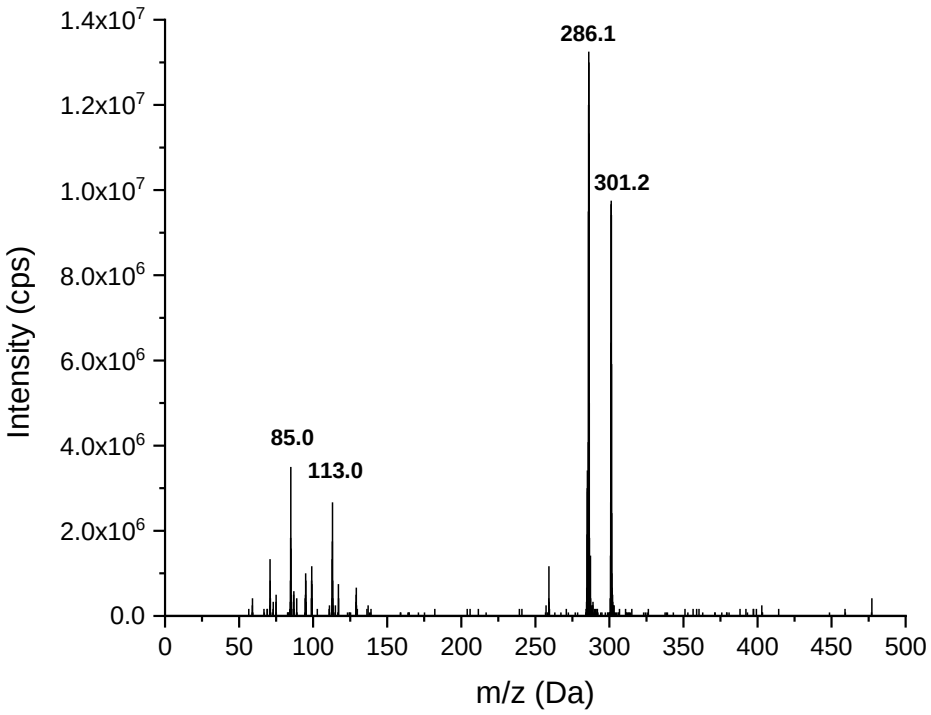

A1.10 Enhanced product ion scan spectrum of the isolated peak at 16 min (suspected 4-MeO-E2-17-G) with a CE of -40 V using the method 4 (Chapter 3.2.1.2).

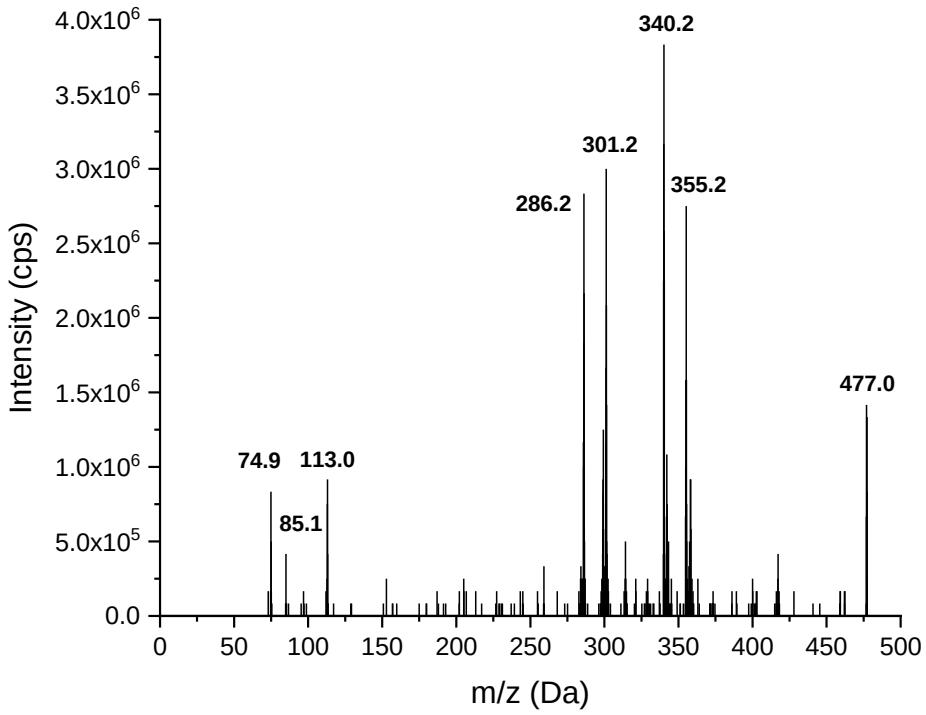

A1.11 HPLC-UV/Vis chromatograms of biosynthesized 2-MeO-E1-d4 (A); a reference of 2-MeO-E1 80µM (B); a blank of the biosynthesis with 2-OH-E1 100 µM (C) and a reference of 2-OH-E1-d4 100 µM (D). The measurement was performed using the method MethoxyE1_E2 (Chapter 3.2.1.1).

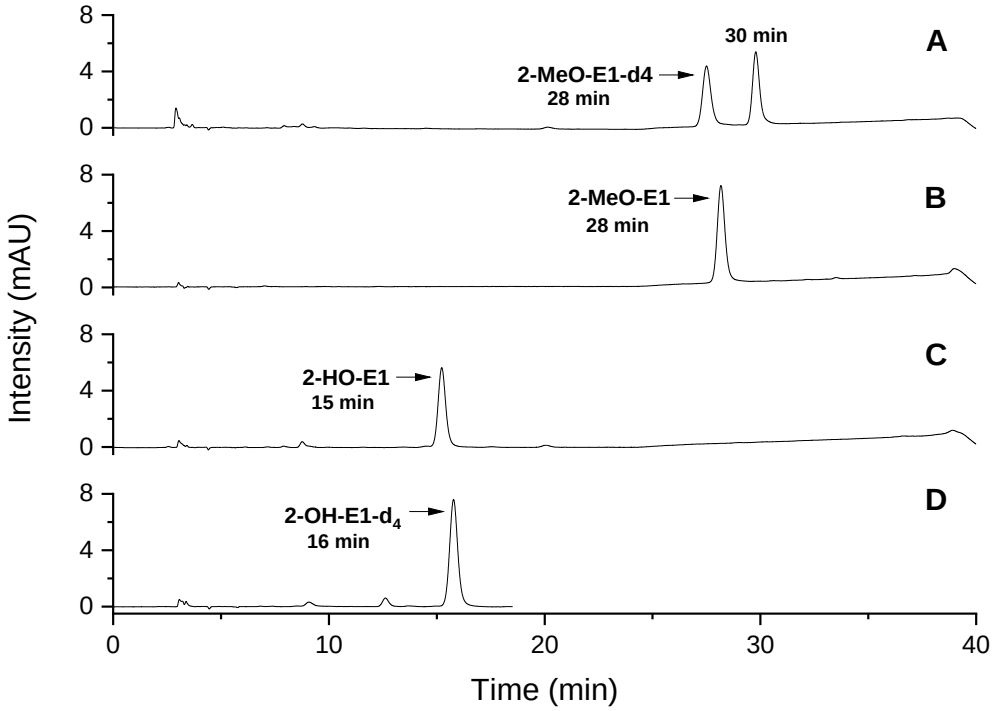

A1.12 HPLC-UV/Vis chromatograms of biosynthesized 4-MeO-E1-d4 (A); a reference of 4-MeO-E1 80 µM (B); a blank of the biosynthesis with 4-OH-E1 100 µM (C) and a reference of 4-OH-E1-d4 100 µM (D). The measurement was performed using the method MethoxyE1_E2 (Chapter 3.2.1.1).

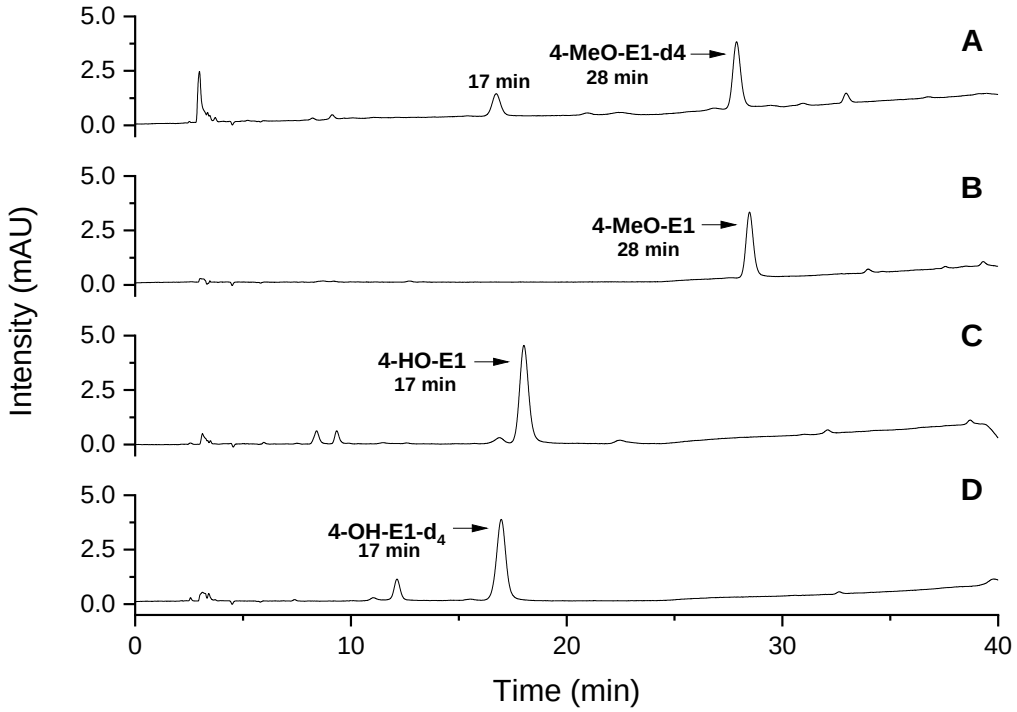

A1.13 HPLC-UV/Vis chromatograms of biosynthesized 2-MeO-E2-d3 (A); a reference of 2-MeO-E2 80 µM (B) and a blank of the synthesis with 2-OH-E2-d3 100 µM (C). The measurement was performed using the method MethoxyE1_E2 (Chapter 3.2.1.1).

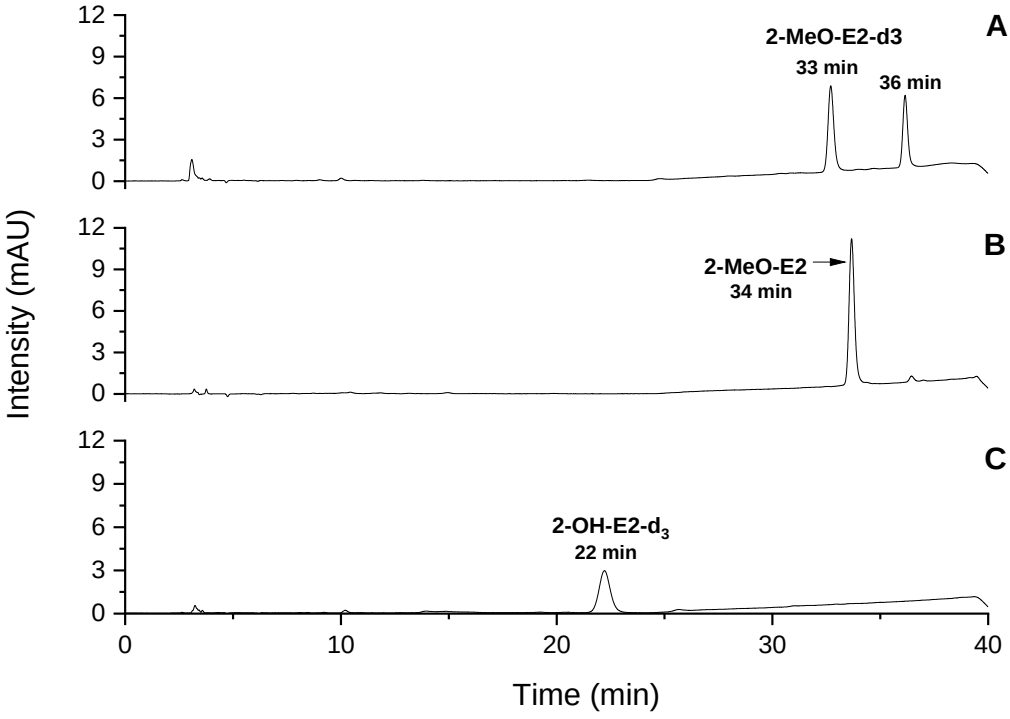

A1.14 HPLC-UV/Vis chromatograms of biosynthesized 4-MeO-E2-d3 (A); a reference of 4-MeO-E2 80 µM (B) and a blank of the synthesis with 4-OH-E2-d3 100 µM (C). The measurement was performed using the method MethoxyE1_E2 (Chapter 3.2.1.1).

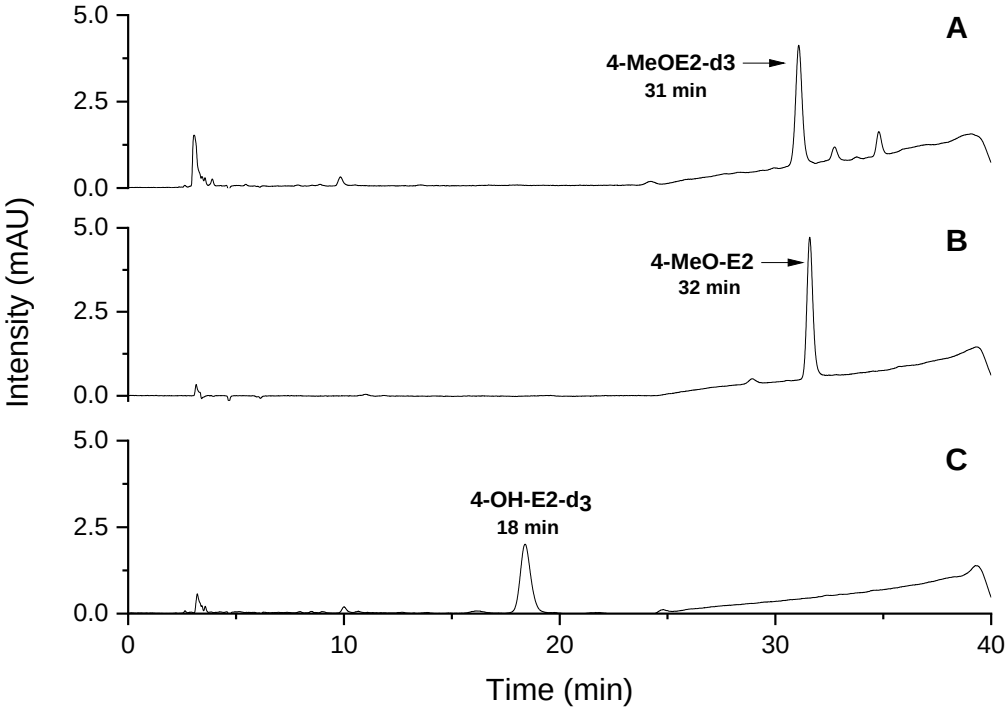

A1.15. Calculation of the concentration of biosynthesized deuterium-labeled 2- and 4-MeO-E1/E2. *The calculation was performed via a 1 point calibration curve, using the rule of proportion. mAU, milli absorbance units.

Biosynthesized reference (stock solution approx. 50 µM)		Peak area of the stock solution (mAU)	Peak area of the non-deuterated reference 80 µM (mAU)	Real concentration of biosynthesized reference (µM)*
2-MeO-E1-d4	1	112.775	176.544	51.10
	2	109.850	171.086	51.37
	3	92.3193	181.119	40.80
4-MeO-E1-d4	1	28.2877	71.5573	31.61
	2	73.1568	46.6977	51.06
	3	73.1568	32.6305	35.68
	4	73.1568	49.3191	53.93
2-MeO-E2-d3	1	177.366	83.4645	37.65
	2	177.366	90.9038	41.00
2-MeO-E2-d3	1	79.5657	40.7918	41.00
	2	79.5657	40.2332	40.45
	3	79.5657	42.6377	42.87

A1.16 HPLC-UV/Vis chromatograms of biosynthesized 2-MeO-E1-G-d4 (A); a blank of the synthesis with 2-MeO-E1 200 µM (B) and a reference of 2-MeO-E1 80 µM (C). The measurement was performed using the method CONJUGATES40_60 (Chapter 3.2.1.1).

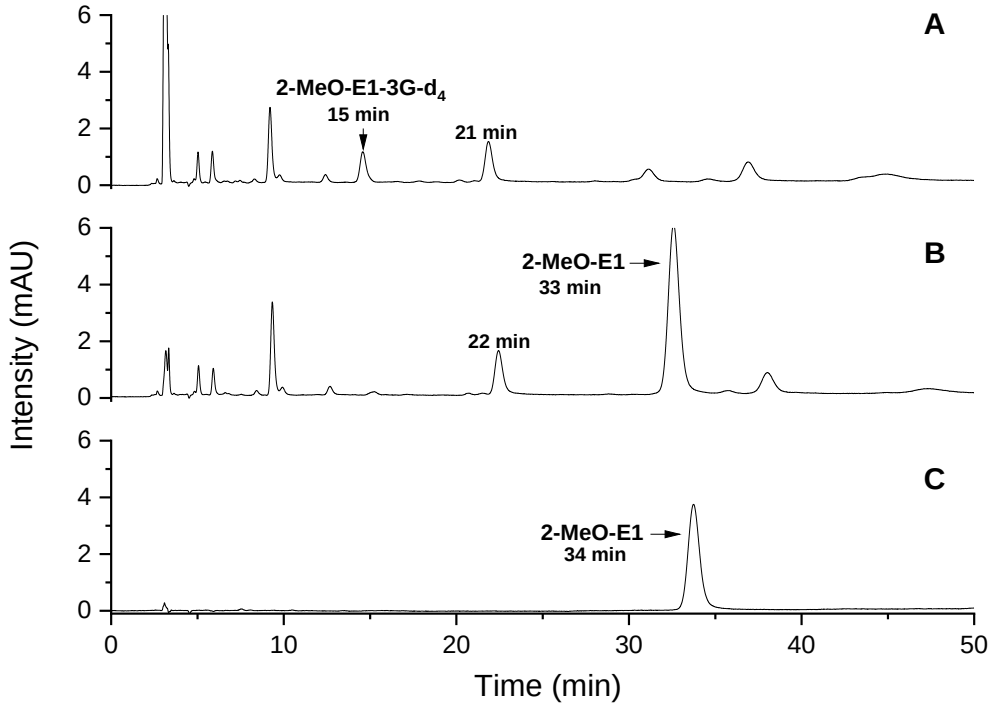

A1.17 HPLC-UV/Vis chromatograms of biosynthesized 4-MeO-E1-G-d4 (A); a blank of the synthesis with 4-MeO-E1 200 µM (B) and a reference of 4-MeO-E1 80 µM (C). The measurement was performed using the method CONJUGATES40_60 (Chapter 3.2.1.1).

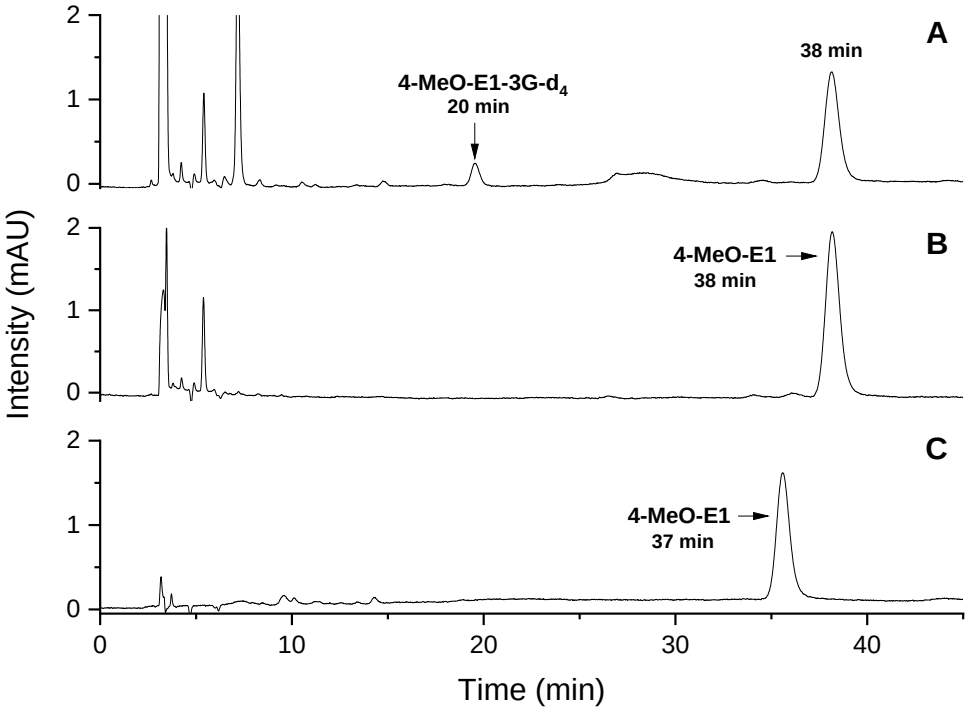

A1.18 HPLC-UV/Vis chromatograms of biosynthesized 2-MeO-E2-3-G-d3 and 2-MeO-E2-17-G-d3 (A); a blank of the synthesis with 2-MeO-E2 200 µM (B) and a reference of 2-MeO-E2 80 µM (C). The measurement was performed using the method CONJUGATES40_60 (Chapter 3.2.1.1).

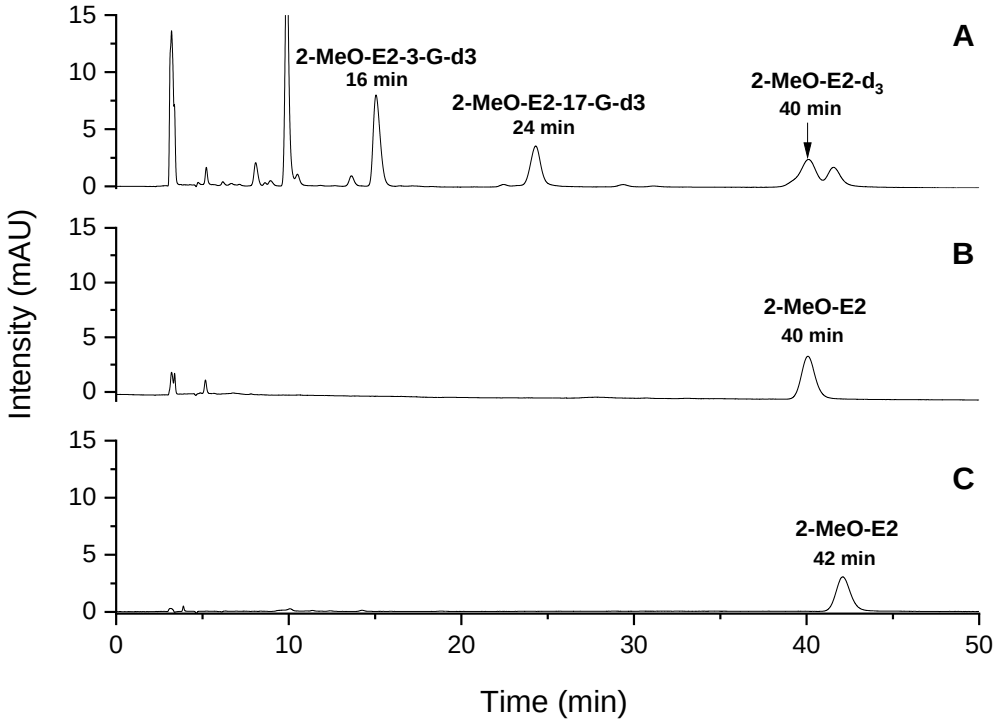

A1.19 HPLC-UV/Vis chromatograms of biosynthesized 4-MeO-E2-3-G-d3 and 4-MeO-E2-17-G-d3 (A); a blank of the synthesis with 4-MeO-E2 200 µM (B) and a reference of 4-MeO-E2 80 µM (C). The measurement was performed using the method CONJUGATES50_50 (Chapter 3.2.1.1).

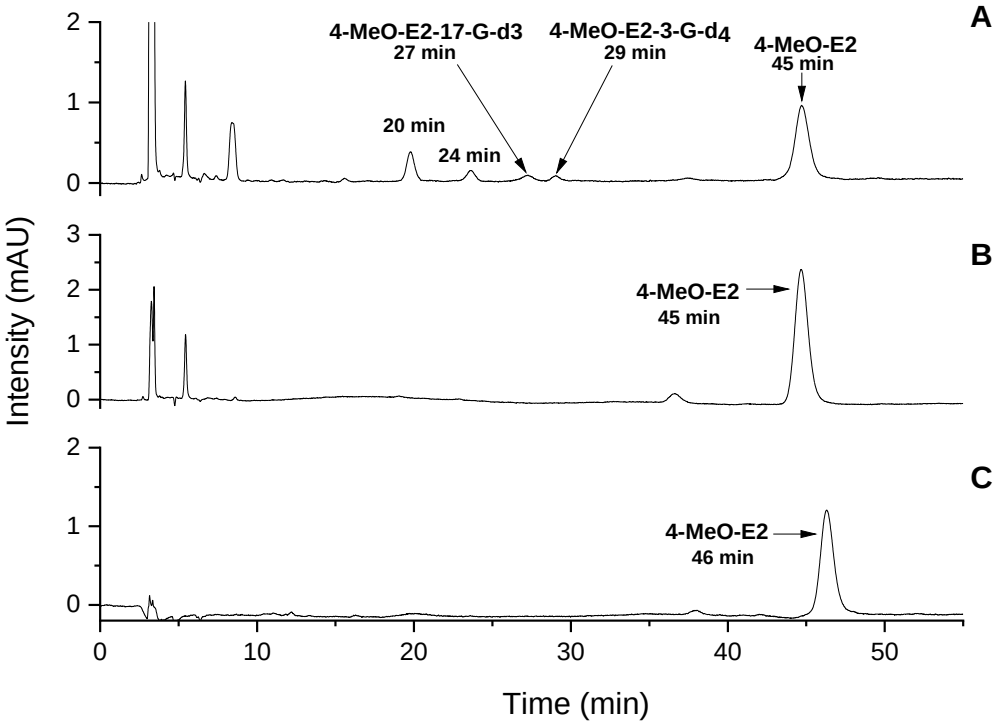

A1.20 Peak area ratio (ratio factor) construction for E1/E1-G = 1.70 ± 0.01. o.c. on column; mAU, mili absorbance units; SD, standard deviation; RSD, relative standard deviation.

pmol o.c. E1/E1-G	Peak area E1 (mAU)	Peak area E1-G (mAU)	Ratio	
		Curve 1		
400	59.5	38.8	1.53	
800	120.1	78.9	1.52	
1200	187.4	124.4	1.51	
1600	251.7	165.2	1.52	
2000	325.0	210.9	1.54	
Mean				1.52
SD				0.01
RSD				0.75
		Curve 2		
400	55.7	30.3	1.83	
800	130.3	70.5	1.85	
1200	209.8	113.0	1.86	
1600	266.9	144.9	1.84	
2000	354.3	189.2	1.87	
Mean				1.85
SD				0.02
RSD				0.85
		Curve 3		
400	51.3	30.1	1.71	
800	108.4	62.5	1.73	
1200	166.4	98.0	1.70	
1600	232.1	135.0	1.72	
2000	297.0	168.4	1.76	
Mean				1.72
SD				0.02
RSD				1.34
		Mean		
400	55.5	33.1	1.69	
800	119.6	70.7	1.70	
1200	187.9	111.8	1.69	
1600	250.2	148.4	1.69	
2000	325.4	189.5	1.72	
Mean				**1.70**
SD				0.01
RSD				0.74

A1.21 Calibration curve of E1 (●) and E1-G (■), each of them as a mean of 3 independent calibration curves. The mean values, SD as well as the linear equation and correlation coefficient are shown. The measurement was performed using the method CONJUGATES40_60 (Chapter 3.2.1.1).

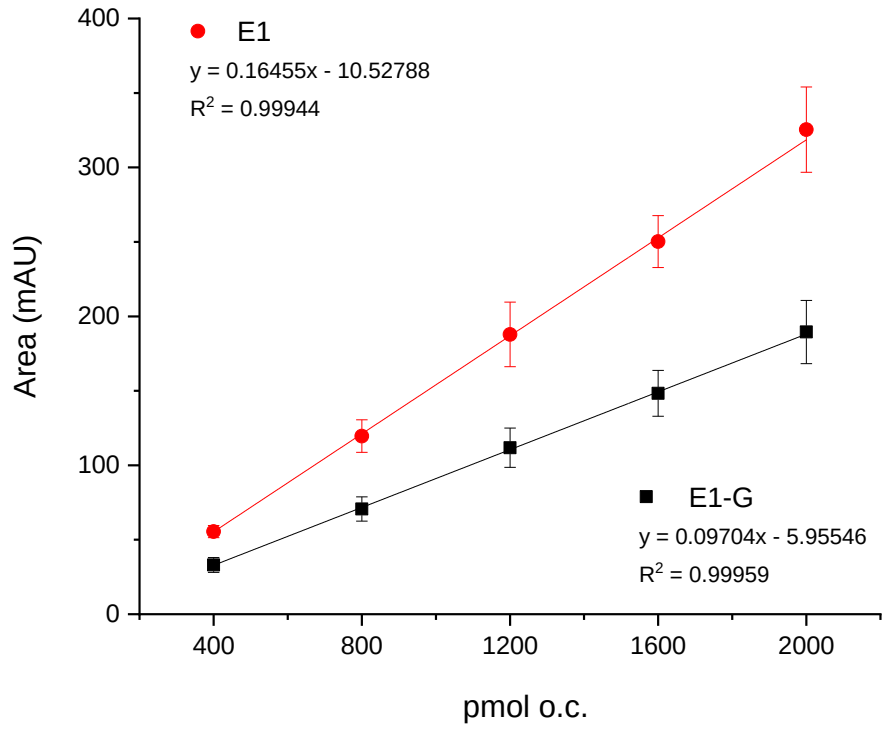

A1.22 Peak area ratio (ratio factor) construction for E2/E2-3-G = 1.80 ± 0.03. o.c. on column; mAU, mili absorbance unit; SD, standard deviation; RSD, relative standard deviation.

pmol o.c. E2/E2-3-G	Peak area E2 (mAU)	Peak area E2-3-G (mAU)	Ratio	
		Curve 1		
400	63.0	37.3	1.69	
800	126.2	73.0	1.73	
1200	189.9	107.1	1.77	
1600	265.4	149.3	1.78	
2000	290.2	164.1	1.77	
Mean				1.75
SD				0.04
RSD				2.17
		Curve 2		
400	56.2	29.4	1.91	
800	109.5	56.8	1.93	
1200	172.1	89.4	1.93	
1600	231.0	119.1	1.94	
2000	289.0	148.8	1.94	
Mean				1.93
SD				0.01
RSD				0.64
		Curve 3		
400	50.3	30.1	1.67	
800	101.8	59.0	1.73	
1200	155.5	88.6	1.76	
1600	210.2	119.4	1.76	
2000	263.1	150.0	1.75	
Mean				1.73
SD				0.04
RSD				2.15
		Mean		
400	56.5	32.3	1.75	
800	112.5	62.9	1.79	
1200	172.5	95.0	1.82	
1600	235.5	129.3	1.82	
2000	280.8	154.3	1.82	
Mean				**1.80**
SD				0.03
RSD				1.68

A1.23 Calibration curve of E2 (●) and E2-3-G (■), each of them as a mean of 3 independent calibration curves. The mean values, SD as well as the linear equation and correlation coefficient are shown. The measurement was performed using the method CONJUGATES40_60 (Chapter 3.2.1.1).

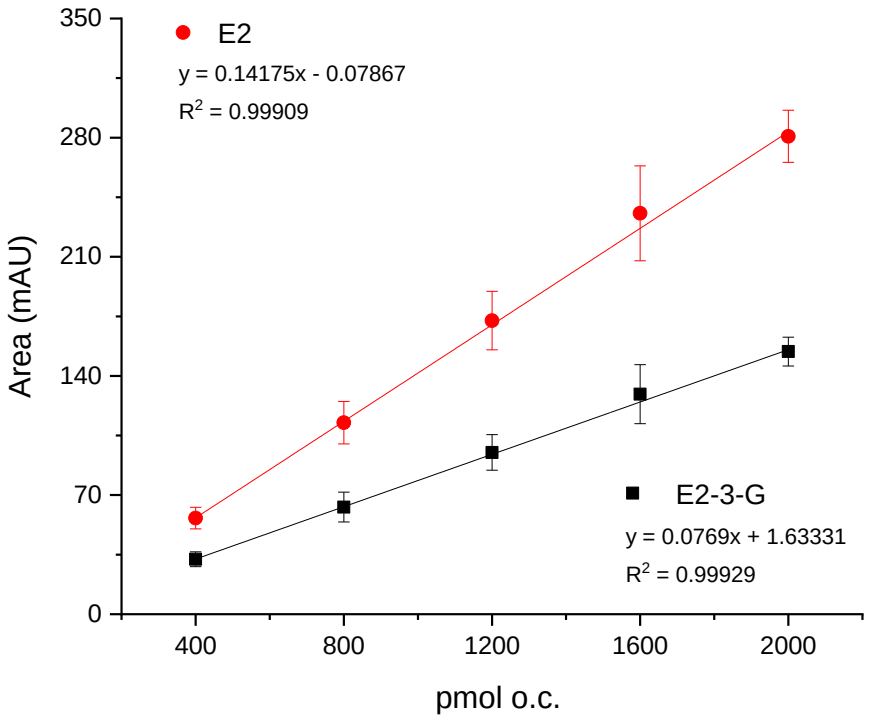

A1.24 Peak area ratio (ratio factor) construction for E2/E2-17-G = 1.07 ± 0.01. o.c. on column; mAU, mili absorbance units; SD, standard deviation; RSD, relative standard deviation.

pmol o.c. E2/E2-17-G	Peak area E2 (mAU)	Peak area E2-17-G (mAU)	Ratio	
		Curve 1		
400	55.5	49.7	1.12	
800	108.0	97.8	1.10	
1200	158.1	142.8	1.11	
1600	210.3	193.5	1.09	
2000	264.7	243.2	1.09	
Mean				1.10
SD				0.01
RSD				1.16
		Curve 2		
400	56.2	53.6	1.05	
800	109.5	105.9	1.03	
1200	172.1	166.3	1.03	
1600	231.0	221.1	1.04	
2000	289.0	277.0	1.04	
Mean				1.04
SD				0.01
RSD				0.61
		Curve 3		
400	50.3	47.2	1.07	
800	101.8	97.1	1.05	
1200	155.5	146.3	1.06	
1600	210.2	195.3	1.08	
2000	263.1	245.9	1.07	
Mean				1.06
SD				0.01
RSD				0.98
		Mean		
400	54.0	50.2	1.08	
800	106.4	100.3	1.06	
1200	161.9	151.8	1.07	
1600	217.2	203.3	1.07	
2000	272.3	255.4	1.07	
Mean				**1.07**
SD				0.01
RSD				0.51

A1.25 Calibration curve of E2 (●) and E2-17-G (■), each of them as a mean of 3 independent calibration curves. The mean values, SD as well as the linear equation and correlation coefficient are shown. The measurement was performed using the method CONJUGATES40_60 (Chapter 3.2.1.1).

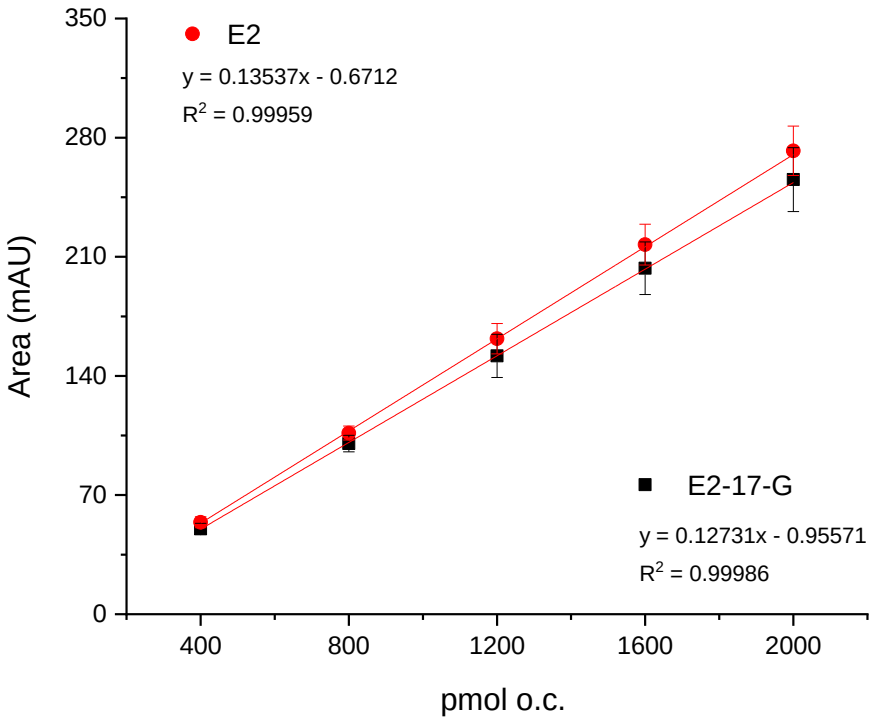

A1.26 Peak areas for the construction of the calibration curve of 2-MeO-E1. o.c. on column; mAU, milli absorbance units; SD, standard deviation; RSD, relative standard deviation.

pmol o.c.	Peak area (mAU)			Mean	SD	RSD
	Curve 1	Curve 2	Curve 3			
400	88.4	73.4	83.8	81.88	7.69	9.39
800	184.1	153.5	181.3	172.97	16.89	9.76
1200	272.4	234.3	263.8	256.83	19.98	7.78
1600	385.4	314.2	331.9	343.84	37.09	10.79
2000	448.1	404.1	436.0	429.39	22.71	5.29

A1.27 Calibration curve of 2-MeO-E1 as a mean of 3 independent calibration curves. The mean values, SD as well as the linear equation and correlation coefficient are shown. The measurement was performed using the method CONJUGATES40_60 (Chapter 3.2.1.1). The calibration curve meets the linearity and homoscedasticity criteria (Valoo 2.8; $p < 0.05$; linearity test 0.0307; homoscedasticity test 8.7350).

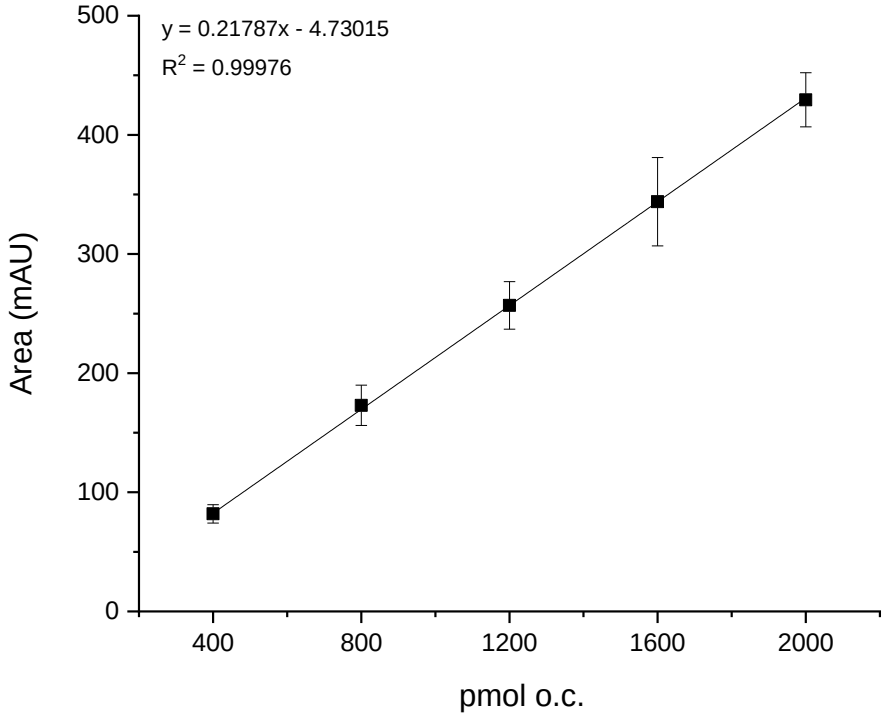

A1.28 Peak areas for the construction of the calibration curve of 4-MeO-E1. o.c. on column; mAU, milli absorbance units; SD, standard deviation; RSD, relative standard deviation.

pmol o.c.	Peak area (mAU)			Mean	SD	RSD (%)
	Curve 1	Curve 2	Curve 3			
400	41.7	49.7	36.8	42.74	6.55	15.33
800	79.5	86.0	71.5	79.00	7.27	9.21
1200	114.9	129.1	113.3	119.09	8.68	7.29
1600	150.5	176.0	152.1	159.54	14.29	8.95
2000	189.2	217.2	188.4	198.29	16.42	8.28

A1.29 Calibration curve of 4-MeO-E1 as a mean of 3 independent calibration curves. The mean values, SD as well as the linear equation and correlation coefficient are shown. The measurement was performed using the method CONJUGATES40_60 (Chapter 3.2.1.1). The calibration curve meets the linearity and homoscedasticity criteria (Valoo 2.8; $p < 0.05$; linearity test 0.0557; homoscedasticity test 6.3442).

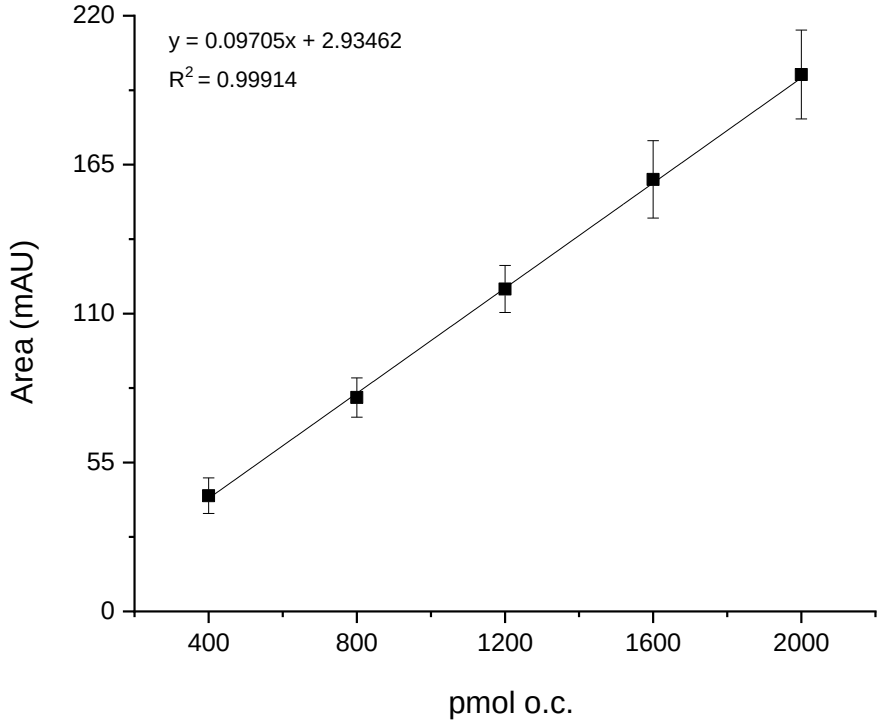

A1.30 Peak areas for the construction of the calibration curve of 2-MeO-E2. o.c. on column; mAU, milli absorbance units; SD, standard deviation; RSD, relative standard deviation.

pmol o.c.	Peak area (mAU)			Mean	SD	RSD (%)
	Curve 1	Curve 2	Curve 3			
400	86.1	92.0	102.9	93.7	8.52	9.10
800	169.8	184.7	191	181.8	10.89	5.99
1200	270.6	278.7	287.8	279.0	8.60	3.08
1600	363.3	400.2	409.0	390.8	24.25	6.20
2000	450.1	457.9	500.5	469.5	27.13	5.78

A1.31 Calibration curve of 2-MeO-E2 as a mean of 3 independent calibration curves. The mean values, SD as well as the linear equation and correlation coefficient are shown. The measurement was performed using the method CONJUGATES40_60 (Chapter 3.2.1.1). The calibration curve meets the linearity and homoscedasticity criteria (Valoo 2.8; $p < 0.05$; linearity test 0.0130; homoscedasticity test 10.1311).

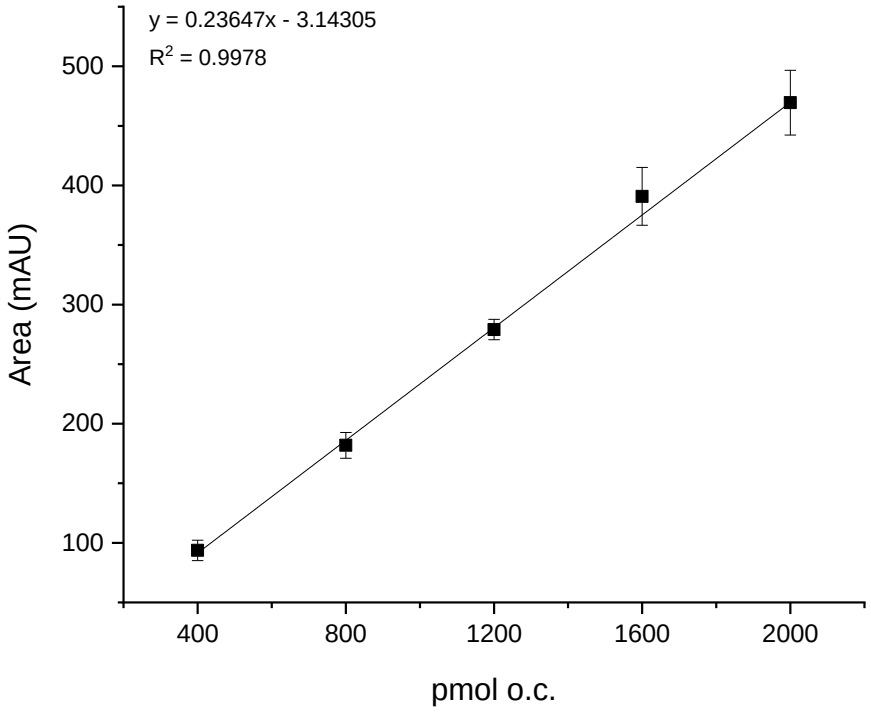

A1.32 Peak areas for the construction of the calibration curve of 4-MeO-E2. o.c. on column; mAU, milli absorbance units; SD, standard deviation; RSD, relative standard deviation.

pmol o.c.	Peak area (mAU)			Mean	SD	RSD (%)
	Curve 1	Curve 2	Curve 3			
400	34.1	35.5	39.5	36.4	2.80	7.71
800	74.3	76.2	73.8	74.8	1.27	1.69
1200	115.1	117.2	119.9	117.4	2.41	2.05
1600	157.4	160.5	159.9	159.3	1.64	1.03
2000	193.3	201.4	200.6	198.4	4.46	2.25

A1.33 Calibration curve of 4-MeO-E2 as a mean of 3 independent calibration curves. The mean values, SD as well as the linear equation and correlation coefficient are shown. The measurement was performed using the method CONJUGATES50_50 (Chapter 3.2.1.1). The calibration curve meets the linearity and homoscedasticity criteria (Valoo 2.8; $p < 0.05$; linearity test 0.0167; homoscedasticity test 2.5359).

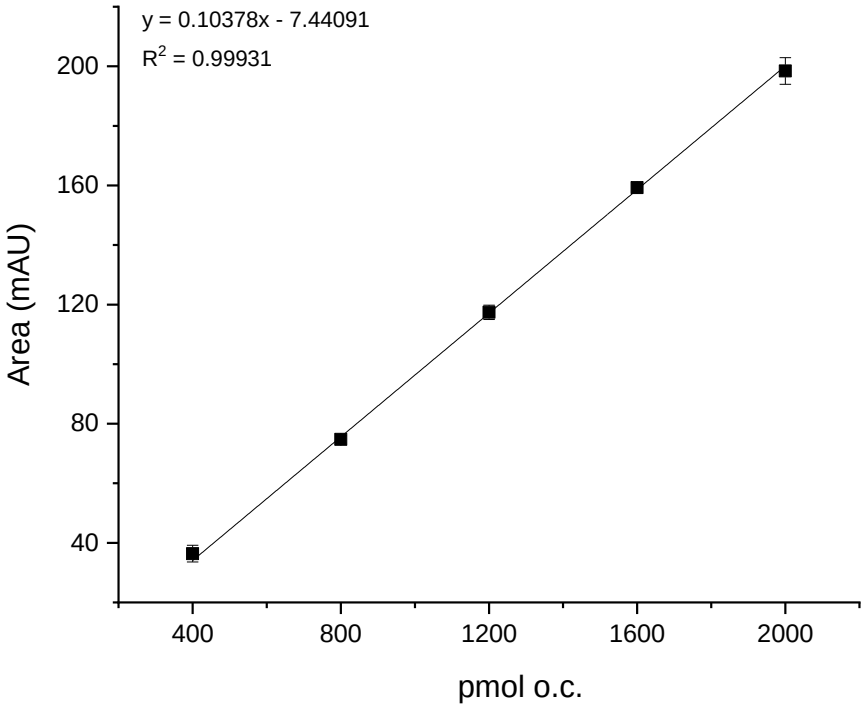

A1.34. Quantification of biosynthesized (deuterated)-methoxyestrogen glucuronides. SD, standard deviation; RSD, relative standard deviation.

2-MeO-E1-G (calibration curve Y= 0.21787 x – 4.7305 and ratio factor 1.70)						
	Peak area	Peak area*1.70	pmol o.c.	pmol in 904.2 µL	Concentration (µM in 904.2 µL)	Amount (µg) in 790 µL
	147.01	249.92	1168.81	105.68	116.88	44.00
	144.41	245.50	1148.52	103.85	114.85	43.24
	140.62	239.06	1118.96	101.18	111.90	42.12
Mean					114.54	43.12
SD					2.51	0.94
RSD					2.19	2.20

2-MeO-E1-G-d4 (calibration curve Y= 0.21787 x – 4.7305 and ratio factor 1.70)						
	Peak area	Peak area*1.70	pmol o.c.	pmol in 580.2 µL	Concentration (µM in 580.2 µL)	Amount (µg) in 540 µL
	95.05	161.58	763.35	44.29	76.33	19.81
	93.36	158.70	750.14	43.52	75.01	19.46
	96.10	163.36	771.52	44.76	77.15	20.02
Mean					76.17	19.76
SD					1.08	0.28
RSD					1.42	1.42

4-MeO-E1-G (calibration curve Y= 0.09705 x + 2.93462 and ratio factor 1.70)						
	Peak area	Peak area*1.70	pmol o.c.	pmol in 539 µL	Concentration (µM in 539 µL)	Amount (µg) in 464 µL
	51.71	87.91	875.63	47.20	87.56	19.36
	51.18	87.01	866.29	46.70	86.63	19.15
	51.79	88.05	877.04	47.27	87.70	19.39
Mean					87.30	19.30
SD					0.58	0.13
RSD					0.67	0.67

4-MeO-E1-G-d4 (calibration curve Y= 0.09705 x + 2.93462 and ratio factor 1.70)						
	Peak area	Peak area*1.70	pmol o.c.	pmol in 362.3 µL	Concentration (µM in 362.3 µL)	Amount (µg) in 322.3 µL
	44.08	74.94	741.90	26.88	74.19	11.49
	43.82	74.48	737.30	26.71	73.72	11.42
	43.64	74.18	734.06	26.59	73.41	11.37
Mean					73.77	11.43
SD					0.39	0.06
RSD					0.53	0.53

2-MeO-E2-3-G (calibration curve Y= 0.23647 x – 3.14305 and ratio factor 1.80)						
	Peak area	Peak area*1.80	pmol o.c.	pmol in 2270 µL	Concentration (µM in 2270 µL)	Amount (µg) in 2140 µL
	119.70	215.50	924.44	209848.57	92.44	94.66
	118.70	213.70	916.83	208120.66	91.68	93.88
	120.50	216.90	930.53	211230.91	93.05	95.29
Mean					92.39	94.61
SD					0.69	0.703
RSD					0.74	0.743

2-MeO-E2-3-G-d3 (calibration curve Y= 0.23647 x – 3.14305 and ratio factor 1.80)						
	Peak area	Peak area*1.80	pmol o.c.	pmol in 2270 µL	Concentration (µM in 2270 µL)	Amount (µg) in 2140 µL
	96.71	174.08	749.44	134.43	74.94	62.65
	97.29	175.12	753.84	135.22	75.38	63.02
	96.84	174.32	750.46	134.61	75.05	62.74
Mean					75.12	62.81
SD					0.23	0.19
RSD					0.31	0.31

4-MeO-E2-3-G (calibration curve Y= 0.10378 x – 7.44091 and ratio factor 1.80)						
	Peak area	Peak area*1.80	pmol o.c.	pmol in 450 µL	Concentration (µM in 450 µL)	Amount (µg) in 415 µL
	49.20	88.60	925.04	41626.91	92.50	18.37
	51.50	92.70	964.93	43422.06	96.49	19.16
	51.80	93.20	970.14	43656.20	97.01	19.26
Mean					95.34	18.93
SD					2.47	0.49
RSD					2.59	2.59

4-MeO-E2-3-G-d3 (calibration curve Y= 0.10378 x – 7.44091 and ratio factor 1.80)						
	Peak area	Peak area*1.80	pmol o.c.	pmol in 180.1 µL	Concentration (µM in 180.1 µL)	Amount (µg) in 125 µL
	29.99	53.98	591.88	10.66	59.19	3.56
	29.86	53.75	589.64	10.62	58.96	3.55
	31.12	56.02	611.49	11.01	61.15	3.68
Mean					59.77	3.60
SD					1.20	0.07
RSD					2.01	2.01

2-MeO-E2-17-G (calibration curve Y= 0.23647 x – 3.14305 and ratio factor 1.07)						
	Peak area	Peak area*1.07	pmol o.c.	pmol in 660 µL	Concentration (µM in 660 µL)	Amount (µg) in 570 µL
	191.80	205.20	881.16	58156.88	88.12	24.03
	193.60	207.20	889.31	58694.44	88.93	24.26
	191.30	204.70	878.90	58007.56	87.89	23.97
Mean					88.31	24.09
SD					0.55	0.14
RSD					0.62	0.62

2-MeO-E2-17-G-d3 (calibration curve Y= 0.23647 x – 3.14305 and ratio factor 1.07)						
	Peak area	Peak area*1.07	pmol o.c.	pmol in 340.3 µL	Concentration (µM in 340.3 µL)	Amount (µg) in 310 µL
	91.90	98.33	429.12	14.60	42.91	6.41
	92.27	98.73	430.79	14.66	43.08	6.43
	91.40	97.80	426.88	14.53	42.69	6.37
Mean					42.89	6.40
SD					0.20	0.03
RSD					0.46	0.46

4-MeO-E2-17-G (calibration curve Y= 0.10378 x – 7.44091 and ratio factor 1.07)						
	Peak area	Peak area*1.07	pmol o.c.	pmol in 200 µL	Concentration (µM in 200 µL)	Amount (µg) in 150 µL
	40.40	43.20	488.23	9764.68	48.82	3.50
	39.70	42.50	481.02	9620.33	48.10	3.45
	38.80	41.50	471.74	9434.75	47.17	3.39
Mean					48.03	3.45
SD					0.83	0.06
RSD					1.72	1.72

4-MeO-E2-17-G-d3 (calibration curve Y= 0.10378 x – 7.44091 and ratio factor 1.07)						
	Peak area	Peak area*1.07	pmol o.c.	pmol in 219.1 µL	Concentration (µM in 219.1 µL)	Amount (µg) in 160 µL
	39.71	42.49	481.09	10.54	48.11	3.71
	39.28	42.03	476.67	10.44	47.67	3.67
	39.75	42.54	481.56	10.55	48.16	3.71
Mean					47.98	3.70
SD					0.27	0.02
RSD					0.56	0.56

A1.35. Quantification of the percentage of hydrolysis of E2-3-G via 1 point calibration curve.

pmol of E2-3-G hydrolyzed:

E2-3-G (standard) 64 nM give 3.445 x 10^5 counts

E2-3-G (hydrolyzed) X nM give 3.060 x 10^4 counts

(64 nM / 3.445 x 10^5) x (3.060 x 10^4) = 20.9 nM which correspond to 2.09 pmol in 100 µL for the analysis

Then, to calculate the % which was not hydrolyzed:

From the 100 µL of the hydrolysis, 60 µL were collected, thus, the pmol collected were

$$2.09 \text{ pmol x } \frac{100\ \mu L}{60\ \mu L} = 3.48 \text{ pmol}$$

$$\text{E2-3-G not hydrolyzed} = \frac{n\ (100\ \mu L\ hydrolysis)}{n\ (\ 0\ \%\ hydrolysis)}\ x\ 100\% = \frac{3.48\ pmol}{3000\ pmol}\ x\ 100 = 0.12\ \%$$

Therefore, 99.88% was hydrolyzed.

A1.36 Peak areas for the construction of the calibration curve of 2-MeO-E2 with internal standard 50 µM of E1. o.c. on column; SD, standard deviation; RSD, relative standard deviation.

pmol o.c. 2-MeO-E2	Peak area 2-MeO-E2	Peak area E1 (50 µM)	Peak area ratio 2-MeO-E2 / E1
	Curve 1		
200	44.0	346.2	0.13
300	102.9	343.8	0.30
400	155.6	339.4	0.46
500	226.8	344.1	0.66
600	324.2	352.7	0.92
700	374.0	334.6	1.12
800	444.4	367.3	1.21
	Curve 2		
200	113.9	565.5	0.20
300	150.4	377.6	0.40
400	193.1	383.0	0.50
500	240.3	377.1	0.64
600	291.1	378.5	0.77
700	348.1	360.7	0.97
800	386.3	373.4	1.03
	Curve 3		
200	72.7	356.0	0.20
300	127.1	323.4	0.39
400	189.1	358.6	0.53
500	237.8	334.4	0.71
600	278.4	344.9	0.81
700	339.8	346.8	0.98
800	387.1	364.8	1.06

pmol (o.c)* 2-MeO-E2	Peak area ratio (mean) 2-MeO-E2 / E1	SD	RSD
200	0.18	0.04	22.88
300	0.36	0.06	15.16
400	0.50	0.04	7.07
500	0.67	0.04	5.38
600	0.83	0.08	9.32
700	1.02	0.08	8.20
800	1.10	0.10	8.77

A1.37 Calibration curve of 2-MeO-E2 (with E1 as internal standard) as a mean of 3 independent calibration curves. The mean values, SD as well as the linear equation and correlation coefficient are shown. The measurement was performed using the method CONJUGATES_GRAD8 (Chapter 3.2.1.1). The calibration curve meets the linearity and homoscedasticity criteria (Valoo 2.8; $p < 0.05$; linearity test 0.6656; homoscedasticity test 4.6697).

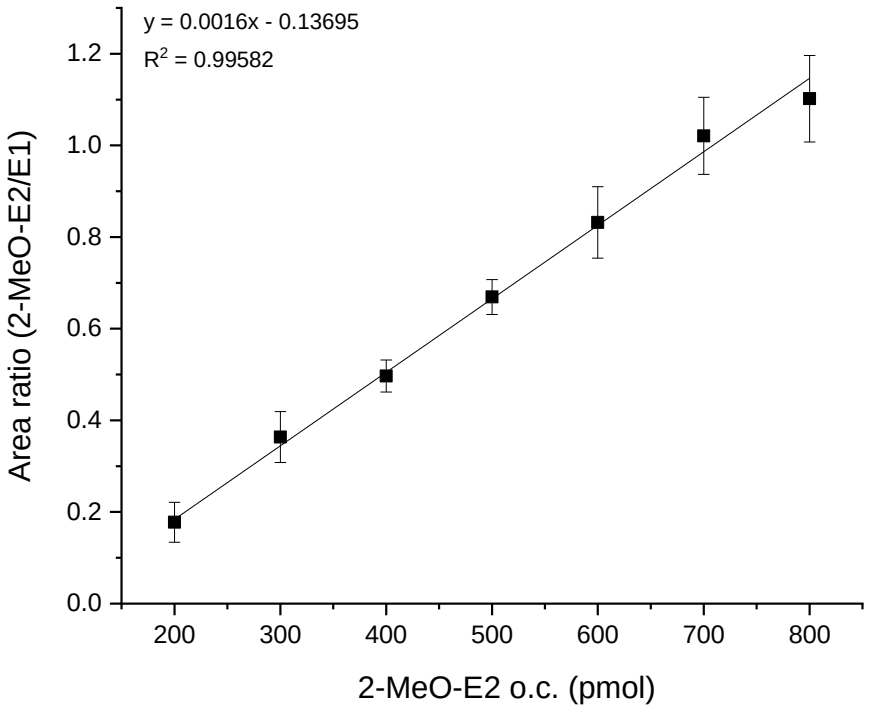

A1.38. Quantification of the 2-MeO-E2 after hydrolysis of 2-MeO-E2-3-G. o.c. on column¸ mAU, milli absorbance units.

Solution	Peak area 2-MeO-E2 (mAU)	Peak area E1	Peak area ratio 2-MeO-E2 / E1	pmol o.c.	pmol in 20 µL	pmol in 40 µL mix
Hydrolysis mix	193.3	192.6	1.0	710.6	710.6	1421.2
Hydrolysis	33.1	51.3	0.6	488.9	651.8	651.8

Therefore, the real pmol of 2-MeO-E2 in the reaction product can be calculated as:

n (hydrolysis mix) – *n* (hydrolysis) =1421.2 pmol – 651. 8 pmol = 769.4 pmol

And in 20 µL of mixture 30 µM (used to spike the reaction product), 600 pmol 2-MeO-E2 were added. Thus, 28% was over quantified:

$$\frac{769.4\ pmol}{600\ pmol}\ x\ 100 = 128\%$$

A1.39. Peak intensities of biosynthesized references for the optimization of the source-dependent parameters (Chapter 3.2.7.2, Table 19). The light-grey line indicates the major intensities given by the combination of the 4 parameters tested. TEM, temperature; IS, ion spray voltage; GS1, nebulizer gas; GS2, turbo gas; cps, counts per second.

Experiment		Intensity (cps)											
		2-MeO-E2-3-G	2-MeO-E2-3-G-d3	2-MeO-E2-17-G	2-MeO-E2-17-G-d3	2-MeO-E1-G	2-MeO-E1-G-d4	4-MeO-E2-17-G	4-MeO-E2-17-G-d3	4-MeO-E2-3-G	4-MeO-E2-3-G-d3	4-MeO-E1-G	4-MeO-E1-G-d4
TEM	1	1.05E+05	1.17E+05	9.30E+04	8.33E+04	1.13E+05	8.39E+04	6.13E+04	6.97E+04	1.39E+05	1.34E+05	1.33E+05	5.99E+04
	2	1.26E+05	1.39E+05	1.10E+05	9.98E+04	1.32E+05	1.06E+05	6.71E+04	7.81E+04	1.63E+05	1.60E+05	1.50E+05	7.65E+04
	3	1.41E+05	1.47E+05	1.18E+05	1.06E+05	1.46E+05	1.07E+05	7.20E+04	8.78E+04	1.78E+05	1.73E+05	1.63E+05	8.71E+04
IS	1	1.15E+05	1.22E+05	9.74E+04	9.13E+04	1.22E+05	8.86E+04	6.32E+04	7.62E+04	1.48E+05	1.44E+05	1.44E+05	7.60E+04
	2	1.30E+05	1.35E+05	1.11E+05	9.98E+04	1.36E+05	9.92E+04	7.55E+04	8.65E+04	1.64E+05	1.59E+05	1.59E+05	7.74E+04
	3	1.34E+05	1.42E+05	1.18E+05	1.03E+05	1.38E+05	1.02E+05	7.75E+04	8.67E+04	1.74E+05	1.63E+05	1.60E+05	7.85E+04
GS1	1	1.25E+05	1.32E+05	1.10E+05	9.98E+04	1.32E+05	9.33E+04	8.16E+04	8.27E+04	1.63E+05	1.51E+05	1.48E+05	7.84E+04
	2	1.38E+05	1.51E+05	1.22E+05	1.12E+05	1.44E+05	1.06E+05	8.85E+04	9.02E+04	1.71E+05	1.73E+05	1.61E+05	8.06E+04
	3	1.46E+05	1.54E+05	1.33E+05	1.24E+05	1.51E+05	1.15E+05	8.85E+04	1.07E+05	1.84E+05	1.76E+05	1.68E+05	9.15E+04
GS2	1	9.92E+04	1.00E+05	8.31E+04	1.50E+04	1.02E+05	7.55E+04	5.74E+04	6.17E+04	1.18E+05	1.12E+05	1.13E+05	6.03E+04
	2	9.90E+04	1.08E+05	9.07E+04	8.08E+04	1.06E+05	8.60E+04	5.90E+04	6.23E+04	1.34E+05	1.30E+05	1.18E+05	5.68E+04
	3	1.05E+05	1.12E+05	9.30E+04	8.72E+04	1.10E+05	8.21E+04	6.11E+04	6.86E+04	1.31E+05	1.27E+05	1.24E+05	6.42E+04

A2 Validation of the extended method for the detection and quantification of methoxyestrogen glucuronides

A2.1 Chromatogram of MRM-transitions of undeuterated and deuterated 2- and 4-methoxyestrone glucuronides. (A) Qn transition of 2/4-MeO-E1-G-d4 with m/z=479.100/112.900; (B) Qn transition of 2/4-MeO-E1-G with m/z=475.100/112.900; (C) Ql transition of 2/4-MeO-E1-G-d4 with m/z=479.100/288.000; (D) Ql transition of 2/4-MeO-E1-G with m/z=475.100/283.900, using the method 2 (Chapter 3.2.1.2).

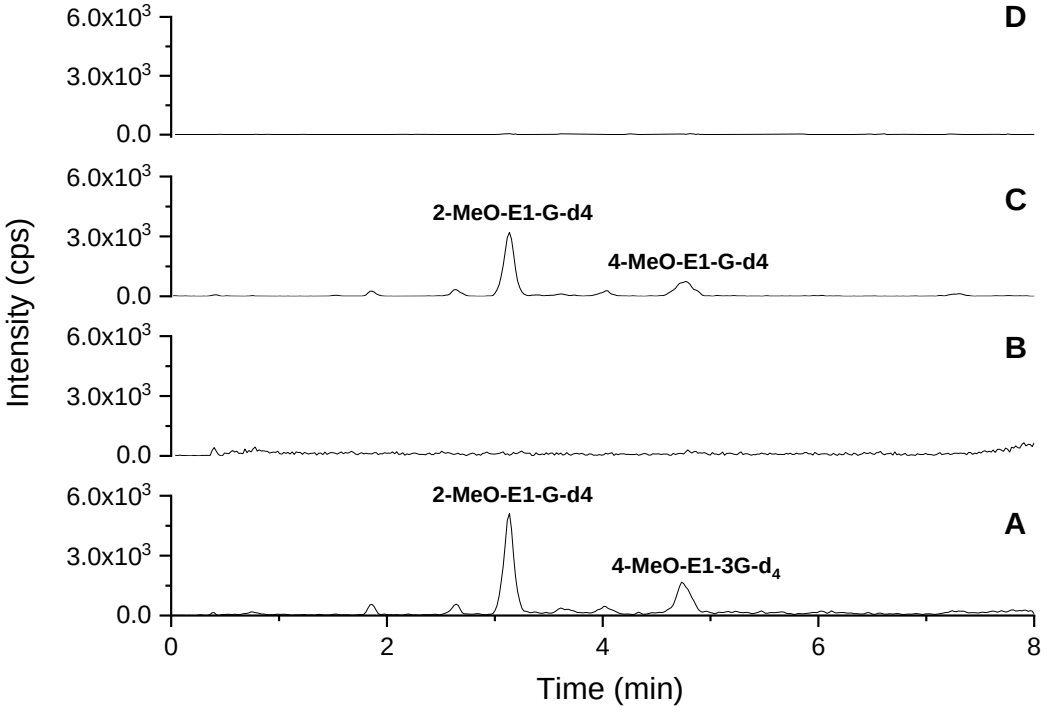

A2.2 Chromatogram of MRM-transitions of undeuterated and deuterated 2- and 4-methoxyestradiol glucuronides. (A) Qn transition of 2/4-MeO-E2-3-G-d3 with m/z=480.100/113.000; (B) Qn transition of 2/4-MeO-E2-3-G with m/z=477.100/113.000; (C) Ql transition of 2/4-MeO-E2-3G-d3 with m/z=480.100/289.100; (D) Ql transition of 2/4-MeO-E2-3-G with m/z=477.100/286.100, using the method 2 (Chapter 3.2.1.2).

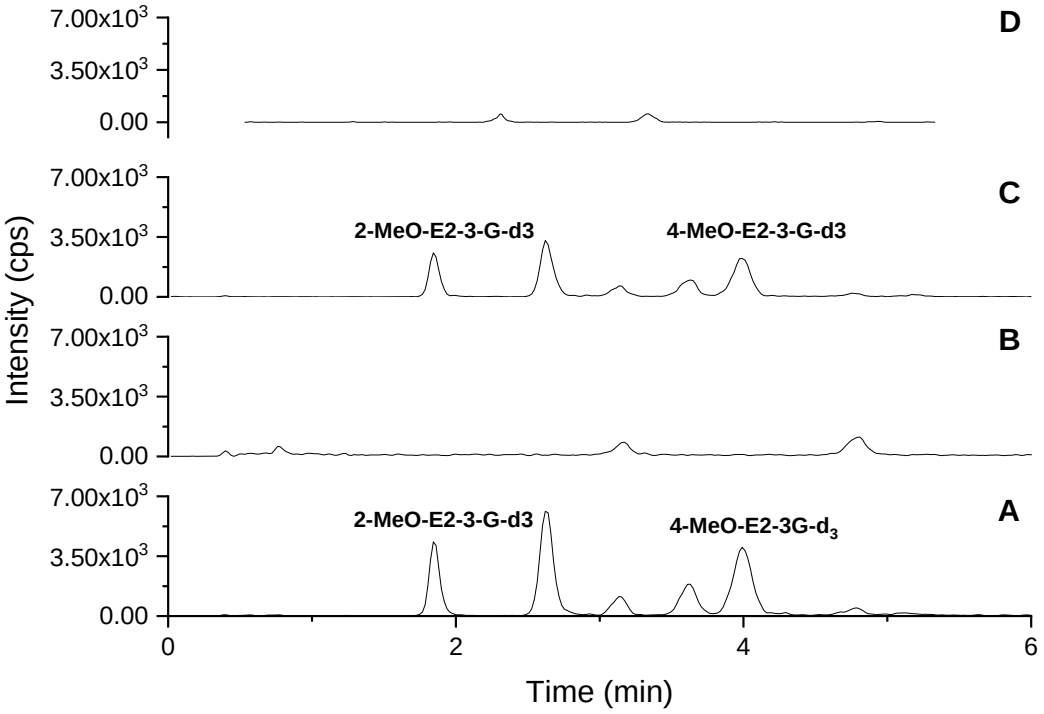

A2.3 Chromatogram of MRM-transitions of undeuterated and deuterated 2- and 4-methoxyestradiol-glucuronides. (A) Qn transition of 2/4-MeO-E2-17-G-d3 with m/z=480.100/113.000; (B) Qn transition of 2/4-MeO-E2-17-G with m/z=477.100/113.000; (C) Ql transition of 2/4-MeO-E2-17-G-d3 with m/z=480.100/304.100; (D) Ql transition of 2/4-MeO-E2-17-G with m/z=477.100/301.200, using the method 2 (Chapter 3.2.1.2).

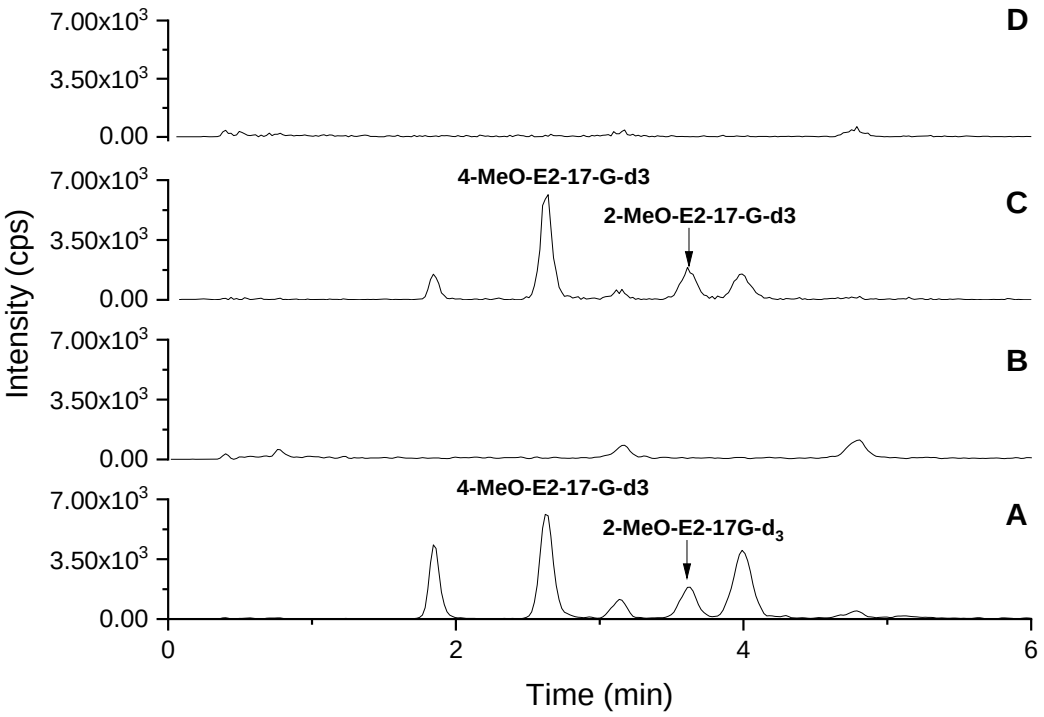

A2.4 Calculation of the peak resolution values between conjugates which eluted adjoining. t_R, retention time; SD, standard deviation; RSD, relative standard deviation.

	Reference	t_R (min)	Reference	t_R (min)	Peak resolution value	
	2-MeO-E2-d3-17-G	3.35	4-MeO-E2-3-G-d3	3.76	2.56	
		3.32		3.67	2.26	
		3.12		3.50	2.81	
		2.85		3.07	1.69	
		2.84		3.26	3.23	
		2.79		3.19	3.33	
		2.57		2.92	3.18	
		2.96		3.33	2.85	
Mean						2.74
SD						0.56
RSD						20.30
	2-MeO-E1-G	1.93	4-MeO-E2-17-G	1.63	2.07	
		1.62		1.92	1.99	
		1.87		2.19	2.00	
		1.83		2.16	2.18	
		1.91		2.24	2.15	
		1.86		2.21	2.03	
		1.91		2.24	1.93	
		1.89		2.22	2.13	
Mean						2.06
SD						0.09
RSD						4.26

A2.5 (Possible) isotopes which may interfere with the identification and quantification of methoxyestrogens glucuronides. t_R, retention time, Qn, quantifier, Ql, qualifier; SD, standard deviation; RSD, relative standard deviation.

	Reference	t_R isotope (min)	Qn/Ql ratio isotope
		5.84	10.03
	2-MeO-E1-G	5.48	10.39
		5.38	10.12
Mean			10.18
SD			0.19
RSD			1.84
		5.93	9.60
	4-MeO-E1-G	5.78	5.23
		5.39	18.79
Mean			11.21
SD			6.92
RSD			61.76
		4.91	7.94
	2-MeO-E2-3-G	4.92	6.77
		4.91	5.56
Mean			6.67
SD			1.19
RSD			17.61
		5.44	9.43
	2-MeO-E2-17-G	5.44	5.14
		5.44	8.47
Mean			7.68
SD			2.25
RSD			29.32
		7.01	7.01
	4-MeO-E2-3-G	7.72	7.72
		6.96	6.96
Mean			7.23
SD			0.42
RSD			5.88
		5.21	6.3
	4-MeO-E2-17-G	5.21	10.0
		5.21	11.12
Mean			9.15
SD			2.52
RSD			27.60

A2.6 Qn/Ql ratios (n = 30) of biosynthesized non-deuterated methoxyestrogen glucuronides obtained from references (n = 10), spiked blanks (n = 10) and spiked plasma samples (n = 10). SD, standard deviation; RSD, relative standard deviation.

	2-MeO-E1-G	4-MeO-E1-G	2-MeO-E2-3-G	2-MeO-E2-17-G	4-MeO-E2-3-G	4-MeO-E2-17-G
Reference	1.44	1.77	1.51	1.42	1.72	1.30
	1.51	1.98	1.56	1.22	1.63	1.22
	1.54	2.10	1.53	1.30	1.75	1.25
	1.69	2.19	1.62	1.19	1.80	1.29
	1.65	2.10	1.71	1.26	1.80	1.28
	1.59	2.11	1.70	1.46	1.95	1.28
	1.62	2.36	1.68	1.59	1.94	1.24
	1.93	2.55	1.72	1.50	1.83	1.34
	1.98	2.35	1.78	1.61	1.98	1.41
	1.53	2.02	1.52	1.45	1.66	1.27
Blank	1.44	1.78	1.25	1.38	1.84	1.29
	1.55	1.99	1.48	1.27	1.68	1.22
	1.49	2.06	1.55	1.50	1.53	1.40
	1.68	2.09	1.69	1.13	1.89	1.26
	1.67	1.66	1.64	1.08	1.77	1.21
	1.63	2.15	1.76	1.64	2.01	1.35
	1.34	1.87	1.78	1.28	1.84	1.14
	2.12	2.53	1.68	1.26	1.92	1.37
	1.89	2.58	1.87	1.69	1.91	1.50
	2.02	2.49	1.73	1.24	1.80	1.21
Plasma	1.36	1.72	2.21	1.17	1.68	1.07
	1.09	1.75	1.86	1.19	2.27	1.42
	1.28	2.47	1.38	1.51	2.15	1.39
	1.39	1.99	1.87	1.22	2.69	1.46
	1.73	1.57	1.47	1.39	1.87	1.12
	1.42	1.20	1.71	1.36	1.67	1.21
	1.32	1.98	2.13	1.50	1.92	1.42
	1.10	1.66	2.04	1.29	1.81	1.16
	1.05	2.01	1.60	1.23	1.96	1.18
	1.29	1.84	1.55	1.39	1.78	1.53
Mean	1.54	2.03	1.69	1.36	1.87	1.29
SD	0.27	0.32	0.21	0.16	0.22	0.11
RSD	17.45	15.97	12.29	11.82	11.65	8.81

A2.7 Qn/Ql ratios (*n* = 30) of biosynthesized deuterated methoxyestrogen glucuronides obtained from references (*n* = 10), spiked blanks (*n* = 10) and spiked plasma samples (*n* = 10). SD, standard deviation; RSD, relative standard deviation.

	2-MeO-E1-G-d4	4-MeO-E1-G-d4	2-MeO-E2-3-G-d3	2-MeO-E2-17-G-d3	4-MeO-E2-3-G-d3	4-MeO-E2-17-G-d3
Reference	1.35	1.82	1.76	1.23	1.68	1.14
	1.61	2.14	1.70	1.22	1.75	1.14
	1.62	2.45	1.72	1.29	1.84	1.14
	1.58	1.67	1.58	1.38	1.78	1.07
	1.48	1.66	1.67	1.17	1.69	1.18
	1.50	1.93	1.53	1.12	1.91	1.18
	1.49	1.95	1.56	1.23	1.99	1.19
	1.73	1.87	1.47	1.11	1.40	1.14
	1.78	2.40	1.72	1.15	1.57	1.07
	1.53	1.83	1.15	1.29	1.63	1.19
Blank	1.42	1.68	1.56	1.07	1.86	1.14
	1.64	2.07	1.70	1.02	1.92	1.19
	1.52	2.23	1.81	1.65	1.82	1.16
	1.53	1.83	1.47	1.21	1.87	1.12
	1.70	1.67	1.53	1.19	1.92	1.13
	1.60	1.80	1.63	1.25	2.10	1.01
	1.40	1.87	1.70	1.18	1.71	1.16
	1.45	1.62	1.41	1.28	1.75	1.20
	1.87	1.94	1.81	1.76	2.08	1.22
	1.76	2.03	1.65	1.06	2.03	1.12
Plasma	1.19	1.24	1.70	1.09	1.76	1.05
	1.50	1.66	1.49	1.03	1.88	1.09
	1.25	1.61	1.77	1.05	1.99	1.01
	1.46	1.32	1.68	1.06	1.63	1.11
	1.68	2.14	1.79	0.91	1.70	1.20
	1.58	2.73	1.60	1.25	1.97	1.23
	1.81	2.52	1.63	1.20	1.59	1.13
	1.55	1.61	1.87	1.27	1.71	1.23
	1.40	1.69	1.74	1.06	1.89	1.13
	1.71	1.71	1.93	1.03	1.98	1.12
Mean	1.56	1.89	1.64	1.19	1.81	1.14
SD	0.16	0.34	0.16	0.17	0.17	0.06
RSD	10.26	17.83	9.47	14.64	9.10	5.10

A2.8 Box-plot chart statistics for recovery levels (%) of methoxyestrogen glucuronides in plasma. Perc, percentile.

Reference	Min.	10 perc.	25 perc.	50 perc. (median)	75 perc.	90 perc.	Max.	n
2-MeO-E1-G	31.13	37.34	45.61	53.21	63.29	76.07	86.09	70
4-MeO-E1-G	26.05	36.89	42.59	50.91	59.04	73.95	94.95	67
2-MeO-E2-3-G	31.89	38.93	47.96	62.17	71.36	80.13	98.74	71
2-MeO-E2-17-G	30.75	38.75	49.60	59.79	69.54	81.38	87.95	59
4-MeO-E2-3-G	37.96	44.97	51.93	59.96	76.79	89.21	98.84	66
4-MeO-E2-17-G	30.44	32.85	40.02	51.12	60.68	65.48	77.98	65

A2.9 Comparison (*p*-values) of expected and obtained ratios of peak areas of non-deuterated/deuterated methoxyestrogen glucuronides in plasma samples. SD, standard deviation; RSD, relative standard deviation; [a] from 2 independent measurements; -, data not available;

2-MeO-E1-G / 2-MeO-E1-G-d4					
Expected ratio	Obtained ratio	Mean	SD	RSD (%)	*p*-value (exact)
0.50	0.62 0.59 0.65	0.62	0.03	4.84	0.01729
1.00	1.13 1.37 1.10	1.20	0.15	12.33	0.1417
2.00	2.61 2.58 2.13	2.44	0.27	11.02	0.00628
4-MeO-E1-G / 4-MeO-E1-G-d4					
Expected ratio	Obtained ratio	Mean	SD	RSD (%)	*p*-value
0.49	0.58 0.68 0.65	0.64	0.05	8.06	0.03847
0.99	0.97 1.51 1.12	1.20	0.28	23.23	0.04773
1.98	2.35 2.08 -	2.22[a]	-	-	0.04972
2-MeO-E2-3-G / 2-MeO-E2-3-G-d3					
Expected ratio	Obtained ratio	Mean	SD	RSD (%)	*p*-value
0.50	0.47 0.57 0.76	0.60	0.15	24.55	0.32512
1.01	1.13 1.26 1.05	1.15	0.11	9.24	0.00857
2.01	2.30 2.70 1.84	2.28	0.43	18.87	0.01873

2-MeO-E2-17-G / 2-MeO-E2-17-G-d3					
Expected ratio	Obtained ratio	Mean	SD	RSD (%)	*p*-value
0.50	- - -	-	-	-	-
1.00	0.40 0.75 -	0.58[a]	-	-	-
2.00	0.76 1.88 1.62	1.42	0.59	41.28	0.11084
4-MeO-E2-3-G / 4-MeO-E2-3-G-d3					
Expected ratio	Obtained ratio	Mean	SD	RSD (%)	*p*-value
0.50	0.58 0.54 -	0.56[a]	-	-	0.17717
1.00	0.99 1.35 1.06	1.13	0.19	16.84	0.02811
2.00	2.52 1.72 -	2.12[a]	-	-	0.15320
4-MeO-E2-17-G / 4-MeO-E2-17-G-d3					
Expected ratio	Obtained ratio	Mean	SD	RSD (%)	*p*-value
0.50	0.66 0.76 0.70	0.71	0.05	7.12	0.01752
1.00	1.22 1.77 1.28	1.42	0.30	21.20	0.03311
2.00	2.99 3.40 2.31	2.90	0.55	18.98	0.01695

A2.10 Box-plot chart statistics of LOD levels (fmol/mL) of methoxyestrogen glucuronides in plasma. Perc, percentile.

Reference	Min.	10 perc.	25 perc.	50 perc. (median)	75 perc.	90 perc.	Max.	n
2-MeO-E1-G	92	112.5	119	183	219.5	268	347	20
4-MeO-E1-G	23	24.5	43.5	66	80	99.5	155	20
2-MeO-E2-3-G	68	90	121	165	204	251	304	18
2-MeO-E2-17-G	299	364	490.5	1021.5	1240.5	1463	1517	12
4-MeO-E2-3-G	32	43	51	76	105	178	222	19
4-MeO-E2-17-G	143	182	247	569	1948	3353	3620	12

A2.11 Individual values for long term stability (%) of biosynthesized references. SD, standard deviation; RSD, relative standard deviation.

	2-MeO-E1-G	4-MeO-E1-G	2-MeO-E2-3-G	2-MeO-E2-17-G	4-MeO-E2-3-G	4-MeO-E2-17-G
			Month 1			
	102.78	105.78	100.69	113.62	111.58	104.15
	97.79	101.15	103.27	113.62	103.00	99.75
	98.74	105.66	103.91	106.33	105.09	100.06
Mean	99.77	104.20	102.62	111.19	106.56	101.32
SD	2.65	2.64	1.71	4.21	4.47	2.46
RSD	2.65	2.53	1.66	3.78	4.20	2.42
			Month 2			
	110.36	117.00	107.89	129.54	118.52	118.12
	100.59	96.03	102.42	124.37	102.18	102.09
	101.63	100.40	112.63	104.78	103.36	103.02
Mean	104.20	104.48	107.65	119.57	108.02	107.74
SD	5.36	11.06	5.11	13.06	9.11	9.00
RSD	5.15	10.59	4.74	10.92	8.43	8.35
			Month 3			
	135.12	133.89	125.86	134.45	131.29	133.45
	118.06	128.39	130.56	144.21	121.47	126.64
	126.65	127.08	125.80	112.32	126.30	121.80
Mean	126.61	129.79	127.41	130.33	126.35	127.30
SD	8.53	3.61	2.73	16.34	4.91	5.85
RSD	6.74	2.78	2.14	12.54	3.88	4.60
			Month 4			
	128.28	122.08	125.25	149.57	144.67	133.64
	120.39	132.63	130.31	137.74	124.28	128.36
	124.92	124.57	124.64	123.89	116.27	118.99
Mean	124.53	126.43	126.73	137.07	128.41	126.99
SD	3.96	5.52	3.11	12.85	14.64	7.42
RSD	3.18	4.36	2.46	9.38	11.40	5.84
			Month 5			
	125.03	121.61	124.02	153.45	127.41	133.86
	111.88	122.36	130.44	131.30	127.61	123.39
	114.96	117.70	121.98	114.31	116.76	118.49
Mean	117.29	120.56	125.48	133.02	123.92	125.25
SD	6.88	2.50	4.41	19.63	6.21	7.85
RSD	5.87	2.08	3.52	14.75	5.01	6.27

A2.12 Individual values for stability (%) of spiked plasma samples after 24 h stored in the autosampler, and adjusted *p*-values by the method of Holm. SD, standard deviation; RSD, relative standard deviation.

	2-MeO-E1-G	4-MeO-E1-G	2-MeO-E2-3-G	2-MeO-E2-17-G	4-MeO-E2-3-G	4-MeO-E2-17-G	*p*-values
	102.38	89.66	109.94	101.80	92.54	96.01	0.420
	107.06	98.76	102.64	110.93	97.76	100.69	0.765
	106.38	85.69	95.95	89.57	99.49	110.44	1.000
Mean	105.27	91.37	102.84	100.77	96.59	102.38	1.000
SD	2.53	6.70	7.00	10.72	3.62	7.36	0.992
RSD	2.40	7.34	6.81	10.64	3.74	7.19	1.000

A2.13 Individual values of stability (%) of spiked plasma samples after freeze/thaw cycles during 4 days, and adjusted *p*-values by the method of Holm. SD, standard deviation; RSD, relative standard deviation.

	2-MeO-E1-G	4-MeO-E1-G	2-MeO-E2-3-G	2-MeO-E2-17-G	4-MeO-E2-3-G	4-MeO-E2-17-G	*p*-values
	105.00	106.86	98.33	104.06	99.51	91.39	1.000
	94.56	105.54	91.55	98.31	91.41	93.76	1.000
	107.60	99.03	108.29	97.85	96.19	103.14	1.000
Mean	102.39	103.81	99.39	100.08	95.71	96.10	1.000
SD	6.90	4.19	8.42	3.46	4.07	6.21	1.000
RSD	6.74	4.04	8.47	3.46	4.25	6.47	1.000

A3. Characterization of the study population

A3.1. Questionnaire.

ÜBERGABEPROTOKOLL (Praxis Prof. Eckert)

Studie: Einfluss Isoflavone auf die Bildung, Aktivierung und Wirkung von 17β-Estradiol in der weiblichen Brustdrüse

Datum: .....

Spenderin (Code): .....

Alter: .....

Anzahl Schwangerschaften: .....

Körpergewicht in kg: .....

Körpergröße: .....

Angaben zum Rauchverhalten:

☐ Raucherin seit: ..... Konsum: .....

☐ Nichtraucherin seit: ..... Konsum bis dato: .....

Angaben zum Alkoholkonsum
(wenn möglich als Menge/Woche und Art der Getränke):

Einnahme von Arzneimitteln mit östrogener Wirkung (Kontrazeptiva, Hormonsubstitution)? ☐ Ja ☐ Nein

Welches Präparat?

Einnahme von Nahrungsergänzungsmittel mit östrogener Wirkung? ☐ Ja ☐ Nein

Welche?

Gewebespende wurde von ..... (AK Lehmann) entgegen genommen.

A4. Analysis of circulating estrogen profiles in women without breast cancer

A4.1. Box-plot chart statistics of levels of E1 (fmol/mL) in plasma samples from women without breast cancer (*n* = 25). Perc, percentile.

Min.	10 perc.	25 perc.	50 perc. (median)	75 perc.	90 perc.	Max.
24	37	53	94	151	243	824

A4.2. Statistical comparison of levels of E1 (fmol/mL) in plasma samples derived from the Isocross study analyzed in 2014 and analyzed again in the present study (2018-2019) (*n* = 10). Through a paired Wilcoxon test, no significant difference was observed (statistical significance would be indicated by a *p*-value < 0.05). Perc, percentile.

Analyzed in	Min.	10 perc.	25 perc.	50 perc. (median)	75 perc.	90 perc.	Max.
2014	35	37	60	105	149	495	790
2018-2019	37	45	75	119	148	525	824

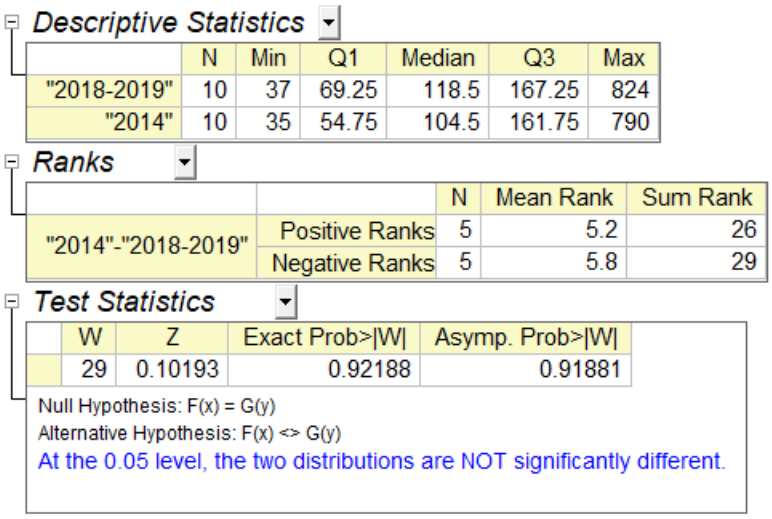

Descriptive Statistics

	N	Min	Q1	Median	Q3	Max
"2018-2019"	10	37	69.25	118.5	167.25	824
"2014"	10	35	54.75	104.5	161.75	790

Ranks

		N	Mean Rank	Sum Rank
"2014"-"2018-2019"	Positive Ranks	5	5.2	26
	Negative Ranks	5	5.8	29

Test Statistics

W	Z	Exact Prob>|W|	Asymp. Prob>|W|
29	0.10193	0.92188	0.91881

Null Hypothesis: F(x) = G(y)
Alternative Hypothesis: F(x) <> G(y)
At the 0.05 level, the two distributions are NOT significantly different.

A4.3. Box-plot chart statistics of levels of E2 (fmol/mL) in plasma samples from women without breast cancer. (**A**) Only with quantified levels (*n* = 22); (**B**) including levels below the LOQ (blue numbers, *n* = 2) and levels below the LOD (red numbers, *n* = 1). Perc, percentile.

	Min.	10 perc.	25 perc.	50 perc. (median)	75 perc.	90 perc.	Max.
A	14	17	22	37	279	385	900
B	7	12	17	33	243	385	900

A4.4. Statistical comparison of levels of E2 (fmol/mL) in plasma samples derived from the Isocross study analyzed in 2014 and analyzed again in the present study (2018-2019) (*n* = 10). Through a paired Wilcoxon test, no significant difference was observed (statistical significance would be indicated by a *p*-value < 0.05). Perc, percentile.

Analyzed in	Min.	10 perc.	25 perc.	50 perc. (median)	75 perc.	90 perc.	Max.
2014	22	27	36	130	260	332	349
2018-2019	14	18	28	162	243	333	385

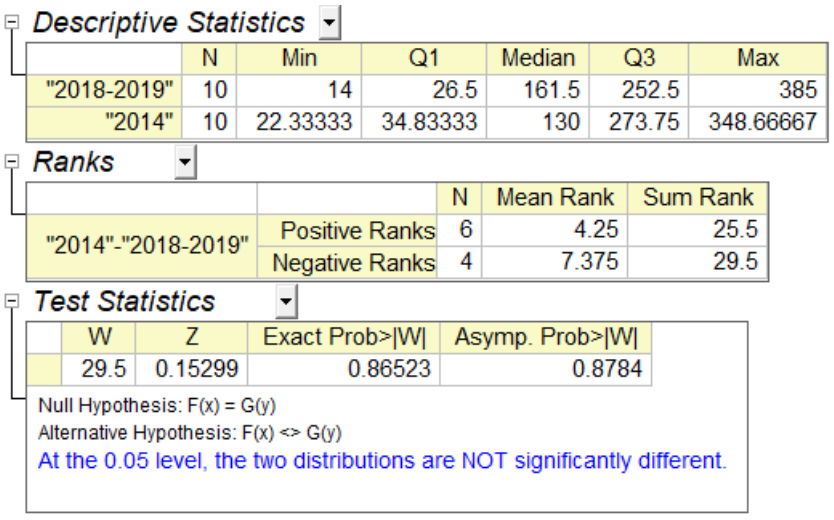

Descriptive Statistics

	N	Min	Q1	Median	Q3	Max
"2018-2019"	10	14	26.5	161.5	252.5	385
"2014"	10	22.33333	34.83333	130	273.75	348.66667

Ranks

		N	Mean Rank	Sum Rank
"2014"-"2018-2019"	Positive Ranks	6	4.25	25.5
	Negative Ranks	4	7.375	29.5

Test Statistics

W	Z	Exact Prob>|W|	Asymp. Prob>|W|
29.5	0.15299	0.86523	0.8784

Null Hypothesis: F(x) = G(y)
Alternative Hypothesis: F(x) <> G(y)
At the 0.05 level, the two distributions are NOT significantly different.

A4.5. Box-plot chart statistics of levels of E1 (fmol/mL) in plasma samples from premenopausal (*n* = 9) and postmenopausal women (*n* = 7) without breast cancer. Perc, percentile.

Menopausal status	Min.	10 perc.	25 perc.	50 perc. (median)	75 perc.	90 perc.	Max.
Premenopausal	37	37	90	138	148	422	422
Postmenopausal	24	24	32	48	75	94	94

A4.6. Box-plot chart statistics of levels of E2 (fmol/mL) in plasma samples from premenopausal (*n* = 9) and postmenopausal women (*n* = 6) without breast cancer. Perc, percentile.

Menopausal status	Min.	10 perc.	25 perc.	50 perc. (median)	75 perc.	90 perc.	Max.
Premenopausal	14	14	28	162	243	900	900
Postmenopausal	17	17	17	22	22	37	37

A4.7. Box-plot chart statistics of ratios of E2 levels to E1 levels (ratios E2/E1) in plasma samples from premenopausal (*n* = 9) and postmenopausal women (*n* = 6) without breast cancer. Perc, percentile.

Menopausal status	Min.	10 perc.	25 perc.	50 perc. (median)	75 perc.	90 perc.	Max.
Premenopausal	0.1	0.1	0.76	1.18	1.79	2.13	2.13
Postmenopausal	0.29	0.29	0.30	0.36	0.40	0.69	0.36

A4.8. Box-plot chart statistics of levels of E1-S (fmol/mL) in plasma samples from women without breast cancer (*n* = 25). Perc, percentile.

Min.	10 perc.	25 perc.	50 perc. (median)	75 perc.	90 perc.	Max.
134	179	328	761	2156	6035	11082

A4.9. Statistical comparison of levels of E1-S (fmol/mL) in plasma samples derived from the Isocross study analyzed in 2014 and analyzed again in the present study (2018-2019) (*n* = 10). Through a paired Wilcoxon test, no significant difference was observed (statistical significance would be indicated by a *p*-value < 0.05). Perc, percentile.

Analyzed in	Min.	10 perc.	25 perc.	50 perc. (median)	75 perc.	90 perc.	Max.
2014	302	360	691	1532	3562	12472	15614
2018-2019	234	312	556	1239	2954	8559	11082

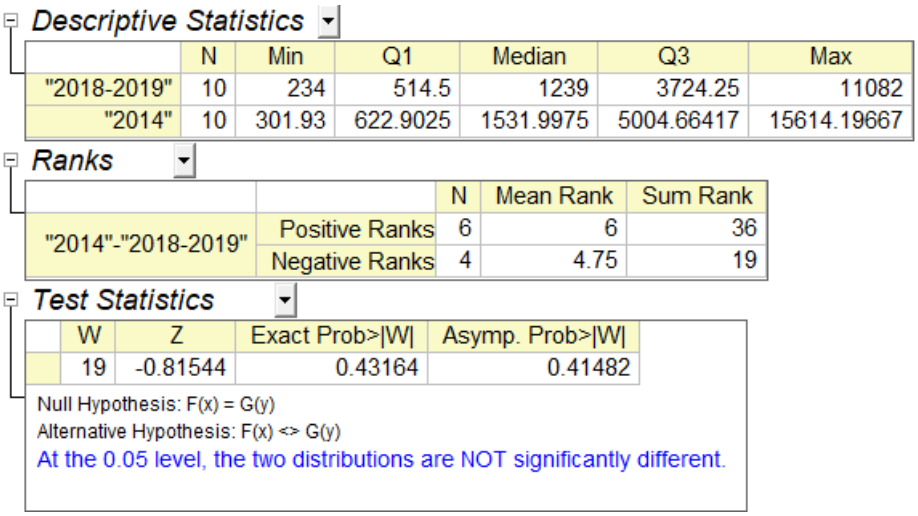

Descriptive Statistics

	N	Min	Q1	Median	Q3	Max
"2018-2019"	10	234	514.5	1239	3724.25	11082
"2014"	10	301.93	622.9025	1531.9975	5004.66417	15614.19667

Ranks

		N	Mean Rank	Sum Rank
"2014"-"2018-2019"	Positive Ranks	6	6	36
	Negative Ranks	4	4.75	19

Test Statistics

W	Z	Exact Prob>|W|	Asymp. Prob>|W|
19	-0.81544	0.43164	0.41482

Null Hypothesis: F(x) = G(y)
Alternative Hypothesis: F(x) <> G(y)
At the 0.05 level, the two distributions are NOT significantly different.

A4.10. Box-plot chart statistics of levels of E1-S (fmol/mL) in plasma samples from premenopausal (*n* = 9) and postmenopausal women (*n* = 7) without breast cancer. Perc, percentile.

Menopausal status	Min.	10 perc.	25 perc.	50 perc. (median)	75 perc.	90 perc.	Max.
Premenopausal	176	176	761	1363	2954	7634	7634
Postmenopausal	179	179	185	404	704	1144	1144

A4.11. Box-plot chart statistics of ratios of E1-S levels to E1 levels (ratios E1-S/E1) in plasma samples from premenopausal (*n* = 9) and postmenopausal women (*n* = 6) without breast cancer. Perc, percentile.

Menopausal status	Min.	10 perc.	25 perc.	50 perc. (median)	75 perc.	90 perc.	Max.
Premenopausal	2.7	2.7	7.7	15.1	21.4	30.1	30.1
Postmenopausal	5.8	5.8	6.8	7.5	9.6	15.9	15.9

A4.12. Box-plot chart statistics of levels of E1-G (fmol/mL) in plasma samples from women without breast cancer. (**A**) Only with quantified levels (*n* = 7); (**B**) including levels below the LOQ (blue numbers, *n* = 6) and levels below the LOD (red numbers, *n* = 9). Perc, percentile.

	Min.	10 perc.	25 perc.	50 perc. (median)	75 perc.	90 perc.	Max.
A	258	258	265	416	540	544	544
B	79	141	158	234	305	534	544

A4.13. Box-plot chart statistics of ratios of E1-G levels to E1 levels (ratios E1-G/E1) in plasma samples from premenopausal women without breast cancer (*n* = 5). Perc, percentile.

Min.	10 perc.	25 perc.	50 perc. (median)	75 perc.	90 perc.	Max.
1.3	1.3	1.8	1.9	2.4	5.5	5.5

A4.14. Box-plot chart statistics of ratios of E1-G levels to E1-S levels (ratios E1-G/E1-S) in plasma samples from premenopausal women without breast cancer (*n* = 5). Perc, percentile.

Min.	10 perc.	25 perc.	50 perc. (median)	75 perc.	90 perc.	Max.
0.07	0.07	0.09	0.09	0.12	0.71	0.71

A4.15. Box-plot chart statistics of levels of E2-3-S (fmol/mL) in plasma samples from women without breast cancer. (**A**) Only with quantified levels (*n* = 6); (**B**) including levels below the LOQ (blue numbers, *n* = 1) and levels below the LOD (red numbers, *n* = 15). Perc, percentile.

	Min.	10 perc.	25 perc.	50 perc. (median)	75 perc.	90 perc.	Max.
A	111	111	126	171	241	329	329
B	27	45	54	105	168	232	329

A4.16. Box-plot chart statistics of ratios of E2-3-S levels to E2 levels (ratios E2-3-S/E2) in plasma samples from premenopausal women without breast cancer (*n* = 5). Perc, percentile.

Min.	10 perc.	25 perc.	50 perc. (median)	75 perc.	90 perc.	Max.
0.4	0.4	0.4	0.7	1.0	6.1	6.1

A4.17. Levels of 16α-HO-E1 (*n* = 22) less than 41 fmol/mL and of 16α-HO-E2 (*n* = 22) less than 370 fmol/mL in plasma samples from women without breast cancer by means of GC-MS/MS (Chapter 3.2.1.3). P, percentile.

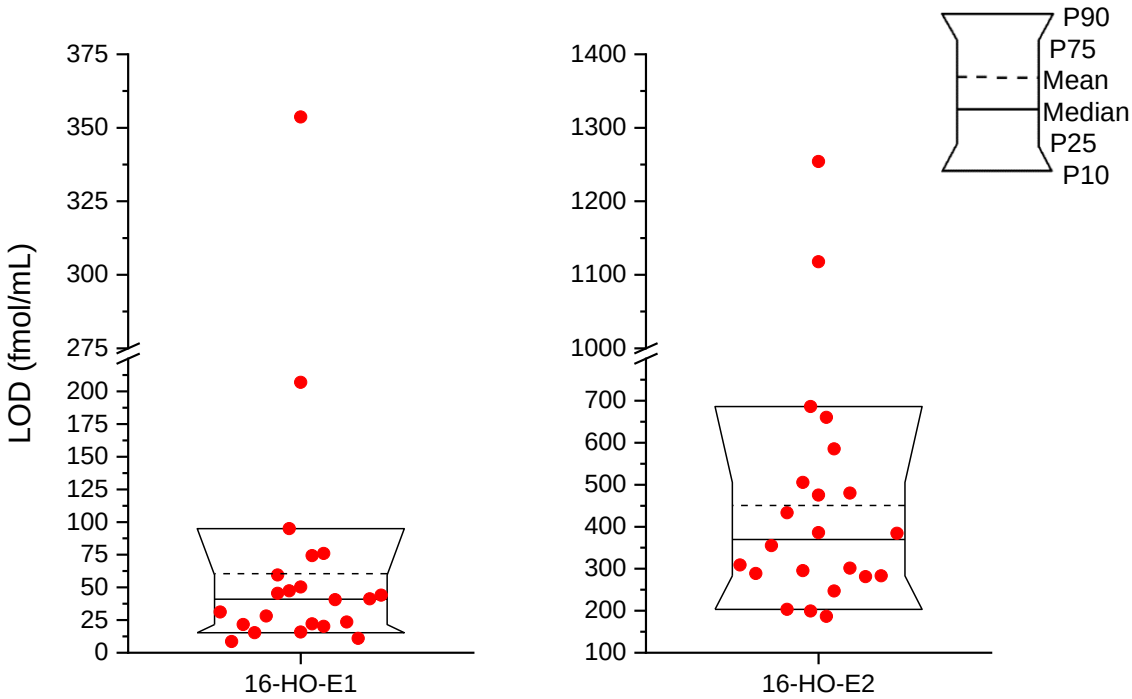

Hydroxyestrogen	Min.	10 perc.	25 perc.	50 perc. (median)	75 perc.	90 perc.	Max.
16α-HO-E1	9	15	22	41	59	95	354
16α-HO-E2	187	203	283	370	505	686	1254

A4.18. Levels of 2-HO-E1 (*n* = 20) less than 748 fmol/mL and of 2-HO-E2 (*n* = 17) less than 1177 fmol/mL in plasma samples from women without breast cancer by means of GC-MS/MS (Chapter 3.2.1.3). P, percentile.

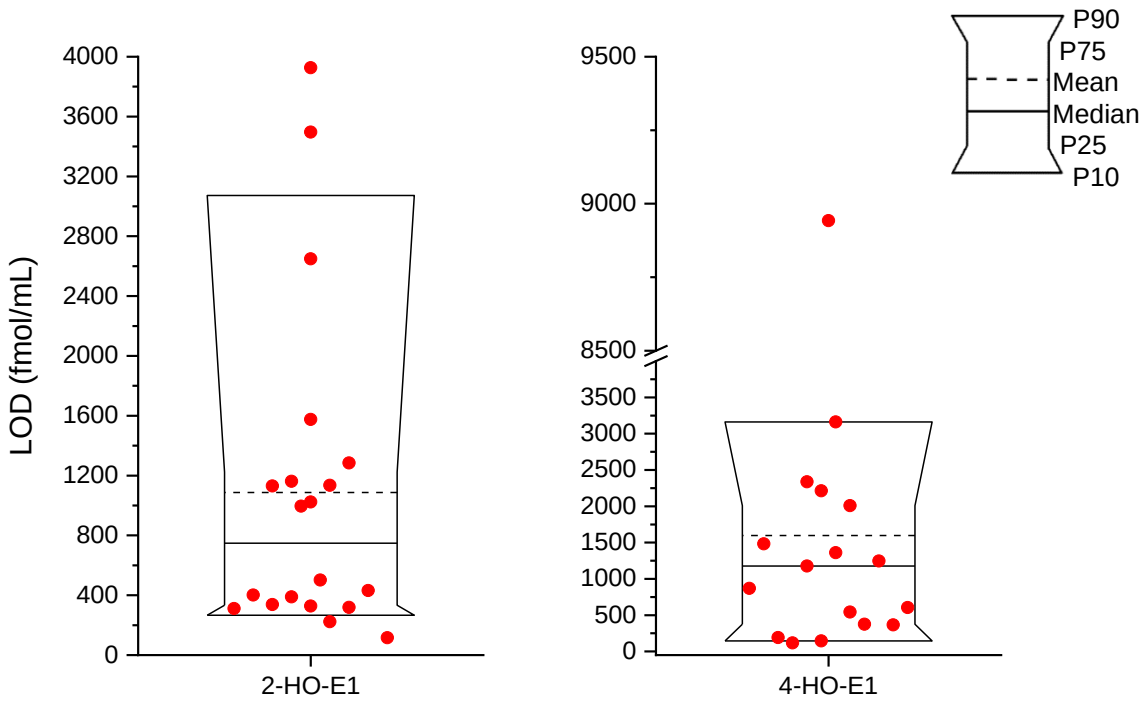

Hydroxyestrogen	Min.	10 perc.	25 perc.	50 perc. (median)	75 perc.	90 perc.	Max.
2-HO-E1	116	267	333	748	1223	3072	3926
2-HO-E2	119	146	375	1177	2009	3163	8942

A4.19. Levels of 4-HO-E1 (*n* = 20) less than 952 fmol/mL and of 4-HO-E2 (*n* = 17) less than 2223 fmol/mL in plasma samples from women without breast cancer by means of GC-MS/MS (Chapter 3.2.1.3). P, percentile.

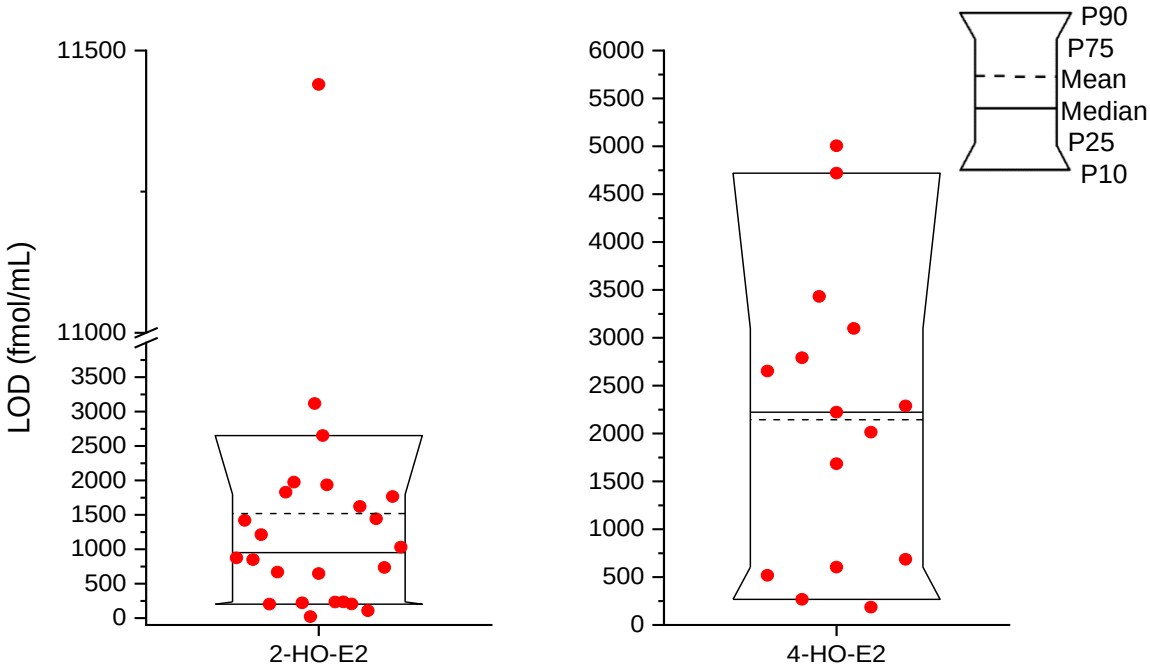

Hydroxyestrogen	Min.	10 perc.	25 perc.	50 perc. (median)	75 perc.	90 perc.	Max.
4-HO-E1	21	203	234	952	1797	2652	11440
4-HO-E2	185	268	604	2223	3097	4719	5005

A4.20. Recovery (%) statistics of hydroxyestrogens in plasma. Perc, percentile.

Hydroxyestrogen	Min.	10 perc.	25 perc.	50 perc. (median)	75 perc.	90 perc.	Max.	n
16α-HO-E1	8	21	37	55	88	122	149	22
16α-HO-E2	16	19	23	32	50	57	91	22
2-HO-E1	9	11	13	15	25	83	94	15
2-HO-E2	3	4	5	11	26	80	120	13
4-HO-E1	6	6	11	25	35	71	82	20
4-HO-E2	6	6	7	16	43	91	99	13

A4.21. Box-plot chart statistics of levels of 2-MeO-E1 (fmol/mL) in plasma samples from women without breast cancer. (**A**) Only with quantified levels (*n* = 5); (**B**) including levels below the LOQ (blue numbers, *n* = 6) and levels below the LOD (red numbers, *n* = 14). Perc, percentile.

	Min.	10 perc.	25 perc.	50 perc. (median)	75 perc.	90 perc.	Max.
A	51	51	71	90	108	164	164
B	4	7	9	12	24	90	164

A4.22. Levels of 4-MeO-E1 (*n* = 25) less than 10 fmol/mL and of 2-MeO-E2 (*n* = 25) and 4-MeO-E2 (*n* = 24) less than 15 fmol/mL in plasma samples from women without breast cancer by means of GC-MS/MS (Chapter 3.2.1.3). P, percentile.

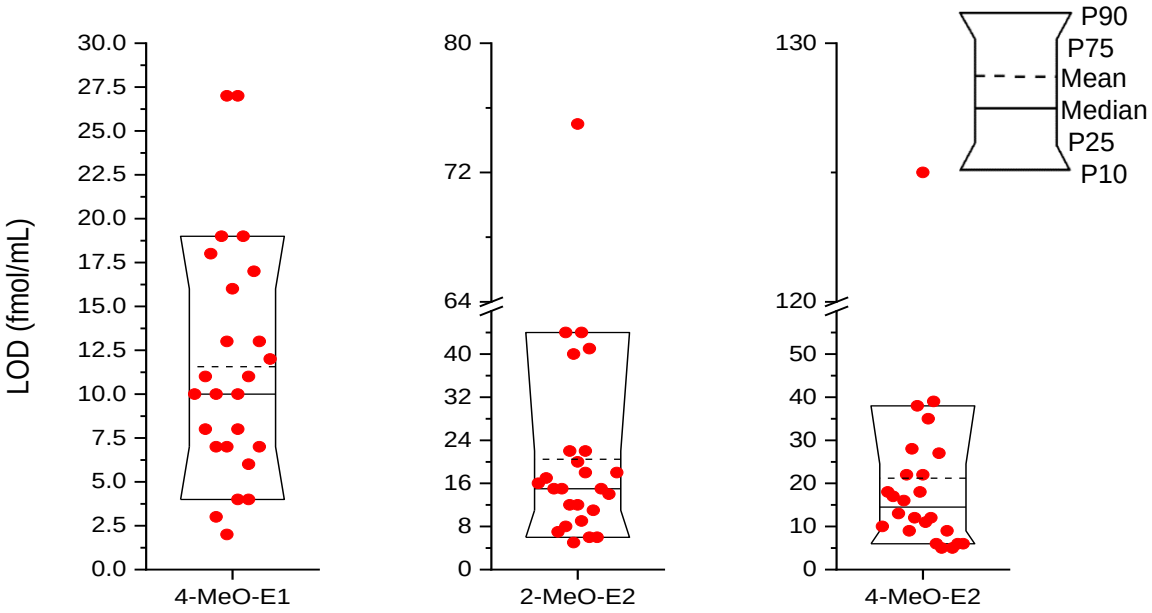

Methoxyestrogen	Min.	10 perc.	25 perc.	50 perc. (median)	75 perc.	90 perc.	Max.
4-MeO-E1	2	4	7	10	16	19	27
2-MeO-E2	5	6	11	15	22	44	75
4-MeO-E2	5	6	9	15	25	38	125

A4.23. Statistical comparison of LOD levels of 4-MeO-E1 (fmol/mL) in plasma samples derived from the Isocross study analyzed in 2014 and analyzed again in the present study (2018-2019) (*n* = 10). Through a paired Wilcoxon test, no significant difference was observed (statistical significance would be indicated by a *p*-value < 0.05). Perc, percentile.

Analyzed in	Min.	10 perc.	25 perc.	50 perc. (median)	75 perc.	90 perc.	Max.
2014	3	5	9	11	16	21	21
2018-2019	2	3	6	9	13	21.5	27

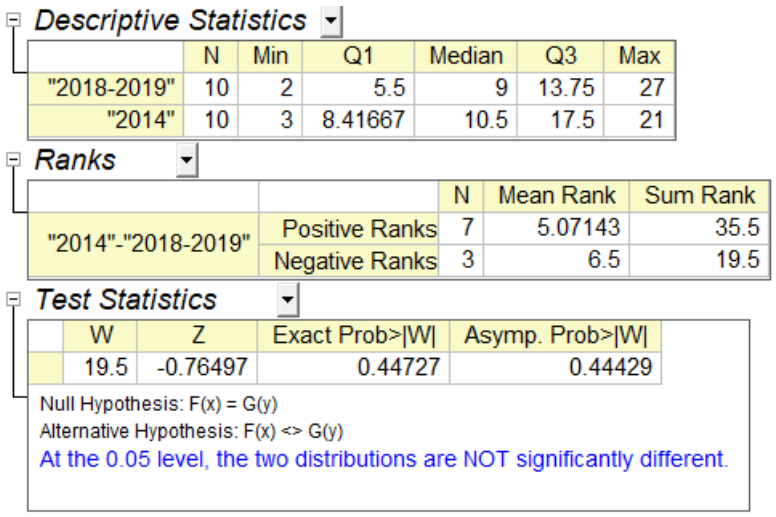

Descriptive Statistics

	N	Min	Q1	Median	Q3	Max
"2018-2019"	10	2	5.5	9	13.75	27
"2014"	10	3	8.41667	10.5	17.5	21

Ranks

		N	Mean Rank	Sum Rank
"2014"-"2018-2019"	Positive Ranks	7	5.07143	35.5
	Negative Ranks	3	6.5	19.5

Test Statistics

W	Z	Exact Prob>|W|	Asymp. Prob>|W|
19.5	-0.76497	0.44727	0.44429

Null Hypothesis: F(x) = G(y)
Alternative Hypothesis: F(x) <> G(y)
At the 0.05 level, the two distributions are NOT significantly different.

A4.24. Statistical comparison of LOD levels of 2-MeO-E2 (fmol/mL) in plasma samples derived from the Isocross study analyzed in 2014 and analyzed again in the present study (2018-2019) (*n* = 10). Through a paired Wilcoxon test, no significant difference was observed (statistical significance would be indicated by a *p*-value < 0.05). Perc, percentile.

Analyzed in	Min.	10 perc.	25 perc.	50 perc. (median)	75 perc.	90 perc.	Max.
2014	5	6	8	9	11	14	16
2018-2019	5	6	9	12	18	32	44

Descriptive Statistics

	N	Min	Q1	Median	Q3	Max
"2018-2019"	10	5	8.25	12	18.5	44
"2014"	10	5	7.83333	9	10.75	16

Ranks

		N	Mean Rank	Sum Rank
"2014"-"2018-2019"	Positive Ranks	3	3.66667	11
	Negative Ranks	6	5.66667	34

Test Statistics

W	Z	Exact Prob>|W|	Asymp. Prob>|W|
34	1.30317	0.20313	0.19252

Null Hypothesis: F(x) = G(y)
Alternative Hypothesis: F(x) <> G(y)
At the 0.05 level, the two distributions are NOT significantly different.

A4.25. Statistical comparison of LOD levels of 4-MeO-E2 (fmol/mL) in plasma samples derived from the Isocross study analyzed in 2014 and analyzed again in the present study (2018-2019) (*n* = 10). Through a paired Wilcoxon test, no significant difference was observed (statistical significance would be indicated by a *p*-value < 0.05). Perc, percentile.

Analyzed in	Min.	10 perc.	25 perc.	50 perc. (median)	75 perc.	90 perc.	Max.
2014	5	6	7	8	11	18	19
2018-2019	5	6	9	12	22	37	38

Descriptive Statistics

	N	Min	Q1	Median	Q3	Max
"2018-2019"	10	5	8.25	12	25.25	38
"2014"	10	5	6.75	7.66667	12.25	19

Ranks

		N	Mean Rank	Sum Rank
"2014"-"2018-2019"	Positive Ranks	2	4	8
	Negative Ranks	8	5.875	47

Test Statistics

W	Z	Exact Prob>|W|	Asymp. Prob>|W|
47	1.93792	0.04688	0.05263

Null Hypothesis: F(x) = G(y)
Alternative Hypothesis: F(x) <> G(y)
At the 0.05 level, the two distributions are significantly different.

A4.26. Box-plot chart statistics of levels of 2-MeO-E1-G (fmol/mL) in plasma samples from women without breast cancer which includes levels below the LOQ (blue numbers, *n* = 2) and levels below the LOD (red numbers, *n* = 21). Perc, percentile.

Min.	10 perc.	25 perc.	50 perc. (median)	75 perc.	90 perc.	Max.
39	51	88	110	147	182	355

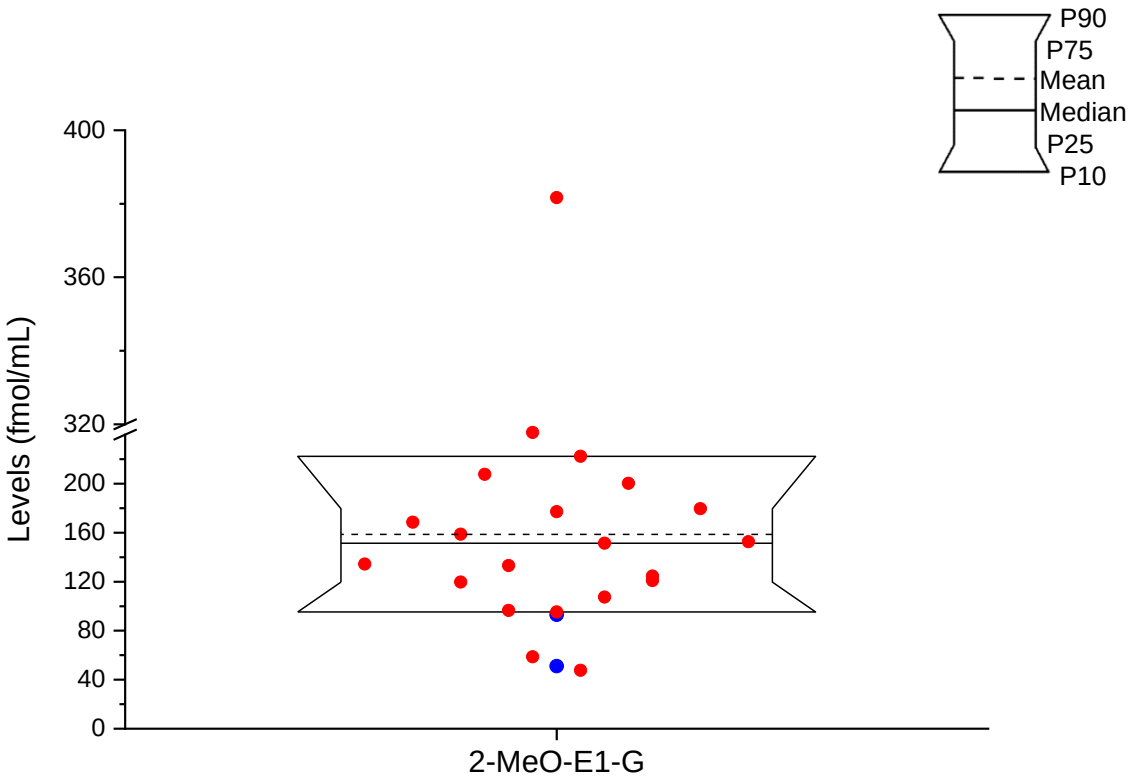

A4.27. Levels of 4-MeO-E1-G (*n* = 25) less than 68 fmol/mL, of 2-MeO-E2-3-G (*n* = 25) less than 121 fmol/mL and of 4-MeO-E2-3-G (*n* = 25) less than 45 fmol/mL in plasma samples from women without breast cancer by means of UHPLC-MS/MS (Chapter 3.2.1.2). P, percentile.

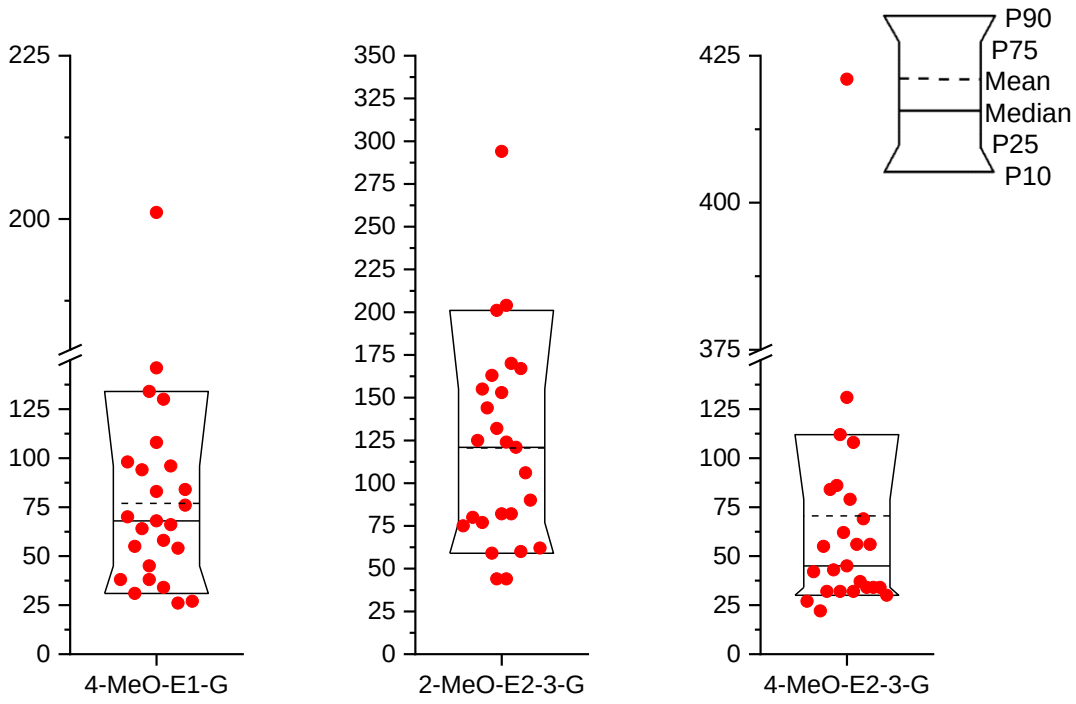

Methoxyestrogen glucuronide	Min.	10 perc.	25 perc.	50 perc. (median)	75 perc.	90 perc.	Max.
4-MeO-E1-G	26	31	45	68	96	134	201
2-MeO-E2-3-G	44	59	77	121	155	201	294
4-MeO-E2-3-G	22	30	34	45	79	112	421

A4.28. Levels of 2-MeO-E2-17-G (*n* = 23) less than 2098 fmol/mL and of 4-MeO-E2-17-G (*n* = 22) less than 2219 fmol/mL in plasma samples from women without breast cancer by means of UHPLC-MS/MS (Chapter 3.2.1.2). P, percentile.

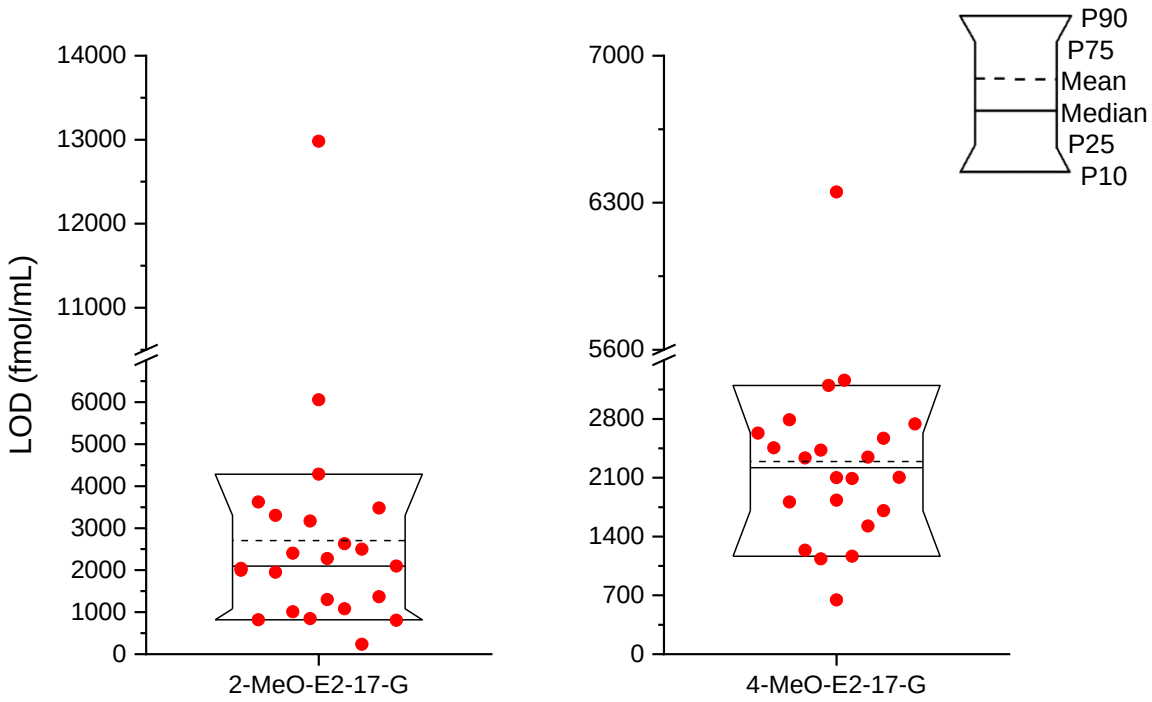

Methoxyestrogen glucuronide	Min.	10 perc.	25 perc.	50 perc. (median)	75 perc.	90 perc.	Max.
2-MeO-E2-17-G	234	820	1079	2098	3305	4284	12982
4-MeO-E2-17-G	645	1165	1707	2219	2631	3198	6351

A4.29. Calculated levels (black numbers), levels below the LOQ (blue numbers), and levels below the LOD (red numbers) (fmol/mL) of free estrogens and estrogen metabolites in pre- (green highlighted), peri-, and postmenopausal women (gray highlighted) without breast cancer. ÜP, übungs plasma; n.d. not determinable.

Woman (sample #)	E1	E2	2-MeO-E1	E1-S	E1-G	E2-3-S	2-MeO-E1-G
28	138	163	24	2954	258	232	182
35	824	385	164	11082	92	n.d.	n.d.
36	90	161	19	1363	229	111	145
37	99	162	8	761	540	42	109
39	75	22	19	556	156	106	124
40	37	28	9	1115	241	173	78
44	225	243	12	6035	534	241	n.d.
46	140	14	90	390	n.d.	47	39
48	148	281	9	2156	265	126	79
49	52	33	11	234	305	45	88
50	42	17	7	404	n.d.	92	130
52	94	34	10	704	143	129	198
53	193	40	22	2142	239	174	98
54	53	12	9	212	141	54	102
55	66	15	11	175.5	n.d.	55	99
56	224	580	51	2754	194	168	51
57	32	22	4	185	190	76	355
58	24	8	9	179	208	52	138
59	72	22	12	1144	160	75	164
60	48	17	6	328	79	104	170
61	422	900	108	7634	544	329	93
ÜP1	151	317	71	3426	416	n.d.	147
ÜP2	66	23	13	639	316	27	110
ÜP3	114	279	27	985	260	n.d.	125
ÜP4	243	7	9	134	158	111	48

A4.30. Ratios of estrogens calculated with reported mean/median/geometric mean levels from the literature in pre- and postmenopausal women. FP, follicular phase; LP, luteal phase; (P), plasma; *median; **mean; †range; -, data not available for comparison; ? healthy status not clearly specified.

Study population		Ratios of levels							Reference
		E2/E1	E1-S/E1	E1-G/E1	E1-G/E1-S	2-MeO-E1/E1	E2-3-S/E2	2-MeO-E1-G/E1	
Premenopausal women (*n* = 20)	healthy	1.52	-	-	-	0.39	-	-	Coburn et al. (2019)**
Postmenopausal women (*n* = 26)	healthy	0.34				0.29			
Postmenopausal women (*n* =110)	healthy	0.17	7.13	-	-	-	-	-	Audet-Delage et al. (2018)*
Premenopausal (*n* = 27)	women	1.44-1.52	-	-	-	-	-	-	Faqehi et al. (2016)† (P) ?
Postmenopausal (*n* = 20)	women	0.65-1.31							
Premenopausal women (*n* = 10)	healthy	0.78	-	-	-	-	-	-	Caron et al. (2015)**
Postmenopausal women (*n* = 20)	healthy	0.25							

Postmenopausal healthy women (*n* = 110)	0.18	7.13	0.75	-	-	-	0.07	Audet-Walsh et al. (2011)*
Premenopausal healthy women (*n* = 29) Postmenopausal healthy women (*n* = 19)	0.55 in the early FP 0.080	-	-	-	-	-	-	Rothman et al. (2011)**
Postmenopausal healthy women (*n* = 110)	0.28	9.14	-	-	-	-	-	Lépine et al., 2010**
Premenopausal healthy women (*n* = 19) Postmenopausal healthy women (*n* = 10)	0.99 (FP); 1.36 (LP) 0.20	12.85 (FP); 19.57 (LP) 10.47	0.85 (FP); 1.13 (LP) 0.58	0.07 (FP); 0.06 (LP) 0.06	-	-	0.11 (FP); 0.16 (LP) 0.11	Caron et al. (2009)**
Premenopausal healthy women (*n* = 4) Postmenopausal healthy women (*n* = 2)	1.26 (FP); 1.34(LP) 0.45	-	-	-	0.27 (FP); 0.29(LP) 0.11	-	-	Xu et al. (2007)**

A4.31. Exact *p*-values from the Spearman's correlation among levels of E1, E2 and E1-S in plasma from pre- (*n* = 9) and postmenopausal (*n* = 7) woman without breast cancer. NA, not applicable.

Menopausal status		E1	E2	E1-S
Pre	E1	NA	0.01252	0.03577
Post		NA	0.04411	0.01370
Pre	E2		NA	0.00094
Post			NA	0.08472
Pre	E1-S			NA
Post				NA

A4.32 Box-plot chart statistics of recovery levels (%) of methoxyestrogen glucuronides in GLT. Perc, percentile.

Reference	Min.	10 perc.	25 perc.	50 perc. (median)	75 perc.	90 perc.	Max.	n
2-MeO-E1-G	2.72	4.00	4.42	5.20	10.89	21.11	49.03	13
4-MeO-E1-G	8.75	8.75	8.75	23.92	38.60	38.60	38.60	3
2-MeO-E2-3-G	2.07	4.16	4.48	6.25	11.91	19.60	40.19	12
2-MeO-E2-17-G	2.64	2.87	3.14	4.07	8.81	10.62	14.16	11
4-MeO-E2-3-G	2.43	4.74	4.76	5.97	15.16	19.54	42.44	11
4-MeO-E2-17-G	2.09	2.21	3.04	3.94	8.59	10.29	11.48	10

A4.33 Box-plot chart statistics of recovery levels (%) of methoxyestrogen glucuronides in ADT. Perc, percentile.

Reference	Min.	10 perc.	25 perc.	50 perc. (median)	75 perc.	90 perc.	Max.	n
2-MeO-E1-G	5.71	7.68	11.05	19.33	36.55	65.52	71.36	12
4-MeO-E1-G	11.22	12.50	17.02	27.15	37.88	59.59	64.50	10
2-MeO-E2-3-G	7.61	10.16	15.10	31.36	50.52	60.06	62.75	12
2-MeO-E2-17-G	3.97	3.97	9.39	12.69	21.80	38.66	38.66	9
4-MeO-E2-3-G	7.01	7.01	16.55	36.58	51.26	63.04	63.04	9
4-MeO-E2-17-G	3.74	4.19	7.09	13.69	23.38	29.83	36.22	12

A4.34 Box-plot chart statistics of LOD levels (fmol/g) of methoxyestrogen glucuronides in GLT. Perc, percentile.

Reference	Min.	10 perc.	25 perc.	50 perc. (median)	75 perc.	90 perc.	Max.	n
2-MeO-E1-G	234	515	587	1396	1954	2148	2644	12
4-MeO-E1-G	354	354	354	436	517	517	517	2
2-MeO-E2-3-G	275	284	316	448	908	1022	2066	11
2-MeO-E2-17-G	150	150	345	399	507	750	750	9
4-MeO-E2-3-G	2825	2825	3613	6249	9219	13616	13616	6
4-MeO-E2-17-G	3992	3992	5428	10523	12930	34989	34989	9

A4.35 Box-plot chart statistics of LOD levels (fmol/g) of methoxyestrogen glucuronides in ADT. Perc, percentile.

Reference	Min.	10 perc.	25 perc.	50 perc. (median)	75 perc.	90 perc.	Max.	n
2-MeO-E1-G	229	270	284	594	893	1035	2061	12
4-MeO-E1-G	212	212	226	241	521	739	739	8
2-MeO-E2-3-G	56	56	95	111	173	373	373	9
2-MeO-E2-17-G	92	92	124	294	429	473	473	9
4-MeO-E2-3-G	293	293	694	1404	4754	8806	8806	9
4-MeO-E2-17-G	1012	1012	2008	3751	5269	10709	10709	9

Further supplementary data can be consulted in the accompanying CD.